THE UNIVERSITY
of EDINBURGH

Characterisation of Nrf2-signalling and the effects of boosting astrocytic Nrf2 in a mouse model of ischaemic stroke

Margaux Aimable BSc MSc

A thesis submitted for the degree of Doctor of Philosophy

College of Medicine and Veterinary Medicine

University of Edinburgh

2019

Table of Contents

DECLARATION **7**

ABSTRACT **9**

LAY SUMMARY **11**

ACKNOWLEDGEMENTS **13**

LIST OF FIGURES **15**

LIST OF TABLES **19**

LIST OF ABBREVIATIONS **21**

1. INTRODUCTION **25**

1.1. General clinical knowledge on ischaemic stroke 25

1.1.1. Definition *25*

1.1.2. Risk factors *27*

1.1.3. Long term effects of ischaemia *29*

1.2. Cellular biology and pathophysiology of cerebral ischaemia 32

1.2.1. Hypoperfusion and penumbra *32*

1.2.2. Ischaemic models *35*

1.2.3. Alterations in neurological function and cognition in animal models of ischaemia *39*

1.2.4. Vascular system disruption *40*

1.2.5. Excitotoxicity and depolarisation waves *41*

1.2.6. Oxidative stress *42*

1.2.7. Inflammation *45*

1.2.8. Apoptosis & necrosis *52*

1.3. Nrf2 signalling 54

1.3.1. An endogenous transcription factor *54*

1.3.2. Nrf2 pharmacological activators and genetically modified models *59*

1.3.3. Beneficial effects of Nrf2-signalling following ischaemia *67*

1.4. Summary 72

1.5. Global hypothesis 73

1.5.1. Aims: *73*

2. MATERIAL & METHODS **75**

2.1. Mice 75

2.1.1. GFAP-Nrf2 mice *75*

2.1.2. Animal maintenance and use *75*

2.2. Focal cerebral ischaemic model 76

2.2.1. Inclusion/exclusion criteria *76*

2.3. Histology 77

2.3.1. Lesion volume assessment *77*

2.3.2. Immunohistochemistry *79*

2.4. qRT-PCR 82

2.5. Behaviour 84

2.5.1. Neuroscore *84*

2.5.2. Novel Object Recognition in a Y maze *86*

2.6. Laser Speckle imaging to determine cerebral blood flow 87

2.7. Statistics 88

3. CHARACTERISATION OF ACUTE AND CHRONIC CEREBRAL ISCHAEMIA AND ITS IMPACT ON NRF2-SIGNALLING PATHWAY **89**

3.1. Introduction 89

3.1.1. Aims *91*

3.2. METHODS 91
3.2.1. Mice and experimental groups 91
3.2.2. Focal cerebral ischaemia model 93
3.2.3. Histology 93
3.2.4. Analysis 94
3.2.5. qRT-PCR 94
3.2.6. Statistics 95
3.3. CHARACTERISATION OF ISCHAEMIC CELL DEATH WITH INCREASING OCCLUSION DURATION 96
3.3.1. Increased neuronal damage with increasing duration of occlusion 96
3.3.2. Increased cortical oxidative stress with increasing duration of occlusion 98
3.3.3. Astrocytic response to acute ischaemia 100
3.3.4. Increased microglia/macrophage density in the acute response to ischaemia 103
3.3.5. Increased cxcl10 expression in the striatum 24 hours after 15 minutes ischaemia 108
3.3.6. Peripheral immune cells infiltrate 24 hours after ischaemia 109
3.3.7. Nrf2 signalling during the acute response to ischaemia 115
3.4. LONG TERM ISCHAEMIA AND NRF2 ACTIVATION 120
3.4.1. Modest duration ischaemia increases neuronal damage in the striatum at chronic time point 120
3.4.2. Modest duration ischaemia increases the oxidative stress marker 3NT in the chronic phase 122
3.4.3. Astrocytic response to chronic ischaemia 124
3.4.4. Microglia/macrophage response 4 weeks after ischaemia 126
3.4.5. Genes il-1β and cxcl10 were increased 4 weeks after modest duration of ischaemia 128
3.4.6. Peripheral immune cells infiltrate 4 weeks after modest duration ischaemia 129
3.4.7. Nrf2 signalling was not activated in chronic ischaemia 132
3.5. DISCUSSION 136
3.5.1. Cerebral ischaemia causes neuronal loss and increase duration of ischaemia increases the damaged area 136
3.5.2. Ischaemia produces oxidative stress environment that persist over time 139
3.5.3. Ischaemia creates an inflammatory environment via modification of glia and infiltration of peripheral immune cells 141
3.5.4. Ischaemia modifies Nrf2 signalling at acute but not chronic response to 15 minutes ischaemia 150
3.5.5. Conclusion 152

4. PROTECTIVE EFFECT OF NRF2 OVEREXPRESSION IN THE ACUTE RESPONSE TO ISCHAEMIA IN MICE 155
4.1. INTRODUCTION 155
4.1.1. Aims 156
4.2. MATERIALS & METHODS 157
4.2.1. Mice and experimental groups 157
4.2.2. Focal cerebral ischaemia 157
4.2.3. Histology and immunohistochemistry 158
4.2.4. qRT-PCR 158
4.2.5. Statistics 159
4.3. RESULTS 160
4.3.1. Overexpression of Nrf2 gene in GFAP-Nrf2 mice 160
4.3.2. Neuroprotection in mice overexpressing Nrf2 in astrocytes 160
4.3.3. Astrocytic overexpression of Nrf2 reduced oxidative stress 163
4.3.4. Nrf2 signalling was boosted in mice that overexpress Nrf2 in astrocytes 167
4.3.5. Reactive astrocytosis was modified with astrocyte specific Nrf2 overexpression 170
4.3.6. Microglial/macrophage response after ischaemia was not altered with astrocyte-specific overexpression of Nrf2 173
4.3.7. Increase of IL-4rα and cxcl10 genes with astrocyte-specific overexpression of Nrf2 175

4.4. DISCUSSION 179
4.4.1. Nrf2 overexpression in astrocytes reduces lesion and oxidative stress induced by ischaemia 179
4.4.2. Nrf2 overexpression and the effects on reactive astrocytes and microglia/macrophages after ischaemia 182
4.4.3. Other possible protective effects of Nrf2 overexpression in astrocytes 188
4.4.4. Other limitations 188
4.4.5. Conclusions 190

5. ASTROCYTIC OVEREXPRESSION OF NRF2 DOES NOT PROTECT NEURONS AND DOES NOT ALTER NEUROLOGICAL FUNCTION OR COGNITIVE DEFICITS IN THE CHRONIC RESPONSE TO A MODEST DURATION OF ISCHAEMIA 191
5.1. INTRODUCTION 191
5.1.1. Aims 192
5.2. MATERIEL & METHODS 193
5.2.1. Mice and experimental groups 193
5.2.2. Focal cerebral ischaemia 194
5.2.3. Sensorimotor and cognitive function tests 194
5.2.4. Histology 195
5.2.5. qRT-PCR 195
5.2.6. Statistics 196
5.3. RESULTS 197
5.3.1. Nrf2 overexpression in astrocytes impaired cognitive functions and did not modify neurological function 197
5.3.2. Neuronal damage was not altered by astrocytic overexpression of Nrf2 200
5.3.3. Oxidative stress in response to ischaemia was unchanged in Nrf2 overexpressing mice compared to wild-type controls 202
5.3.4. Nrf2-signalling was increased in the GFAP-Nrf2 mice 204
5.3.5. Nrf2 overexpression did not alter levels of reactive astrocytes 4 weeks after modest duration ischaemia (15 minutes) 205
5.3.6. Astrocytic overexpression of Nrf2 increased microglia/macrophages response 4 weeks after mild ischaemia 206
5.3.7. Nrf2 overexpression in astrocytes reduced c3 gene expression after ischaemia but did not modify the expression of cxcl10, il-1β or il-4rα genes 208
5.4. DISCUSSION 210
5.4.1. Neurological deficits improved at 7 days in the GFAP-Nrf2 animals 210
5.4.2. Novel object recognition (NOR) to test cognitive function 211
5.4.3. Neuronal damage unaltered with overexpression of Nrf2 in astrocytes 213
5.4.4. Increased Nrf2-signalling in GFAP-Nrf2 animals compared to wild-type animals ... 216
5.4.5. Oxidative stress was unchanged in GFAP-Nrf2 animals compared to wild-type littermates after modest duration ischaemia 217
5.4.6. Astrocyte reactivity unchanged in GFAP-Nrf2 animals compared to their wild-type littermates 217
5.4.7. Microglia/macrophages increased in the striatum of the GFAP-Nrf2 animals compared to wild-types 219
5.4.8. Inflammatory-related genes expression 219
5.4.9. Conclusions 221

6. DISCUSSION 223
6.1. SUMMARY AND IMPLICATIONS 223
6.2. LIMITATIONS AND FUTURE DIRECTIONS 228

7. REFERENCES 231

8. APPENDIXES 281
8.1. REAGENT RECIPES 281

8.2. GLIAL RESPONSE IN THE PERI-INFARCT COMPARED TO THE CORE OF CHRONIC ISCHAEMIA AND COMPARED WITH LESION 282
8.2.1. Peri-infarct results in the chronic phase of ischaemia were a mean value of core and healthy for Glial marker GFAP and Iba1 282
8.2.2. Correlations of the lesion volume with GFAP and Iba1 marker in the chronic response to ischaemia 283
8.3. ASTROCYTIC OVEREXPRESSION OF NRF2 DID NOT MODIFY CEREBRAL BLOOD FLOW 4 WEEKS AFTER ISCHAEMIA 284

Declaration

I declare that this thesis has been composed solely by myself, that it has not been submitted for any previous degree or qualification, and that the work described within this thesis comprises my own original work except where stated otherwise in the text.

The author contributions are outlined in the material & methods of each chapter; however, the majority of the work was carried out by me with contributions from Lizi Hegarty, Katharina Nagassima Rodrigues dos Reis and Dr Jill Fowler, and was under the supervision of Dr Jill Fowler.

Margaux Aimable

Date: 12/10/19

Signature: 

Abstract

Stroke is the leading cause of disability for adults and the second leading cause of death worldwide. It is characterised by a sudden weakness or numbness of the face, arm or leg, most often on one side of the body. The most common type of stroke is an ischaemic stroke, the blockage of a cerebral vessel and is causing dementia. Nuclear Factor Erythroid 2 (NF-E2)-Related Factor 2 (Nrf2) is a transcription factor and master regulator of a battery of antioxidant and anti-inflammatory genes such as Heme oxygenase-1 (*hmox1*), NAD(P)H dehydrogenase quinone 1 (*nqo1*), glutamate-cystine antiporter (xCT; gene *slc7a11*), sulfiredoxin 1 (*srxn1*). As astrocytes play a central role in the neuroprotective effects of boosting Nrf2, the overarching hypothesis of the present work is that boosting the Nrf2 pathway in astrocytes will prevent oxidative stress and pro-inflammatory damage caused by ischaemia/reperfusion and thereby protect neurons from damage and diminish cognitive deficits and neurodegeneration that may lead to dementia.

A mouse model of transient focal cerebral ischaemia was chosen to reproduce ischaemia in controlled conditions, by occluding the middle cerebral artery. Modest duration of ischaemia (15 minutes) was sufficient to cause ischaemic neuronal damage in the striatum and to significantly increase oxidative stress, inflammatory markers and to activate Nrf2-signalling. Furthermore, oxidative stress and inflammation were found despite reperfusion and in areas spared of neuronal death, suggesting they may still be at risk of cellular damage. Despite persistent elevations in oxidative stress, inflammatory glial cells and cytokines 4 weeks after ischaemia, there were no alterations to Nrf2-signalling suggesting that boosting Nrf2-signalling may confer protective effects.

Nrf2 overexpression in GFAP-expressing astrocytes in a mouse model (GFAP-Nrf2 mice) has been shown to confer protection against inflammation and oxidative stress in neurodegenerative models. Following ischaemia, GFAP-Nrf2 mice presented a significant reduction of neuronal damage, oxidative stress was markedly reduced, and levels of reactive astrocytes were increased in the peri-infarct of the cortex. This was paralleled with a significant increase of *cxcl10* and anti-inflammatory *il-4rα* cytokine gene expression.

These promising results led to next study the potential protective effects of boosting Nrf2 in astrocytes on cognitive and neurological deficits 4 weeks after ischaemic stroke. In this experiment, ischaemia impaired cognitive functions at 4 weeks and this was paralleled with oxidative stress and inflammation. Neuronal damage caused by ischaemia was not significantly altered between wild-type and GFAP-Nrf2 animals despite upregulated Nrf2-signalling in GFAP-Nrf2 mice compared to wild-types. Nrf2 overexpression in astrocytes increased microglial response and reduced inflammatory *c3*, but their cognitive functions were further impaired compared to wild-types.

Altogether these studies suggest that Nrf2 exerts different effects after ischaemia depending on the severity of stroke and the timepoint analysed. Furthermore, these results suggest that there is ongoing signalling between microglia and astrocytes. This work provides an original contribution to understanding the potential protective effects of Nrf2 overexpression in astrocytes and its limitations.

Lay summary

Stroke is the leading cause of disability for adults and the second leading cause of death worldwide. The first symptom is a sudden numbness of the face, arm or leg, most often on one side of the body, and in the long term it can impair cognitive functions, the mental processes by which we think, remember, learn and make decisions. These processes depend on neurons, the main cell type of the brain, and their environment. The main cause of stroke is a blockage of a vessel in the brain, called cerebral ischaemia. It leads to a cascade of damaging mechanisms that can cause dysfunction and death of neurons. These damaging mechanisms include alterations to the immune defence system called inflammation. Another damaging mechanism is called oxidative stress and is characterised by an overproduction of toxic molecules called oxidants that can damage cells. The brain normally produces antioxidants to balance it out, however after stroke, these defences are reduced and overwhelmed. These two features of ischaemia endanger neurons to the point that it might lead to their death and cause cognitive decline. Nrf2 is a protein known for its antioxidant and anti-inflammatory effects and is thus a promising candidate for treatment of stroke patients. In this thesis, the impact of stroke on Nrf2 was studied together with the potential protective effect of boosting Nrf2 on neuron damage after stroke. It was found that Nrf2 is activated during the first day after stroke and that these changes were associated with increased oxidative stress and inflammation. However, four weeks after ischaemia, oxidative stress and inflammation persisted whereas the Nrf2 system was no longer activated.

The protective effects of Nrf2 are dependent on another cell type in the brain called astrocytes, that provide a supporting role for neurons that includes providing them with antioxidants. A model has been developed in which Nrf2 levels are boosted specifically in astrocytes, and other studies have shown that this has beneficial effects in several neurodegenerative diseases such as Parkinson's disease. In the second part of this thesis, the effects of boosting Nrf2 in astrocytes was studied in a model of stroke. Boosting Nrf2 in astrocytes was shown to modestly decrease damage to neurons and reduce inflammation and oxidative stress 1 day after a large stroke. This promising result led on to a second experiment to determine if boosting Nrf2 could protect neurons and cognition in the longer term (4 weeks) response to a smaller stroke. Interestingly, in this experiment, boosting Nrf2 in astrocytes did not alter neuronal damage and oxidative stress after ischaemia although alterations to inflammation were detected. Surprisingly, it was found that boosting Nrf2 in astrocytes impaired cognitive function. Altogether these studies suggest that Nrf2 exerts different effects after ischaemia depending on the severity of stroke and the time point analysed. Further experiments are required to understand these mechanisms.

Acknowledgements

Non est arbor solida nec fortis nisi quam frequens ventus incursant. Lucius Annaeus Seneca.
No tree becomes rooted and sturdy unless many a wind assails it, Seneca the younger.
L'arbre ne devient solide et fort qu'en subissant les assauts répétés du vent. Sénèque le Jeune.

First, to Jill Fowler that saw potential in me, that gave me a brilliant project, I am very grateful. I appreciate the patience and determination. Thank you ever so much.

I would like to thank Karen Horsburgh for the scientific excellence that guided me throughout this journey. I thank Jeffrey Johnson, Giles Hardingham, Anjie Harris and Ferenc Anthony for their help, very precious for this work. Special thanks to Tara Spires-Jones, Dies Meijer and Joyce Yau for the support and the kindness. I would like to thank Alzheimer's Research UK for funding my scholarship for this PhD.

Very special thanks to Katharina Nagassima and Lizi Hegarty who participated in this work, they have been amazing colleagues and amazing persons. For, Jemma, thanks for everything, for singing in French in the kitchen, for singing Katatonia late at night in the lab, for the smile, the creativity, the fire!!!! I love you, you're amazing, keep going!

George, pour me suivre dans mes conneries, pour les bières et les cours de grec, d'histoire, de bio et d'étymologie. Alex pour m'avoir toujours aidée, écoutée, comprise. Ça me manque de me faire appeler "Paupiette". Florian, pour m'avoir appris à prendre de la distance et à reconnaître ce qui est important.

The Horsburgh team for great support and help whenever I needed it: Emma, Jess, Juraj, Edel, Mosi, Stefan, Josh, Gaia, Sanny, Martina, Alessio, Akihiro. So many great people around: Chiara, YK, Dimitra, Ana, Jazz, Rand, Liv, Nat, Max, Megan, Annelise, Jamie, Makis, Vlad, Sofia, Hannah, Themis, Greg, Kathy, Cathy, Sarah, Hannah, Julie, Melissa, David & Gavin… I'd like to thank the LF1 and LF2 technicians always keen on helping, teaching, especially Duncan, Larraine, John and Will.

J'aimerai remercier mes amis de l'autre côté de la Manche, pour le soutien, les visites, les rires et les surprises : Hugo, Jen & Cyril, Marie, Léna & Quent2, Jéro & Séb, Aly, Mareva, Héloïse, Elisa, Antoine, Auriane, Pauline et Lisa. "Parce qu'on est des bonhommes" : PJ & PR, Lydie & Adrien, Yon & Julie (Nadine). Merci à la famille Divay pour m'avoir toujours soutenue et pour avoir pensé à moi, malgré les visites rares mais appréciées.

Edinburgh is amazing but better because of the people there: Chris, for taking care of myself better than I did (I'm better now though ;)), for the support anytime of the day... you're amazing. Jake, for the support, for the impeccable taste and the exploration of this amazing city. Emily, Ben, Chiara and Annika for the morning or night philosophical and psychological discussion that always got me going. Amaya for the laughs, trust and support from the very beginning.

Ante penultimate: Sushi. Merci de m'avoir aidé, d'avoir partagé mes rires et mes larmes, d'avoir cru en moi.

Penultimate: Merci à mon Papa pour avoir été là. Merci à Stéphane pour avoir toujours su me faire marrer. Merci à Didie de toujours m'avoir écouté et pris soin de moi. Enfin, Merci Maman pour m'avoir attendu, pour avoir pensé à moi.

Last but not least: Bon Clovis, bière ? Vas-y viens on va griller des trucs, ou les frire ! Et on mangera de la pâte à cookie cru en regardant des séries. Merci d'avoir toujours su trouver les mots, merci pour ton soutien sans faille, plus que précieux à mes yeux.

List of Figures

Figure 1-1 Diagram representing ischaemic versus haemorrhagic stroke in the human brain. 26
Figure 1-2 Vascular cognitive impairment is a nomenclature for diverse cerebro-vascular pathologies (from Iadecola, 2013). 31
Figure 1-3 Simplified diagram of the interrelated pathophysiological mechanisms of cerebral ischaemia. 33
Figure 1-4 Cascade of damaging events after cerebral ischaemia (from Dirnagl et al., 1999). 34
Figure 1-5 The penumbra can be seen with the mismatch or perfusion and diffusion weighted MRI images (From Moskowitz et al., 2010). 34
Figure 1-6 The neurogliovascular unit and blood-brain barrier. 41
Figure 1-7 Conditions for Nrf2-signalling activation. 55
Figure 1-8 Indirect glutathione production from astrocyte increases neuronal glutathione levels (GSH). 58
Figure 2-1 Nine coronal brain levels were used to map the infarct area. 78
Figure 2-2 Three coronal level were selected to perform the immunohistology studies. 79
Figure 2-3 Depending on the lesion size, the pictures for peri-infarct and core were selected in the cortex and striatum in the same area. 81
Figure 2-4 Schematic of the mouse brain dissection for biochemistry cohorts. 82
Figure 2-5 Schematic of the modified rat Y-maze for mouse novel object recognition. 86
Figure 2-6 Objects used for the NOR. 86
Figure 3-1 Neuronal damage was detected with Haematoxylin & Eosin staining, 24 hours after ischaemia. 96
Figure 3-2 Increased duration of ischaemia increases neuronal damage in cortex and striatum, 24 hours after ischaemia. 97
Figure 3-3 Increased duration of ischaemia increases oxidative stress in cortex and striatum, 24 hours after ischaemia. 99
← **Figure 3-4** Increased duration of ischaemia modifies reactive astrocytes assessed with GFAP in the cortex and the striatum, 24 hours after ischaemia. 102
Figure 3-5 Increased gene expression for gfap in the cortex and striatum, 24 hours after ischaemia. 102
← **Figure 3-6** Increased duration of ischaemia modifies microglia/macrophage marker Iba1 in the cortex and the striatum, 24 hours after ischaemia. 105
Figure 3-7 Increased duration of ischaemia increases Iba1-positive cells in the cortex and the striatum but not Iba1 gene aif1 expression, 24 hours after ischaemia. 107
Figure 3-8 Inflammatory gene cxcl10 was upregulated in the striatum 24 hours after 15 minutes of ischaemia. 109
Figure 3-9 Ischaemia increases neutrophil infiltration, 24 hours after ischaemia. 110
Figure 3-10 Representative images of TMEM119 and Iba1 co-immunostaining in the cortex, 24 hours after ischaemia. 112
Figure 3-11 Representative images of TMEM119 and Iba1 co-immunostaining in the striatum, 24 hours after ischaemia. 113
Figure 3-12 Ischaemia increases microglia/macrophage cells in the cortex and striatum, 24 hours after ischaemia. 114
Figure 3-13 Increased duration of ischaemia increases heme oxygenase-1 in the cortex and the striatum, 24 hours after ischaemia. 116
Figure 3-14 Nrf2 gene and its related genes were upregulated 24 hours after ischaemia. 119

F**igure 3-15** Ischaemia increases neuronal damage in the striatum but not the cortex 4 weeks after 15 minutes ischaemia. 121
F**igure 3-16** Modest duration ischaemia increases oxidative stress in the striatum but not the cortex 4 weeks after 15 minutes ischaemia. 123
F**igure 3-17** Astrocytic marker GFAP was increased in striatum and cortex 4 weeks after 15 minutes ischaemia. 125
← **Figure 3-18** Modest duration ischaemia (15 minutes) increases microglia/macrophage marker Iba1 4 weeks post injury. 128
F**igure 3-19** Inflammatory gene cxcl10 and il-1β were upregulated 4 weeks after 15 minutes of ischaemia. 129
F**igure 3-20** Modest duration ischaemia increases neutrophil infiltration 4 weeks after 15 minutes ischaemia. 130
← **Figure 3-21** Ischaemia increases microglia/macrophage cells with reduced TMEM119 expression 4 weeks after 15 minutes ischaemia. 132
F**igure 3-22** Modest duration ischaemia (15 minutes) does not modify heme oxygenase-1 four weeks post injury. 133
F**igure 3-23** Nrf2 related genes were no longer upregulated 4 weeks after 15 minutes ischaemia. 135
F**igure 3-24** Incomplete circle of Willis in C57Bl/6J (from McColl et al., 2004). 137
F**igure 3-25** Magnetic resonance imaging used determine striatal cerebral blood flow. 139
F**igure 4-1** Mice overexpressing Nrf2 in astrocytes (GFAP-Nrf2 mice) have over two-fold increase of Nrf2 gene nfe2l2 mRNA expression compared to wild-type (WT). 160
F**igure 4-2** Nrf2 overexpression in astrocytes reduced neuronal damage 24 hours after 60 minutes ischaemia. 162
F**igure 4-3** Nrf2 overexpression in astrocytes reduced oxidative stress 24 hours after 60 minutes ischaemia. 164
F**igure 4-4** Nrf2 overexpression in astrocytes reduced oxidative stress spread out beyond the lesion 24 hours after 60 minutes ischaemia. 166
F**igure 4-5** Nrf2 overexpression in astrocyte increased HO1 expression, 24 hours after 60 minutes ischaemia. 168
F**igure 4-6** Nrf2 overexpression in astrocyte increased Nrf2-related genes 24 hours after 60 minutes ischaemia in the cortex peri-infarct. 170
F**igure 4-7** GFAP immunostaining was increased at 24 hours after 60 minutes ischaemia in both cortex and striatum and GFAP-Nrf2 sham animals had increased GFAP immunostaining in the cortex. 172
F**igure 4-8** Nrf2 overexpression in astrocytes did not alter levels of the microglia/macrophage marker Iba1, 24 hours after 60 minutes ischaemia. 174
← **Figure 4-9** Nrf2 overexpression in astrocyte increases cxcl10 and IL-4rα genes 24 hours after 60 minutes ischaemia in the peri-infract of the cortex. 178
F**igure 5-1** After modest duration (15 minutes) ischaemia, animals present neurological deficits and recovered quickly. 197
F**igure 5-2** Novel object recognition on wild-types mice. 198
F**igure 5-3** Cognitive deficit was observed 4 weeks after 15 minutes ischaemia compared to sham controls. 199
F**igure 5-4** Discrimination of the novel object compared to the familiar was performed twice on naïve animals of both genotype with three weeks apart. 200
F**igure 5-5** Nrf2 overexpression in astrocytes did not modify neuronal damage 4 weeks after modest duration of ischaemia (15 minutes). 201
F**igure 5-6** Nrf2 overexpression in astrocytes does not modify oxidative stress marker 3NT 4 weeks after 15 minutes ischaemia. 203

F**igure 5-7** Nrf2 overexpression in astrocyte increases Nrf2-related genes in the striatum 4 weeks after 15 minutes ischaemia. 204
F**igure 5-8** Astrocytic Nrf2-overexpression does not modify astrocyte reactivity after 15 minutes ischaemia 4 weeks post-injury. 205
F**igure 5-9** Nrf2 overexpression in astrocytes modifies microglia/macrophage levels 4 weeks after modest duration ischaemia (15 minutes). 207
F**igure 5-10** Nrf2 overexpression in astrocyte decreases complement 3 (c3) gene but not cxcl10, il-1β or il-4rα in the striatum 4 weeks after 15 minutes ischaemia. 209
F**igure 8-1** GFAP immunostaining quantified with %area was increased in the peri-infarct 4 weeks following ischaemia. 282
F**igure 8-2** Iba1 immunostaining quantified with %area was increased in the peri-infarct 4 weeks following ischaemia. 282
F**igure 8-3** GFAP %area in the cortex peri-infarct is correlated with the lesion volume at 4 weeks but not the core. 283
F**igure 8-4** Iba1 %area in the cortex is correlated with the lesion volume at 4 weeks 283

List of Tables

Table 1-1 Reactive oxygen and nitrogen species with their formula and structure. 43
T**able 1-2** Infarct volume of Nrf2 knockout mice compared to wild-types following ischaemia. 62
T**able 1-3** Summary of the modulation of Nrf2, Keap1 and Nrf2-related protein following ischaemia. 69
T**able 2-1** Antibodies used for immunohistochemistry study. 80
T**able 2-2** Antibodies used for free-floating immunofluorescence. 81
T**able 2-3** Forward end reverse strand of the primers used for the qPCR..... 84
T**able 2-4** Neuroscore test with score ranging from 0 indicating no deficit to 36 indicating maximal impairment. 85
T**able 3-1** Summary of the group size of each group for the histologic and the biochemistry cohorts. 92
T**able 4-1** Summary of the group size of each group for histologic and biochemistry cohorts. 157
T**able 5-1** Summary of the group size of each group after exclusion for histologic and biochemistry cohorts. 194
T**able 6-1** Main results from chapter 4 and chapter 5 following ischaemia for wild-type and GFAP-Nrf2 animals. 226
T**able 6-2** Main discrepancies between chapter 4 and chapter 5 following ischaemia comparing GFAP-Nrf2 to wild-type animals. 227

List of Abbreviations

3NT: 3-Nitrotyrosine

4-HNE: 4-Hydroxynonenal

8-OHDG: 8-Hydroxydeoxyguanosine

A1/A2: Reactive astrocyte phenotype neurotoxic or neuroprotective

AD: Alzheimer's disease

AIF1: Allograft inflammatory factor 1

ALDH1L1: Aldehyde dehydrogenase 1 family member l1

ALS: Amyotrophic lateral sclerosis

ARE: Antioxidant response elements

ATP: Adenosine triphosphate

BBB: Blood-brain barrier

C3: Complement component 3

CBF: Cerebral blood flow

CCL2: Chemokine ligand 2

CD: Cluster of differentiation

CNC: Cap'n'collar

DAB: 3,3'-Diaminobenzidine

DAM: disease-associated microglia

DAMPs: damage-associated molecular patterns

DAPI: 4',6-diamidino-2-phenylindole

DMF: Dimethyl fumarate

DNA: Deoxyribonucleic acid

Gclc: Glutamate—cysteine ligase catalytic subunit

Gclm: Glutamate-Cysteine Ligase Modifier Subunit

GFAP: Glial fibrillary acidic protein (gene: *gfap*)

GSH: Glutathione (reduced form)

H&E: Haematoxylin & eosin

HO1: Heme oxygenase-1 (gene *hmox1*)

Iba1: Ionised calcium binding adaptor molecule 1 (gene *aif1*)

IFNγ: Interferon gamma

IGF-1: Insulin-like growth factor-1

IgG: Immunoglobulin G

IL: interleukin

Keap1: Kelch-like erythroid cell-derived protein with CNC homology-associated protein 1 (gene *keap1*)

KO: Knock-out

LPS: Lipopolysaccharide

M1/M2: Reactive microglial phenotypes (M1 is pro-inflammtory or classically activated, M2 is anti-inflammatory alternatively activated)

MAP2: Microtubule-associated protein 2

MCA: Middle cerebral artery

MCAo: Middle cerebral artery occlusion

MDA: malondialdehyde

MRI: Magnetic resonance imaging

mRNA: messenger ribonucleic acid

NAD(P)H: Nicotinamide adenine dinucleotide phosphate (reduced form)

NO: Nitric oxide

NOR: novel object recognition

NQO1: NAD(P)H dehydrogenase quinone 1 (gene *nqo1*),

Nrf2: Nuclear factor (erythroid derived 2)-related factor 2 (gene *nfe2l2*)

NGVU: Neurogliovascular unit

OGD: Oxygen and glucose deprivation

PCR: Polymerase chain reaction

qRT-PCR: quantitative reverse transcriptase polymerase chain reaction

ROS: Reactive oxygen species

RNA: Ribonucleic acid

RNS: Reactive nitrogen species

rtPA: Recombinant tissue-type plasminogen activator

siRNA: small interfering RNA

shRNA: short hairpin RNA

SOD: superoxide dismutase

SRXN1: sulfiredoxin 1 (gene *srxn1*)

STAT3: Signal transducer and activator of transcription 3

TGFβ1: Transforming growth factor-beta 1

TMEM: Transmembrane protein

TNFα: Tumour necrosis factor alpha

UCCAo: Unilateral common carotid artery occlusion

VaD: Vascular dementia

VCI: Vascular cognitive impairment

WHO: World Health Organisation

WT: Wild-type

xCT: Glutamate-cystine antiporter (also known as Xc-; gene *slc7a11*)

1. Introduction

1.1. General clinical knowledge on ischaemic stroke

1.1.1. Definition

1.1.1.1. Acute Symptoms

Stroke is characterised by the World Health Organisation as sudden weakness or numbness of the face, arm or leg, most often on one side of the body. Other symptoms include confusion, difficulty speaking or understanding speech; difficulty seeing with one or both eyes; difficulty walking, dizziness, loss of balance or coordination; severe headache with no known cause; fainting or unconsciousness (reference from WHO; Siegler et al., 2013). Clinically, stroke is defined as a sudden onset of focal neurological symptoms or signs that should last more than 24 hours, that must be caused by disturbances in cerebral blood flow and not explained by other disease processes (Abbott et al., 2017). A mnemonic campaign was launched to help recognize signs of a stroke called "FAST" which is defined by **F**acial drooping, **A**rm weakness, **S**peech difficulties and **T**ime to call emergency services (Harbison et al., 2003). A revised mnemonic was recently proposed with the addition of **B**alance and **E**yes termed "BE-FAST" (Aroor et al., 2017).

1.1.1.2. Epidemiology

Every year, around 14 million people worldwide suffer from a stroke (Johnson et al., 2019). Stroke is the leading cause of disability for adults and the second leading cause of death worldwide. Over 55 years of age, the risk doubles every 10 years (Rojas et al., 2007). In the United Kingdom, there are more than 100 000 strokes each year, and there are currently over 1.2 million stroke survivors; it is the third leading cause of death in Scotland (Association, 2018). It has a significant health cost to the United Kingdom economy, estimated to be around £26 billion in 2018 including productivity loss, treatment and care (Patel et al., 2017).

1.1.1.3. Ischaemia or Haemorrhage

In 87% of cases, stroke is caused by a blockage of a vessel by a thrombus or embolus; this event is termed ischaemia (Mozaffarian et al., 2016; Neuhaus et al., 2017). The remaining 13% of strokes are haemorrhagic, caused by a burst vessel (Fig. 1.1). In both cases, the symptoms are similar, and a differential diagnosis must be undertaken using magnetic resonance imaging (MRI) techniques.

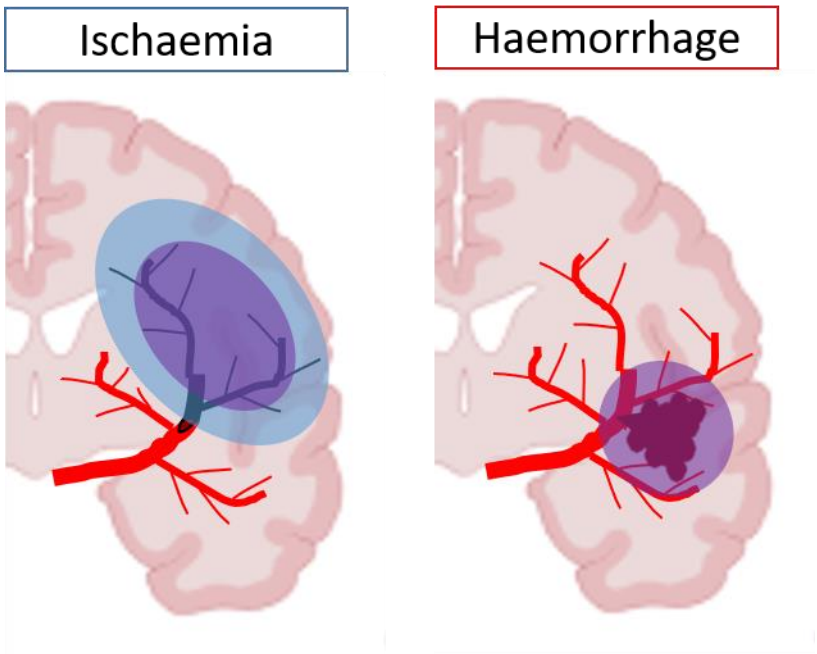

Figure 1-1 Diagram representing ischaemic versus haemorrhagic stroke in the human brain.

Cerebral ischaemia is characterised by a blockage of a cerebral vessel. It leads to hypoperfusion of the following vessels (in black) and thus hypoxia (in blue) and dysfunction leading to cell death (area in purple). Cerebral haemorrhage is a burst of a cerebral vessel which leak blood in the parenchyma and is very toxic for the brain cells causing their death (area in purple).

The word ischaemia comes from the ancient greek *ἴσχω* (pronounced *iskho*) that means "holding back" and *αἷμα* (pronounced *haima*) that means "blood". The vessel is blocked by coagulated blood (a blood clot is also named thrombus). Ischaemia can be permanent or temporary. During ischaemia, oxygen and nutrient supplies are interrupted; resulting in a cascade of events that are detrimental such as excitotoxicity, depolarisation, oxidative stress, inflammation, blood-brain barrier leakage and apoptosis (Dirnagl et al., 1999; Puig et al., 2018).

1.1.1.4. Acute Treatment of Ischaemic Stroke: Reperfusion

The only drug approved and used for ischaemia since 1996 is called Alteplase; its active substance is the recombinant tissue-type plasminogen activator (rtPA; FDA Application No.: 103172-Suppl. 1055). It is a serine protease; it cleaves plasminogen into its activated form plasmin, which is known for its clot lysis effect. Consequently, it breaks the thrombus and liquefies the blood. However, the use of this method is beneficial only during the acute period. When first approved, rtPA treatment improved the outcome by 11% if used in the first 3 hours after the onset (National Institute of Neurological Disorders and Stroke rt-PA Stroke Study Group, 1995). Since then, the therapeutic window has been extended to 4 hours and 30 minutes (Hacke et al., 2004). Thrombolysis on patients with unknown time of onset has shown beneficial outcomes, when used on a selection of patient (Thomalla et al., 2018).

In the last years, another technique called mechanical thrombectomy to remove the clot was developed using stent retrievers. The first clinical trials showed improved survival and functional recovery, but only a few neurosurgeons are trained, and a few centres are equipped for this procedure. This new technique can potentially expand the time window treatment (Baek et al., 2014; Jovin et al., 2015; Mokin et al., 2018) to 16 or 24 hours after the onset for all patient (Albers et al., 2018; Nogueira et al., 2017).

1.1.2. Risk factors

1.1.2.1. Age and Gender

As discussed previously, age is an important factor in ischaemic stroke occurrence, for 95% of strokes occurred at the age of 45 and older (Grau et al., 2001). Furthermore, the risk of having a stroke doubles every 10 years past 55-years old (Rojas et al., 2007).

Before 70 years old, the risk is higher for men than women. However the prevalence for stroke is more elevated for women after 80 years-old compared to men (Andersen et al., 2010). Two thirds of stroke patients older than 80 years are women; but this result is biased as life expectancy for women is greater than men. The reduced incidence of stroke in young women is thought to be due to the neuroprotective effect of oestrogen (Honarpisheh &

McCullough, 2019; Zhang et al., 2018) or immune system differences (Freitas-Andrade et al., 2017; Seifert et al., 2017).

1.1.2.2. Comorbidities and risk factors

As the probability of having a stroke gets greater with age, it also increases the possibility of comorbidities. These comorbidities significantly increase the risk of having a stroke and they worsen the stroke outcome. These are diabetes, cancer, hypertension, obesity, coronary and cardiac diseases (Allen & Bayraktutan, 2008; Gallacher et al., 2018; Moskowitz et al., 2010; Rojas et al., 2007).

Arrhythmia, and notably atrial fibrillation, is a dysregulation of the normal pumping blood function of the heart. It leads to stagnation of blood in the heart. It eventually causes blood to coagulate forming a blood clot and can be injected in the rest of the vascular system. The clot gets bigger with platelet aggregation due to immune detection. It is more likely to block vessels that are narrowed; this phenomenon is called stenosis and can happen with aggregation of cholesterol (atherosclerosis). With age, blood vessels are weakened and harden (arteriosclerosis), this leads to hypertension and increases the risk of cerebral ischaemia (Oladiran & Nwosu, 2019; Wolf et al., 1998).

Atherosclerosis happens more frequently in cases of obesity, hyperlipidaemia, hypercholesterolemia or diabetes. Diabetes is characterised by hyperglycaemia caused by insulin resistance. Diabetes potentially leads to hypertension, hypercholesterolemia and atrial fibrillation. Thus it increases the risk of developing atherosclerosis and ischaemic stroke (Béjot & Giroud, 2010; Luitse et al., 2012). Hypertension, notably with blood pressure at higher than 140/90, increases vascular diseases and notably is found in 66 to 69% of ischaemic patient (Grau et al., 2001; Lewington et al., 2002; McManus & Liebeskind, 2016).

1.1.2.3. Other risk factors

Studies of stroke prevalence amongst diverse ethnic groups revealed greater risks for black and Hispanic people than white, possibly due to higher risk of hypertension and diabetes

(Centers for Disease Control and Prevention (CDC), 2001; Kissela et al., 2005; Ohira et al., 2006; White et al., 2005). These groups showed greater insulin resistance, obesity rates and possibly some genetic differences in the fat distribution, lipolysis and metabolic rate compared to other ethnic groups (Akinyemi et al., 2019; Caprio et al., 2008; Saab et al., 2015; Spanakis & Golden, 2013). To note that modifiable risk factors such as smoking and low physical activity are also thought to be generally reduced in those populations, increasing obesity (Akinyemi et al., 2019; Caprio et al., 2008; Spanakis & Golden, 2013).

Smoking is an important risk factor for stroke, with a dose dependent effect with more cigarettes smoked per day causing an increased relative risk of stroke (Boehme et al., 2017; Hankey, 1999; Thun et al., 2000; Wolf et al., 1988).

1.1.3. Long term effects of ischaemia

Ischaemia may lead to disability or death within hours. However, advances in the treatment and prevention of stroke have produced a decline in mortality (Hankey, 2017; Khandelwal et al., 2016), and one consequence is an increased number of stroke survivors (Macrae & Allan, 2018; Muruet et al., 2018; Pendlebury & Rothwell, 2009); there are currently 1.2 million stroke survivors in the UK (Association, 2018). As previously explained, these patients are for the most part elderly; and aging impairs recovery (Knoflach et al., 2012; Macciocchi et al., 1998). After recovery, less than half of the patients regain independence (Hankey, 2017). Ischaemic patients may present cognitive decline faster than healthy age-matched people (Levine et al., 2015). Around 80% of them will present mild cognitive impairments (Barbay et al., 2018). Cognitive impairment may appear immediately or within month or years (Pendlebury & Rothwell, 2009, 2019; Zamboni et al., 2017).

Dementia and cognitive impairment are now recognised to be associated with vascular causes (Iadecola, 2013). Ischaemia can contribute mechanistically to dementia including vascular cognitive impairment (VCI). VCI is an umbrella term that encompasses any form of cognitive deficit associated with and presumed to be caused by cerebrovascular disease (O'Brien et al., 2003). As first termed by O'Brien and colleagues (2003), VCI encompasses many types of dementia such as multiple-infarct dementia, post-stroke dementia, small vessel disease, hereditary vascular dementia CADASIL, Alzheimer's disease with vascular dementia, and more (O'Brien et al., 2003) as seen in Fig 1.2 (Iadecola, 2013). At a National

Institute for Neurological Disorders and Stroke (NINDS) workshop, Hachinski et al (2006) identified standards for identifying and describing individuals with VCI, notably by recommending the development of MRI techniques, psychological assessments and physio-pathological evidence (Hachinski et al., 2006). Gorelick et al (2011) reviewed the literature on VCI and published a statement on vascular contributions to cognitive impairment and dementia for healthcare professionals. This statement highlighted the importance of vascular contributions to dementia and the importance of detection and control of traditional risk factors for stroke and cardiovascular disease for the prevention of VCI (Gorelick et al., 2011).

VCI commonly features a decline in cognitive functions and cerebrovascular lesion are demonstrated with MRI (Gorelick et al., 2016; Rodríguez García & Rodríguez García, 2015). The cerebrovascular lesion can comprise strategic infarct (one small to medium infarct), multi infarct encephalopathy (several large vessel infarcts), lacunar infarcts (ischaemia of small artery), hypoxic-ischaemic encephalopathy (with hypotension or cardiac arrest), cerebral haemorrhage, mixed cerebrovascular disease (which is a combination of the above) and Alzheimer's disease with vascular dementia (Rodríguez García & Rodríguez García, 2015). The presence of microinfarcts and notably in the white matter (named white matter hyperintensities) is highly associated with VCI (Ferro et al., 2019) and the burden of white matter hyperintensities is correlated with the extent of cognitive deficits. VCI symptoms are heterogeneous depending on the cerebrovascular pathology, and can include amnesia, aphasia (neurological impairment of language), agnosia (neurological impairment of visuospatial processing), and executive function (such as planning and making decision) impairment to name just a few (Gorelick et al., 2011; Rodríguez García & Rodríguez García, 2015; Skrobot et al., 2018).

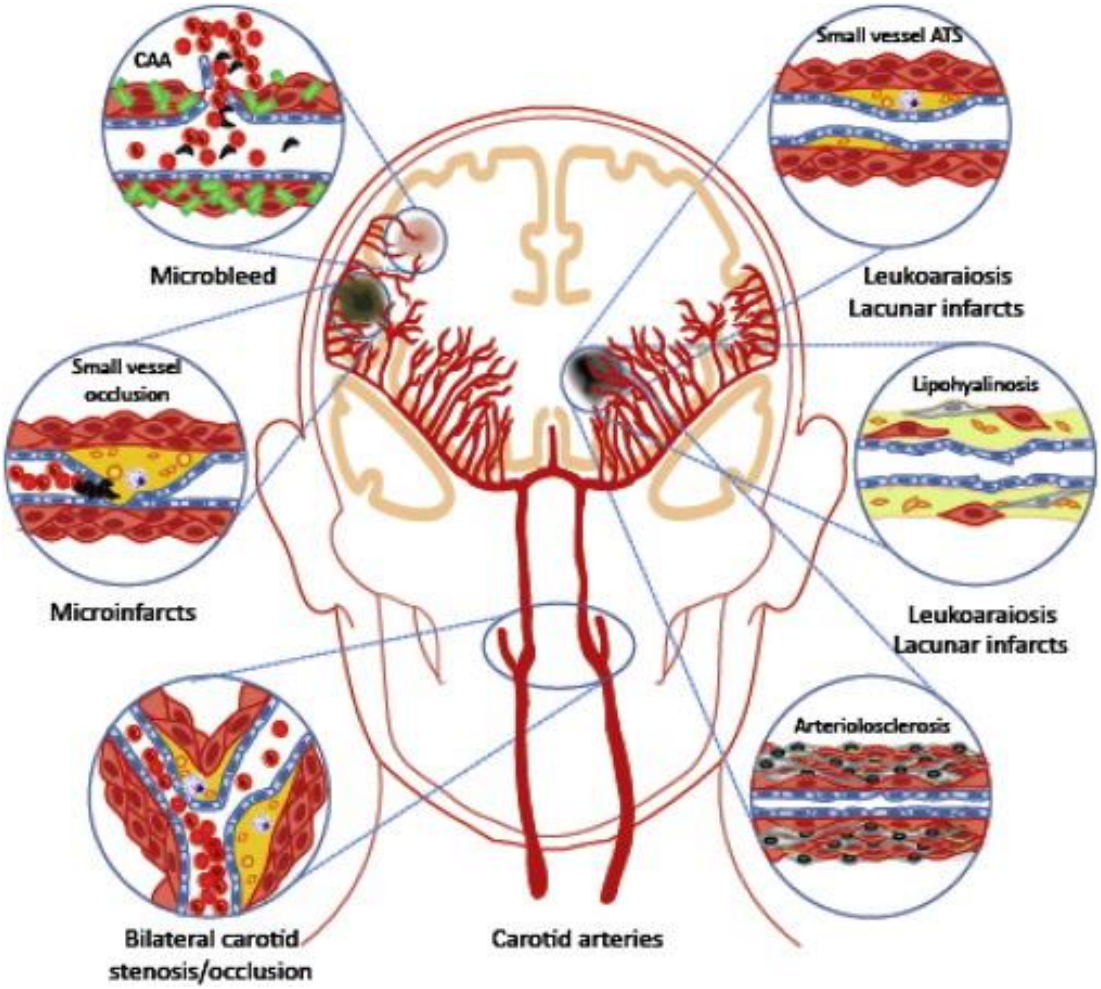

Figure 1-2 Vascular cognitive impairment is a nomenclature for diverse cerebro-vascular pathologies (from Iadecola, 2013).

Alzheimer's disease (AD) is a neurodegenerative disease, which causes memory loss, confusion and mood deterioration. Stroke more than doubles the risk of AD in the elderly (Vermeer et al., 2003). Stroke pathology is present in one third of AD cases at post mortem autopsy (Kalaria, 2000). Stroke was found to enhance amyloid precursor protein and its cleavage into Amyloid β (Nihashi et al., 2001; Saido et al., 1994). Amongst the cascade of detrimental events triggered by ischaemia, oxidative stress and inflammation are accused of leading to Alzheimer's disease (Daulatzai, 2016; Gorelick et al., 2011; Pluta et al., 2009; Rojas-Gutierrez et al., 2017). In recent years, the blood-brain barrier and alterations in the integrity of astrocytes have been linked to cognitive decline in AD (Avila-Muñoz & Arias, 2014; Chen et al., 2016; Hase et al., 2017).

1.2. Cellular biology and pathophysiology of cerebral ischaemia

1.2.1. Hypoperfusion and penumbra

Cerebral ischaemia is a reduction in the blood supply to the brain. Any reduction in the blood supply is called hypoperfusion and it leads to oxygen and nutrient deprivation in cells. The brain accounts for only 2% of the body mass, however, it uptakes 20% of glucose and energy (Erbsloh et al., 1958; Klocke et al., 1969; Magistretti & Allaman, 2015; Mink et al., 1981). It is the most sensitive organ to glucose and oxygen deprivation due to its high metabolic rate.

With ischaemia, oxygen and nutrient supplies are suboptimal and can be completely interrupted in some areas. It causes brain cell malfunctioning and triggers a cascade of pathogenic mechanisms that are detrimental such as excitotoxicity, depolarisation, oxidative stress, inflammation, blood-brain barrier leakage and apoptosis (Fig 1.3; Dirnagl et al., 1999; Moskowitz et al., 2010), all of which will be reviewed in this section. These pathophysiologic events appear at different timepoints after the onset of ischaemia and are proposed to have different durations (Fig 1.4).

During the acute phase of ischaemia, the lesion is divided into two parts: penumbra and core. The lesion's core represents irreversible damage to cells as they die from hypoxia. Whereas the penumbra represents a suboptimal irrigated area leading to decrease energy production disrupting ion pump (Astrup et al., 1981). The perfusion rate of the penumbra is below 20 ml/min/100 g and the core below 10 ml/min/100 g whilst normal perfusion is about 55 ml/min/100 g (Hossmann, 1994).

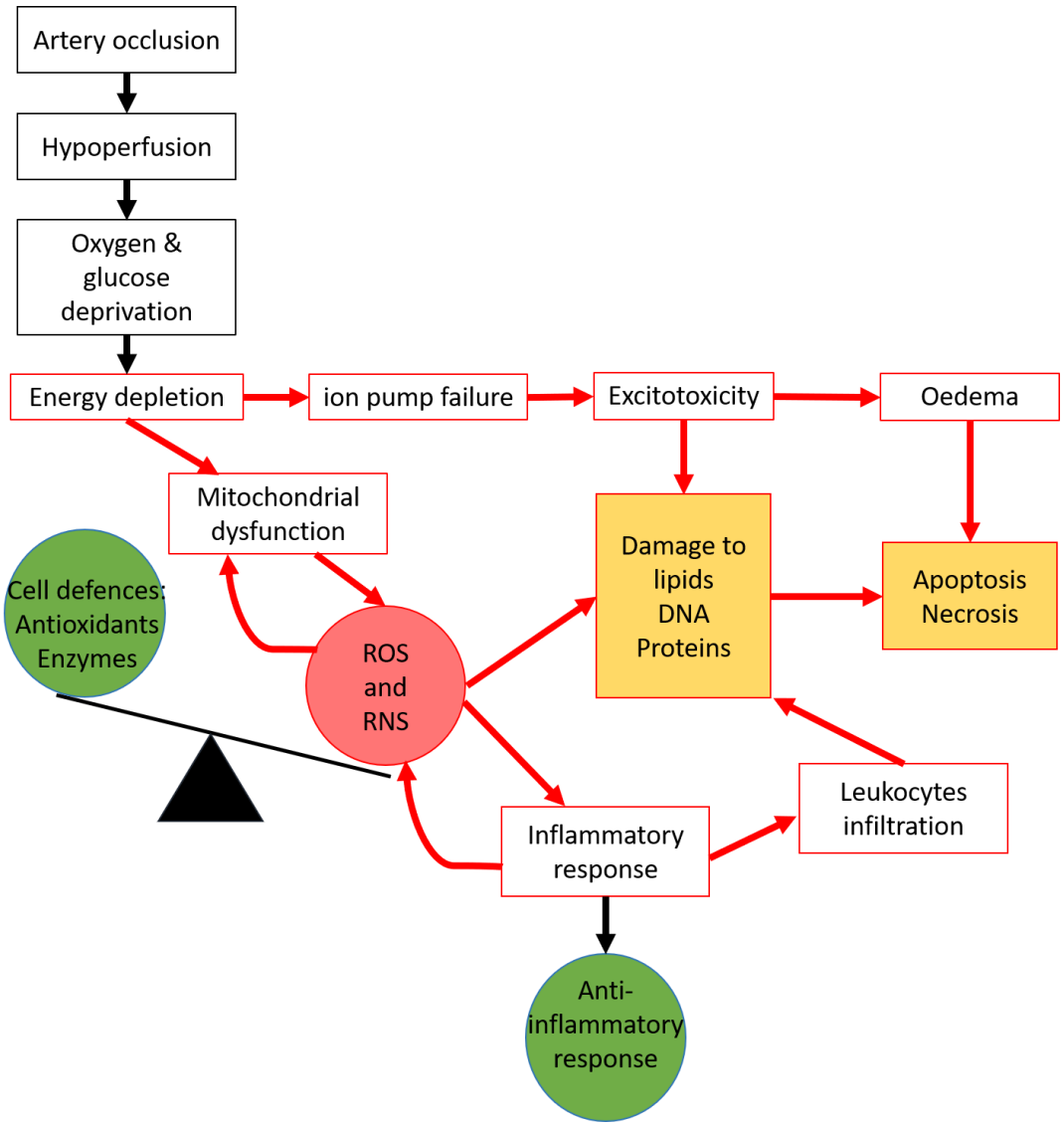

Figure 1-3 Simplified diagram of the interrelated pathophysiological mechanisms of cerebral ischaemia.

The artery occlusion reduces blood supply to the brain and lead to energy deprivation in the cell. Many functions of the cell rely on this constant supply on energy to maintain the cell homeostasis, notably mitochondria and ion pumps. These dysfunctions are at the beginning of a number of detrimental cascades. Ion pumps failure initiate calcium accumulation promote cytotoxic oedema and lead to excitotoxic cell death. Mitochondrial dysfunction increases reactive oxygen species (ROS) and reactive nitrogen species (RNS) while antioxidant enzymes are reduced resulting in imbalance named oxidative stress that damage cell compounds (lipids, DNA, proteins). Oxidative stress initiate cytokines productions that activate immune cells with notably astrocytes and microglia. These cells have different response signatures, some are neuroprotective, but others are aggressive and cytotoxic. This inflammatory state promotes peripheral immune cell infiltration such as macrophages and leukocytes. Leukocytes are known for their production of matrix metalloproteinases (MMPs) that are highly toxic to neurons and endothelial cells.

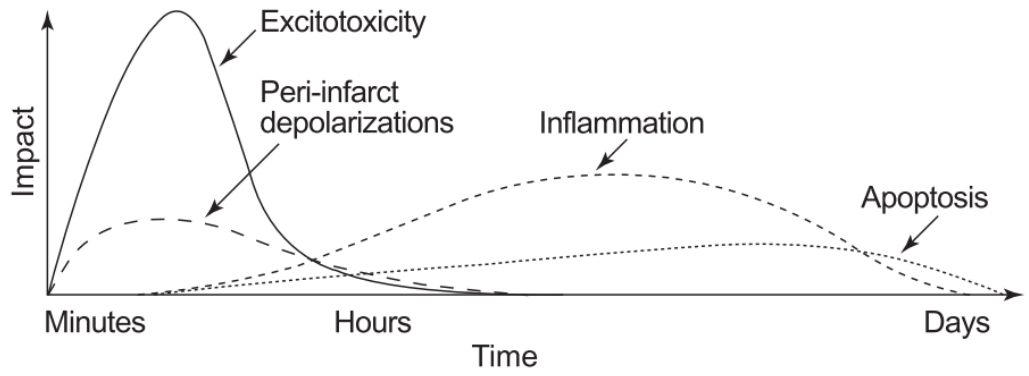

Figure 1-4 Cascade of damaging events after cerebral ischaemia (from Dirnagl et al., 1999).

The penumbra can be imaged with MRI using perfusion weighted and diffusion weighted images (Moskowitz et al., 2010). Diffusion weighted images shows the ischaemic necrosis, identifying the core of the lesion. Perfusion weighted image shows the blood flow reduction hence the entire area at risk. The mismatch of the perfusion weighted image with the diffusion weighted image inform on the penumbra (Fig 1.5).

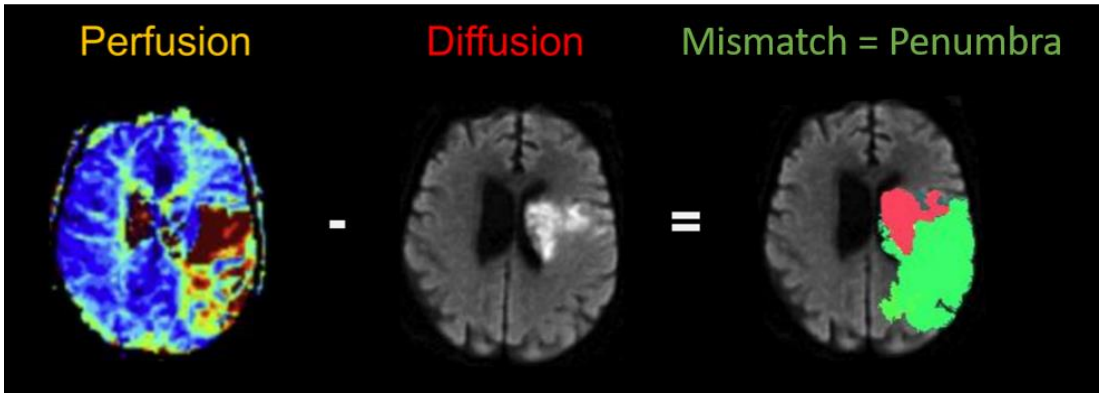

Figure 1-5 The penumbra can be seen with the mismatch or perfusion and diffusion weighted MRI images (From Moskowitz et al., 2010).

The longer the duration of hypoperfusion, the larger the infarct (Memezawa et al., 1992). Without reperfusion, cells in the penumbra die leading to expansion of core the lesion. However, restoration of blood flow in the penumbra is beneficial to a certain extent; the infarct volume plateaus between 18 and 24 hours in rodents and cats (Hartings et al., 2003; Heiss, 2000; Mulcahy et al., 2003) and thus the penumbra cannot be rescued anymore

(Baron, 2018; Hossmann, 2012; Robertson et al., 2015). Reperfusion is beneficial as long as the penumbra is still detectable, during the first hours after the onset for humans and mouse models (Hossmann, 2012; McCabe et al., 2018; Morris et al., 2018; Paciaroni et al., 2009). However, recent advances in the field showed beneficial effects of reperfusion at 16 to 24 hours after the onset (Albers et al., 2018; Nogueira et al., 2017; Wardlaw & Bath, 2019).

1.2.2. Ischaemic models

1.2.2.1. In vitro models of ischaemia

Most commonly undertaken using cell culture of primary neurons from rodents or cell lines, *in vitro* models reduce the use of animals, reduce costs and time, and are mostly used to understand mechanisms underlying the response to treatment or drugs and to evaluate their toxicity or protective effects. Depending on the protocol used, some *in vitro* techniques were developed to explore the responses of single-cells rather than mixed cell culture and it facilitates the use of transfection to knock-in and knock-out (KO) genes and silencing of RNA (Engelhardt et al., 2015; Liddelow & Barres, 2017; Lipton, 1999; Mcdonough et al., 2017; Pekny & Nilsson, 2005; Shih et al., 2005a).

Regarding ischaemia/reperfusion research, oxygen and glucose deprivation (OGD) models have been used to mimic hypoxic conditions and nutrient deprivation by modifying the culture oxygenation and medium (Bell et al., 2011a; Ryou & Mallet, 2018; Shih et al., 2005a). Common endpoints include the measure of cell death or cell viability, mRNA and protein levels. Ischaemia triggers a cascade of events that can lead to neurotoxicity, such as inflammation and oxidative stress. To mimic these events, there are *in vitro* models of inflammation induced by lipopolysaccharide (LPS; Catorce & Gevorkian, 2016; Hoogland et al., 2015) and free radicals for oxidative stress injury such as hydrogen peroxide (H_2O_2; Gille & Joenje, 1992; Reddy et al., 2007).

An important criticism of these models is the discrepancies between cultured cells and *in vivo* cells. Cultured astrocytes tend to have a reactive phenotype with increased antioxidant glutathione production (Shih et al., 2003) and cultured neurons present important variations of glutathione levels throughout the literature, most likely due to the preparation protocol used (Dringen et al., 1999). Discrepancies between *in vivo* and *in vitro* models are caused by

maturation differences (Desestret et al., 2013; Hellwig et al., 2013). Development of organotypic brain slice culture emerged to address this problem (Humpel, 2015; Khalilov et al., 1997). Primary culture cells are not developed in terms of structural aspects of the brain such as white matter and vascular supply. Stroke research needs a systemic approach with a vascular system and a multi-organ context. Recently, an *in vitro* model reproducing the multi-cell aspect of the brain was developed (Xue et al., 2013). It consists in 3 layers of primary cell culture: neurons, astrocytes and endothelial cells. This model was notably used in hypoxic conditions mimicked by ODG techniques (Tian et al., 2016; Zhao et al., 2019). As *in vitro* techniques are limited, more *in vivo* techniques to mimic stroke have been developed.

1.2.2.2. In vivo models of ischaemia

To study ischaemic stroke, many models have emerged, each with specific advantages and limitations. Depending on the hypothesis, the technique used must be carefully chosen. To perform occlusion of a vessel, the approach can be extravascular (external to the vessel) using coagulation, clips or ligation; or endovascular (internal to the vessel, through the lumen) using intraluminal filament, emboli or photochemical methods (Fluri et al., 2015; McCabe et al., 2018).

All extravascular techniques require a craniotomy that can trigger complications and potentially impair food consumption, which is crucial for the recovery after ischaemia. Furthermore, advanced surgical skills are necessary for these techniques. However, these are highly reproducible and have a high success rate (Fluri et al., 2015; McCabe et al., 2018).

Electrocoagulation permanently occludes the vessel using diathermy machine (Tamura et al., 1981). As this model is permanent, an alternative to this model is the use of clip or ligation that can be removed to perform a transient ischaemia (Buchan et al., 1992).

A method that reduces invasiveness and that does not require advanced surgical skills would be the injection of endothelin-1, a long-lasting vasoconstrictor (Robinson et al., 1990). Using a cannula, it can be used on conscious animals to avoid anaesthetic cross effects (Bogaert et al., 2000). However, this technique showed major disadvantages as it triggers astrocytosis and axonal sprouting (Uesugi et al., 1998) and the timing of occlusion could not be controlled, giving high variability.

Two endovascular models of occlusion use injection of either autologous blood or thrombin that closely mimics human pathology and are both used to model thrombolysis. Embolic methods have very little control over the final site of clot lodgement and limit the control of occlusion timing reducing reproducibility (Zhang et al., 2015). Thromboembolic models are characterised by injection of thrombin in distal arteries using small craniotomy, that will create a fibrin clot (Orset et al., 2007). Due to its superficial location, it creates only small infarct, and thus there is low mortality and high reproducibility. Furthermore, it is clinically relevant as it mimics a limited time window for alteplase treatment (Orset et al., 2007).

Another endovascular model is the photo-thrombosis technique that consists of injection of Rose Bengal in the blood stream, then illumination of the area chosen for occlusion with light. It leads to reactive oxygen species mediated damage to endothelial cells, by activating platelets causing their aggregation and thrombi formation (Watson et al., 1985). It is a simple technique with low variability due to controlled location of the lesion and is minimally invasive. However, it is uncharacteristic of human stroke as it creates an early vasogenic oedema and is unsuitable for neuroprotective drug experimentation as it creates very little penumbra (Fluri et al., 2015; McCabe et al., 2018).

The last endovascular technique is the intraluminal filament model, mainly undertaken to occlude the origin of the middle cerebral artery (MCA), as it is the most common ischaemic location in the human brain (O'Sullivan & Schmitz, 2007). At its origin, the MCA is shaped like a "Y" with two downstream branches finer than the upstream one. As the MCA is placed right after the common carotid artery, any clot is thus easily driven there and can become trapped (O'Sullivan & Schmitz, 2007).

The insertion of the thread in an artery leads to permanent ligation of that artery afterwards in order to reperfuse and avoid haemorrhage. The model used in this thesis utilises unilateral common carotid artery occlusion (UCCAo) to enable the thread to be inserted via the internal carotid (Hata et al., 1998). Other have performed this surgery by inserting the thread in the external carotid (McColl et al., 2004; Morris et al., 2016; Trotman-Lucas et al., 2017). A comparison of the two methods demonstrated a lower mortality rate, bigger infarcts and more neurological deficits with the insertion of the thread by the external carotid artery (Smith et al., 2015). However, insertion of the thread by the external carotid damages the

mouth vasculature hence it impairs mastication that is crucial for recovery of post-stroke body weight loss (Boyko et al., 2010; Dittmar et al., 2003).

Insertion of a thread can damage intraluminal vessel wall and increases risk of haemorrhage; this problem has been reduced by optimisation of the filament size (Tsuchiya et al., 2003). Other limitations are filament diameter not optimal for the vessel and filament misplaced (i.e. not being advanced far enough, hence not leading to complete occlusion; Fluri et al., 2015; Hata et al., 1998; Morris et al., 2016). Knowing these limitations, a short range of animal weights was selected to match the filament diameter. This method has controlled limitation and many advantages such as reproducibility and high proportion of successful procedures, the creation of a penumbra, and control over time of occlusion, furthermore it mimics mechanical thrombectomy.

These models have been performed mainly on rodents, but strain is also a factor to take in account in the design of the study. In rats, 5 strains have shown significantly different infarct sizes, notably because of hypertension (Cipolla et al., 2018; Duverger & MacKenzie, 1988). Age and sex are important variability factor and needs to be duly controlled (Zhang et al., 2018). In mice, different strains showed different susceptibility regarding ischaemic lesion size as some presented bigger infarcts compared with other strains within the same study (Barone et al., 1993; Zhang et al., 2018). This is potentially due to anatomical differences between strains (Barone et al., 1993; Maeda et al., 1998). The mouse model C57Bl/6J, commonly used, also have variability regarding sex and sub-strains (Zhao et al., 2017).

The model used in this thesis is 15-, 30- or 60-minutes duration ischaemia. This model is giving neuronal damage in a defined area with no recovery at 24 hours. These outcomes do not mimic the transient ischaemic attack (TIA) that is supposedly leaving no defined lesion but possibly small diffuse lesion, difficult to perceive with MRI study or CT scans and neurological signs and symptoms disappear 24 hours after the injury (Easton et al., 2009). Others have reported that ischaemia for 2.5 to 10 minutes in mice left no discernible lesion on MRI, whereas from 12.5 minutes the lesion was visible in either cortex or striatum (Pedrono et al., 2010). Recent advancements in high resolution MRI might classify a greater number of minor stroke amongst those TIA patient (with symptoms not lasting beyond 24 hours; Kernan et al., 2014), and research on new biomarkers emerge to help the diagnosis

(Dolmans et al., 2019), especially since TIA often lead to greater ischaemia (Coutts, 2017).

1.2.3. Alterations in neurological function and cognition in animal models of ischaemia

Ischaemia causes sudden weakness, confusion, loss of balance or coordination. In the long term, ischaemic patients might be disabled by hemiparesis, language impairments and cognitive decline. Behavioural assessment in preclinical research tests sensorimotor functions using notably neurological score (called neuroscore). Many tests have been developed around the different sensorimotor functions observed in mice (reviewed by Balkaya et al., 2013; Trueman et al., 2017). Ischaemic animals present general sensorimotor impairment following the injury but then recover during the first week (Deng et al., 2016; Macrez et al., 2011; Omura et al., 2006; Orset et al., 2007; Titova et al., 2011).

In order to investigate cognitive deficits, tests were developed around learning and memory paradigms. The most commonly used test is the Morris water maze, evaluating the spatial memory of an animal (Morris, 1984) but it is very stressful for the mice and time consuming for the experimenter. Novel object recognition (NOR) memory has been studied in various disease models and thus a plethora of protocols have been developed (Antunes & Biala, 2012). These tasks are based on rodent's innate preference to explore novel over familiar stimuli in their environment and can be used to infer memory for the familiar stimulus (Berlyne, 1950; Ennaceur & Delacour, 1988). It is a two-phase test with a familiarisation phase in which the animal is left to explore an object and its duplicate, followed by a retention test to determine whether the animal remember the familiarised object and thus spent more time exploring the novel object. In the context of stroke models, NOR has been used with a 24 hours retention paradigm showing impairment from 7 to 28 days post-injury (Wang et al., 2012; White et al., 2012; Yabuki & Fukunaga, 2013; Zhu et al., 2015). Because many tests were used for different severity of ischaemia, recommendations by Leger and colleagues were used to design the experiment in this thesis (Leger et al., 2013): Handling the animal must be done before performing any experiment; ideally, animals should have an habituation phase of the apparatus 24 hours before; familiarisation and test is at most 10 minutes.

1.2.4. Vascular system disruption

1.2.4.1. The neurogliovascular unit (NGVU)

For the neuron to function, it needs a suitable environment to support it. Neurons together with astrocytes, microglia, endothelial cells and pericytes, form the neurogliovascular unit (NGVU; Fig 1.6).

Astrocytes and microglia have crucial roles in this unit as they contribute to the different pathological features of ischaemia in beneficial and detrimental cascades (Magaki et al., 2018). Astrocytes bring essential energy and support to the neuron in homeostatic conditions; After an insult, astrocytes adapt their response to maintain neuronal needs (Verkhratsky & Nedergaard, 2017; Weber & Barros, 2018). In the same way, microglia modulate the neuronal environment for their growth and bring trophic support in a resting state; after an insult or in the context of a disease, microglia become activated, changing their functions to evolve and adapt to the situation (Butovsky & Weiner, 2018).

In the NGVU, astrocytes, pericytes and endothelial cells have a role in maintaining a physical barrier, controlling exchange between blood from the vessel lumen and parenchyma: the blood brain barrier (BBB). It comprises vessel walls, composed by endothelial cells, and on the parenchyma side, astrocytes and pericytes surround vessels (Fig. 1.6). To investigate its integrity, researchers can either study the proteins of the tight junction between the endothelial cell spaces (such as occludin, claudin-5, ZO1), aquaporin-4 (AQP4), a water channel on astrocyte end-feet or by analysing leakage of blood to the parenchyma named extravasation (Fig. 1.6).

BBB breakdown is thought to contribute to neurodegenerative diseases (Zlokovic, 2008). Following focal cerebral ischaemia (MCAo), BBB permeability is increased from 2 hours post-injury and is reported to return to baseline after 18 days using Evans Blue extravasation (Wu et al., 2014).

Neurovascular coupling is a system defining vascular adaptation to neuronal activity (Phillips et al., 2016). It requires astrocytes to elicit vessel dilatation (Zonta et al., 2003). Cerebral ischaemia impacts on neurovascular coupling as it damages endothelial cells and promote BBB breakdown (Del Zoppo & Mabuchi, 2003; Salinet et al., 2015). In physiological conditions, CBF is maintained to a certain level despite perfusion changes; this phenomenon is called

autoregulation and is found at perfusion rate from 50 to 150 mmHg (Kunz & Iadecola, 2009). It is possible through vasoconstriction and vasodilatation finely tuned by glia that constantly adapt CBF to neuronal demands (Girouard & Iadecola, 2006). However during ischaemia, the perfusion rate is too low, and autoregulation is lost (Salinet et al., 2015).

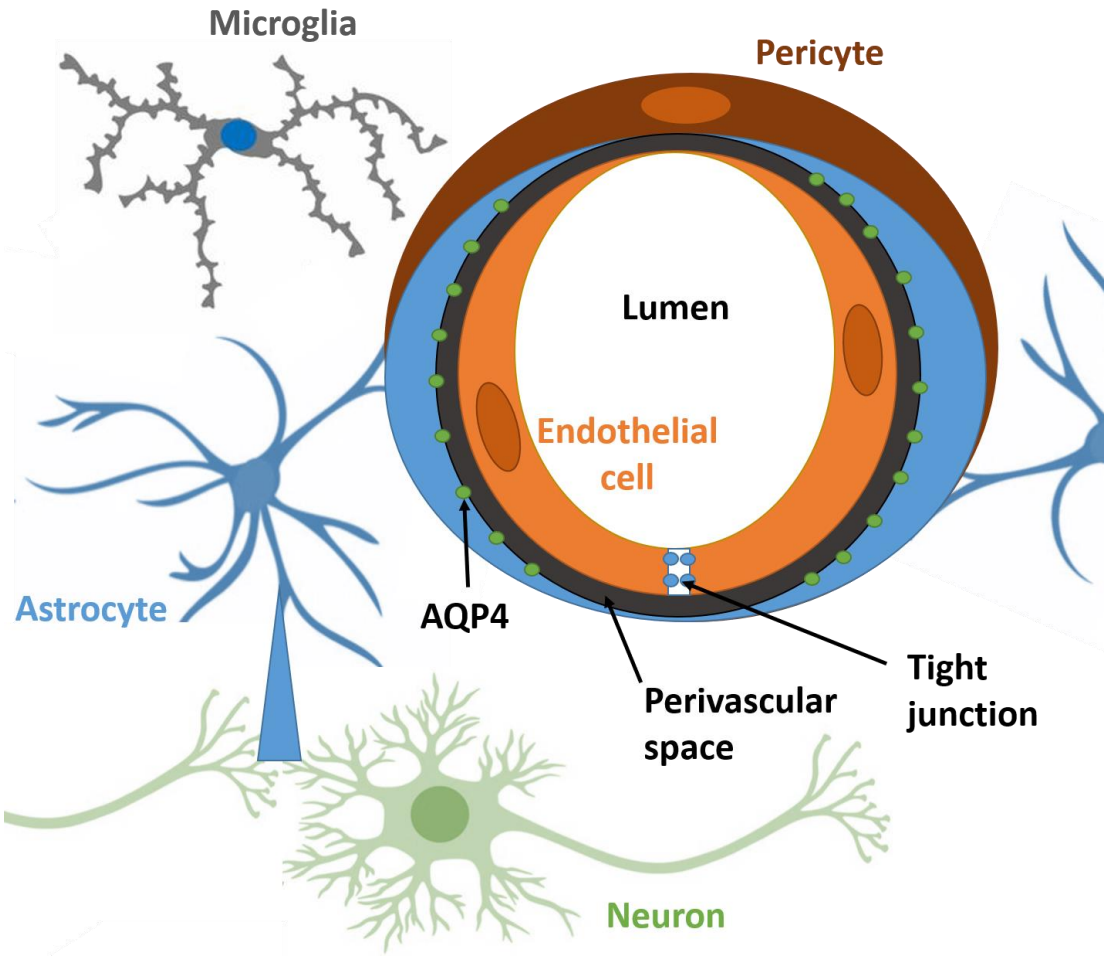

Figure 1-6 The neurogliovascular unit and blood-brain barrier.

1.2.5. Excitotoxicity and depolarisation waves

One of the acute detrimental events that is triggered by ischaemia and reperfusion is excitotoxicity. It was first discovered that injection of glutamate on the retina tissue lead to its degeneration; and later on this concept was extended to neurons of the brain (Lucas & Newhouse, 1957; Olney, 1969). This concept, later named “excitotoxicity” by Olney, was associated with excess influx of calcium via N-Methyl-D-Aspartate (NMDA) receptors after ischaemia (Choi, 1988; Tymianski et al., 1993). These authors described the loss of energy of

the cell leading to malfunction of the active calcium pumps. Calcium enters the cell via NMDA receptors and cannot be ejected causing its accumulation and eventual neuronal death. Reducing excitotoxicity is still the focus of ongoing research to develop novel therapies for stroke, such as novel compounds that target the NMDA-R signalling pathways (Bano & Ankarcrona, 2018; Wu & Tymianski, 2018).

With ischaemia, the accumulation of calcium and other ions, normally regulated with active pumps, leads to the depolarisation of the neurons (Branston et al., 1977). As neurons die, their death leads to their fragmentation, liberating excess calcium in the extracellular medium. This creates "depolarisation waves" that propagate to the penumbra and induce a cascade of detrimental events such as inflammation and apoptosis (Hossmann, 1996; Dirnagl et al., 1999; Fig 1.3).

1.2.6. Oxidative stress

1.2.6.1. Definition

A reduction of oxygen concentration in the blood is called hypoxia, from the Greek *υπό* (hypo) meaning under and *οξύς* (oxus) oxygen. Cells in the brain depend on this oxygen to function, a mechanism termed as aerobic from the Greek *ἀήρ* (aero) air and *βίος* (bios) life.

The brain is the most sensitive organ to glucose and oxygen deprivation due to its high metabolic rate and has poor anti-oxidative defences (Kohen et al., 1988) and is therefore more prone to damage caused by oxidative stress (Lebel & Bondy, 1991). Oxidative stress occurs when there is an imbalance between the production of oxidants and the cell's capacity to neutralise them through intrinsic antioxidant defences.

Oxidants are radicals that have at least one unpaired electron, thus they tend to interact with other elements to get them paired. By doing so, they are reduced and the element they interact with is oxidised. The oxidation of cell elements (such as DNA, proteins or the cytoplasmic membrane) leads to their degradation and thus dysfunction of the cell (Sun et al., 2018).

Some radicals are derived from oxygen and thus are called Reactive Oxygen Species (ROS); they are also named free radicals because of their unpaired electron(s). Other free radicals are derived from nitrogen; they are called Reactive Nitrogen Species (RNS; see table 1.1).

Name	Formula	Structure	Lewis Structure
Superoxide	O_2^-	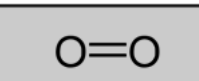	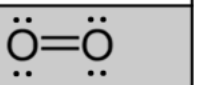
Hydrogen peroxide	H_2O_2	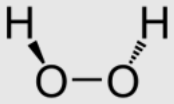	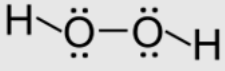
Nitric oxide	NO	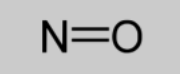	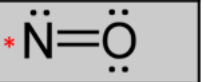
Peroxynitrite	$ONOO^-$	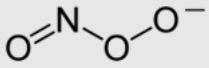	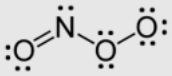

Table 1-1 Reactive oxygen and nitrogen species with their formula and structure.

Although elevation of ROS is detrimental, basal level maintenance of ROS is important for homeostasis (Angelova & Abramov, 2018; Ye et al., 2015). Particularly fine tuning of ROS production and regulation is critical as both high and low ROS levels impact at different time point the physiological development of nervous system cells (Olguín-Albuerne & Morán, 2018; Schippers et al., 2012) notably neurons (Kennedy et al., 2012). Furthermore, ROS are essential for vascular homeostasis and function, immune response, haematopoiesis (Vara & Pula, 2014).

1.2.6.2. Oxidative stress following ischaemia

During ischaemia, levels of ROS increase to the extent that they overwhelm endogenous scavenging systems. This is hypothesized to be due to mitochondria dysfunction (Sun et al., 2018; Zhang et al., 2016). In anaerobic conditions, mitochondria cannot provide energy to the rest of the cell with the consequence that many physiological mechanisms are interrupted. To study oxidative stress *in vitro,* oxygen and glucose deprivation (OGD) has been used to demonstrate that reduced energy causes astrocytes to die (Yager et al., 1994). Mitochondrial dysfunction produces ROS and nitric oxide (NO); a second messenger in cells that inhibits cellular respiration thus leading to cell death (Cleeter et al., 1994). NO and ROS

together generate peroxynitrite ($ONOO^-$), a highly aggressive element (Beckman, 1991). It is important to note that following reperfusion, by recanalization of the blocked vessel (mostly attain by thrombolysis), there is an exacerbation of ROS production (Enzmann et al., 2018).

There is also evidence of oxidative stress in human; a meta-analysis showed increased lipid peroxidation and equal or decreased levels of antioxidant activities in patient following stroke (Cherubini et al., 2005). In the following months after the onset, radicals from phagocytes were still increased with equal antioxidant defences contained in the blood leading to oxidative damage to lipid following ischaemic stroke in patient compared to controls (Alexandrova & Bochev, 2005). Interestingly, patient with MCA occlusion had increased oxidative stress biomarkers compared to controls on admission before tPA injection, and 1, 2, 12 and 24 hours after tPA injection (Domínguez et al., 2010). Oxidative stress was correlated positively with ischaemia severity and recovery as poorly or not recovering patient had decreased antioxidant and increased radicals at admission, 6 hours after, 1, 3, 5 and 7 days after compared to patient with functional recovery at 2 weeks (Cherubini et al., 2000). Reducing oxidative stress using uric acid reduced growth and improved functional recovery in hyperglycaemic ischaemic patients (Amaro et al., 2015).

Cognitive impairments were correlated with higher oxidative stress in patients following ischaemic stroke (Wang et al., 2018). Both increased NO and MDA in ischaemic stroke patient during the first 48 hours was negatively correlated with neurological score (Ozkul et al., 2007).

Many have pointed out that oxidative stress might be the link between ischaemia and these types of dementia (Bennett et al., 2008; Luca et al., 2015; Tönnies & Trushina, 2017; Tramutola et al., 2017). At early stage of AD, anti-oxidative enzymes are decreased (Mangialasche et al., 2009; Nunomura et al., 1999) and radicals are increased (Resende et al., 2008). Oxidative stress is involved in the generation of amyloid-β and the onset and progression of AD (Akbar et al., 2016; Obrenovich et al., 2006; Pratico et al., 2001; Reddy, 2006).

Oxidative stress is found also found in VaD patients (Aguilar-Navarro et al., 2016; Choi & Lee, 2017; Luca et al., 2015). Ischaemia, AD and VaD share common risk factors such as ageing, hypercholesterolemia, hyperglycaemia, smoking, cardiovascular disease, hypertension (Vijayan & Reddy, 2016), and these risk factors increases or are increased by oxidative stress

(Choi & Lee, 2017). Oxidative stress is found beneath molecular and cellular mechanisms underlying VaD (Calabrese et al., 2016; Vijayan & Reddy, 2016). Furthermore, increased oxidative stress is positively correlated with cognitive decline in VaD patients (Li et al., 2010).

1.2.7. Inflammation

1.2.7.1. Definition

Inflammation is a mechanism that defines activation of immune defences. Cells that undergo an injury produce and release messengers to attract immune cells called damage-associated molecular patterns (DAMPs; Shi et al., 2019). In the brain, glial cells respond to those messengers, they get activated and respond with production of cytokines (Liu et al., 2017). Inflammation is a major detrimental mechanism of cerebral ischaemia; it is closely related to other mechanisms of ischaemia-induced damage to neurons. But some inflammatory mechanisms are beneficial and thus its modulation could be a potentially target for the development of novel therapeutic approaches for the treatment of stroke (Anrather & Iadecola, 2016; Shi et al., 2019). Two notable glial cells activated in the parenchyma during ischaemia are microglial cells and astrocytes. The messengers can also attract immune cells from the blood circulation, such as macrophages and neutrophils.

Inflammation is found in human patient using blood samples, post-mortem studies and PET scans (Shi et al., 2019) in a chronic manner (Narasimhalu et al., 2015) but also in remote places to the injury (Shi et al., 2019). Inflammation is associated with cognitive decline in ischaemic patients (Kliper et al., 2013). Mild cognitive impairment patients have increased inflammation notably pro-inflammatory TNF-α, and its receptor is positively correlated with increased cognitive decline (Shen et al., 2019). Inflammation is increased in VCI, VaD and AD patients (De Strooper & Karran, 2016; Iadecola, 2013; Wallin et al., 2017). Inflammation is found in most cellular mechanisms of VaD such as BBB disruption, white matter damage (Albers et al., 2018; Calabrese et al., 2016). Oxidative stress and inflammation are intertwined cascades both increasing vascular disruption and participating in promoting neuronal damage themselves closely related to cognitive decline (Gorelick et al., 2011).

1.2.7.2. Glial response following ischaemia

Astrocytes

Astrocytes undertake numerous roles in the central nervous system (CNS) to maintain homeostasis and modulation of the immune response. Astrocytes have a support role for neurons by producing and releasing neurotrophic factors, antioxidants and energy precursor glycogen and lactate; they also regulate the neuronal transmission by buffering excessive glutamate at the synapse, re-up-take of neurotransmitters, releasing vasoconstrictor or vasodilator mediators and modifying the extracellular matrix (Verkhratsky & Nedergaard, 2017; Weber & Barros, 2018).

Any brain damaging disease exerts a modification of astrocyte morphology, gene expression and thus their functions (Burda & Sofroniew, 2014; Liu & Chopp, 2016; Pekny et al., 2016). In this case, astrocytes are reactive, and the global phenomenon is also called astrocytosis. Interestingly, it has been found that different injuries lead to heterogeneity of astrocyte function and gene expression (Zamanian et al., 2012). In this paper, they showed that LPS-inflammation challenge upregulated many pro-inflammatory genes in astrocytes whereas ischaemia upregulated many anti-inflammatory and antioxidant genes but also thrombospondins that promote synaptogenesis (Zamanian et al., 2012). Since this discovery, more reports have highlighted an important diversity in the response of astrocytes depending on the insult (Matias et al., 2019). Furthermore, as astrocytes could potentially be guided toward neuroprotective phenotypes, it became a potential therapeutic target for cerebral disease (Pekny et al., 2019).

One protein commonly used to detect reactive astrocytes is glial fibrillary acidic protein (GFAP; Sofroniew, 2009). GFAP is essential for astrocytosis and glial scar formation (Herrmann et al., 2008; Pekny & Pekna, 2004). GFAP knockout mice have increased lysosomal degradation and inflammatory responses in an Alzheimer's Disease model (Kamphuis et al., 2015), increased paralysis and disease severity in a multiple sclerosis model (Liedtke et al., 1998) and increased inflammation and impaired functional recovery following ischaemia (Li et al., 2008; Liu et al., 2014). Altogether, these studies suggest that reactive astrocytes have a protective role against these insults.

Following cerebral ischaemia, anaerobic conditions lead to a loss of astrocytes (Liu et al., 1999; Shannon et al., 2007) but also morphological changes for the remaining ones, in and around the infarct (Ding, 2014; Lukaszevicz et al., 2002). Astrocytes become elongated in the penumbra (Ding, 2014), they develop more extensions, and their processes gets larger (Ding, 2014; Lukaszevicz et al., 2002; Wagner et al., 2013). Furthermore, astrocytes gain phagocytic functions and help clear debris (Koizumi et al., 2018; Morizawa et al., 2017). Importantly, astrocytes are known for their antioxidant support to neurons (Baxter & Hardingham, 2016) and their neuroprotective role during an oxidative challenge (Drukarch et al., 1997; Kraft et al., 2004; Shih et al., 2003). Regarding ischaemia, astrocytes represent a target for the development of therapeutic strategies as they modulate the immune response, synaptic connectivity, angiogenesis and neurogenesis but also control most of the antioxidant production and maintain the BBB (Becerra-Calixto & Cardona-Gómez, 2017; Koizumi et al., 2018; Liu & Chopp, 2016). Notably, ischaemic tolerance observed after preconditioning was found mediated by astrocytes (Hirayama et al., 2015). In this mechanism, one important aspect is the upregulation of antioxidant by astrocytes that was found essential for neuroprotection following ischaemia (Bell et al., 2011a; Shih et al., 2003; Shih et al., 2005b). Overall, neuroprotective effects of reactive astrocytes were associated with improved neurological recovery after ischaemia (Sims & Yew, 2017).

However, in the recent years, potential detrimental roles of reactive astrocytes where found and notably through the upregulation of inflammatory cytokines (Becerra-Calixto & Cardona-Gómez, 2017). As part of the immune system defence, astrocytes can be aggressive and neurotoxic (Liddelow et al., 2017). Ben Barres group conducted a transcriptomic study of reactive astrocytes and found heterogeneity of reactive astrocytes depending on the injury (Zamanian et al., 2012). In 2017, they advanced this work to demonstrate two populations of reactive astrocytes (Liddelow et al., 2017). Their main features are their transcriptomic differences leading to different cellular behaviour. Using the so-called microglia M1/M2 phenotype (despite controversy, see Ransohoff, 2016) Barres used this nomenclature for astrocytes, naming one phenotype as neuroinflammatory/neurotoxic (A1) whereas the other is protectant/neurotrophic (A2). Liddelow et al (2017) showed that an activation of the A1 phenotype with pro-inflammatory microglia was neurotoxic and led to synapse destruction. On the other hand, A2 phenotype upregulates neurotrophic factors (Liddelow & Barres, 2017). Even though this classification is pertinent and highlights the heterogeneity of reactive

astrocytes in different disease states, subsequent *in vivo* studies tend to show a diversity of response (Lin et al., 2017) suggesting that this classification is very reductive.

Following ischaemia, different publications found either aggressive and neurotoxic phenotypes (Villarreal et al., 2016), but also neuroprotective phenotype (Zamanian et al., 2012), and others found both simultaneously at different areas of the lesion (Rakers et al., 2018). One critic of Zamanian et al (2012) is the use of very young (P30) mouse brains, which could explain discrepancies with the response of adult mice. Furthermore, this paper analysed whole brain samples whereas the first paper analysed only one time point after ischaemia. Several papers show that ischaemia first leads to increased levels anti-inflammatory cytokines during the first hours/days and that they later decline, then pro-inflammatory cytokines are increased (Amantea et al., 2018; Hu et al., 2012; Zhang et al., 2018). Furthermore, some have found that there are different inflammatory responses depending on the location of the lesion (Hu et al., 2012; Perego et al., 2011). As astrocytes play an important part in the modulation of inflammation and in the production of these cytokines, it suggests that there are heterogenous responses of reactive astrocytes throughout the lesion. Rakers and colleagues (2018) recently reported diverse gene expression in reactive astrocyte upregulated in the core and in the peri-infarct (Rakers et al., 2018).

This heterogeneity in astrocyte gene expression and function is also found in physiological conditions through different parts of the brain (Lin et al., 2017; Morel et al., 2018; Lanjakornsiripan et al., 2018). There are two main types of astrocytes: protoplasmic found in the grey matter and fibrous in the white matter (Miller & Raff, 1984) and it appeared that fibrous astrocytes are more sensitive to injury than protoplasmic (Shannon et al., 2007) However, others found the opposite (Lukaszevicz et al., 2002). Although diverse injuries exert different reactive astrocyte response (Lin et al., 2017), aging was also found to modulate the phenotype of reactive astrocytes (Boisvert et al., 2018).

First discovered in Alzheimer's disease neuropathology by Alois Alzheimer in 1910, (Alzheimer, 1910) astrocytes with lost processes have been observed after ischaemic challenges such as OGD and anaerobic glycolysis (Mercatelli et al., 2016). The term 'clasmatodendrosis' that defines this phenomenon was first reported in the literature in 1926 (Google N-gram viewer) and termed "clasmatodendrosis" by Cajal (Penfield, 1928). It defines

astrocyte with swelling and vacuolisation in the soma and disintegrated processes (Friede & Van Houten, 1961; Hulse et al., 2001; Tomimoto et al., 1997, Davies et al., 1998). The first *in vitro* model to study clasmatodendrocytes has demonstrated that anaerobic glycolysis, indicated by increased medium acidity, is a key mechanism of tissue damage (Friede & Van Houten, 1961; named here klasmatodendrosis). More recently this concept was associated with white matter hyperintensities and cognitive decline found in both human and mouse (Chen et al., 2016; Hase et al., 2017; Sahlas et al., 2002).

Microglia

Microglia are the body of immune cells in the CNS. Microglia modulate the neuronal environment and provide trophic support in a resting state; after an insult or in the context of a disease, microglia become activated, changing their function and gene expression (Hammond et al., 2018). These small cells with short processes can migrate and proliferate. As scavenger cells, microglia phagocyte damaged and unused cells or infectious agents (Puig et al., 2018). Reactive microglia produce ROS and NO-derived elements that can exacerbate oxidative stress (Zhao et al., 2017). They may also promote cell survival and repair via the production of anti-inflammatory cytokines and growth factors (Chen & Trapp, 2016).

One of the challenges in microglia research has been to define their homeostatic phenotype and to differentiate them from infiltrated peripheral macrophages (Butovsky & Weiner, 2018). In physiologic conditions, microglia are in a resting state. This phenotype potentially restrains any inflammatory response to maintain homeostasis (Salter & Stevens, 2017). However, with an injury, microglia shift to an adaptative phenotype, which depends on the injury (Hammond et al., 2018).

In vitro studies have distinguished different phenotypes of microglia after an injury. Depending on the treatment, two main populations have been defined (for review, Zhao et al., 2017):

- M1: classical – pro-inflammatory phenotype:

They are induced by LPS, IFNγ, TNFα, IL-1β and produce cytokines such as IL-1β, IL-6, TNFα and CCL2, but also ROS and NO. This phenotype is believed to be cytotoxic and to promote

tissue re-modelling, neurodegeneration, tumour destruction (for review, Zhao et al., 2017).

- M2: alternative – anti-inflammatory, pro-resolving, quiescent phenotype:

These are induced by IL-4, IL-13 and IL-10 and produce factor such as IL-10, IL-13, TGFβ1, IL-4, IGF-1. They are known for phagocytosis, resting signals, survival signals, tumour promotion (Puig et al., 2018).

The M1/M2 dichotomy was named after a similar classification of T helper 1 and 2 cells. However, this characterisation is very controversial as there are probably a spectrum of phenotypes rather than only two and these polarised phenotypes have not been reported *in vivo* (For review: Ransohoff, 2016). Nevertheless, the concept of pro and anti-inflammatory microglia is still used as many studies investigate modulators of inflammatory phenotype and recent evidence suggested that diseases and injuries had prevalence of one of the two phenotypes (Cherry et al., 2014; Tang & Le, 2016).

Several papers showed that ischaemia first led to increased anti-inflammatory cytokines in the first hours/days and that these later declined, after which pro-inflammatory cytokines were increased (Amantea et al., 2018; Hu et al., 2012; Zhang et al., 2018). Furthermore, a different spatial distribution of diverse microglia/macrophage inflammatory phenotypes were observed from 24 hours to 14 days after ischaemia (Hu et al., 2012; Perego et al., 2011). Some have found upregulated M2 markers in the core and M1 markers in the peri-infarct (Perego et al., 2011). Others found upregulated M2 markers in the peri-infarct from 1 to 7 days, but then these markers decreased and M1 markers were upregulated from 5 days up to 14 days (Hu et al., 2012). These studies used immunohistochemistry and rt-qPCR; thus their conclusions are limited as these cytokines and chemokines are produced by different cells, and not only microglia/macrophages. To overcome this limitation, cell sorting or single cell RNA-sequencing could be used. Studies have suggested that modulating these phenotypes following ischaemia is possible (Liu et al., 2017; Zhao et al., 2017) and that therapeutic strategies promoting an anti-inflammatory phenotype seem promising (Wang et al., 2018).

Macrophages and neutrophils infiltration

After cerebral ischaemia, peripheral immune system cells are detected in brain parenchyma. After 30 to 60 minutes of MCAo in mice, neutrophils were found immediately after the onset of the ischaemia and peaked between 18 hours to 3 days after the onset (Grønberg et al., 2013; Vaas et al., 2017). Then, neutrophil number decreased whereas macrophage peak infiltration was observed between 3 to 14 days and seemed to decline only after 3 weeks (Grønberg et al., 2013). This infiltration of neutrophils and monocyte-derived macrophages was reported to be both detrimental and beneficial (Benakis et al., 2015; Enzmann et al., 2018).

Neutrophils produce matrix metalloproteinases (MMPs), enzymes that degrade the collagen of the extracellular matrix but also cellular components. They notably worsen BBB breakdown after stroke by damaging endothelial cells when releasing MMP 9 and exacerbating the inflammatory response (Turner & Sharp, 2016). They also participate in ROS production, exacerbating oxidative stress in the parenchyma (Matsuo et al., 1995; Satoh et al., 1999; Turner & Sharp, 2016). Therapies blocking neutrophil adhesion to endothelial cells were found to decrease their infiltration, ameliorate ischaemia and reduce infarct volume (Francis & Baynosa, 2017). It is possible that neutrophils may have different inflammatory phenotypes as suggested after discovering that their infiltration was associated with the production of anti-inflammatory markers (Cuartero et al., 2013).

Macrophages are morphologically like microglia and express a large number of similar markers (Bennett et al., 2016; Satoh et al., 2016). Macrophages may also have both anti- and pro-inflammatory phenotypes in the vicinity of an ischaemic lesion (Zrzavy et al., n.d.). Macrophages produce neurotoxic factors that worsen the infarction but also have anti-inflammatory properties; and thus as microglia, they can be classified as the M1/M2 system (Benakis et al., 2015). Modification of macrophages from pro-inflammatory phenotype to anti-inflammatory phenotypes reduces the production of those neurotoxic factors (Kadl et al., 2010; Naito et al., 2014).

Glial scar

Within weeks, the ischaemic infarct has increased levels of reactive glial cells. Astrocytes, microglia and macrophages are found in the lesion, notably in the core. All activated, they form an intertwined pattern of cells, named the glial scar (Sofroniew, 2009). It was first thought to be neuroprotective because it limits inflammation spreading (Bush et al., 1999; Wanner et al., 2013). Signal transducer and activator of transcription 3 (STAT3) is important for the glial scar formation and astrocyte activation. In a model of spinal cord injury, selective deletion of STAT3 in astrocytes impeded their activation and formation of the scar, leading to an expansion of inflammatory cell infiltration, increased lesion size, demyelination, delayed and attenuated motor recovery (Herrmann et al., 2008; Okada et al., 2006; Wanner et al., 2013). However, the glial scar was found to be permeable, as oedema and neuronal damage were observed beyond the scar and were associated with clearance mechanisms such as drainage and phagocytosis at the border of the scar (Zbesko et al., 2018). Furthermore, it was observed that astrocytes gained phagocytic functions and helped the clearing of debris (Koizumi et al., 2018; Morizawa et al., 2017).

Recent studies also suggested a possible detrimental effect of the glial scar. Reactive astrocytes notably produce axonal repair inhibitors (Liu & Chopp, 2016) and studies in human suggest that the glial scar can impede neuronal growth and thus repair (Huang et al., 2014). This finding is however controversial as further evidence suggested that the glial scar produced multiple axonal growth factors; and by preventing the glial scar formation, it resulted in the reduction of these growth factors (Anderson et al., 2016).

1.2.8. Apoptosis & necrosis

Apoptosis is a mechanism of programmed cell death, particularly useful during normal development and homeostasis (Geden et al., 2019; Grilo & Mantalaris, 2019). It is composed of several steps: condensation of the chromatin and shrinking of the cell, blebbing (which is defined by the formation of protrusions around the cell) and fragmenting (Kerr et al., 1972). Necrosis is defined as the unprogrammed cell death as opposed to apoptosis. It is composed of different steps, such as blebbing, swelling and finally membrane rupture leading to the leakage of the cell contents. This leakage triggers an immune response and oedema (Cullen, 2010; Martin et al., 1998; Snider et al., 1999). Excitotoxicity and oxidative stress lead to

apoptosis and necrosis (Dirnagl et al., 1999). Apoptosis is observed after mild injury and found in the penumbra of the ischaemic lesion compared to necrosis that is mostly found in acute phase of severe injury, and thus mainly found in the core of the ischaemic lesion (Kerr et al., 1972; Radak et al., 2017).

1.3. Nrf2 signalling

1.3.1. An endogenous transcription factor

1.3.1.1. Definition

The Nuclear Factor Erythroid 2 (NF-E2)-Related Factor 2 (Nrf2) signalling pathway has been identified as a new therapeutic target to prevent damage caused by elevated oxidative stress and inflammation (Sandberg et al., 2014). It is a transcription factor of the Cap'N'Collar family and the basic leucine zipper sub-family (Chan & Paolo, 1995; Itoh et al., 1995). Nrf2 upregulates a battery of antioxidant and anti-inflammatory genes that contain an antioxiant response element (ARE) on their upstream promotor regions that initiates their transcription (ARE; Itoh et al., 1997; Rushmore et al., 1991).

Nrf2 was discovered in 1994 (Moi et al., 1994) and two years later, its antioxidant properties were demonstrated (Venugopal & Jaiswal, 1996). The phase II detoxyfying enzyme response was established by Rushmore in 1991 and relates to antioxiant response elements (ARE) upregulated during oxidative challenge (Rushmore et al., 1991). The phase II response was found altered with neurologic diseases and its activation was demonstrated to be neuroprotective (Zhang et al., 2013; Venugopal & Jaiswal, 1996). Since then, Nrf2 has been described as a master regulator of antioxidants, and notably of ARE, and a target for therapy in diseases involving elevated levels of oxiditive stress-related disease therapy could be developed (Ma, 2013; Ma & He, 2012).

Keap1 – ARE

In physiological conditions, Nrf2 is sequestered in the cytoplasm by homodimerised Keap1 (Kelch-like erythroid cell-derived protein with CNC homology-associated protein 1) at two sites (Fig 1.7). Nrf2 binding to Keap1, complexed with Cullin 3 (Cul3) and Ring box 1 (RG1), leads to Nrf2 ubiquitination (Ub) and thus degradation, ensuring that Nrf2 levels are kept low. Oxidation by radicals, alkylation by electrophiles or metal chelation of the cysteine 151, 273 or 288 changes the conformation of Keap1 that downregulates Nrf2 ubiquitination and releases Nrf2 (Yamamoto et al., 2008). Once freed, Nrf2 translocates to the nucleus where it

upregulates a battery of over 200 cytoprotective genes by binding to the antioxidant response elements (ARE) of certain genes (Fig 1.7; Itoh et al., 1997).

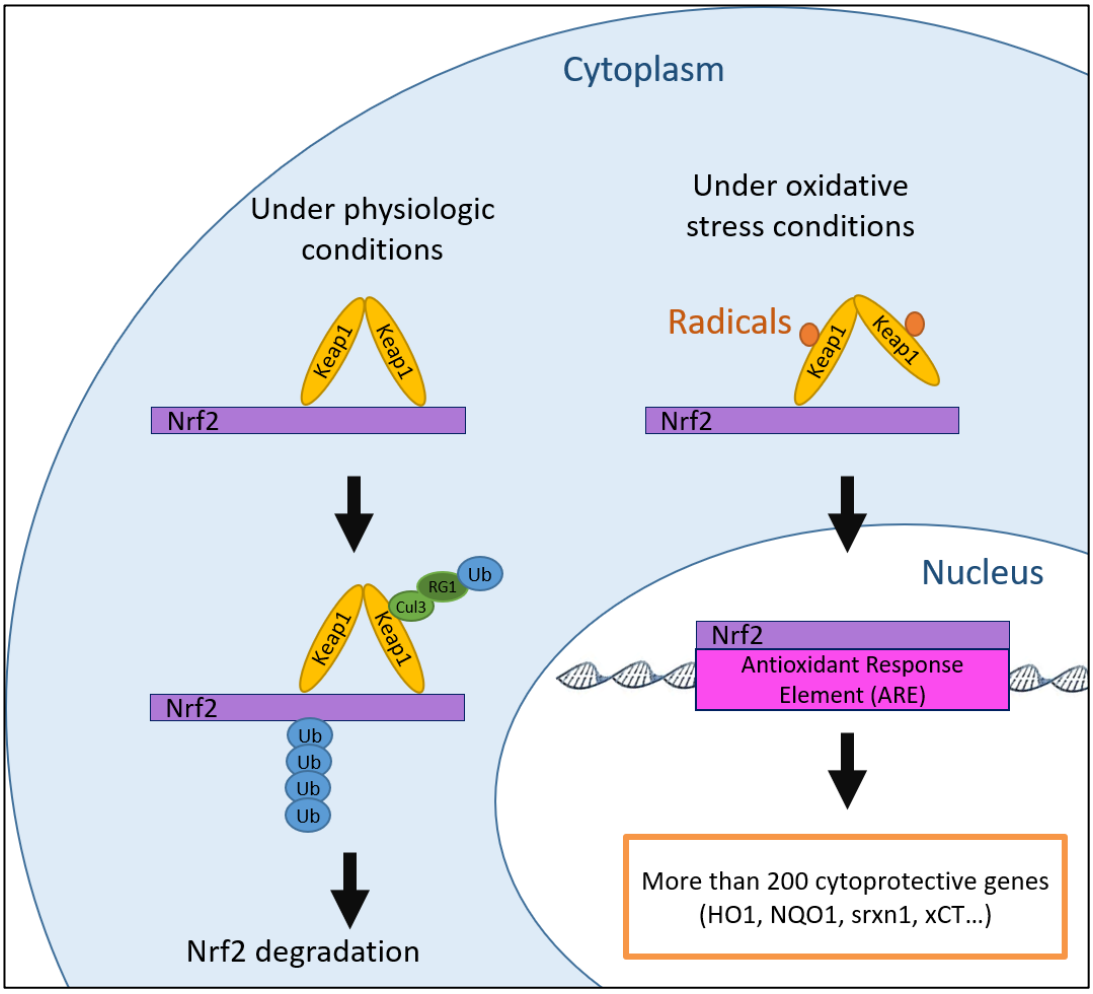

Figure 1-7 Conditions for Nrf2-signalling activation.

Nrf2 is sequestered by Keap1 and degraded in physiological conditions. With oxidative stress, Keap1 conformation is changed and Nrf2 is free to translocate to the nucleus where it activates Nrf2-signalling by binding to the antioxidant response element (ARE) sequence of more than 200 cytoprotective genes.

Nrf2 detection using immunohistochemistry is limited at present due to a lack of specificity of the commercially available antibodies (Kemmerer et al., 2015). In order to analyse Nrf2-signalling activation, different methods have emerged. Nrf2-signalling activation is characterised by its translocation to the nucleus and the upregulation of its related downstream genes. Therefore, alternative methods exist such as measuring Nrf2 nuclear

fraction compared to Nrf2 cytoplasmic fraction (Chen et al., 2016; Lei et al., 2016; Mao et al., 2018), or mRNA levels of Nrf2-related genes such as HO1, NQO1 (Dai et al., 2018; Liu et al., 2019; Yao et al., 2016).

1.3.1.2. Downstream proteins of the Nrf2/ARE pathway

Heme oxygenase-1 (HO1)

Heme contains an iron atom, which is cytotoxic, notably by lipid peroxidation which leads to DNA damage. Heme oxygenase-1 (HO1) is a heat shock protein (Hsp 32) known to degrade heme elements into free ferrous iron, carbon monoxide and biliverdin, which further degrades to bilirubin. Both biliverdin and bilirubin have radical-scavenging properties (Bergeron et al., 1997; Ryter & Tyrrell, 2000; Stocker et al., 1987). HO1 is induced with Nrf2 pathway activation (Alam et al., 1999; Zeynalov et al., 2009). HO1 is upregulated in the ischaemic lesion and confers neuroprotective effects (Alfieri et al., 2013; Ding et al., 2014). HO1 has been described as co-localised with astrocytes at the peri-lesional site from 4 to 72 hours after reperfusion and with microglia in the core at 72 hours after reperfusion in rats after focal cerebral ischaemia (Bergeron et al., 1997; Min et al., 2006). It was also shown that HO1 is expressed in the vessels in the perilesional sites (Alfieri et al., 2013).

NQO1

NQO1 (Nicotinamide adenine dinucleotide phosphate (NADPH) quinone oxidoreductase 1) is a downstream protein of the Nrf2 pathway (Lee et al., 2003; McMahon et al., 2001). Furthermore, its expression depends on Nrf2 activation, as it is not expressed in Nrf2 knockout models (Yeager et al., 2009).

NQO1 is an antioxidant, it catalyses the reduction of NADP (oxidised form) into NADPH (reduced form) and is also an electrophile detoxifier. Electrophiles are produced when there is increased oxidative stress (Dinkova-Kostova & Talalay, 2010), notably lipid peroxidation (degradation of the lipids by oxidation) and can lead to DNA damage (Koenitzer & Freeman, 2010).

Sulfiredoxin 1 (srxn1)

Activation of the Nrf2 pathway also leads to the transcription of sulfiredoxins, notably sulfiredoxin 1 (srxn1) a scavenger that protects against hypoxia, excitotoxicity and Amyloid β toxicity (Soriano et al., 2008, 2009; Zhu et al., 2012). This effect is particularly interesting following ischaemia/reperfusion as Srxn1 knockout increases lesion volume, neurological deficits and oxidative stress (Wu et al., 2017).

The protective effect of sulfiredoxin1 seems to involve peroxiredoxin, an antioxidant that exists in six forms (noted from I to VI). Peroxiredoxin can be inactivated by hyper-oxidation and srxn1 catalyses the reduction of peroxiredoxin (Soriano et al., 2009, 2008) from peroxiredoxin I to IV, but not V and VI (Woo et al., 2005). Peroxiredoxin VI has an ARE sequence and thus is upregulated with Nrf2 pathway activation (Chowdhury et al., 2009).

Glutathione system and xCT

Glutathione (GSH) is an antioxidant mainly produced by astrocytes and released in the extracellular space where it can reduce ROS (Drukarch et al., 1998). GSH secretion by astrocytes enhances neuronal levels of GSH (Bolaños et al., 1996; Dringen et al., 1999) however, neurons cannot uptake GSH directly. GSH derives from cysteine that is unstable in the extracellular space and becomes oxidized in cystine (Meister, 1995). There, cystine can be taken up by neurons via the glutamate-cystine antiporter (xCT) and then transformed back to GSH (Fig 1.8; Dringen et al., 1999).

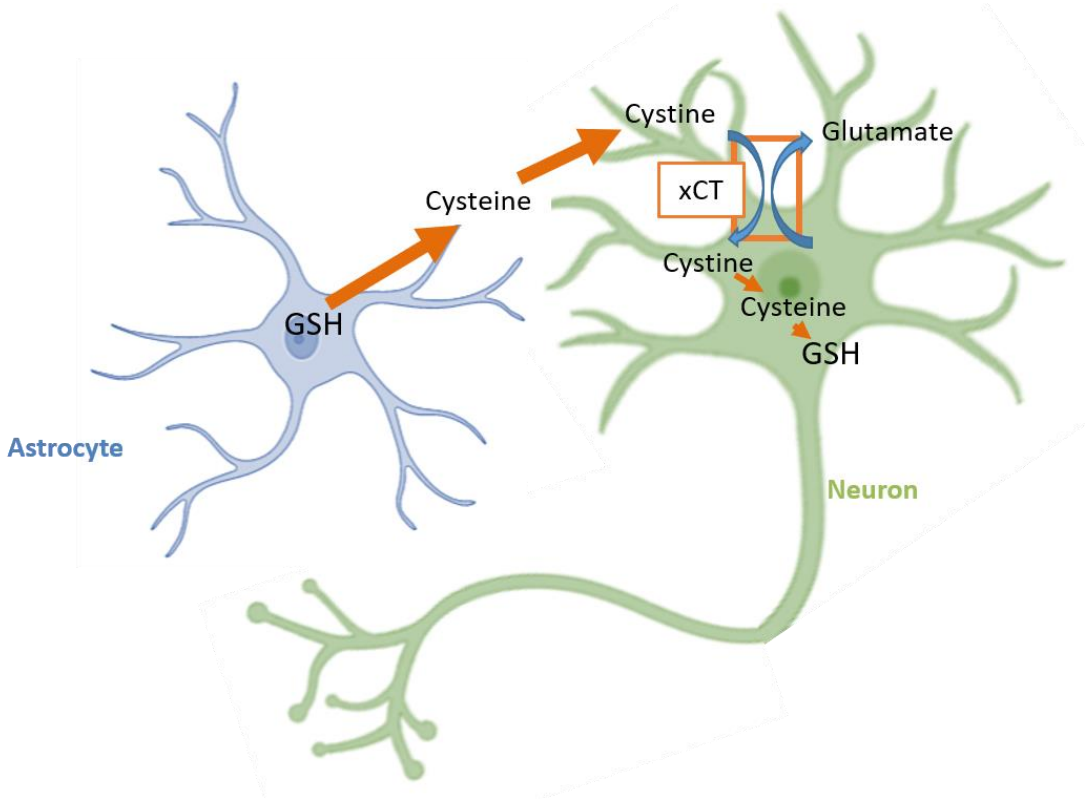

Figure 1-8 Indirect glutathione production from astrocyte increases neuronal glutathione levels (GSH).

Glutathione expression depends on Nrf2-signalling (McMahon et al., 2001). Gene precursors of GSH and xCT both contain ARE sequences and thus are upregulated with Nrf2-signalling activation (Sasaki et al., 2002). GSH knockout increases cell death but it is rescued with forced expression of xCT by transfection (Mandal et al., 2010). Itself, xCT protects against lipid peroxidation, possibly because it reduces extracellular radicals (Banjac et al., 2008). Following ischaemia, there was increased oxidative stress in xCT knockout mice and aggravated infarct damage (Shibasaki et al., 2009).

1.3.1.3. Cells expressing Nrf2

Nrf2 is expressed in many organs and systems including the CNS, digestive system, female and male-sex organs, skin and endocrine organs and it is highly expressed in the muscles and kidney but also in heart, lungs, liver and brain (Fagerberg et al., 2014; Moi et al., 1994).

In the brain, Nrf2 is produced by neurons *in vitro* (Habas et al., 2013), but this production is repressed *in vivo* in adult neurons (Bell et al., 2015). Forced Nrf2 expression in neurons during

the early days of development leads to reduced synapse density, retarded electrophysiological maturation and outgrowth of dendritic arborescence. It was suggested that this detrimental effect of Nrf2 was mediated via the reduction of ROS (Bell et al., 2015). As ROS-pathways are crucial for synaptogenesis, neuronal differentiation during early life development (Bell et al., 2015; Hardingham & Do, 2016), Nrf2 repression in cortical neurons is a critical part of their development and synaptogenesis.

Nrf2 is also expressed in astrocytes (Habas et al., 2013), microglia (Rojo et al., 2010) and endothelial cells (Chen et al., 2003) in physiological conditions. After ischaemia, immunohistochemical double labelling studies show that Nrf2 is upregulated in microglia, astrocytes and neurons (Dang et al., 2012). However, this result is controversial since Nrf2 detection using immunohistochemistry lacks specificity (Kemmerer et al., 2015). Nrf2 is upregulated on the ischaemic side of rat brains (Srivastava et al., 2013) at 4 and 24 hours and other studies show an increase of HO1 at 4, 7 and 24 hours (Alfieri et al., 2013). However, alterations of Nrf2-signalling in the more chronic response to ischaemia have not been defined.

1.3.2. Nrf2 pharmacological activators and genetically modified models

1.3.2.1. Nrf2-signalling pharmacological activators

DMF/MMF

The FDA have approved Dimethyl fumarate (DMF) and its precursor monomethyl fumarate (MMF) for the treatment of multiple sclerosis. They exhibit antioxidant effects by activating Nrf2-signalling pathway (Scannevin et al., 2012). DMF releases Nrf2 from Keap1 by alkylation of several of its cysteines, whereas MMF is less efficient as it only alkylate one of Keap1 cysteine (Ahuja et al., 2016; Takaya et al., 2012).

In models of ischaemia, several papers reported a protective effect of DMF through Nrf2 activation. It reduced neurological deficits and infarct volume, glial activation, oxidative stress, BBB breakdown and thus reduced vasogenic oedema and peripheral immune cell infiltration (Kunze, 2017; Kunze et al., 2015; Lin et al., 2016; Liu et al., 2019; Yao et al., 2016). These effects were lost with in Nrf2 deficient mice (Kunze et al., 2015; Liu et al., 2019; Yao et

al., 2016) suggesting that the compound protective effects were dependant on the activation of Nrf2-signalling.

tBQH and Sulforaphane

Sulforaphane and *tert*-butyl hydroquinone (tBHQ) showed Nrf2-dependant protective effects after *in vivo* ischaemia or an oxidative challenge *in vitro* (Lee et al., 2003; Mao et al., 2018; Shih et al., 2005a). Both compounds are electrophiles that act to downregulate Nrf2 ubiquitination by reacting on the cysteine 151, 273 and 288 of Keap1 (Abiko et al., 2011; Hong et al., 2005; Kobayashi et al., 2006; Zhang & Hannink, 2003). In a model of ischaemia, tBHQ reduced infarct and improved neuroscore in a Nrf2-dependant manner (Shih et al., 2005) and Sulforaphane reduced lesion propagation, BBB breakdown and consequently reduced cognitive dysfunction (Alfieri et al., 2013).

Curcumin

Curcumin has been shown to have protective effects following ischaemia such as modulation of inflammation from pro- to anti-inflammatory (Liu et al., 2017), reduction of lesion volume, oxidative stress and oedema and improved neurological deficit (Li et al., 2016; Yang et al., 2009) and these effects were associated with activation of Nrf2 signalling. However, these publications did not prove that the protective effects of Curcumin were dependant on Nrf2. Curcumin acts via Nrf2-independent mechanisms such as iron-chelating properties (Jiao et al., 2009). This could be investigated by examining if the protective effects of curcumin are lost in Nrf2 knockout mice.

CDDO

Bardoxolone-methyl or 1-(2-cyano-3,12-dioxooleana-1,9[11]-dien-28-oyl) imidazole (CDDO-Im) protects from cell from oxidative stress-induced death *in vitro* (Bynum et al., 2015), and is a very potent activator of Nrf2-signalling (Kensler & Wakabayashi, 2010; Liby et al., 2005). However, it also has many Nrf2-independent protective effect (Walsh et al., 2014).

Furthermore, triterpenoids, such as CDDO, have cytotoxic effects in high doses (Kensler & Wakabayashi, 2010; Liby et al., 2005; Liby et al., 2007; Magesh et al., 2012).

Limitation of these Nrf2-signalling activators

Many activators of Nrf2-signalling exist but they can also have Nrf2-independent effects. For example, DMF is known to additionally modulate HCAR2 signalling, IκB kinase, transforming growth factor-β signalling (Kensler & Wakabayashi, 2010; Liby et al., 2007; Parodi et al., 2015). Interestingly, inflammation also activates IκB kinase, transforming growth factor-β signalling (Amantea et al., 2015; Islam et al., 2018; Kondylis et al., 2017), and they are also modulated with oxidative stress (Barcellos-Hoff & Dix, 1996; Korn et al., 2001; Leonardi et al., 2000). Electrophiles, such as DMF, Sulforaphane and tBHQ, can react with other proteins on the sulfhydryl groups of their cysteine or on amino and hydroxyl group of nucleic acid that leads to carcinogenicity and genotoxicity (Abed et al., 2015; Magesh et al., 2012). ARE inducers in general have cytotoxic effect in high dose (Dimmock et al., 1999; Kensler & Wakabayashi, 2010; Magesh et al., 2012). Finally, a review found that non-natural Nrf2-pathway activators have oxidative effects (Eggler et al., 2008).

In conclusion, pharmacological compounds that activate Nrf2-signalling can be limited due to their off-target effects and their potential toxicity.

1.3.2.2. Nrf2-repressing models

In order to investigate the potential protective role of Nrf2 signalling, genetic modification of Nrf2 expression levels is a more specific tool than pharmacological compounds that activate Nrf2-signalling. The first models developed to study the modification of Nrf2 were designed by knock out the gene of interest or its translation to a protein using RNA silencing.

Nrf2 Knock-out

Following ischaemia, Nrf2 KO animals had increased inflammation and worsened neurological deficits compared to wild-type animals (Rojo et al., 2010; Sandberg et al., 2014;

Shah et al., 2007). It was also reported that Nrf2 KO mice had increased infarct volume compared to wild-type at 24 hours following 90 minutes ischaemia or at 48 hours or 7 days following permanent ischaemia (Shah et al., 2007; Shih et al., 2005; Wang et al., 2012). However, another paper did not find a detrimental effect on infarct volume in Nrf2 KO mice at 24 hours following 60 minutes ischaemia (Narayanan et al., 2015). In Shih et al (2005), Nrf2 KO mice had greater infarct in the cortex 7 days after permanent distal MCAo but not at 24 hours (Shih et al., 2005). Altogether, these findings suggest that Nrf2 KO detrimental effect on the lesion volume depends on the survival time or duration of ischaemia (see table 1.2). In the same manner, neurological deficits were greater in Nrf2 KO mice compared to wild-types at 24 hours following 90 minutes ischaemia (Shah et al., 2007) whereas it has no effect at 1 hour after 90 minutes ischaemia or at 48 hours following permanent ischaemia (Shah et al., 2007; Wang et al., 2012). Therefore, the main difference in these papers was due to changes in the severity of the ischaemia (60 minutes compared with 90 minutes or permanent occlusion) and survival time points (1 hour versus 24 hours, and 24 hours versus 7 days).

		Survival			
		24 hours	**48 hours**	**7 days**	**References**
MCAo duration	**60 minutes**	equal			Narayanan et al., 2015
	90 minutes	increased			Shah et al., 2007
	Permanent	equal		increased	Shih et al., 2005
	Permanent		increased		Wang et al., 2012

Table 1-2 Infarct volume of Nrf2 knockout mice compared to wild-types following ischaemia.

In diverse conditions, Nrf2 knock-out mice had either equal or increased infarct volumes compared to wild-types (Narayanan et al., 2015; Shah et al., 2007; Shih et al., 2005; Wang et al., 2012).

Lack of Nrf2 from birth might lead to the development of compensatory mechanisms (El-Brolosy & Stainier, 2017). This finding stimulated the development of alternative methods such as conditional knock-out, to allow temporal or spatial control of Nrf2 knockout, or silencing models. Furthermore, Nrf2-KO models can be cell specific, allowing a clearer understanding of the cell interaction mechanisms at stake.

Nrf2 knock-out (KO) models have also been used to prove the Nrf2 dependent mechanisms of action of pharmacological compounds targeting Nrf2 signalling. For example, DMF, Sulforaphane or tBHQ were found protective in models of increased oxidative stress, cerebral

haemorrhage, hypoxia/ischaemia but not when administered to Nrf2 KO mice (Jakel et al., 2007; Lin et al., 2016; Scannevin et al., 2012; Zhao et al., 2007). *In vitro*, Nrf2 KO cells showed increased vulnerability to oxidative stress and mitochondria dysfunction (Jakel et al., 2007; Lee et al., 2003; Lee et al., 2003b; Narayanan et al. , 2015).

Silencing Nrf2 by interfering with its RNA

Small interfering RNA (siRNA) and short hairpin RNA (shRNA) have been predominantly used *in vitro* to test whether a drug has protective effects that were dependant on the Nrf2-signalling pathway. Many drugs lose their protective effects when administered in combination with Nrf2 siRNA (Ding et al., 2014; Jing et al., 2013; Kunze et al., 2015; Li et al., 2018; Ling et al., 2015; Wang et al., 2016). For some compounds, Nrf2 signalling was found to act in concert with other signalling pathways to mediate the protective effect of that drug (Hao et al., 2013; Hu et al., 2018).

Some Nrf2 activators showed anti-inflammatory effects, for example by reducing pro-inflammatory cytokines following LPS treatment, but with Nrf2 silencing, they lose effect using microglial or endothelial cell cultures (Li et al., 2018; Wang et al., 2018). Furthermore, Nrf2 siRNA increased toxicity and reduced cell viability after oxidative injury (Yang et al., 2017; Zhang et al., 2010) and LPS-induced decreased BBB proteins (Li et al., 2018). Interestingly, in most papers there is no difference in cell viability when comparing an injury coupled with Nrf2 siRNA, to the injury alone, meaning that silencing Nrf2 does not worsen the injury: One paper did an injection of LPS *in vivo* on the cardiac muscle cells (Hao et al., 2013), and the other an OGD *in vitro* on cortical neurons (Ling et al., 2015). In the same manner, inflammatory levels were not worsen following LPS treatment with Nrf2 silencing compared to LPS alone (Li et al., 2018; Wang et al., 2018).

SiRNA has also been used to determine the potential detrimental effect of Nrf2 silencing. In an *in vivo* accelerated senescence model, Nrf2 siRNA increased glial response and worsened cognitive functions (Ren et al., 2018). Two papers used Nrf2 silencing in combination with MCAo models. Nrf2 siRNA increased pro-inflammatory and pro-apoptotic proteins (Hou et al., 2018) and reduced the protective effect of hyperbaric oxygen preconditioning (Xue et al., 2016).

The worsening effect of Nrf2 siRNA is found in the *in vivo* papers working on brain cells (Hou et al., 2018; Ren et al., 2018; Xue et al., 2016); whereas the equal cell viability or inflammation comparing an injury coupled with Nrf2 siRNA, to the injury alone, is observed either *in vitro* or *in vivo* on cardiomyocytes (Hao et al., 2013; Li et al., 2018; Ling et al., 2015; Wang et al., 2018).

1.3.2.3. Models boosting Nrf2 expression

Injection of Nrf2 adenovirus/lentivirus

In a mouse model of Alzheimer's disease, Nrf2 overexpression by adenovirus or lentivirus reduced amyloid-β-induced apoptosis, decreased astrocyte activation and improved spatial learning (Kanninen et al., 2009, 2008; Wang et al., 2014). Nrf2 overexpression also reduced the neuronal lesion caused by mitochondria dysfunction mediated by *in vivo* injection of the mitochondrial complex inhibitor malonate (Calkins et al., 2005; Shih et al., 2005b). Furthermore, Nrf2 overexpression by adenovirus or lentivirus reduced cell vulnerability to oxidative stress and glutamate toxicity (Dowell & Johnson, 2013; Jakel et al., 2007; Kraft et al., 2004; Li et al., 2005; Shih et al., 2005b).

Overexpression of Nrf2 in astrocytes: the GFAP-Nrf2 model

Astrocytes are known for their support to neurons and especially their production of antioxidants (Baxter & Hardingham, 2016). Neurons have very little antioxidant defences and notably Nrf2 (Shih et al., 2003). Co-cultured with astrocytes, neurons have greater survival, development of branching and are less sensitive to oxidative challenge compared to neurons on their own (Shih et al., 2003; Kraft et al., 2004). Indeed, neurons have very little antioxidant defences and notably Nrf2 compared to astrocytes (Baxter & Hardingham, 2016; Bronstein et al., 1995; Desagher et al. 1996; McNaught & Jenner, 1999; Min et al., 2006; Tanaka et al., 1999; Shih et al., 2003). Furthermore, neuron survival to an oxidative challenge was improved with the presence of astrocytes, an effect that was abolished with depletion of glutathione, suggesting a pivotal role for both astrocytes and glutathione production for neuron survival (Drukarch et al., 1997). As explained previously, glutathione is an antioxidant that is produced

by astrocytes which enhances neuronal levels of glutathione (Bolaños et al., 1996; Dringen et al., 1999). Glutathione expression depends on Nrf2-signalling as its precursors and uptake receptor have ARE sequences (McMahon et al., 2001; Sasaki et al., 2002). Furthermore, activation of Nrf2-signalling with pharmacological compounds predominantly targetted astrocytes but not neurons (Eftekharpour et al., 2000; Johnson et al., 2002; Murphy et al., 2001) and Nrf2 adenovirus is selectively taken up by astrocytes and not neurons (Kraft et al., 2004).

Glutamate toxicity can be reduced if neurons are co-cultured with glia; and this protective effect is lost if Nrf2 is knocked out (Shih et al., 2003). Nrf2 adenovirus is selectively up taken by astrocytes preferentially compared to neurons (Kraft et al., 2004). Furthermore, tBHQ treatment increased neuronal survival following an oxidative challenge and this was mediated through Nrf2 activity in astrocytes (Kraft et al., 2004). Taken together, these papers suggest a pivotal role of astrocytes to rescue neurons during oxidative challenges. Furthermore, pharmacological activation of Nrf2-signalling predominantly has effects on astrocytes but not neurons (Eftekharpour et al., 2000; Johnson et al., 2002; Murphy et al., 2001). Neurons have very little Nrf2 and its related proteins compared to glia (Shih et al., 2003).

In order to find therapies for ischaemia, the concept of preconditioning emerged. It is defined by a brief, sub-lethal injury that can improve the tolerance to neurons to a subsequent, lethal injury (Dirnagl et al., 1999). A preconditioning of 90 min OGD performed 24 hours before another OGD insult lead to 66% decreased in cell death compared to non-conditioned neurons (Bell et al., 2011a). Interestingly this effect was lost in Nrf2 KO cocultures. Bell et al. (2011) then went on investigate Nrf2 signalling in preconditioning and found increased expression of glutathione system genes both *in vivo* and *in vitro* (Bell et al., 2011b). Taken together, most of the papers cited above found glutathione as one of the most prominent Nrf2-downstream system in the astrocyte neuroprotection. However other studies revealed astrocytic neuroprotection with Nrf2 activation via HO1 in the context of ischaemic insults and oxidative challenge (Alfieri et al., 2013; Bergeron et al., 1997; Min et al., 2006).

These discoveries led to the development of a model that overexpressed Nrf2 specifically in astrocytes using a GFAP promoter (GFAP-Nrf2). This model has been used to study the protective effect of astrocytic Nrf2 overexpression in amyotrophic lateral sclerosis (ALS)

models. This disease is characterised by the degeneration of motor neurons during adulthood, leading to progressive muscle control loss and eventual death from respiratory failure (Kiernan et al., 2011). The most widely used mouse model of ALS is obtained by expressing a mutation of superoxide dismutase 1 (SOD1) that causes rapid degeneration of motor neurons, paralysis and eventually death (Morrice et al., 2018). Firstly, co-culturing motor neurons with primary astrocytes overexpressing Nrf2, motor neuron survival was increased, an effect that was lost with glutathione inhibitor or activity. Secondly, by crossing the SOD1 ALS mouse model with the GFAP-Nrf2 model, motor neuron degeneration was prevented, mouse survival was increased and the onset of disease symptoms was delayed compared to ALS mice (Vargas et al., 2008).

Parkinson's disease is a progressive neurodegenerative disease that primarily causes tremor and then impaired movement, posture, balance and speech. It is characterised by an accumulation of misfolded alpha-synuclein proteins that lead to degeneration of dopaminergic neurons involved in motor control (Konnova & Swanberg, 2018). Mouse models that can reproduce Parkinson's pathology involve expression of mutant alpha-synuclein, or injection of the mitochondrial complex inhibitor 1-methyl-4-phenyl-1,2,3,6-tetrahydropyridine (MPTP) that damages dopaminergic neurons in the substantia nigra (Chen et al., 2009). Nrf2 signalling pathway was increased in the substantia nigra and decreased in the striatum 2 days after 5 days injection of MPTP. Furthermore, dopaminergic neurons were lost with MPTP injection, and further decreased in Nrf2 deficient mice compared with wild type mice (Chen et al., 2009). However, when MPTP was administered to GFAP-Nrf2 mice, there was reduced neuronal toxicity compared to wild-type animals. In addition, crossing GFAP-Nrf2 mice with the mutated alpha-synuclein model resulted in increased mouse survival and motor neuron viability in crossed animals compared with the disease model controls. This protective effect was associated with a reduction of alpha-synuclein accumulation, oxidative stress and glial activation (Gan et al., 2012).

Alexander's disease is a neurodegenerative disease due to a mutation in the GFAP gene that causes developmental delays, seizures and juvenile death (Brenner et al., 2001; Prust et al., 2011). A mouse model of Alexander's disease involving expression of human mutant GFAP demonstrates similar pathophysiologic features: increased GFAP protein and mRNA levels, neurotoxic astrocytic protein aggregates called Rosenthal fibres, seizures and oxidative stress. When mutant GFAP mice were crossed with GFAP-Nrf2 mouse model, there was

decreased GFAP protein and mRNA levels, reduced Rosenthal fibres and increased body mass (LaPash Daniels et al., 2012).

Malonate is an inhibitor of mitochondrial function that damages neurons and induces oxidative stress and glial activation (Calkins et al., 2010; Calkins et al., 2005; Shih et al., 2005b). Following instrastrial injection of malonate *in vivo*, wild-type animals developed a small lesion with increased Nrf2 signalling around it. Malonate injection into Nrf2 KO animals produced a larger lesion and Nrf2-signalling was minimal (Calkins et al., 2010). However, when malonate was injected into GFAP-Nrf2 animals, neuronal damage was decreased, and this was paralleled by increased Nrf2-signalling activity around the lesion compared with wild type mice.

Hypoperfusion induced by bilateral common carotid stenosis leads to 40% reduction of cerebral blood flow, an impairment in spatial working memory, white matter damage and inflammation in the optic tract (Sigfridsson et al., 2018). However, when hypoperfusion was induced in GFAP-Nrf2 mice, astrocytic overexpression of Nrf2 improved cognitive deficits, reduced white matter damage, dampened microgliosis and astrocytosis and complement component C1q and C4 in the optic tract when compared with wild type mice.

Collectively, these studies suggest that astrocytic overexpression of Nrf2 can reduce oxidative stress and inflammation in a diverse range of neurodegenerative models. *In vitro* models that mimic aspects of focal cerebral ischaemia suggest that astrocytic Nrf2 may mediate neuroprotective effects, however this has not been investigated in an *in vivo* model of ischaemia.

1.3.3. Beneficial effects of Nrf2-signalling following ischaemia

Ischaemia/reperfusion is not always possible due to the limited time window, and if reperfusion is possible, the oxygen flow can increase ROS (Enzmann et al., 2018). Thus, antioxidant and anti-inflammatory therapy has been of an area of research to develop an adjunct to thrombolysis or thrombectomy.

As previously explained, Nrf2-silencing models tend to show a detrimental effect of the lack of Nrf2 suggesting a pivotal role of Nrf2 in the endogenous protective response against

injuries. Conversely, pharmacological compounds that activate Nrf2-signalling and Nrf2 overexpressing models protect neurons against oxidative stress, inflammation and consequently improved neurological function. The beneficial effects of Nrf2 following ischaemia are reviewed in this section.

1.3.3.1. Nrf2-signalling modulation following ischaemia

Activation of Nrf2 signalling can lead to increased transcription of antioxidant genes such as *GSH, HO1, srxn1* or *NQO1*. These Nrf2-dependent genes are found to be upregulated from 4 hours to 3 days post ischaemia (Alfieri et al., 2013; Bell et al., 2011a; Bell et al., 2011b; Ding et al., 2014; Tanaka et al., 2010; Yang et al., 2009). The gene that encodes Nrf2 itself was also upregulated in the lesion 4 to 72 hours after the onset (Alfieri et al., 2013; Lin et al., 2016; Srivastava et al., 2013; Zhai et al., 2013) because Nrf2 has an ARE sequence in its gene (Kwak et al., 2002; Raghunath et al., 2018), suggesting auto-regulation. At the same time, Keap1 was decreased from 2 to 72 hours (Ling et al., 2015; Tanaka et al., 2010). Similar finding were reported from *in vitro* studies that demonstrated that OGD increases oxidative stress, which in return releases Nrf2 from keap1, permitting the activation of the Nrf2-signalling pathway (Itoh et al., 1997).

Looking closely at the spatial distribution of Nrf2 alterations, it was upregulated in the peri-infarct of the ischaemic lesion (Alfieri et al., 2013; Dang et al., 2012; Srivastava et al., 2013; Tanaka et al., 2010), and has been reported to be upregulated in microglia, astrocytes and neurons after ischaemia (Alfieri et al., 2013; Bergeron et al., 1997; Dang et al., 2012; Min et al., 2006).

HO1 and Nrf2 proteins levels peaked during the first week (Alfieri et al., 2013; Lin et al., 2016; Mao et al., 2018) and tended to return to baseline at 14 days (Lin et al., 2016). However, no investigation on Nrf2 levels has not been conducted beyond that time point.

Article	Animals	Type	Duration	Quantification	Nrf2 increased	Nrf2-related genes upregulated	Keap1 decreased
Yang et al., 2009	SD rats	pMCAo	perman.	Prot. & mRNA	from 3 h to 72 h	HO1 is increased from 3 h to 72 h	
Tanaka et al., 2010	ICR mice	tMCAo	60 mins	positive-cell count	at 8, 24, 72 h		at 2, 8, 24 and 72 h
Bell et al., 2011a	C57Bl/6J mice	tMCAo	15 mins	mRNA		hmox1 and srxn1 upregulated at 4 h	
Bell et al., 2011b	C57Bl/6J mice	tMCAo	15 mins	mRNA		gclc, gclm, slc7a11 upregulated at 4 h	
Alfieri et al., 2013	SD rats	tMCAo	70 mins	immuno-reactivity	at 4, 24 but not 72 h	HO1 increased at 4, 24 and 72 h	
Srivasta et al., 2013	SD rats	tMCAo	70 mins	nuclear Nrf2	at 24 h		
Zhai et al., 2013	SD rats	tMCAo	90 mins	prot. & mRNA	at 24 h		
Ding et al., 2014	SD rats	tMCAo	120 mins	prot. & nuclear Nrf2	at 48 h	HO1 increased at 48 h	
Ling et al., 2015	SD rats	tMCAo	60 mins	prot. & nuclear Nrf2	at 3 d		at 3 d
Lin et al., 2016	SD rats	tMCAo	120 mins	prot.	at 3, 7 d but not 14 d	HO1 increased at 3 and 7 d but not 14 d	
Wu et al., 2017	SD rats	tMCAo	60 mins	prot.	at 24 h	NQO1, srxn1 and prdx increased at 24 h	
Mao et al., 2018	SD rats	2VO	perman.	prot. & nuclear Nrf2	at 3 and 7 d	HO1 increased at 3 and 7 d	
Liu et al., 2019	C57Bl/6J mice	CCAo + hypoxia	60 mins	prot. & mRNA	at 6, 12, 24 h	HO1 & NQO1 increased at 6, 12, 24 h	

Table 1-3 Summary of the modulation of Nrf2, Keap1 and Nrf2-related protein following ischaemia.

Abbreviated as follow, for the animal and model: SD: Sprague-Dawley rats; 2VO: bilateral common carotid arteries occlusion; CCAo: common carotid artery occlusion; tMCAo: transient middle cerebral artery; Perm.: permanent; Prot.: protein; h: hours; d: days.

For the Nrf2-related genes: HO1: heme oxygenase 1; NQO1: NAD(P)H dehydrogenase quinone 1 (gene nqo1), Gclc: Glutamate—cysteine ligase catalytic subunit gene; Gclm: glutamate-cysteine ligase modifier subunit gene; slc7a11: xCT gene; srxn1: sulfiredoxin1.

1.3.3.2. Antioxidant effect of Nrf2-signalling following ischaemia

Nrf2 overexpression reduced cell vulnerability to oxidative stress during oxidative challenge (Jakel et al., 2007; Kraft et al., 2004; Li et al., 2005; Shih et al., 2005b). This is explained by the transcription role of Nrf2 that leads to the upregulation of a battery of cytoprotective genes and notably antioxidants such as NQO1, srxn1 and xCT (Banjac et al., 2008; Dinkova-Kostova & Talalay, 2010; Soriano et al., 2009; Soriano et al., 2008; Zhu et al., 2012). Repressing Nrf2 expression increased the vulnerability to oxidative stress, reducing cell viability after oxidative injury after ischaemia or oxidative challenge (Zhang et al., 2010; Jakel et al., 2007; Lee et al., 2003b; Narayanan et al., 2015). In addition, pharmacological activators of Nrf2-

signalling reduced oxidative stress resulting from ischaemia (Alfieri et al., 2013; Li et al., 2016; Yao et al., 2016; Jakel et al., 2007; Lin et al., 2016; Scannevin et al., 2012; Zhao et al., 2007; Kunze, 2017; Kunze et al., 2015; Liu et al., 2019; Bynum et al., 2015).

As previously explained in section 1.3.2.3, the neuroprotective effect of Nrf2 is dependent on astrocytes and notably through antioxidant upregulation (Shih et al., 2003; Kraft et al., 2004). Furthermore, activation of Nrf2-signalling with pharmacological compounds predominantly targetted astrocytes but not neurons (Eftekharpour et al., 2000; Johnson et al., 2002; Murphy et al., 2001) and Nrf2 adenovirus is selectively taken up by astrocytes and not neurons (Kraft et al., 2004).

1.3.3.3. Nrf2 and Inflammation

Nrf2 and its role on polarisation of glial cells

Besides the production of a battery of antioxidants, Nrf2-signalling has anti-inflammatory effects. In response to oxidative stress, Nrf2 can modulate microglial phenotype by elevating Nrf2, HO1, srxn1 and thioredoxin1 protein production (Kadl et al., 2010). In presence of heme elements, microglia switch to a phenotype that produces more HO1 (Boyle et al., 2012). HO1 has been discovered to alter the phenotype of macrophages to an anti-inflammatory phenotype (Naito et al., 2014). Furthermore, in the absence of Nrf2, pro-inflammatory cytokine production is increased and anti-inflammatory cytokines are reduced in a Parkinson's disease model (Rojo et al., 2010). Nrf2-signalling pharmacological activation or forced expression lead to decreased pro-inflammatory cytokine production whereas anti-inflammatory cytokine production is increased (Kobayashi et al., 2016; Liu et al., 2017; Peng et al., 2016; Liu et al., 2019).

Nrf2-signalling modifies the glial response following ischaemia

Following ischaemia, astrocytes and microglia are activated in the lesion and they produce pro- and anti-inflammatory cytokines. Interestingly, pharmacological activation of Nrf2-signalling with Ginseng, DMF or MMF causes a modulation of the glial response to ischaemia

(Lin et al., 2016; Liu et al., 2019; Yao et al., 2016). Lin and colleagues (2016) found a 50% decrease in microglia/macrophage activation 3 and 7 days after ischaemia in the penumbra of mice treated with DMF compared to vehicle treated mice (Lin et al., 2016). Furthermore, Yao and colleagues also reported a reduction of GFAP and Iba1-positive cells using DMF and MMF (Yao et al., 2016) in a model of ischaemia. More recently, Nrf2-signalling activators Ginseng and DMF were shown to alter the glial response after ischaemia, however they found different results depending on the time point (Liu et al., 2019), with increased GFAP staining and cell number at 24 hours and decreased GFAP staining without an alteration to GFAP-positive cell number at 6 hours. On the other hand, microglia/macrophage staining Iba1 was reduced with both activators at 6 and 24 hours.

BBB leakage, immune cell infiltration and Nrf2

Nrf2 knockout increases vasogenic oedema and decreases AQP4 expression (Liu et al., 2019; Yao et al., 2016), whereas Nrf2 activation reduces vasogenic oedema (Alfieri et al., 2013; Clausen et al., 2017; Kunze et al., 2015; Li et al., 2016; Liu et al., 2019; Yang et al., 2009; Yao et al., 2016), increases BBB proteins occludin, claudin-5, AQP4 and reduces MMP9 after ischaemia (Kunze et al., 2015; Liu et al., 2019). Furthermore, DMF reduced neutrophil and T cell infiltration from 3 to 14 days after ischaemia (Lin et al., 2016).

1.3.3.4. Nrf2 and its potential role to ameliorate functional recovery and cognition after ischaemia

Sensorimotor recovery after ischaemia is improved by Nrf2-signalling activation or Nrf2 overexpression

Deficiency of Nrf2 in Nrf2-knockout mice or silencing of srxn1 RNA led to neurological deficits (Shah et al., 2007, Wu et al., 2017) after ischaemia. Although it has been reported that there is an increased infarct volume with knockout of Nrf2, there was no significant difference on neurological deficit score (Wang et al., 2012). Furthermore, these authors found that trichostatin A, an inhibitor of histone deacetylase, activated Nrf2-signalling, reduced the cortical infarct and neurological deficits 2 days after ischaemia.

Other studies using pharmacological activators of Nrf2 signalling have demonstrated reductions of neurological deficits: lipoxin A4 improved neurological scores at 24 hours (Wu et al., 2013), DMF improved neurological score from 3 to 14 days after ischaemia (Lin et al., 2016) and RS9 improved motor recovery at 24 hours after ischaemia (Yamauchi et al., 2016). More importantly, some papers found that the reduction of neurological deficits with Nrf2 activators DMF, MMF, Ginseng and tBHQ were lost in Nrf2 deficient mice (Liu et al., 2019; Shih et al., 2005a; Yao et al., 2016).

Nrf2-signalling activation ameliorates cognitive functions after ischaemia

Very few papers focus on potential protective effects of Nrf2-signalling on cognitive impairment after ischaemia. Of these few, Sulforaphane improved cognitive function after ischaemia (Mao et al., 2018) and glutathione improved discrimination in novel object recognition (NOR) after ischaemia (Yabuki & Fukunaga, 2013). However, these papers do not use RNA silencing or genetic KO to prove the direct and sole effect of Nrf2 signalling on cognition.

Finally, Nrf2 overexpression models using lentiviral Nrf2 transfection showed improved spatial memory in AD model (Kanninen et al., 2009; Wang et al., 2014) and Nrf2 overexpression in astrocytes improved spatial memory following hypoperfusion (Sigfridsson et al., 2018). However, the effects of boosting Nrf2 in astrocytes has not been tested on a mouse model of focal cerebral ischaemia.

1.4. Summary

Ischaemia is known to raise the risk of neurodegeneration and dementia. Two major mechanisms triggered by cerebral ischaemia may be involved: neuroinflammation and oxidative stress. Nrf2-signalling pathway has been highlighted as an important therapeutic target as it reduces oxidative stress and inflammation. Nevertheless, there are gaps in the literature about the chronic state of this pathway after ischaemia. Furthermore, this pathway is upregulated at acute stage after ischaemia because of oxidative conditions. Pharmacological activation of Nrf2-signalling can cause “off-target” effects. Astrocytes have

an important role in the production of antioxidants to protect neurons. Furthermore, Nrf2-signalling is preferentially activated in astrocytes during ischaemia or oxidative challenges and astrocytes are necessary for the neuroprotective effect of Nrf2. The GFAP-Nrf2 model is found to reduce oxidative stress, inflammation and neurodegeneration in a number of models of neurodegenerative diseases; it can be used to address specific questions about Nrf2 mediated astrocyte-neuronal interactions; however, it has never been used for ischaemia.

1.5. Global hypothesis

This work has been designed to test the hypothesis that boosting the Nrf2 pathway in astrocytes will prevent oxidative stress and pro-inflammatory damage caused by ischaemia/reperfusion and thereby diminish cognitive deficits and neurodegeneration that may lead to dementia.

1.5.1. Aims:

This thesis will be divided in three parts. Firstly, a characterisation of a mouse model of ischaemia will be undertaken to investigate alterations to Nrf2-signalling at acute and chronic time points, and how it parallels with alterations in oxidative stress and inflammatory glial cell changes. The second chapter will focus on the use of a model where Nrf2 is specifically overexpressed in astrocytes (GFAP-Nrf2) to determine if it has neuroprotective effects in the acute response to ischaemia. Furthermore, the effects of boosting astrocytic Nrf2 will be determined on inflammatory glial cell activation, inflammatory cytokine production and oxidative stress. Finally, the effects of boosting astrocytic Nrf2 will be studied in the chronic response to ischaemia to determine if there is a protective effect on neurological function, cognition, neurons, oxidative stress and inflammation.

2. Material & Methods

2.1. Mice

2.1.1. GFAP-Nrf2 mice

GFAP-Nrf2 transgenic mice were made in Prof. Jeffrey Johnson's laboratory at the University of Wisconsin (Vargas et al., 2008). The mice overexpress Nrf2 under the control of a GFAP promoter. This has been achieved by using a pCMV*β* plasmid (BD Biosciences) excised of its CMV promoter to be replace with a custom multiple cloning site with insertion of hGFAP promoter containing the mNrf2 sequence from a pEF-Nrf2. The construct was microinjected on fertilised eggs on B6/SJL background which is a cross between a C57BL/6J (B6) female and an SJL/J (SJL) male (Calkins et al., 2010; Gan et al., 2012). Transgenic mice were identified by genotyping ear or tail biopsies on NaOH-extracted DNA (50 mM at 100°C for 7 minutes) with a PCR of 35 cycles as follow: 30 seconds at 95°C, 30 seconds at 54°C and 30 seconds at 72°C; and a final extension of 5 minutes at 72°C. The PCR was performed using GoTaq Green Master Mix (M7822; Promega) and these primers: Nrf2 Left 5'-GCC TGA GAG CTG TAG GCC C–3', Nrf2 Right 5'-GGA ATG GAA AAT AGC TCC TGC C-3', GFAP Forward: 5'-CTT CAT AAA GCC CTC GCA TC-3' and GFAP Reverse 5'-TCT TGC CTC CAA AGG ATG TC-3'. Nrf2 product is 262 bp and GFAP Product is 400 bp. The product was run on 2% agarose gel (v3121; Promega) prepared with Tris/Borate/EDTA buffer with an electrophoresis tank (Mini-Sub Cell GT Cell; Bio Rad). Mice were genotyped prior to surgery and genotype status was confirmed from tail samples at the end of the experiment.

2.1.2. Animal maintenance and use

Two to four months old male C57Bl/6J mice (Charles River, UK; 25 - 30g) or GFAP-Nrf2 (with C57Bl/6J background) were used. Animals were group housed on a 12:12 hr light/dark cycle and had access to food and water ad libitum. All experiments were conducted in accordance with the Animals (Scientific Procedures) Act 1986 and local ethical approval at the University of Edinburgh and were performed under personal and project licenses granted by the Home Office. The experiments were performed following the ARRIVE guidelines (Kilkenny et al., 2010; www.nc3rs.org.uk/arrive-guidelines). All animals were randomly assigned into groups using random function in Microsoft Excel. The function generate a number between 0 and 1

for each animal, when above 0.5, it was assigned as an ischaemic animal. All data collection and analysis were performed by experimenter blind to the group.

2.2. Focal cerebral ischaemic model

Animals were subjected to a transient focal ischaemia by an occlusion of the right middle cerebral artery (MCAo) for different duration of ischaemia (15, 30 or 60). Mice were initially anaesthetised in an induction box with 5% isoflurane in a mix of 30% oxygen and 70% nitrous oxide before isoflurane levels were reduced to 1.5-2% during the operation. To induce the occlusion, the protocol from Hata and colleagues was followed (Hata et al., 1998). The right common carotid (CCA), external carotid (ECA), and internal carotid (ICA) arteries and their branches were exposed through a midline cervical incision. A 6–0 silk suture was tied around the CCA proximal to the bifurcation of the ECA and ICA and then a second suture tied around the ECA distal to the superior thyroid artery (STA). The STA and occipital artery (OA) were closed by electrocoagulation. A silicone-coated monofilament (diameter 220 μm) was introduced into the CCA via a small incision and advanced 10mm distal to the carotid bifurcation to occlude the MCA (Monofilament 6-0 medium A MCAO suture L34 PK10; Doccol). The sham procedure involved the operation without the insertion of the thread. To withdraw the thread, mice were re-anaesthetised with isoflurane anaesthesia as before. After wound was sutured, the anaesthesia was discontinued, and mice received 0.5ml saline (0.9%) subcutaneously by injection before being transferred to an incubator (30 °C) for 2 hours. The mice were weighed and monitored every day in order to assess the severity of the ischaemia injury. All ischaemia surgery was undertaken by Dr Jill Fowler who was blinded as to genotype. Aseptic techniques were used.

2.2.1. Inclusion/exclusion criteria

Animals that underwent MCA occlusion but had no evidence of ischaemic neuronal damage were excluded from the study. In addition, animals were excluded if their weight loss exceeded 25%, if they had a poor response to the procedure or if they presented signs of infarction, which is defined pan necrosis of cells and a cluster of infiltrated cells and glia in an atrophied lesion and is diagnosed post-mortem on haematoxylin and eosin staining.

2.3. Histology

Recipes for all reagents and buffers used are defined in the Appendix section 8.1. (i.e. phosphate buffer (PB), phosphate buffer saline (PBS), tris buffer (TB) and paraformaldehyde (PFA))

After 24 hours or 4 weeks of survival since the onset of ischaemia, animals were re-anaesthetised with 5% isoflurane in a mix of 30% oxygen and 70% nitrous oxide then transferred to a face mask where anaesthesia was maintained with 3% isoflurane during the operation. In order to perfuse the brain, the animals were transcardially perfused-fixed. The heart was exposed by dissection of the animal's thorax, accessed by cutting the skin below the sternum and the diaphragm. Once the needle was placed in the left ventricle, mice were perfused with 20 ml of 0.9% heparinised phosphate buffered saline followed by 20 ml of 4% paraformaldehyde (PFA) prepared in phosphate buffer (PB; made with mono-sodium phosphate NaH_2PO_4 and di-sodium phosphate Na_2HPO_4, purchased from Sigma). Shortly after the beginning of the perfusion, the right atrium was opened to allow for bleeding and to wash the blood from the body. The perfusion pump (PHD Ultra Syringe Pump, Harvard) infused solution at a rate of 2.1 ml/min. Animals were then decapitated and heads post-fixed in PFA 4% made in PB for 24 hours, followed by a further 2 hours in PFA 4% once the brain was dissected from the skull. Brains were then transferred to 30% sucrose in PBS for three days before freezing them in isopentane at -42 °C for 2 minutes. Twenty-µm sections were cut with a cryostat (CM1950. Leica) and retained in cryoprotective solution (30% glycerol, 30% Ethylene glycol in PB).

2.3.1. Lesion volume assessment

2.3.1.1. Haematoxylin and eosin (H&E)

Sections were washed in PBS and then dehydrated through a series of increasing concentrations of ethanol baths (70% for 2mins, 90% for 2 mins, 100% for 5 mins) to delipidise sections, then immersed in a xylene bath for 15 minutes followed by decreasing concentrations of ethanol baths (100% for 5 mins, 90% for 2 mins, 70% for 2 mins). The sections were incubated in haematoxylin (Harris) for 3 mins then differentiated in 1% acid alcohol (1% HCl in 70% ethanol) for 10 seconds. After 2 minutes in Scott's tap water substitute

(0.35% Sodium bicarbonate $NaHCO_3$ and 2% magnesium sulphate $MgSO_4$ in distilled water), the sections were placed in eosin (Shandon Eosin Y Alcoholic) for 1 minute. Finally, the sections were de-hydrated in increasing concentration of ethanol baths (70%, 90%, and 100%) for 15 minutes, 5 minutes and 5 minutes, placed in xylene for 10 minutes and coverslips mounted with DPX (Thermo Fisher).

2.3.1.2. Analysis of the lesion volume

Infarct volume (mm^3) was assessed using haematoxylin and eosin (H&E) stained sections, in addition to MAP2 and NeuN immunostaining. Nine coronal brain levels were used to calculate infarct volume (coordinates from Bregma +2.58; +1.54; +0.98; +0.74; -0.10; -1.06; -2.06; -2.92; -4.48 mm). Lesion area was mapped onto each coronal level on a line diagram (Fig. 2.1) and area (mm^2) calculated with Image J (Fiji, NIH). Lesion volume (mm^3) was calculated using area under the curve in GraphPad Prism (v7).

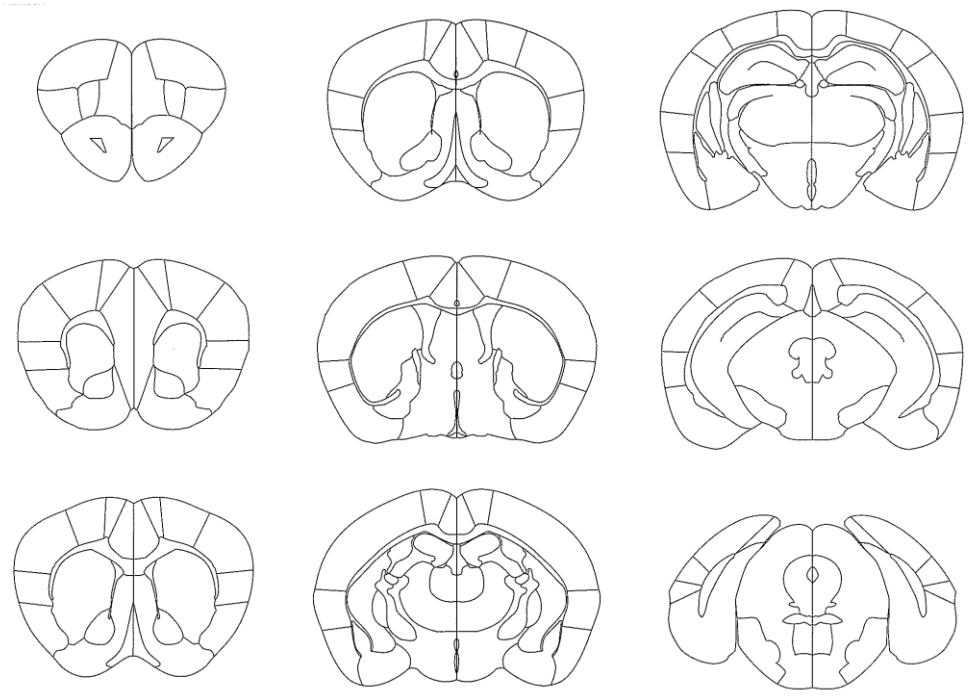

Figure 2-1 Nine coronal brain levels were used to map the infarct area.

(Distance to Bregma: +2.58; +1.54; +0.98; +0.74; -0.10; -1.06; -2.06; -2.92; -4.48).

2.3.2. Immunohistochemistry

2.3.2.1. Immunohistochemistry study of the quantifiable markers for light microscopy

Immunohistochemistry was performed on 3 sections of each brain representing three different levels of the brain (Bregma +0.98; -0.10; -2.06; Fig 2.2). After washing off the cryoprotective solution with phosphate buffer saline (PBS; PB with sodium chloride NaCl, purchased from Sigma; pH 7.4; 3 washes for 15 mins each), and tris buffer (TB; made with Trizma HCl and Trizma Base, purchased from Sigma; pH 7.6; 2 washes for 15 mins each) sections were floated out in Tris buffer and mounted on Superfrost slides (J1800AMNZ; Thermo fisher). To delipidise sections, slides went through a series of increasing concentrations of ethanol baths (70% for 2mins, 90% for 2 mins, 100% for 5 mins and 100% for 10 mins) and a xylene bath for 10 minutes. This was followed by two baths of 100% ethanol for 10 minutes and 5 minutes and a methanol and 3% H_2O_2 bath for 30 minutes to block endogenous peroxide activity. Sections were then blocked for 1 hour with 0.5% BSA (Sigma) and normal horse or goat serum (Vector) depending on the secondary antibody species. Triton X 0.3% was incorporated in the block to permeabilise sections for HO-1 staining. Then primary antibodies (see table 1) were diluted in the appropriate blocking solution and incubated overnight at 4 °C. A negative control omitting the primary antibody was used.

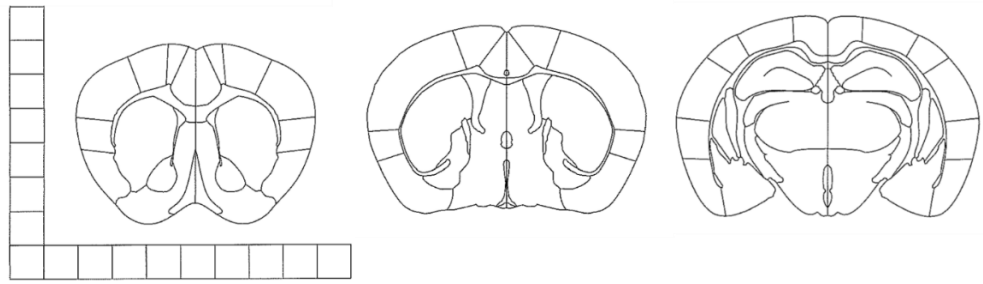

Figure 2-2 Three coronal level were selected to perform the immunohistology studies.

(Bregma +0.98; -0.10; -2.06; Scale: one square is 1mm²).

Sections were then washed two times for 10 minutes with PBS and incubated with the appropriate secondary antibodies (biotinylated-horseradish peroxidase-conjugated; purchased from Vector) used at 1:100 for 1 hour (see table 2.1). After another two times 10 minutes wash with PBS, the signal was amplified with an ABC kit (Vectastain, Vector, California) for 1 hour at room temperature. Finally, after a further two 10 minutes washes with PBS, the sections were stained with 3,3'-diaminobenzidine (DAB) in the presence of

hydrogen peroxide for 3 minutes (DAB Peroxidase Substrate kit, Vector, California). Slides were then rehydrated by different ethanol dilution baths (70% for 2mins, 90% for 2 mins, 100% for 5 mins and 100% for 5 mins) and a xylene bath for 10 minutes and hard mounted in DPX (Thermo fisher) with 1µm thick coverslips (VWR).

Target	Host	M/P	Brand	Reference	Dilution	Secondary	Reference
GFAP	Rat	Monoclonal	Invitrogen	Cat13-300	1:500 to 1000	Goat anti-rat	BA 9401
Iba1	Rabbit	Polyclonal	Menarini	MP 290 CR05	1:250 to 1000	Horse anti-rabbit	BA 1100
3-NT	Mouse	Monoclonal	Abcam	Ab61392	1:800	Horse anti-mouse	BA 2001
HO1	Rabbit	Polyclonal	αDiagnosic	ADI PSA 895	1:1000	Horse anti-rabbit	BA 1100
MAP2	Mouse	Monoclonal	Sigma	M9942	1:2000	Horse anti-mouse	BA 2001
NeuN	Mouse	Monoclonal	Merck	MAB377	1:8000	Horse anti-mouse	BA 2001
Neutrophils	Rabbit	-	-	SJC-neutrophil	1:10000	Horse anti-rabbit	BA 1100

Table 2-1 Antibodies used for immunohistochemistry study.

Microglia and macrophages were stained with Iba1 (Ionised calcium binding adapting molecule 1) antibody, reactive astrocytes were immunostained with a GFAP (Glial Fibrillary Acidic Protein) antibody, oxidative stress was evaluated via the study of peroxynitrite generation with 3-Nitrotyrosine (3-NT). To investigate neuronal damage, anti-MAP2 (microtubules associated protein 2) and anti-NeuN were used. The use of anti-NeuN required a 10 minutes citric acid heat-retrieval before the contact with the primary antibody. the sThe SJC-neutrophil antibody was kindly provided by Drs. Daniel Anthony and Sandra Campbell, University of Oxford, UK.

2.3.2.2. Immunofluorescence on mounted sections and free-floating sections

Microglia and macrophages were both stained with Iba1 antibody. To investigate the infiltration of macrophages in the parenchyma, the antibody anti-TMEM-119 was used (see table 2). The co-labelling of these markers was performed on free-floating sections of level 5 (Bregma -0.10) for each animal. Sections were washed 3 times 10 minutes in PBS to clear them from cryoprotectant. Then the sections were pre-treated with PBS-Triton X 0.1% for 15 minutes. The sections were blocked for two hours with 10% donkey serum and 10% horse serum in PBS at Room temperature. The primary antibodies were prepared in the block and left overnight at 4 °C overnight.

Target	Host	M/P	Brand	Reference	Dilution	Secondary	Reference
Iba1	Goat	Polyclonal	Abcam	Ab107159	1:250	Horse anti-goat biotinylated (1:100)	BA9500
						Then streptavidin anti-biotin AF546 (1:100)	S11225
TMEM119	Rabbit	Monoclonal	Abcam	Ab209064	1:500	Donkey anti-rabbit AF488 (1:500)	A21206

Table 2-2 Antibodies used for free-floating immunofluorescence.

The following day, sections were washed three times 10 minutes in PBS. Iba1 antibody was detected with biotinylated horse anti-goat at 1:100 prepared in PBS for an hour at room temperature. After a further three times wash with PBS, the fluorescent secondary antibodies were applied for an hour at room temperature. Before mounting, the sections were washed 10 minutes with PBS and two times 10 minutes with PB. Sections were mounted on Superfrost slides (J1800AMNZ; Thermo fisher), and coversliped (no. 1; VWR) with DAPI (Vectastain).

2.3.2.3. Analysis

Images from immunofluorescence were captured using a Zeiss confocal microscope (LSMZ10). Light microscopy of the immunostaining was undertaken with a Zeiss Axio Scope A1 microscope. For each section, an image of the cortex and the striatum in the peri-infarct and the core of the ischaemic lesion was taken (Figure 2.3). The peri-infarct was defined as the closest area of the lesion with no neuronal damage. The core of the lesion was inside the neuronal damage area. Images from an equivalent region in the contralateral hemisphere was also captured. Images were analysed using the software Image J (Fiji, NIH) after cropping the images to a region of 0.285mm^2 and transformation into 8-bit images. In order to use a threshold, the background was subtracted with 50 pixels rolling ball radius. For Iba1 and GFAP immunostained sections, the %area was calculated automatically on Image J (Fiji, NIH) with the selection of the specific staining by an auto-threshold (Triangle method). An average of the three sections in either the striatum or the cortex was calculated.

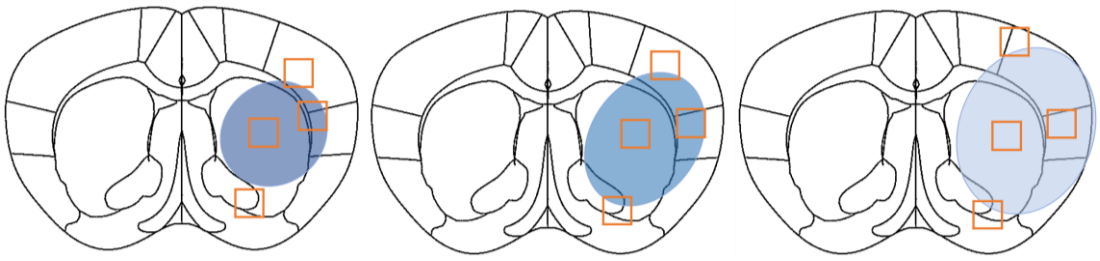

Figure 2-3 Depending on the lesion size, the pictures for peri-infarct and core were selected in the cortex and striatum in the same area.

For HO1 and 3NT staining, the area of immunostaining was mapped onto each coronal level and area (mm^2) calculated with Image J (Fiji, NIH). Area were delineated by stained parenchymal cell bodies only. Volume of HO1 or 3NT immunostaining (mm^3) was calculated using area under the curve in GraphPad Prism (v7).

2.4. qRT-PCR

To evaluate gene expression, mRNA was quantified with quantitative real-time reverse transcriptase polymerase chain reaction (qRT-PCR). Brains were dissected immediately after dislocation of the animal neck. Three 2 mm sections of the brains were collected (Fig. 2.4). For each section, the striatum and the cortex of the ipsilateral and contralateral hemisphere were collected. Tissue was frozen in liquid nitrogen and stored at -80 °C. RNA extraction was undertaken using the RNAeasy Lipid tissue kit (Qiagen). The samples were homogenised in a 2 ml Eppendorf tube with 1 ml of Quiazol reagent (Qiagen) and shaken with a metal bead for two times 2 minutes using a tissue ruptor at 20 Hertz (Qiagen). RNA extraction was conducted with the Qiazol kit (RNeasy Lipid Tissue) according to manufacturer instructions: Homogenised samples were mixed with 200 µl of chloroform then centrifuge for 15 minutes at 4 °C to separate the different phases. The upper phase was collected and mixed with 70% ethanol. The sample was then filtered in a spin column at 8000 rpm for 15 seconds. The sample was then mixed with 700 µl RW1 and centrifuged at 8000 rpm for 15 seconds then mixed with 500 µl RPE and centrifuged at 8000 rpm for 15 seconds twice. After a final centrifuge for 14000 rpm, RNA was eluted in 40 µl of RNA grade water.

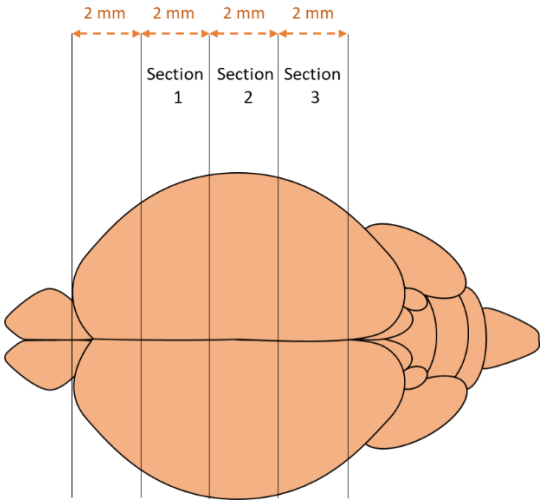

Figure 2-4 Schematic of the mouse brain dissection for biochemistry cohorts.

The RNA concentration was measured with a nanodrop machine (NanoDrop One, Thermo Scientific) in duplicates of 1 µl. To remove genomic DNA, the extracted RNA was then purified with DNAse I treatment (Thermo Scientific). One µg of the RNA was mixed with 1 µl of DNAse and 1 µl of magnesium chloride ($MgCl_2$), mixed with PCR-grade water to get a final volume of 10 µl. This mix was incubated at 37 °C for 30 minutes. Then, 1 µl of 50 mM EDTA was added to the mix and incubated at 65 °C for 10 minutes. The extracted RNA was then reverse transcripted into complementary DNA (cDNA) with the Roche cDNA synthesis kit (Transcriptor First Strand cDNA Synthesis Kit) and a PCR machine (10 minutes at 25 °C, 30 minutes at 55 °C and 5 minutes at 85 °C). The kit was composed of Transcriptor Reverse Transcriptase; Transcriptor RT Reaction Buffer; 5x concentrated, Protector RNase Inhibitor; dNTP Mix, PCR Grade; Anchored Oligo $(dT)_{18}$ Primer; Random Hexamer Primer and PCR-grade water.

Samples were diluted to a concentration of 3 ng/µl for qRT-PCR. cDNA (5.76ul) was mixed with the primers at 0.4 µmol/L (see table 2.3), then 7.4 µl of SyBr Green (Dynamo flash SyBr green, Roche) was added together with 5.3 µl of PCR-grade water. Samples were then pipetted onto a 96 well plate and placed in a PCR machine (CFX96, BioRad) for 40 cycles. Each primer was used with its optimal cycle's programs: When the annealing temperature was 60 °C, the protocol was as follows: Denaturation for 30 seconds at 95 °C, annealing for 40 seconds at 60 °C, and elongation for 30 seconds at 72 °C. For an annealing temperature was 62.5 or 65 °C, the protocol was as follows: denaturation for 10 seconds at 95 °C, annealing for 30 seconds at the temperature stated in table 3, and elongation for 30 seconds at 72 °C. Gene expression was normalised to a housekeeping gene (18s), and data were normalised as fold change of sham or wild type sham expression. For each pair of primers, the annealing temperature was optimised and tested to get efficiency close to 100% (±10%). Two negative controls were used, one with water to replace the sample and one with a sample that was not reverse transcribed.

Gene	Forward	Reverse	Annealing
18S	GTGGAGCGATTTGTCTGGTT	CAAGCTTATGACCCGCACTT	60, 62.5 or 65
nfe2l2 (Nrf2)	CAGCTCAAGGGCACAGTGC	GTGGCCCAAGTCTTGCTCC	65
hmox1	AGCACAGGGTGACAGAAGAG	GGAGCGGTGTCTGGGATG	60
nqo1	ACCTTGCTTTCTATCACCACTG	TGAATCGGCCAGAGAATGAC	60
srxn1	GACGTCCTCTGGATCAAAG	GCAGGAATGGTCTCTCTCTG	60
Slc7a11 (xCT)	ATACTCCAGAACACGGGCAG	AGTTCCACCCAGACTCGAAC	65
keap1	AAGGACCTTGTGGAAGACCA	CCCTGTCCACTGGAATTGAT	65
gfap	TCCTGGAACAGCAAAACAAG	CAGCCTCAGGTTGGTTTCAT	60
aif1 (Iba1)	GTCCTTGAAGCGAATGCTGG	CATTCTCAAGATGGCAGATC	60
il-6	ACAACCACGGCCTTCCCTACTT	CACGATTTCCCAGAGAACATGTG	62,5
il-1β	GGGCCTCAAAGGAAAGAATC	TACCAGTTGGGGAACTCTGC	65
cxcl10	AAGTGCTGCCGTCATTTTCT	GTGGCAATGATCTCAACACG	60
il-4ra	TCACGTGGTACAACCACTTCC	TGCTGAAGTAACAGAACAGGCA	60
complement3	AGCTTCAGGGTCCCAGCTAC	GCTGGAATCTTGATGGAGACGC	65
amigo2	GAGGCGACCATAATGTCGTT	GCATCCAACAGTCCGATTCT	65
stat3	GCCCCGTACCTGAAGACCAA	ACACTCCGAGGTCAGATCCA	60

Table 2-3 Forward end reverse strand of the primers used for the qPCR.

In brackets the name of the protein if different from the gene name.

2.5. Behaviour

To investigate the effects of ischaemia and overexpression of Nrf2 in astrocytes on cognition and neurological function, behavioural tests were undertaken on mice that survived for 4 weeks after ischaemia. Cognitive functions, notably memory, were tested with a Novel Object Recognition task (NOR) 1 week and 4 weeks after ischaemia. For each behaviour test, the mice were moved to the behavioural room 30 minutes prior to the experiment. The light of the room was homogenous to avoid shadows and dimly lit (13 to 16 lux). Each trial/test was video recorded.

2.5.1. Neuroscore

Neurological deficits were assessed at 1, 3, 7, 10, 14, 21 and 28 days post-ischaemia using a neuroscore test based on a protocol from Clark et al., 1997; De Simoni et al., 2003 and Orsini et al., 2012. Scores range from 0 to 36, with a score of 0 indicating no deficit and a score of 36 indicating maximal impairment. The score represents the sum of the results obtain in diverse categories to assess grooming (hair, eyes and coat), sensorial response (whisker

stimulation), posture and gait, spontaneous activity, symmetry, circling and gripping. The score was evaluated by an experimenter blinded to the groups.

Section	Observation	Score
Hair	neat/clean	0
	piloerection and dirty nose/eyes	1
	piloerection and dirty coat	2
Ears	laterally & behind, straightening with noise	0
	laterally, react to noise	1
	laterally and don't react	2
Eyes	open and clear	0
	open & milky white or dark mucus	1
	closed	3
whisker	symmetrical response	0
	light. Withdraws	1
	prominent. No response on one side	2
	absent on one side and slow response ctrltl	3
	absent bilaterally	4
Posture (rock the animal in your palm)	upright, parallel, stabilise	0
	humpbacked, lowers during rocking	1
	head or part of the trunk lies in the palm	2
	reclines on one side	3
Spontaneous activity	alert & explore	0
	seems alert but calm & quiet, start and stop exploring	1
	listless, sluggish moves, no exploration	2
	lethargic or stuporous, barely moves for 60sec	3
Body symmetry	trunk elevated, fore and hind limbs beneath, tail straight	0
	asymmetry: leans on one side & tail slightly bent	1
	moderate: leans on one side, limbs stretched out, tail bent	2
Gait	flexible, symmetric & quick	0
	stiff, inflexible, humpbacked, slower	1
	limping with asymmetric movements	2
	severe limping, drifting, falling with obvious deficits	3
	no spontaneous walk, (stimulation) no more than 3 steps	4
Circling	absent	0
	predominantly one-sided	1
	circles to one side, not constantly	2
	circling constantly	3
Forelimb asymmetry (suspension by tail)	forelimb extended towards the bench & move actively	0
	light. Contralateral forelimb not extended	1
	marked. Ctrltl forelimb extend towards trunk, body bent on side	2
	prominent. Contralateral forelimb adheres to trunk	3
	slight asymmetry. No body/limb movement	4
Compulsory circling	absent. Extension both forelimbs	0
	both forelimbs extended but circling	1
	circles on one side and slower motion	2
	pivots to one side sluggishly, not rotate in full circle	3
Gripping	grasps the grid firmly and tries place hind paws	0
	less power, slight pull	1
	cannot grip with the impaired forelimb	2
	cannot grip	3

Table 2-4 Neuroscore test with score ranging from 0 indicating no deficit to 36 indicating maximal impairment.

2.5.2. Novel Object Recognition in a Y maze

Prior to the experiment, mice were handled in order to habituate them. To avoid the stress of open spaces, Novel Object Recognition (NOR) was performed in a rat Y-maze (arms 49 cm long, 17 cm wide and walls 32 cm; Easter Roads Plastics Ltd, Edinburgh). Because this apparatus was too big for mice, it was modified for the experiment (Fig 2.5). One unmodified arm was the "starting arm" (49 cm long), was closed and used to place the animal at the beginning of the experiment and during the habituation phases. The two other arms were closed mid-length and were used to place the objects (24 cm long; Fig 2.6).

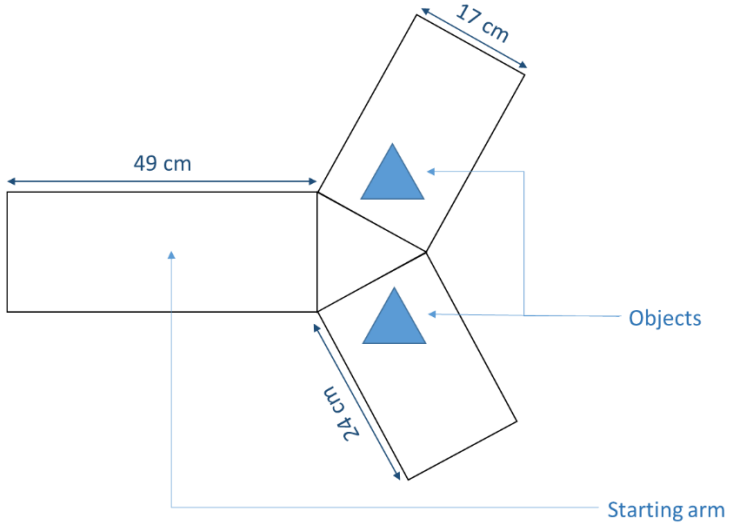

Figure 2-5 Schematic of the modified rat Y-maze for mouse novel object recognition.

Figure 2-6 Objects used for the NOR.

Habituation of 10 minutes per animal were carried out 48 and 24 hours prior to familiarisation in the "starting arm" closed. Objects were bigger than the mouse and stable, such as upside-down glass, decorative pear, Lego© construction, upside down light bulb, plant pot. They were placed at the centre of the two "object arms". Objects were cleaned with ethanol between the tests of two different animals. Objects used and arms selected for first new object were randomised. Trials were video recorded with ANY-maze software. The analysis was based on the time spent exploring the objects. A pilot test showed that the animals were interested in the object mainly during the 3 first minutes. As a result, the 3 first minutes of exploration were used. A discrimination index (DI) has been used to normalise the time spent on the new arm on the total time spent in the apparatus.

An animal that did not explore the objects during the 3 minutes of familiarisation would be excluded. In the study, one animal was excluded following this rule.

$$DI = \frac{(\text{Time on Novel object} - \text{Time on Familiarised Object})}{(\text{Time on Novel object} + \text{Time on Familiarised Object})}$$

2.6. Laser Speckle imaging to determine cerebral blood flow

A semi-quantitative measure of cerebral blood flow was undertaken by using laser speckle imaging (Moor FLPI2 Speckle Contrast Imager, Moor Instruments, UK) before surgeries (for the baseline) and 4 weeks after the surgeries. Mice were anesthetised with 5% isoflurane in a mix of 30% oxygen and 70% nitrous oxide before transfer to stereotaxic frame where they were maintained with2.5 to 3 % isoflurane during the operation. Body temperature was monitored throughout the experiment using a rectal probe and maintained within the range of 36.5–37.5 °C using a heat blanket. The head was fixed in place using ear and tooth bars and an incision was made over the midline. The scalp was retracted, the skull was cleaned of fur and a thin layer of ultrasound gel applied to prevent the skull drying. Images were captured from the MCA territory of the ipsilateral hemisphere of the ischaemia and normalised to the contralateral hemisphere of the ischaemia. Speckle contrast images were analysed using MoorFLPI-2 Review software (version 4.0). Blood flow was expressed as a percent of the contralateral CBF.

2.7. Statistics

Data were expressed mean ± S.E.M. and statistical analysis was performed using GraphPad Prism software (v7.0). For parametric analysis on the wild-type study in chapter 3, unpaired t-test or one-way analysis of variance (ANOVA) followed by *post-hoc* Bonferroni test to correct for multiple comparisons. Mann-Whitney U test or Kruskal-Wallis Test were performed for non-parametric analysis. Normality of the distribution was tested with Shapiro-Wilk test.

In chapter 4 and 5, to compare the genotype and the surgery effect, statistical analysis was undertaken on the four groups with a two-way ANOVA followed by post-hoc Bonferroni test for multiple comparisons. In chapter 5, to analyse neuroscore, two-way ANOVA with repeated measures were performed. To analyse discrimination and preference for the novel object in the NOR test, one-sample t-test was used to compare the results to zero, (i.e. no preference).

Correlation between total lesion volume and GFAP or Iba1 immunostaining %area was assessed with Spearman R.

The difference between experimental groups was deemed statistically significant for a p-value $P<0.05$.

3. Characterisation of acute and chronic cerebral ischaemia and its impact on Nrf2-signalling pathway

3.1. Introduction

Ischaemic stroke is a leading cause of disability and the second leading cause of death worldwide, affecting 15 million people per year. Ischaemia can contribute to dementia including both vascular cognitive impairment (VCI) and Alzheimer's disease (AD), however there is no therapy to date. Cerebral ischaemia can be modelled in rodents *in vivo* with endovascular techniques, to allow disease mechanisms to be studied and to investigate novel therapeutic approaches. As outlined in the introduction, a number of different techniques can be used in rodents to induce focal cerebral ischaemia. One of the most commonly used techniques involves transient intraluminal thread occlusion of the origin of the MCA with a thread introduced via the ligated external carotid artery. Hata et al (1998) developed a technique to occlude the MCA that involves thread insertion via the common carotid artery, which is permanently ligated. Therefore, this technique involves unilateral common carotid artery occlusion in combination with transient middle cerebral artery occlusion. This paper showed that this model produces an infarct core with a depletion of ATP and a penumbra where protein synthesis was reduced, acidity increased, ATP levels were preserved. They also used MRI techniques to highlight the difference between diffusion and perfusion weighted imaging, used to distinguish the penumbra from the core. This model has been previously characterised, showing astrocyte reactivity and microglial activation from 12 hours to 7 days following ischaemia (Alawieh et al., 2015; Petrovic-Djergovic et al., 2012; Strecker et al., 2011), however glial cell activation at later time points than 7 days have not been defined using this model.

Following ischaemia, neuronal damage is caused by initially by hypoxia but also with oxidative stress and inflammation. Due to its high metabolic rate and poor anti-oxidative defences, the brain is prone to oxidative stress (Kohen et al., 1988; Lebel & Bondy, 1991). Radicals and notably ROS oxidise cell elements such as DNA, proteins or the cytoplasmic membrane, leading to their degradation and thus dysfunction of the cell (Sun et al., 2018).

For many decades, Ischaemic research was predominantly focused on neurons but there is now a growing interest on glial cells and their response after ischaemia as a target for stroke

treatment (Liu & Chopp, 2016; Xia et al., 2015). Microglia are immune cells that phagocyte damaged and unused cells or infectious agents. Astrocytes support neurons in many ways (production and release of neurotrophic factors, antioxidants and energy precursors) but additionally regulate neuronal transmission, glutamate levels, homeostasis and vasomodulation (Sofroniew & Vinters, 2010). With an injury, microglia become activated and astrocytes become reactive; they exert morphological and transcriptomic changes. These changes can be classified in two main populations, one aggressive and potentially neurotoxic and the other anti-inflammatory and neurotrophic. After ischaemia both phenotypes were to be found in the vicinity of the lesion (Liddelow & Barres, 2017; Zamanian et al., 2012; Zhang et al., 2018; Zhao et al., 2017). Microglia and astrocytes contribute to ongoing inflammation and oxidative stress and may exacerbate neuronal damage (Block et al., 2007; Liddelow et al., 2017; Villarreal et al., 2016) or provide neuroprotection by producing anti-inflammatory cytokines, anti-oxidant and neurotrophic factors (Becerra-Calixto & Cardona-Gómez, 2017; Chen & Trapp, 2016).

Nrf2-signalling is a potential therapeutic target in diseases involving oxidative stress and inflammation. This transcription factor drives the production of cytoprotective genes such as heme oxygenase-1 (HO1; gene *hmox1*), NAD(P)H dehydrogenase quinone 1 (NQO1; gene *nqo1*), sulfiredoxin 1 (SRXN1, gene *srxn1*) and glutamate-cystine antiporter (xCT; gene *slc7a11*), reducing cellular oxidative damage and inflammation. Nrf2 is upregulated in microglia, astrocytes and neurons after ischaemia (Dang et al., 2012). Even modest durations of ischaemia (15 minutes) can lead to the activation of the Nrf2 signalling pathway at 4 hours (Bell et al., 2011). Upregulation of Nrf2-related genes has been reported from 4 hours to 3 days post ischaemia (Alfieri et al., 2013; Bell et al., 2011a; Bell et al., 2011b; Ding et al., 2014; Tanaka et al., 2010; Yang et al., 2009) however, more chronic time points have not been examined. Therefore, a characterisation of ischaemia at the cellular level coupled with an investigation of alterations to the Nrf2 pathway was carried out in the present chapter. This study will test the hypothesis that activation of Nrf2 signalling is associated with oxidative stress and inflammation and in the acute and chronic response to focal cerebral ischaemia.

3.1.1. Aims

The aim of the current study was to characterise the acute and chronic effects of ischaemia on inflammatory glial cells, oxidative stress and Nrf2 signalling.

I. To characterise inflammatory glial cell changes and determine how Nrf2 signalling is altered in the acute response to focal cerebral ischaemia in mice.
   a. To study inflammatory glial cell changes (reactive astrocytes and microglia/macrophages) and oxidative stress following increasing durations (15, 30 and 60 minutes) of ischaemia.
   b. To determine how Nrf2-related genes are altered in response to ischaemia.

II. To characterise glial cell changes and determine how Nrf2 signalling is altered in the chronic response to focal cerebral ischaemia in mice.
   a. To determine inflammatory glial cell changes and oxidative stress in the chronic response to ischaemia.
   b. To determine how Nrf2-related genes are altered in the chronic response to ischaemia.

3.2. Methods

3.2.1. Mice and experimental groups

To address these aims, three experiments were designed. Three to four-month-old male C57Bl/6J mice underwent middle cerebral artery occlusion (MCAo) or sham surgery and their brains harvested at acute (24 hours) or chronic (4 weeks) time points.

The first experiment was designed to study cellular responses to increasing duration of ischaemia (15-60 minutes; n=6-8 per group) at acute time points (24 hours after injury) using histology and immunohistochemistry techniques. The second experiment was developed to study Nrf2-related genes and inflammatory-related genes after modest duration ischaemia (15 minutes) at three early time points after injury (2, 4 and 24 hours; n=5-6 per group) using quantitative reverse transcriptase polymerase chain reaction (qRT-PCR). In the last experiment, the impact of chronic ischaemia (4 weeks post-injury) was studied after modest

duration ischaemia (15 minutes) with a histology and immunohistochemistry cohort (n=7-9) and a qRT-PCR cohort (n=7-9). Mice were allocated to groups in a randomised fashion.

3.2.1.1. Inclusion/exclusion criteria

In the histology acute cohort, three animals in ischaemic group did not present neuronal damage and thus have been excluded and three animals from the ischaemic group were culled early due to a poor response to the procedure. In the histology chronic cohort, two animals from the ischaemic group were culled due to either a poor response to the procedure or weight loss, and one animal was excluded due to the presence of an infarction defined by a cluster of infiltrated cells and glia in an atrophied lesion. For the biochemistry cohorts, one sham and one ischaemic animal were excluded due to poor response to the procedure.

	Histochemistry cohorts			
	24 hours		4 weeks	
Duration	Initial size	Final size	Initial size	Final size
sham	6	6	7	7
15 min	9	6	12	9
30 min	10	8		
60 min	7	6		

	Biochemistry cohorts			
	24 hours		4 weeks	
Survival	Initial size	Final size	Initial size	Final size
sham	6	5	7	7
2 hours	5	5		
4 hours	5	5		
24 hours	6	6		
4 weeks			10	9

Table 3-1 Summary of the group size of each group for the histologic and the biochemistry cohorts.

Histologic cohorts and the biochemistry cohorts depending on the surgery and the duration of occlusion and the survival (time between the ischaemia and the sacrifice).

3.2.2. Focal cerebral ischaemia model

Male mice were subjected to a transient focal ischaemia by an occlusion of the right middle cerebral artery (MCAo) for differing durations of ischaemia (15, 30 or 60) minutes under anaesthesia with 5% isoflurane in a mix of 30% oxygen and 70% nitrous oxide before and 1 to 1.5% isoflurane during the operation.

As previously explained in the section 2.2 of the Materials & Methods chapter, a monofilament was introduced into the CCA via a small incision and advanced 10mm distal to the carotid bifurcation to occlude the MCA (Monofilament 6-0 medium A MCAO suture L34 PK10; Doccol). Sham experiments involved the same procedure, including unilateral common carotid artery ligation, however but the thread was not inserted into the CCA. To withdraw the thread, mice were re-anaesthetised with isoflurane anaesthesia. Mice received 0.5ml saline (0.9%) subcutaneously by injection and transferred to an incubator (30 °C) for 2 hours. The mice were weighed daily and monitored at least twice a day for the first 72 hours, and then daily, in order to assess the severity of the ischaemia injury. All ischaemia surgery was undertaken by Dr Jill Fowler. Aseptic techniques were used.

3.2.3. Histology

Histology and immunohistochemistry techniques were performed as described in section 2.3. Lesion volume was assessed by drawing areas of ischaemic neuronal death assessed in haematoxylin and eosin (H&E) stained sections from 9 coronal levels as outlined in section 2.3. The assessment of lesion volume in mice that survived for 1 month was undertaken with H&E stained sections as well as MAP2 immunostained sections because loss of neurons after 4 weeks was harder to detect with H&E stained sections alone. There was a loss of dendrites in MAP-2 immunostained sections as previously described (Dawson & Hallenbeck, 1996; Popa-Wagner et al., 1999). Oxidative stress was detected using 3-nitrotyrosine antibody and then mapped at 3 coronal levels and the volume of oxidative stress was determined as outlined in section 2.3. Microglia/macrophages and astrocytes were studied using Iba1 and GFAP immunostaining respectively and quantified with %area as outlined in section 2.3. Neutrophils and microglia were labelled with a specific antibody (SJC-Neutrophil antibody and TMEM119 respectively) and quantified as described in section 2.3. Finally, HO1 immunostaining was used to assess HO1 upregulation as an index of Nrf2-signalling

activation and the area of HO1 immuno-positive staining was quantified at 3 coronal levels as outlined in section 2.3. All experiments were conducted by an experimenter blinded to the groups.

3.2.4. Analysis

Images of GFAP and Iba1 immunostained sections were taken with a Zeiss microscope (LSMZ10) at 20x magnification. For each section, an image of the cortex and the striatum in the peri-infarct and the core of the ischaemic lesion was taken, using the lesions maps to determine the peri-infarct and core areas. They were analysed using the software Image J (Fiji, NIH) after cropping the images to a region of 0.285mm2 and transformed into 8-bit images. Images were captured from 3 coronal levels (Bregma +0.98; -0.10; -2.06) and the final result was expressed as an average of these three sections for either the striatum or the cortex.

For Iba1 and GFAP immunostained sections, the %area was calculated automatically using Image J (Fiji, NIH) with the selection of the specific staining by an auto-threshold (Triangle method) on inverted images. For 3-nitrotyrosine staining, the area of immunostained cells was mapped onto three coronal levels and area (mm2) calculated with Image J (Fiji, NIH). Lesion volume (mm3) was calculated using area under the curve in GraphPad Prism (v7).

3.2.5. qRT-PCR

To study gene expression, qRT-PCR was undertaken as explained in the methods section 2.4. For this first study, inflammation and glial response were assessed by investigated alterations to *gfap*, *aif1*, *cxcl10* and *il-1β* mRNA levels. For Nrf2-related gene expression, alterations to *nfe2l2*, *hmox1*, *nqo1, srxn1* and *slc7a11* genes were investigated. For each animal, the level of expression was normalised to the housekeeping gene *18S* and normalised to levels of sham. All analyses were carried out with the experimenter blinded to groups.

3.2.6. Statistics

Data were expressed mean ± S.E.M. using GraphPad Prism software. For parametric analysis, unpaired student's t-test or one-way analysis of variance (ANOVA) followed by *post-hoc* Bonferroni test were performed for multiple comparison. $P<0.05$ was deemed statistically significant. Mann-Whitney U test was performed for non-parametric analysis. Normality of the distribution was tested with Shapiro-Wilk test.

3.3. Characterisation of ischaemic cell death with increasing occlusion duration

3.3.1. Increased neuronal damage with increasing duration of occlusion

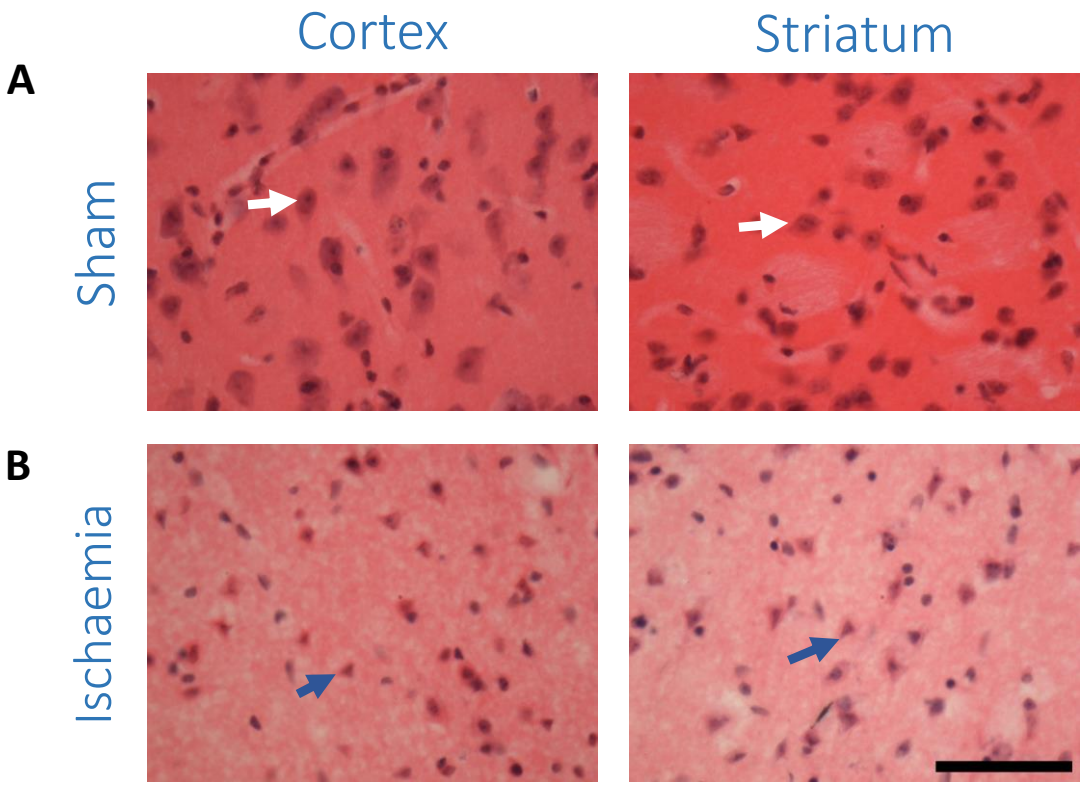

Figure 3-1 Neuronal damage was detected with Haematoxylin & Eosin staining, 24 hours after ischaemia.

(A) Morphologically normal appearing cells and neurons (white arrow) in shams.

(B) Damaged tissue in the core of the lesion in the cortex displays shrunken neurons with an eosinophilic cytoplasm and triangular perikarion (blue arrow). Scale bar 100 µm.

The ischaemic lesion was detected with haematoxylin and eosin (H&E) staining. In the lesion, the tissue appeared vacuolated and ischaemic neurons appeared shrunken with a triangular perikarion and eosinophilic cytoplasm (Fig 3.1 B) whereas undamaged tissue contained round cell bodies and no vacuolisation (Fig 3.1 A). Areas of tissue containing ischaemic neurons were delineated onto line diagram from 9 coronal levels throughout the brain (Fig 3.2 A).

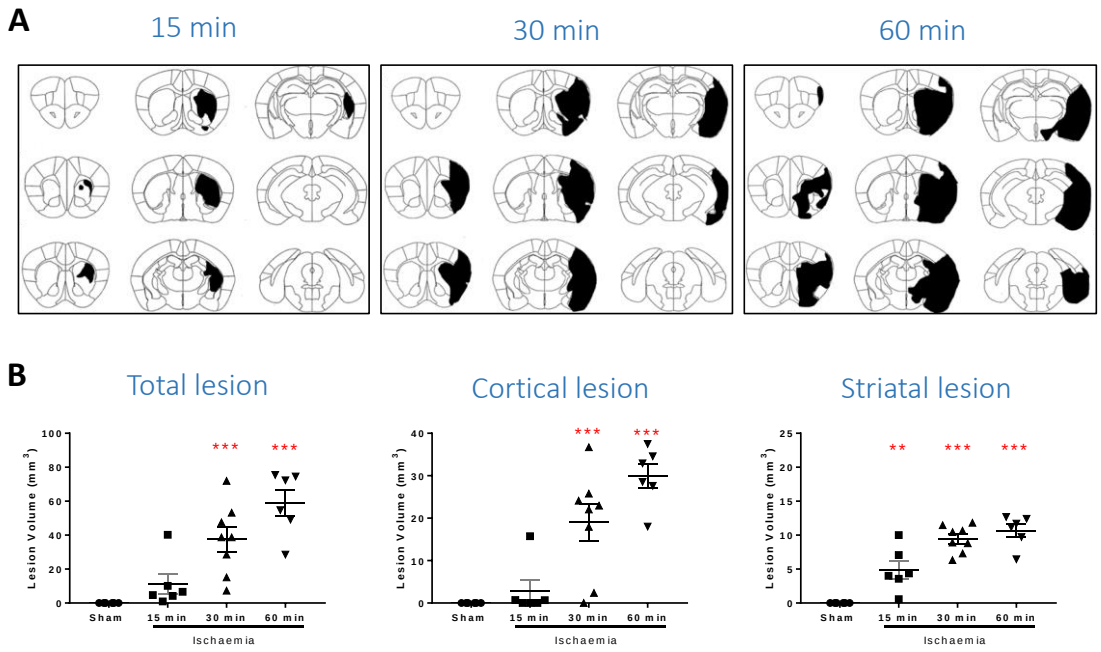

Figure 3-2 Increased duration of ischaemia increases neuronal damage in cortex and striatum, 24 hours after ischaemia.

(A) Representative line diagram with ischaemic neuronal damage in black from median animals (coordinates from Bregma +2.58; +1.54; +0.98; +0.74; -0.10; -1.06; -2.06; -2.92; -4.48 mm).

(B) Quantification of neuronal damage mapping showed significant differences between groups in total lesion ($F_{(3, 22)}$=16.31, p<0.0001), cortex ($F_{(3, 22)}$=17.88, p<0.0001) and striatum ($F_{(3, 22)}$=30.49, p<0.0001). There was a significant increase in every region with 30 or 60 minutes of ischaemia (p<0.0001). Interestingly, after 15 minutes of ischaemia, the lesion was increased in the striatum (p=0.0024) but not the cortex (p>0.05).

*Data presented as mean ± S.E.M. One-way ANOVA followed by post hoc comparisons with Bonferroni (N=6 to 8 per group). **p<0.01, ***p<0.001.*

No ischaemic cell death was observed in sham animals. There was a significant difference between the groups in total lesion ($F_{(3, 22)}$=16.31, p<0.0001), cortex ($F_{(3, 22)}$=17.88, p<0.0001) and striatal lesion $F_{(3, 22)}$=30.49, p<0.0001) with an increase in the lesion volume with increasing duration of ischaemia (p<0.0001 for all groups; Fig 3.2 A and B). Post-hoc comparisons revealed differences in the lesion volume after 30 and 60 minutes in the total lesion and cortex compared to shams (p<0.0001, Fig 3.2 B) and from 15, 30 and 60 minutes ischaemia in the striatum compared with shams (p=0.0024, Fig 3.2 B). Therefore with longer occlusion, the there was an increase in lesion volume (Fig 3.2 B) as reported in the literature (Popp et al., 2009). Given these results, the lesion seems to extend from striatum to cortex with increasing duration of ischaemia.

3.3.2. Increased cortical oxidative stress with increasing duration of occlusion

Ischaemia and reperfusion can induce oxidative stress via increased reactive oxygen species and nitric oxide (Iadecola et al., 1995; Olmez & Ozyurt, 2012). Together, they form peroxynitrite (Radi et al., 1991) that nitrates tyrosine residues in proteins. This phenomenon can be detected with 3-Nitrotyrosine (3NT) immunohistochemistry (Giannessi et al., 2010). There was minimal 3NT immunostaining in the shams, whereas 3NT labelled cells were detected in the ischaemic animals (Fig 3.3 A). Morphologically, the staining appeared similar with increasing duration of ischaemia.

Quantification of areas containing 3NT labelled cells was assessed by the mapping the immunostaining observed in 3 coronal sections (Bregma +0.98, -0.10. -2.06). There was a significant difference between groups in the total lesion ($F_{(3, 22)}$=17.28, p<0.0001), cortical ($F_{(3, 22)}$=12.92, p<0.001) and striatal lesion ($F_{(3, 22)}$=25.11, p<0.0001). Post hoc comparisons showed significant increase in 3NT staining with all durations of ischaemia. A modest duration of ischaemia (15 minutes) significantly increased 3NT immunostaining at 24 hours in the total ipsilateral hemisphere, cortex and striatum compared to shams (p=0.0008, p=0.0097 and p<0.0001 respectively; Fig 3.3 B). With 30 minutes ischaemia and 60 minutes ischaemia, 3NT immunostaining was significantly increased in the total ipsilateral hemisphere, cortex and striatum (p<0.0001 for every region for both group; Fig 3.3 B).

This result suggests the presence of oxidative stress in the lesion after ischaemia. Interestingly, 24 hours after 15 minutes ischaemia, the cortex contained minimal ischaemic neuronal death (Fig 3.2 B) but had elevated 3NT staining (Fig 3.3 B). Therefore, the area of 3NT immunostaining was compared with area of neuronal damage area for animals that underwent 15 minutes of ischaemia (Fig 3.3 C). The blue line represents area of tissue containing 3NT immunostained cells on the three coronal sections whereas black line represents area of tissue containing ischaemic neuronal damage in the same three coronal sections. This comparison demonstrated that there is a greater area of 3NT expression compared to the neuronal damage area on these three coronal levels for both cortex and striatum (Fig 3.3 C). It is important to note that oxidative stress was found beyond the area of lesion in morphologically normal appearing tissue.

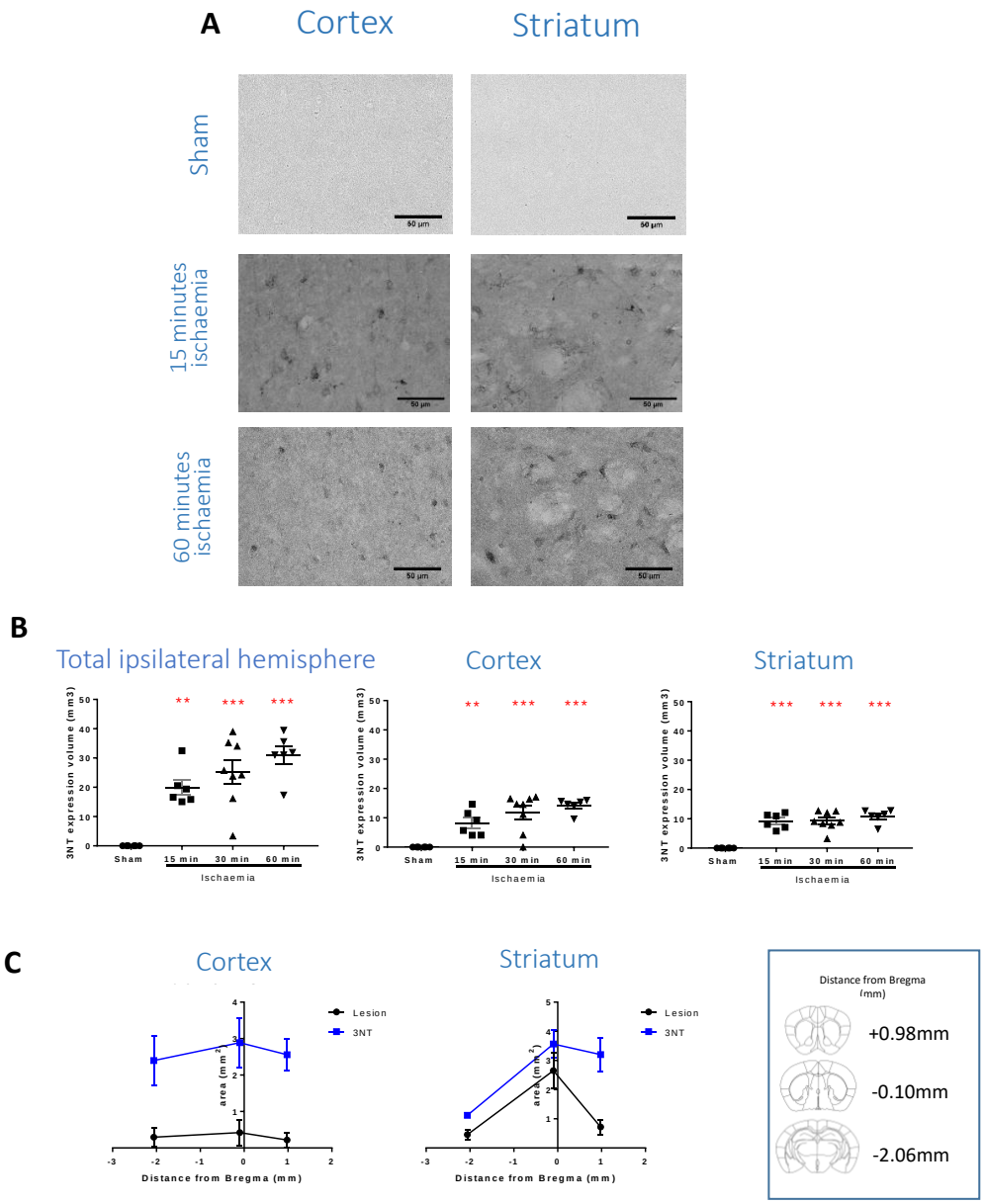

Figure 3-3 Increased duration of ischaemia increases oxidative stress in cortex and striatum, 24 hours after ischaemia.

(A) Representative images of 3-Nitrotyrosine (3NT) immunostaining showing peroxide nitrite generation in the cytoplasm of cells in cortex and striatum after ischaemia and minimal staining in shams.

*(B) Quantification of 3NT staining by mapping the positive immunostaining. There was a significant difference between groups in the total ipsilateral hemisphere ($F_{(3, 22)}$=17.28, p<0.0001), cortex ($F_{(3, 22)}$=12.92, p<0.001) and striatum $F_{(3, 22)}$=25.11, p<0.0001). There was a significant increase in every region with 15 minutes or longer ischaemia (**p<0.01, ***p<0.001). Interestingly, even after 15 minutes of ischaemia, there was increased oxidative stress increased in the cortex (p=0.0097) despite minimal ischaemic neuronal damage in that region.*

(C) Profile area of 3Nt immunostaining compared to the area of neuronal damage in three coronal sections of the 15 minutes ischaemia group demonstrated that 3NT expression extended beyond the lesion site. The blue line represents area of tissue containing 3NT immunostained cells on the three coronal sections whereas black line represents area of tissue containing ischaemic neuronal damage in the same three coronal sections.

*Data presented as mean ± S.E.M. One-way ANOVA followed by post hoc comparisons with Bonferroni (N= 6 to 8 per group). **p<0.01, ***p<0.001.*

3.3.3. Astrocytic response to acute ischaemia

To investigate how reactive astrocytes are altered by ischaemia, glial fibrillary acidic protein (GFAP) immunostaining was undertaken. In shams, 15- and 30-minutes ischaemic animals, astrocytes had small cell bodies and long and thin processes with many branches (Fig. 3.4 A). In 60-minutes ischaemic animals, processes were fragmented in the peri-infarct and were not detectable in the core. In both locations after 60 minutes of ischaemia, cell bodies were bigger (Fig. 3.4 A).

Quantification of the GFAP immunostaining using %area revealed a significant difference between groups for the four locations: cortex peri-infarct ($F_{(3, 22)}$=8.498, p=0.0006), cortex core ($F_{(3, 22)}$=3.455, p=0.033), striatum peri-infarct ($F_{(3, 22)}$=6.011, p=0.0035) and striatum core ($F_{(3, 22)}$=10.26, p=0.0002; Fig 3.4 B). Post hoc tests revealed no significant differences between shams and any duration ischaemia in the cortex core (p>0.05). In the striatum core, GFAP %area was decreased in the core of the lesion in the striatum following 30- and 60-minutes ischaemia compared to shams (p=0.0318 and p=0.0012). This might be linked to astrocytic death observed early on after ischaemic injury (Liu et al., 1999). In the peri-infarct, post hoc test revealed a significant increase between sham and 60 minutes ischaemia for the cortex and striatum (p=0.0019 and p=0.0025 respectively; Fig. 3.4 B). Other comparisons were not found significantly different.

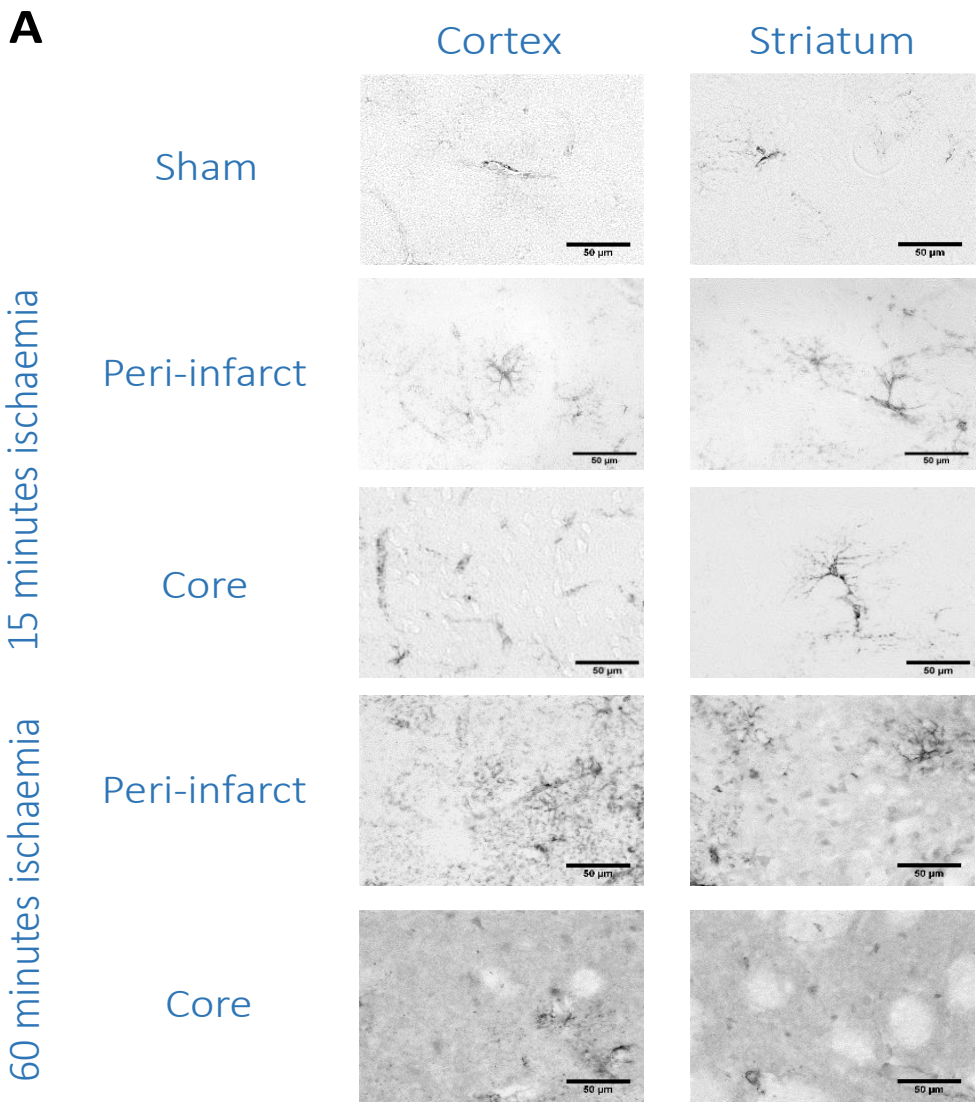
A
Cortex
Striatum
Sham
15 minutes ischaemia
Peri-infarct
Core
60 minutes ischaemia
Peri-infarct
Core
50 µm

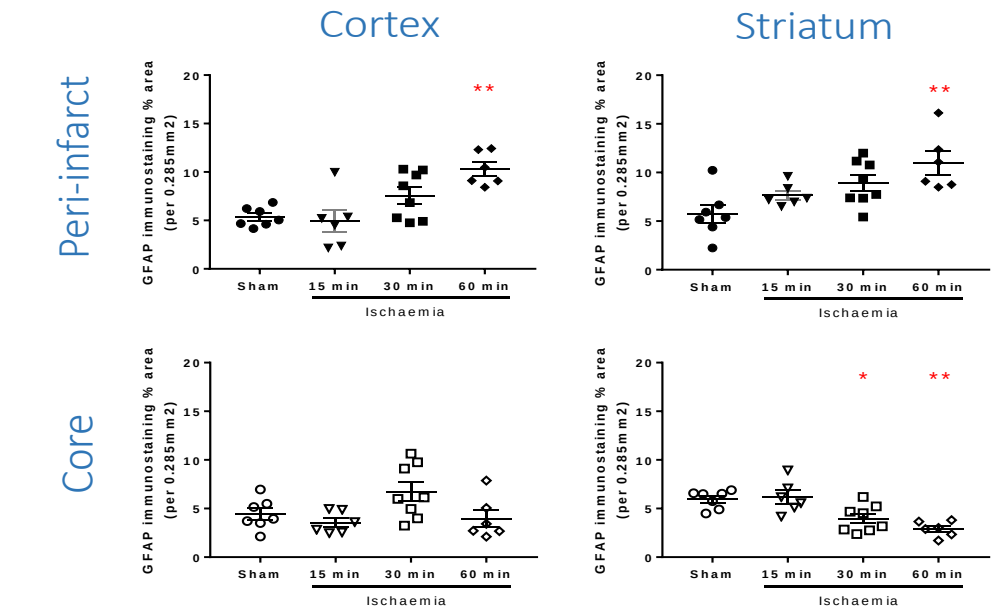
B
Cortex
Striatum
Peri-infarct
Core
GFAP immunostaining % area (per 0.285mm2)
Sham
15 min
30 min
60 min
Ischaemia
**
*

← Figure 3-4 Increased duration of ischaemia modifies reactive astrocytes assessed with GFAP in the cortex and the striatum, 24 hours after ischaemia.

(A) Representative images of GFAP immunostaining showing an increase in the peri-infarct for the cortex and the striatum after ischaemia compared to shams for the 60 minutes ischaemia group. However, 15 minutes ischaemia did not modify GFAP immunostaining.

(B) Quantification of GFAP staining assessed by %area showed significant differences between groups in the cortex peri-infarct ($F_{(3, 22)}$=8.498, p=0.0006), the cortex core ($F_{(3, 22)}$=3.455, p=0.033), the striatum peri-infarct $F_{(3, 22)}$=6.011, p=0.0035) and the striatum core ($F_{(3, 22)}$=10.26, p=0.0002). There was a significant increase of GFAP immunostaining following 60 minutes of ischaemia in the peri-infarct of the cortex and striatum (p=0.0019 and p=0.0025 respectively) compared to shams. In the striatum core, GFAP immunostaining was decreased significantly following 30 and 60 minutes of ischaemia (p=0.0318 and p=0.0012 respectively). For the other comparisons, there was no statistical difference between ischaemic animals and shams.

*Data presented as mean ± S.E.M. One-way ANOVA followed by post hoc comparisons with Bonferroni (N= 6 to 8 per group). *p<0.05, **p<0.01.*

To build on these findings, GFAP mRNA level was investigated in a cohort of animals that received 15 minutes of ischaemia and 24 hours survival. Levels of *gfap* gene expression were significantly increased at 24 hours in the striatum and the cortex (p<0.0001 for both; Fig 3.5). Taken together, these results show that ischaemia modifies GFAP at protein and gene level and that there are increased levels of reactive astrocytes in peri-infarct regions.

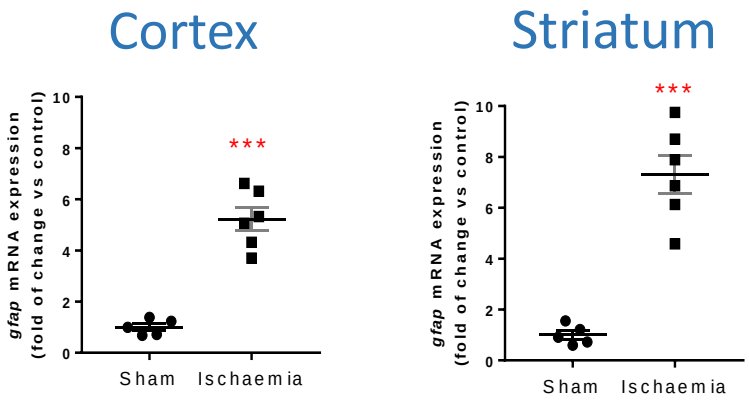

Figure 3-5 Increased gene expression for gfap in the cortex and striatum, 24 hours after ischaemia.

GFAP gene gfap mRNA expression (normalised to 18s) was significantly increased in both cortex ($t_{(9)}$=8.092, p<0.0001) and striatum ($t_{(9)}$=7.409, p<0.0001) 24 hours after 15 minutes of ischaemia compared to shams.

*Data presented as mean ± S.E.M. Student's t-test for gene expression study (N= 5 to 6 per group). ***p<0.001.*

3.3.4. Increased microglia/macrophage density in the acute response to ischaemia

Ischaemia triggers morphological alterations and recruitment of the microglia/macrophages at the core and peri-infarct regions of the ischaemic lesion (Fumagalli et al, 2015; Morrison & Filosa, 2013; Ito et al., 2001). The morphological modification appears when microglia/macrophages are activated after hypoxia and during inflammation (Bachiller et al., 2018; Hirbec et al., 2017; Hoogland et al., 2015; Patel et al., 2013). Iba1 immunostaining of resident microglia and infiltrated macrophages (Ito et al., 2001) was undertaken and % area of immunostaining was quantified in the cortex and striatum.

Sham animals had Iba1-positive cells with small cell bodies and small and thin processes. Following ischaemia, Iba1-positive cells had larger, darker cell bodies and the processes were thicker and more intensely stained (Fig 3.6 A). For some Iba1-positive cells, the processes were lost, giving then an amoeboid shape as reported previously (Giulian, 1987; Schilling et al., 2003).

Quantification of the %area of Iba1 immunostaining with revealed a significant effect of the ischaemia in every locations: cortex peri-infarct ($F_{(3, 22)}$=21.51, p<0.0001), cortex core ($F_{(3, 22)}$=11.56, p<0.0001), striatum peri-infarct $F_{(3, 22)}$=22.28, p<0.0001) and striatum core ($F_{(3, 22)}$=16.01, p<0.0001; Fig 3.6 B). Post hoc comparisons with Bonferroni revealed a significant increase in the striatum core and peri-infarct following 15 minutes ischaemia (p<0.0001). Following 30 minutes ischaemia, Iba1 %area was significantly increased compared to shams for every location (p<0.0001; Fig 3.6 B).

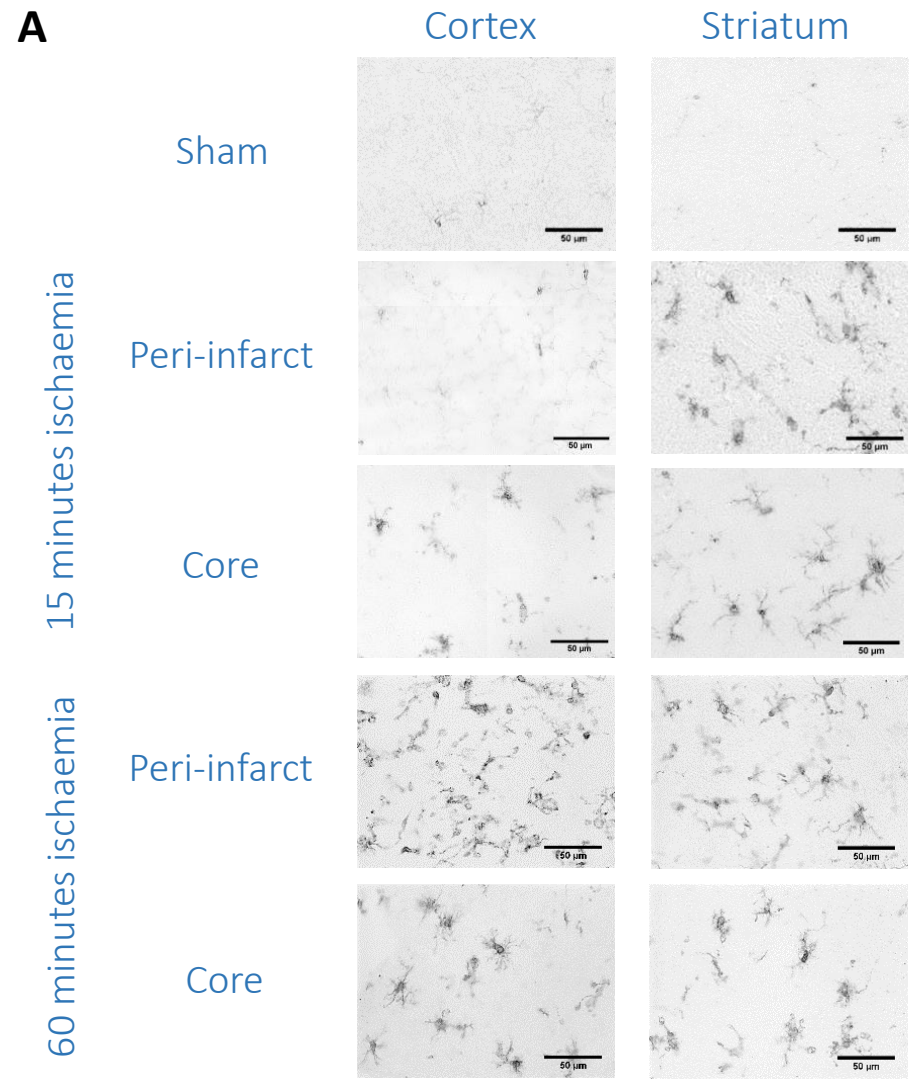
A
Cortex
Striatum
Sham
Peri-infarct
Core
Peri-infarct
Core
15 minutes ischaemia
60 minutes ischaemia
50 µm

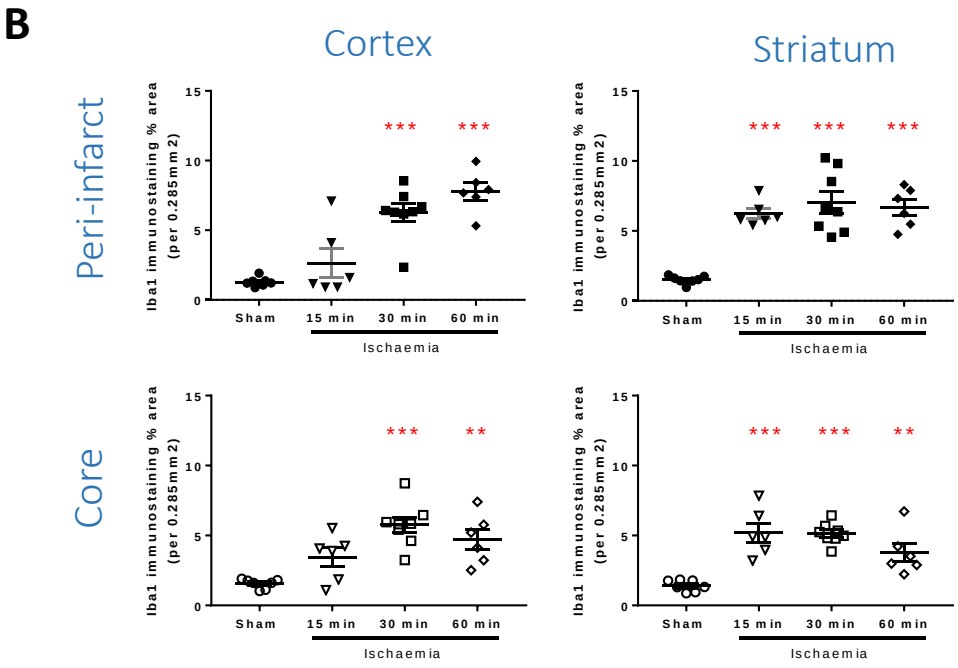
B
Cortex
Striatum
Peri-infarct
Core
Iba1 immunostaining % area (per 0.285mm2)
Sham
15 min
30 min
60 min
Ischaemia
***
**

← Figure 3-6 Increased duration of ischaemia modifies microglia/macrophage marker Iba1 in the cortex and the striatum, 24 hours after ischaemia.

(A) Representative images of Iba1 immunostaining showing an increase in the density of cells in the peri-infarct and core of the cortex and the striatum after ischaemia compared to shams. Following ischaemia, cells were larger, with thicker, darker processes.

(B) Quantification of Iba1 staining by %area showed significant differences between groups in the cortex peri-infarct ($F_{(3, 22)}$=21.51, p<0.0001), the cortex core ($F_{(3, 22)}$=11.56, p<0.0001), the striatum peri-infarct $F_{(3, 22)}$=22.28, p<0.0001) and the striatum core ($F_{(3, 22)}$=16.01, p<0.0001). Post hoc comparisons revealed no significant differences between 15 minutes ischaemia and shams in the cortex peri-infarct (p=0.979) and cortex core (p=0.156). There was a significant increase in the striatum with 15 minutes (p<0.0001). With 30 minutes ischaemia, Iba1 %area was significantly increased compared to shams for every location (p<0.0001). There was a significant increase of the Iba1 % area after 60 minutes ischaemia in the peri-infarct cortex and striatum (both p<0.0001), in the cortex core (p=0.0037) and in the striatum core (p=0.0088). For the other comparisons, there was no statistical difference between ischaemic animals and shams.

*Data presented as mean ± S.E.M. One-way ANOVA followed by post hoc comparisons with Bonferroni (N= 6 to 8 per group). **p<0.01, ***p<0.001.*

To further investigate alterations to microglia/macrophages, Iba1-positive cell counts were undertaken to assess recruitment at the lesion site. Quantification of cell counts revealed a significant alteration of Iba1-positive cells for all durations of ischaemia compared with shams (cortex peri-infarct $F_{(3, 22)}$=17.97, p<0.0001, cortex core $F_{(3, 22)}$=5.491, p=0.0054, striatum peri-infarct $F_{(3, 22)}$=9.591, p=0.0003 and striatum core $F_{(3, 22)}$=3.552, p=0.0301; Fig 3.7 A).

Post hoc comparisons with Bonferroni revealed a significant increase in the striatum peri-infarct with 15 minutes ischaemia (p=0.0076) but not in the cortex peri-infarct, cortex core or striatum core (p=0.893, p=0.358 and p=0.254 respectively; Fig 3.7 A). With 30 minutes ischaemia, Iba1-positive cells were significantly increased compared to shams in the cortex peri-infarct and core (p=0.0002 and p=0.0034 respectively) and striatum peri-infarct (p=0.0002) but not in the striatum core (p=0.154; Fig 3.7 A). There was a significant increase of Iba1-positive cells in the peri-infarct for both cortex and striatum compared to shams after 60 minutes ischaemia (p<0.0001 and p=0.0058) but not in the striatum peri-infarct or core (p>0.999 for both; Fig 3.7 A).

To further investigate Iba1 alterations, levels of the Iba1 gene *aif1* were investigated. At 24 hours, there was no significant difference in Iba1-gene *aif1* levels between the shams and ischaemic animals in the striatum (p=0.585) and in the cortex (p=0.081; Fig 3.7 B).

In the peri-infarct, Iba1 %area and Iba1-positive cell counts are both significantly increased for the same groups, suggesting that microglia/macrophages migrate to the lesion site. However, in the core of the lesion, Iba1 %area increase is not paralleled with an increased number of positive cells, suggesting that the morphology has changed in this area compared to shams. As *aif1* is not modified, microglia/macrophages do not seem to proliferate.

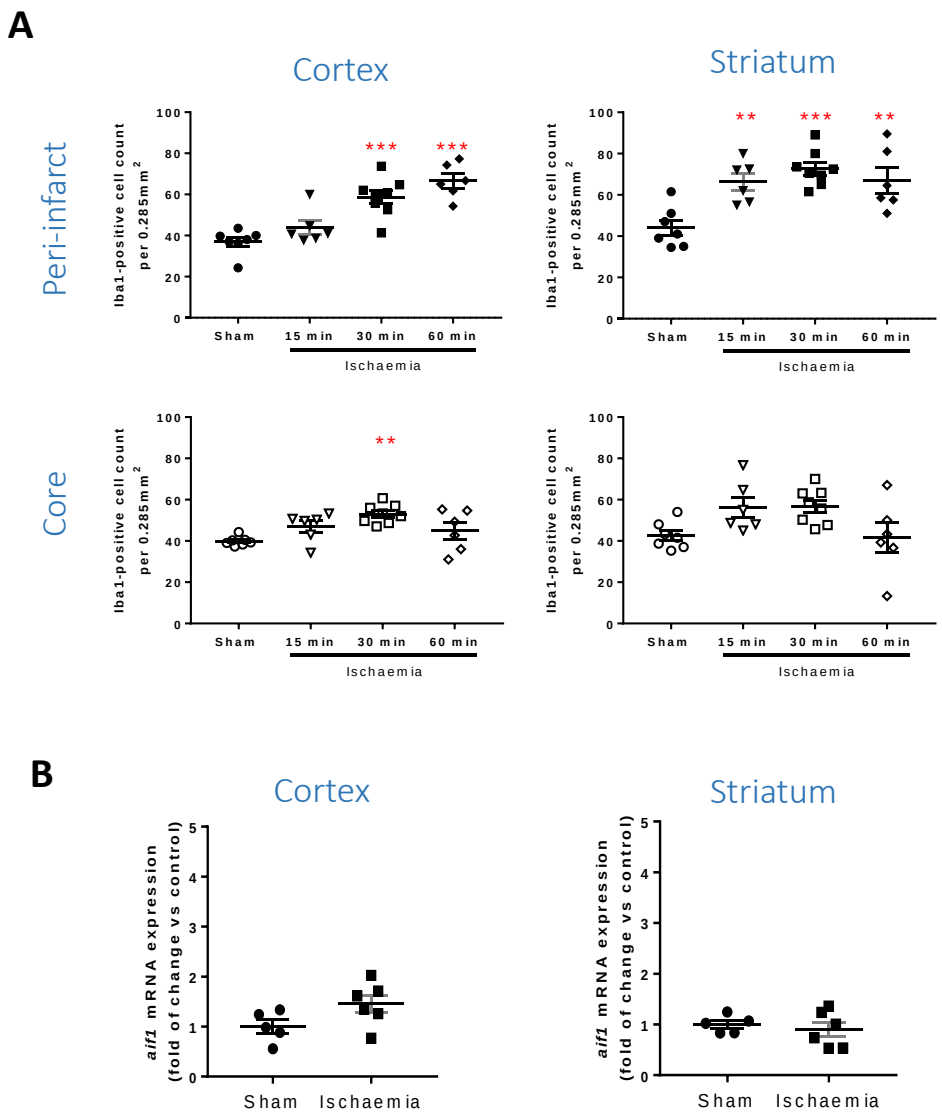

Figure 3-7 Increased duration of ischaemia increases Iba1-positive cells in the cortex and the striatum but not Iba1 gene aif1 expression, 24 hours after ischaemia.

(A) Quantification of the number of Iba1-positive cells. There were significant differences in the number of Iba1 immunostained cells in the cortex peri-infarct ($F(3, 22)=17.97$, $p<0.0001$), the cortex core ($F(3, 22)=5.491$, $p=0.0054$), the striatum peri-infarct $F(3, 22)=9.591$, $p=0.0003$) and the striatum core ($F(3, 22)=3.552$, $p=0.0301$). There was a significant increase in the striatum peri-infarct with 15 minutes ischaemia ($p=0.0076$). With 30 minutes ischaemia, Iba1-positive cells were significantly increased compared to shams in the cortex peri-infarct and core ($p=0.0002$ and $p=0.0034$ respectively) and striatum peri-infarct ($p=0.0002$). There was a significant increase of Iba1-positive cells in the peri-infarct for both cortex and striatum compared to shams after 60 minutes ischaemia ($p<0.0001$ and $p=0.0058$). For the other comparisons, there was no statistical difference between ischaemic animals and shams.

(B) There was no significant difference in mRNA expression of the Iba1 gene aif1 in the cortex ($t(9)=1.962$, $p=0.081$) and striatum ($t(9)=0.566$, $p=0.585$) 24 hours after 15 minutes of ischaemia compared to shams.

*Data presented as mean ± S.E.M. One-way ANOVA followed by post hoc comparisons with Bonferroni (N= 6 to 8 per group). Student's t-test for gene expression study (N= 5 to 6 per group). **$p<0.01$, ***$p<0.001$.*

3.3.5. Increased *cxcl10* expression in the striatum 24 hours after 15 minutes ischaemia

Cytokines are produced by neurons, glial cells and immune cells and serve as messengers that induce and modulate glial activation and response. Recruitment of glial cells at the injury is possible via increased production of chemokines. Interleukin 1 beta (Il-1β) is a cytokine found in the pro-inflammatory environment that can promote activation of microglia (Rider et al., 2011; Fogal et al., 2005). C-X-C motif chemokine 10 (CXCL10) is produced by microglia, astrocytes, neurons, leukocytes, macrophages and T cells (Chai et al., 2015; Harikumar et al., 2014; Klein et al., 2005; Nakamichi et al., 2004; Singh et al., 2008). It is notably expressed by reactive astrocytes and is known to promote microglia recruitment (Cross & Woodroofe, 1999; Rappert et al., 2004).

In the cortex, *cxcl10* and *il-1β* levels were not significantly altered when comparing ischaemia and sham groups (Mann–Whitney U=6 p=0.125 and Mann–Whitney U=9 p=0.329 respectively; Fig. 3.8). In the striatum, *cxcl10* mRNA expression was significantly increased compared to sham following ischaemia (Mann–Whitney U=0 p=0.0043; Fig. 3.8), whereas there was no significant difference in the levels of *il-1β* mRNA expression compared to shams (Mann–Whitney U=11 p=0.536; Fig 3.8).

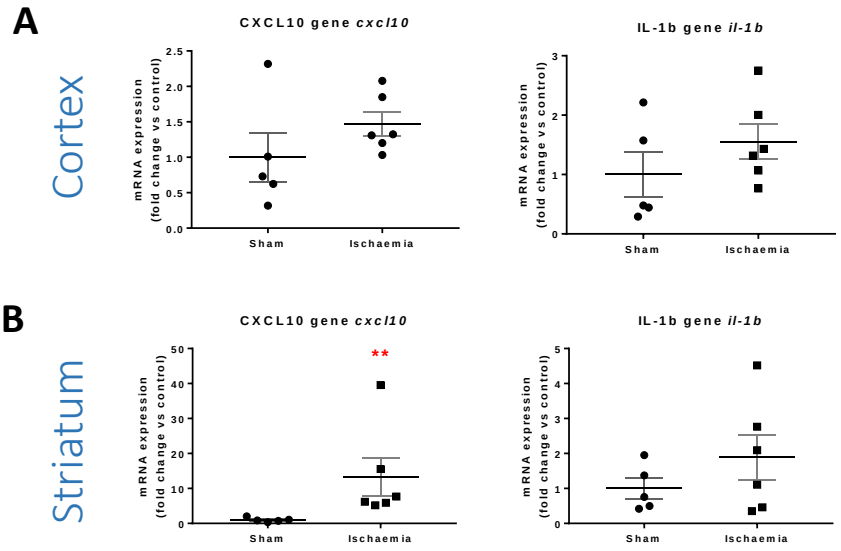

Figure 3-8 Inflammatory gene cxcl10 was upregulated in the striatum 24 hours after 15 minutes of ischaemia.

(A) In the cortex, cxcl10 and il-1β levels were not significantly altered ischaemia and sham groups (Mann–Whitney U=6 p=0.125 and Mann–Whitney U=9 p=0.329 respectively).

(B) In the striatum, cxcl10 mRNA expression was significantly increased compared to sham (Mann–Whitney U=0 p=0.0043). Study of il-1β mRNA expression showed no significant differences compared to shams (Mann–Whitney U=11 p=0.536).

*Data presented as mean ± S.E.M. Student's t-test or Mann-Whitney U test $n_1 = 5$ and $n_2 = 6$, two-tailed (N= 5 to 6 per group). **p<0.01.*

3.3.6. Peripheral immune cells infiltrate 24 hours after ischaemia

Ischaemia is associated with peripheral immune cell infiltration through the blood brain barrier (BBB). The previous result demonstrated that the gene that encodes the chemokine CXCL10 was upregulated and Iba1 staining was increased. Therefore, infiltrating peripheral immune cells were examined. Neutrophils and peripheral macrophages can be studied with immunostaining.

Neutrophil staining was performed on this cohort and was detected in ischaemic brains (Fig 3.9 A). To quantify neutrophils, their presence or absence was determined in the experimental groups (Fig 3.9 B). Neutrophils were absent in sham controls. Neutrophils were detected in the cortex and striatum of ischaemic animals. Interestingly, only one animal of the 15 minutes ischaemia group contained neutrophils. After verification, this animal had the biggest lesion within this group (Fig 3.9 B). The probability of neutrophil infiltration to the parenchyma occurring following ischaemia was unchanged with 15-minutes ischaemia

(p>0.999) and increased with 30- and 60-minutes ischaemia (p=0.0003 and p=0.0022, Fisher's exact test). In the cortex, the probability was unchanged with 15 minutes ischaemia (p>0.999) and increased with 30- and 60-minutes ischaemia (p=0.0047 and p=0.0022). In the striatum, the probability was unchanged with 15-minutes ischaemia (p>0.999) and increased with 30- and 60-minutes ischaemia (p=0.0097 and p=0.0152).

A

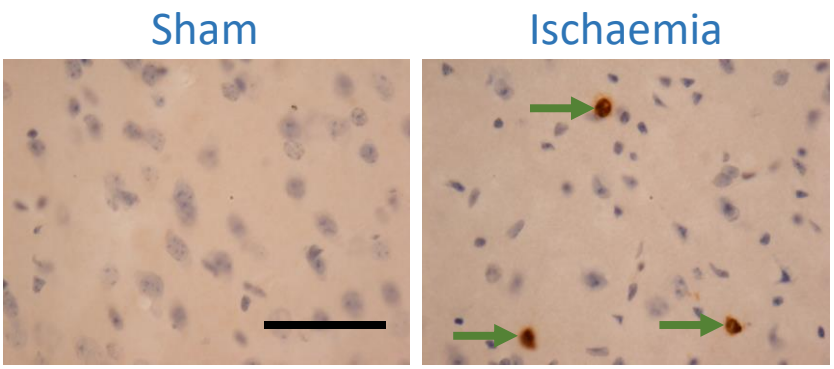

B

Anatomical Area		MCAo		
	Sham	15 minutes	30 minutes	60 minutes
Ispilateral	0 of 6	1 of 6	8 of 8	6 of 6
Cortex	0 of 6	1 of 6	7 of 8	6 of 6
Striatum	0 of 6	1 of 6	6 of 8	5 of 6

Figure 3-9 Ischaemia increases neutrophil infiltration, 24 hours after ischaemia.

(A) Representative images of neutrophil immunostaining in the cortex after 60 minutes ischaemia. No neutrophils were to be found in the shams. Nuclei were counterstained with DAPI, in blue, and neutrophil in brown (green arrows). Scale bar 100 µm.

(B) Quantification of the presence of neutrophils revealed only one animal of the 15 minutes ischaemia group had neutrophil infiltration. On the contrary, every animal receiving 30 minutes or longer ischaemia had neutrophils.

The infiltration of neutrophils suggested that peripheral macrophages may also infiltrate the brain. Since Iba1 immunostaining cannot discriminate between innate microglia and infiltrated macrophages, another marker was investigated. TMEM 119 is expressed by resident microglia but not peripheral macrophages (Bennett et al., 2016; Satoh et al., 2016). In order to distinguish them, Iba1 and TMEM 119 co-labelling was undertaken.

In sham animals, each Iba1-positive cell co-labelled with TMEM 119 suggesting the presence of microglia but not macrophages (Fig 3.10 and 3.11). Furthermore, these cells had a comparable morphology to the immunostaining studied previously (Fig 3.6 A). After ischaemia, Iba1-positive cells were bigger and processes thicker or lost in the lesion as seen previously (Fig 3.6 A). This activated resident microglia had reduced TMEM staining. This might be due to morphological changes (Fig 3.10 and 3.11).

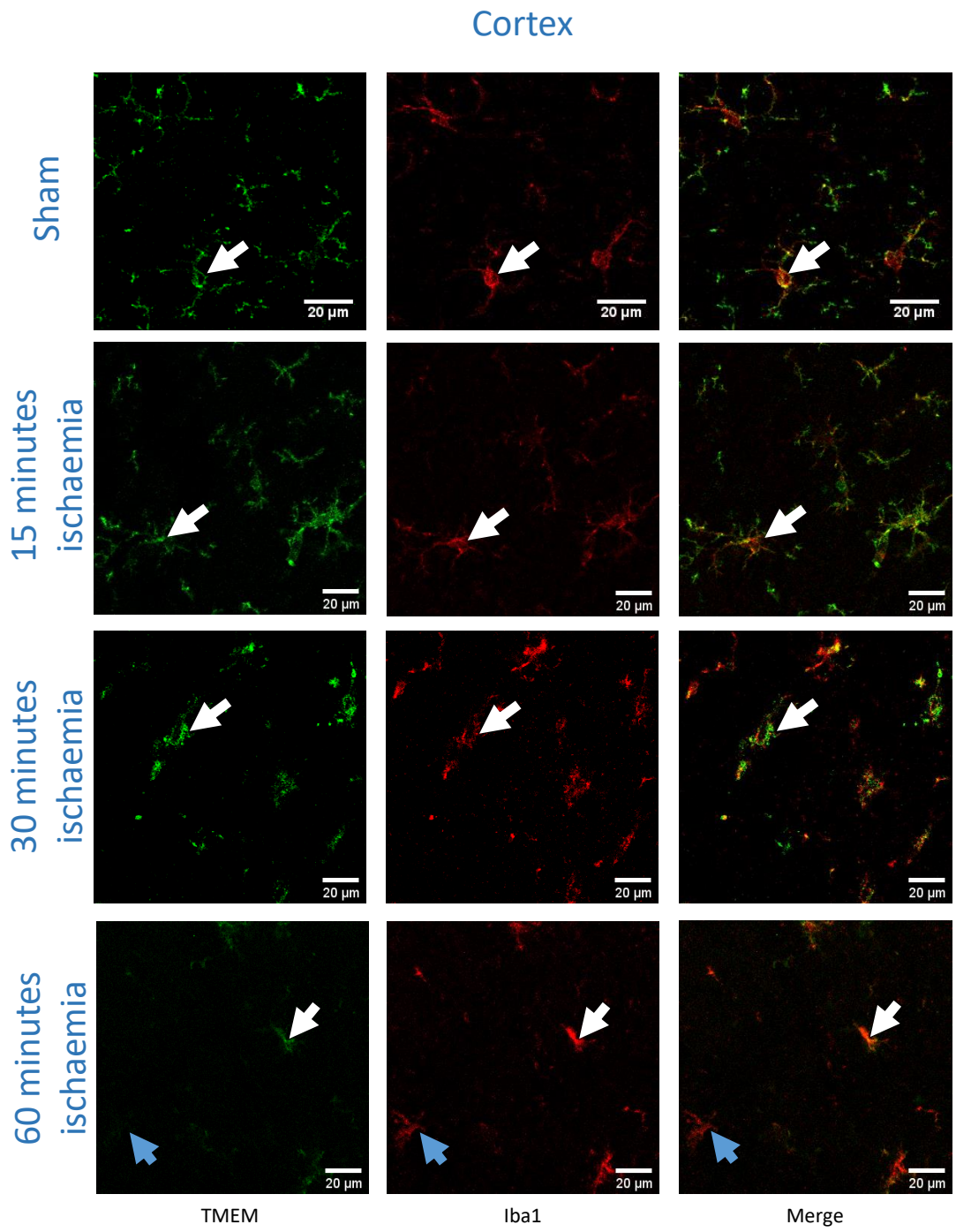

Figure 3-10 Representative images of TMEM119 and Iba1 co-immunostaining in the cortex, 24 hours after ischaemia.

In sham animals, Iba1-positive cells were co-labelled with TMEM119, suggesting they are microglia and not macrophages (white arrows). With ischaemia, Iba1-positive cells had bigger cell bodies and thicker processes, notably after 15- and 30-minutes ischaemia, and some Iba1-positive cells had an amoeboid form with no processes, notably after 60-minutes ischaemia. TMEM119 was co-labelling most of the Iba1-positive cells, suggesting they are microglia (white arrows). However, a few Iba1-cells were not co-labelled with TMEM119 (blue arrows).

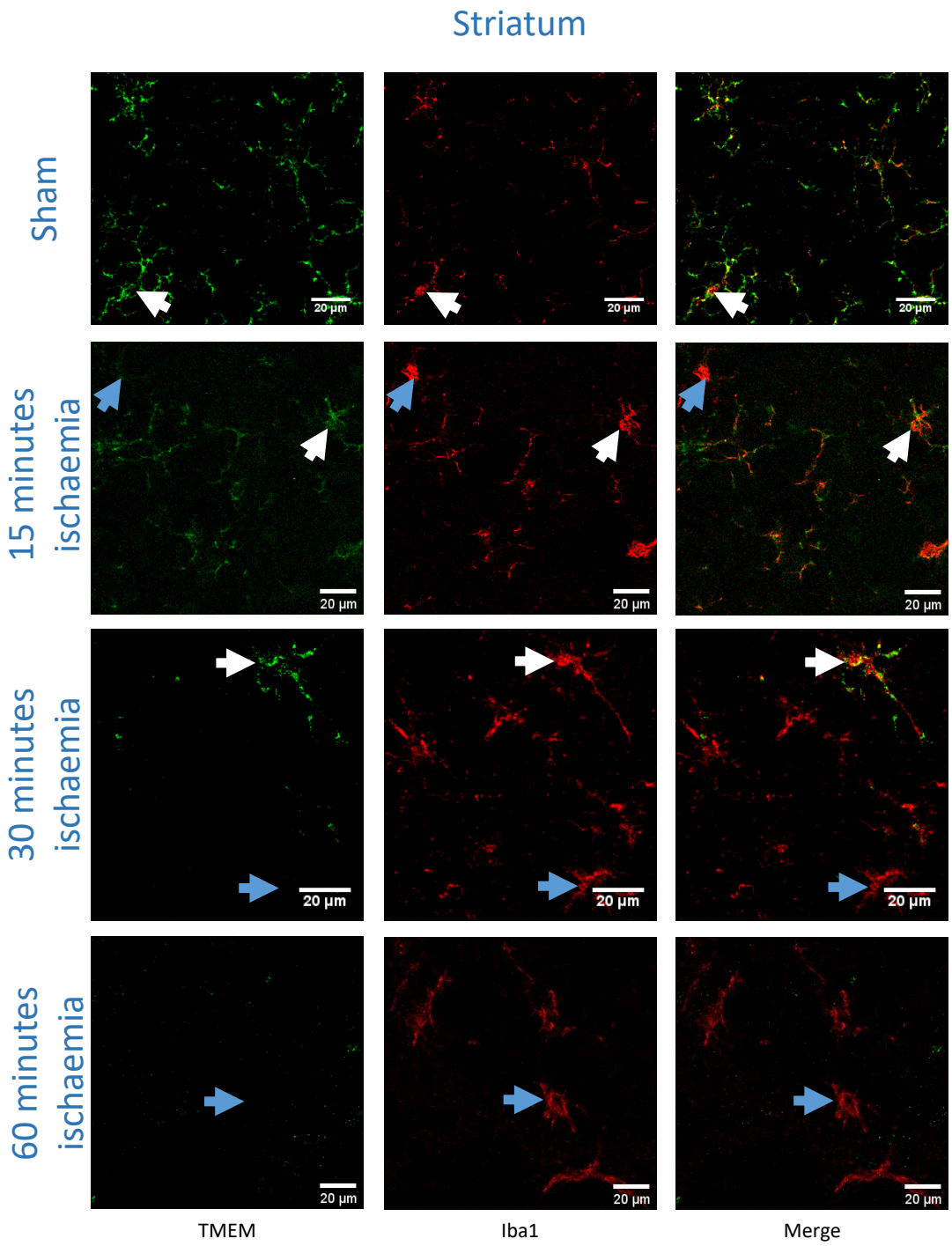

Figure 3-11 Representative images of TMEM119 and Iba1 co-immunostaining in the striatum, 24 hours after ischaemia.

In sham animals, Iba1-positive cells were co-labelled with TMEM119, suggesting they are microglia and not macrophages (white arrows). With ischaemia, Iba1-positive cells had bigger cell bodies and thicker processes, notably after 15- and 30-minutes ischaemia, and some Iba1-positive cells had an amoeboid form with no processes, notably after 60-minutes ischaemia. TMEM119 was reduced or not observable in some Iba1-positive cells after 15-, 30- or 60-minutes ischaemia (blue arrows).

In order to quantify these results, microglia (Iba1-positive/TMEM-positive cells; $Iba1^+/TMEM^+$) and macrophages (Iba1-positive/TMEM-negative cells; $Iba1^+/TMEM^-$) were counted. Counting of $Iba1^+/TMEM^-$ cells (dots on the graph) revealed no significant difference between groups in the cortex peri-infarct ($F_{(3, 22)}=2.01$, p=0.1419) and core ($F_{(3, 22)}=1.098$, p=0.3709; Fig 3.12). There was significant differences in the striatum peri-infarct ($F_{(3, 22)}=5.561$, p=0.0054) and post hoc comparison revealed there was a significant increase of $Iba1^+/TMEM^-$ cells in the 15, 30 and 60 minutes ischaemia group compared to shams (p=0.0117, p=0.0027 and p=0.0478 respectively; Fig 3.12). There was also a significant increase in $Iba1^+/TMEM^-$ cells in the striatum core of ischaemic animals and post hoc comparison showed that there was a significant increase ($F_{(3, 22)}=6.849$, p=0.0020) in the 15- and 30-minutes ischaemia group compared to shams (p=0.048 and p=0.0007 respectively) but not with 60-minutes ischaemia when compared with shams (p=0.417; Fig 3.12). This result showed there is an alteration of TMEM staining that might be attributed to resident microglia modification and/or macrophage infiltration.

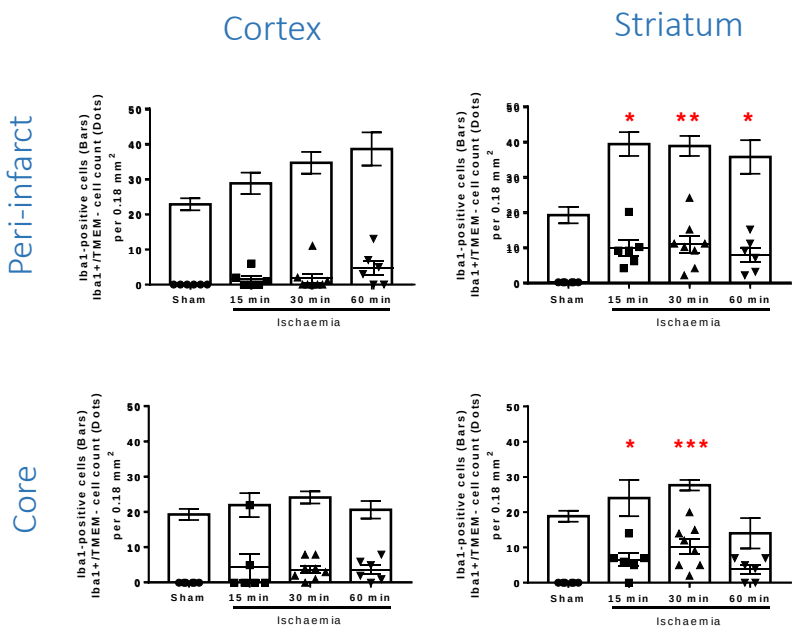

Figure 3-12 Ischaemia increases microglia/macrophage cells in the cortex and striatum, 24 hours after ischaemia.

Counting of Iba1-positive/TMEM-negative cells ($Iba1^+/TMEM^-$; dots) revealed significant differences in the striatum peri-infarct ($F_{(3, 22)}=5.561$, p=0.0054) with a significant increase of $Iba1^+/TMEM^-$ cells in the 15, 30 and 60 minutes ischaemia group compared to shams (p=0.0117, p=0.0027 and p=0.0478 respectively). A significant effect of the ischaemia in the striatum core ($F_{(3, 22)}=6.849$, p=0.0020) showed significant differences for 15 and 30 minutes ischaemia group compared to shams (p=0.048 and p=0.0007 respectively). There was no significant difference between groups in the cortex peri-infarct ($F_{(3, 22)}=2.01$, p=0.1419) and core ($F_{(3, 22)}=1.098$, p=0.3709).

*Data presented as mean ± S.E.M. One-way ANOVA followed by post hoc comparison with Bonferroni (N= 6 to 8 per group). *p<0.05, **p<0.01, ***p<0.001 comparing infiltrating macrophages (Iba1^{+}/TMEM^{-}; dots) for 15-, 30- or 60-minutes ischaemia to shams*

3.3.7. Nrf2 signalling during the acute response to ischaemia

Nrf2 detection using immunohistochemistry is limited at present due to a lack of specificity of the commercially available antibodies (Kemmerer et al., 2015). Consequently, to assess Nrf2-pathway activation, downstream genes or proteins of this pathway were studied. The following immunohistochemical study is based on heme oxygenase-1 (HO1), one of the most upregulated protein of Nrf2-pathway activation, previously shown to be upregulated with ischaemia (Alfieri et al., 2013).

HO1 immunostaining was minimal in shams and after 15 minutes ischaemia; however, levels were upregulated in the cortex and striatum, in both peri-infarct and core of the lesion after 30- and 60-minutes of ischaemia (Fig 3.13 A). Quantification of %area of HO1 immunostaining revealed a significant difference in the cortex peri-infarct ($F_{(3, 22)}$=10.21, p=0.0002), the cortex core ($F_{(3, 22)}$=11.08, p<0.0001), striatum peri-infarct ($F_{(3, 22)}$=3.96, p=0.021) but not the striatum core ($F_{(3, 22)}$=2.88, p=0.0585).

Post hoc comparisons with Bonferroni showed no differences between 15-minutes ischaemia and shams in the cortex peri-infarct and core (p>0.999 for both), in the striatum peri-infarct and core of the lesion (p=0.347 and p=0.496 respectively; Fig 3.13). After 30-minutes ischaemia, HO1 immunostaining was significantly increased in the peri-infarct cortex and striatum (p=0.0044 and p=0.0157 respectively) but not in the core cortex and striatum (p=0.158 and p=0.311 respectively; Fig 3.13). HO1 was significantly increased with 60 minutes of ischaemia in the peri-infarct for both cortex and striatum (p=0.0004 and p=0.0269 respectively) and in the core for both cortex and striatum (p<0.0001 and p=0.0228 respectively; Fig 3.13).

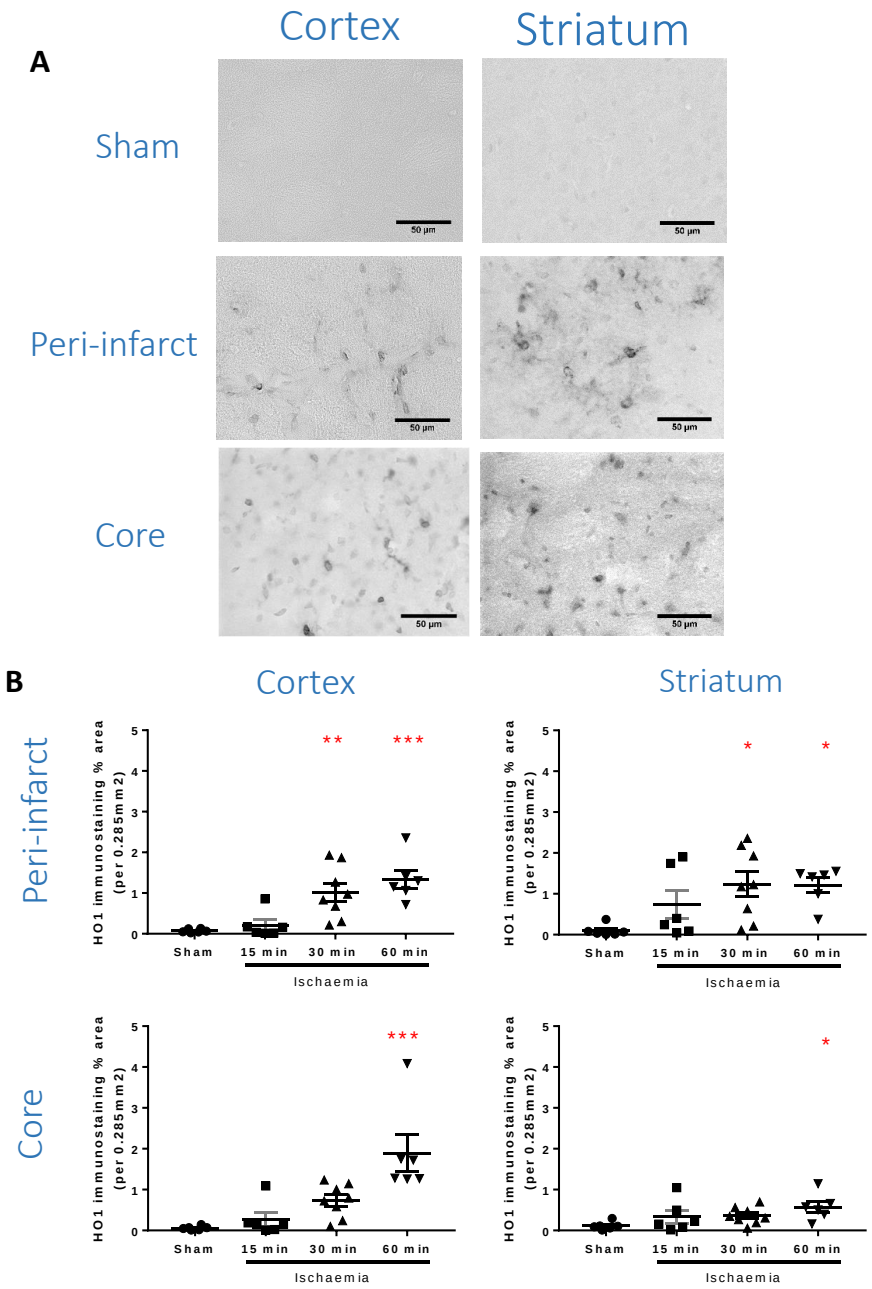

Figure 3-13 Increased duration of ischaemia increases heme oxygenase-1 in the cortex and the striatum, 24 hours after ischaemia.

(A) Representative images of heme oxygenase-1 (HO1) immunostaining showing increased levels in the cortex and the striatum after 60 minutes ischaemia but not in shams.

(B) Quantification of HO1 immunostaining by %area showed significant differences between groups in the cortex peri-infarct ($F_{(3, 22)}$=10.21, p=0.0002), the cortex core ($F_{(3, 22)}$=11.08, p<0.0001), striatum peri-infarct ($F_{(3, 22)}$=3.96, p=0.021) but not the striatum core ($F_{(3, 22)}$=2.88, p=0.0585). There was a significant increase in peri-infarct cortex with 30- and 60-minutes ischaemia (p=0.0044 and p=0.0004 respectively). In the striatum peri-infarct, HO1 was significantly increased with 30- and 60-minutes ischaemia (p=0.0157 and p=0.0269 respectively). In the core of the lesion, HO1 immunostaining was increased with 60 minutes ischaemia in the cortex (p<0.0001) and striatum (p=0.0228).

*Data presented as mean ± S.E.M. One-way ANOVA followed by post hoc comparisons with Bonferroni (N= 6 to 8 per group). *p<0.05, **p<0.01, ***p<0.001.*

Nrf2 is a transcription factor and thus leads to the expression of downstream proteins via an upregulation of their genes by binding on their ARE sequences. Nrf2-related gene expression has been measured with qRT-PCR on a cohort of animals that received 15 minutes ischaemia or sham surgery, with collection of brain samples at 24 hours. The downstream protein genes chosen were as follow: heme oxygenase-1 (*hmox1*), NADPH quinone oxidoreductase 1 (*nqo1*), sulfiredoxin 1 (*srxn1*), xCT (*slc7a11*). Furthermore, Nrf2 gene *nfe2l2* expression was also measured.

There were no differences between the groups for *nfe2l2* in the cortex ($F_{(3, 17)}$=1.892, p=0.169), however there was a significant difference in the striatum ($F_{(3, 17)}$=3.831, p=0.0290). Post hoc comparisons however did not show any differences between shams and 2-, 4- or 24-hours survival (p=0.257, p>0.999, and p=0.0561 respectively; Fig 3.14).

There was a significant difference between the groups for *hmox1* in the cortex ($F_{(3, 17)}$=3.991, p=0.0254), and in the striatum ($F_{(3, 17)}$=27.93, p<0.0001). Post hoc comparisons revealed a significant increase of *hmox1* 4 hours after ischaemia compared to shams in the cortex (p=0.0135) and 24 hours after ischaemia in the striatum p<0.0001; Fig 3.14). Other comparisons did not reveal any statistical difference.

There was a significant difference between the groups for *nqo1* in the cortex ($F_{(3, 17)}$=3.532, p=0.0374), however there was no difference in the striatum ($F_{(3, 17)}$=0.583, p=0.633). Post hoc comparisons with Bonferroni a significant increase of *nqo1* 24 hours after ischaemia in the cortex (p=0.0175; Fig 3.14) and no statistically significant difference between shams and the other timepoints (p > 0.05).

There was a significant difference between the groups for *srxn1* in the cortex ($F_{(3, 17)}$=9.534, p=0.0006), and in the striatum ($F_{(3, 17)}$=8.211, p=0.0013). Post hoc comparisons revealed a significant increase of *srxn1* 4 hours after ischaemia compared to shams in the cortex (p=0.001) and at 24 hours for both cortex and striatum (p=0.0023 and p=0.0016; Fig 3.14). Other comparisons did not reveal any statistical difference.

There was a significant difference between the groups for *slc7a11* in the cortex ($F_{(3, 17)}$=7.679, p=0.0019), and in the striatum ($F_{(3, 17)}$=18.8, p<0.0001). Post hoc comparisons revealed a significant increase of *slc7a11* 24 hours after ischaemia compared to shams in the cortex and

striatum ($p=0.0007$ and $p<0.0001$; Fig 3.14). Other comparisons did not reveal any statistical difference.

Taken together, these results show that Nrf2-pathway was activated at 4 and 24 hours after even a modest duration of 15 minutes ischaemia.

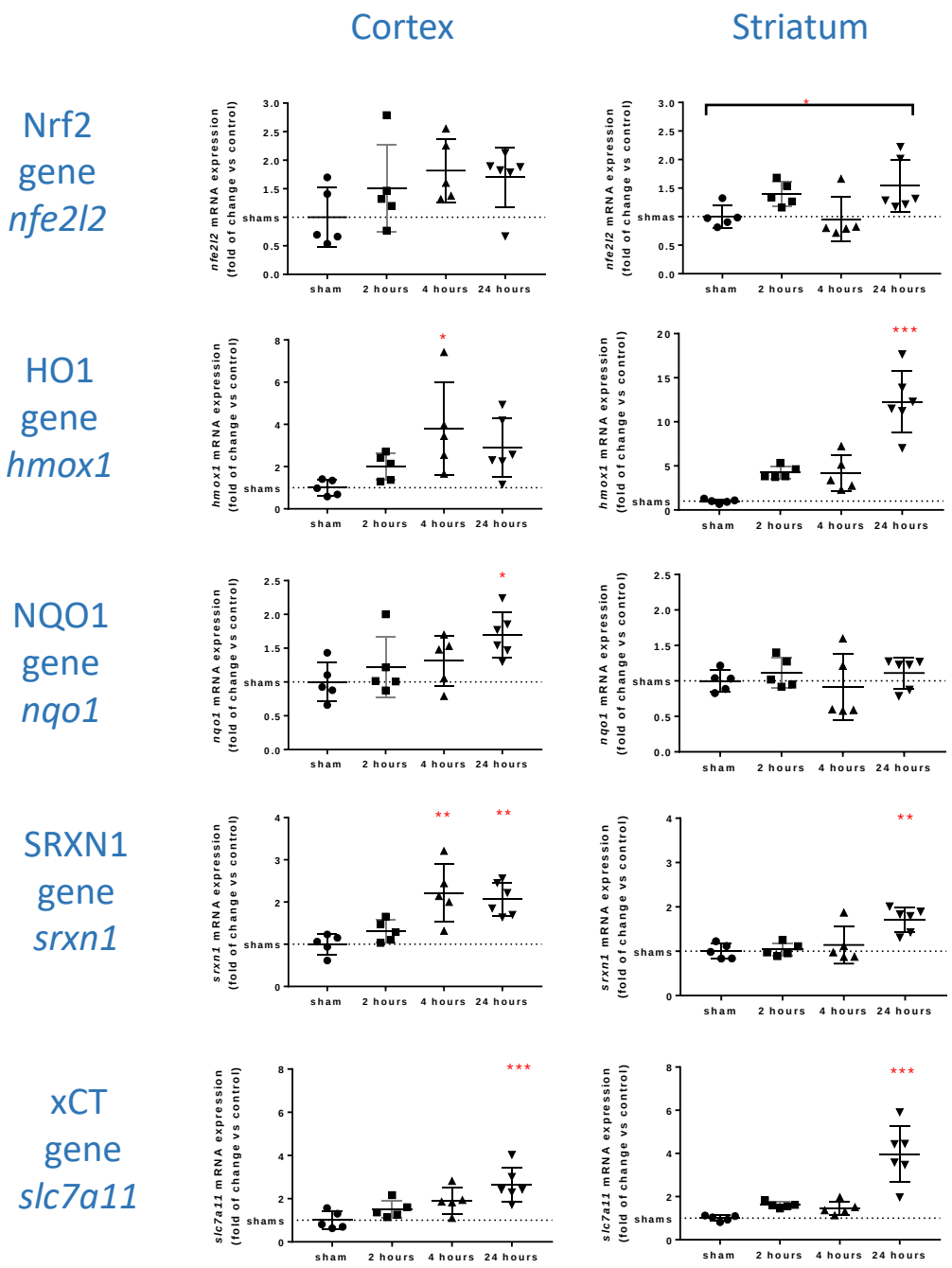

Figure 3-14 Nrf2 gene and its related genes were upregulated 24 hours after ischaemia.

mRNA expression of Nrf2 gene (nfe2l2) and its related genes in the cortex showed a significant difference in the striatum for nfe2l2 ($F_{(3, 17)}$=10.21, p=0.0002) for hmox1 in the cortex ($F_{(3, 17)}$=3.991, p=0.0254), and in the striatum ($F_{(3, 17)}$=27.93, p<0.0001) for nqo1 in the cortex ($F_{(3, 17)}$=3.532, p=0.0374), for srxn1 in the cortex ($F_{(3, 17)}$=9.534, p=0.0006), and in the striatum ($F_{(3, 17)}$=8.211, p=0.0013) for slc7a11 in the cortex ($F_{(3, 17)}$=7.679, p=0.0019), and in the striatum ($F_{(3, 17)}$=18.8, p<0.0001).

*Dotted line indicates average sham level. Data presented as mean ± S.E.M. One-way ANOVA followed by post hoc comparisons with Bonferroni (N= 5 to 6 per group). *p<0.05, **p<0.01, ***p<0.001.*

3.4. Long term ischaemia and Nrf2 activation

A modest duration of ischaemia (15 mins) induced ischaemic neuronal death, oxidative stress, activation of microglial cells and these changes were paralleled by activation of Nrf2 signalling. To determine if oxidative stress and inflammation were present and Nrf2-signalling was activated at a chronic time point after stroke, a cohort of mice underwent 15 mins of focal cerebral ischaemia and mice survived for 4 weeks.

3.4.1. Modest duration ischaemia increases neuronal damage in the striatum at chronic time point

Lesion volume was mapped out onto line diagrams of coronal anatomical levels using H&E stained sections coupled with microtubule associated protein 2 (MAP2) immunostained sections (Fig 3.15 A, B and C).

High magnification images of H&E showed evidence of vacuolisation in the lesion, loss of cells with the morphological appearance of neurons, and the tissue was shrunken. MAP2 staining was performed to help the distinction (Fig 3.15 A). MAP2 immunostaining showed homogenous staining in the healthy tissue. After ischaemia, the lesion had reduced MAP2 immunostaining (Fig 3.15 B).

No neuronal damage was observed in the sham groups. With 15 minutes of ischaemia, the lesion was mainly contained in the striatum at 4 weeks post-injury. Quantification of lesion volume revealed a significant increase in the total ipsilateral hemisphere and striatal lesion compared to shams at 4 weeks after the ischaemia ($t_{(14)}$=4.552, p=0.0005 and $t_{(14)}$=5.046, p=0.0002; Fig 3.15 D). There was no significant difference in the volume of neuronal damage between ischaemic animals and shams in the cortex ($t_{(14)}$=1.534, p=0.147 respectively; Fig 3.15 D).

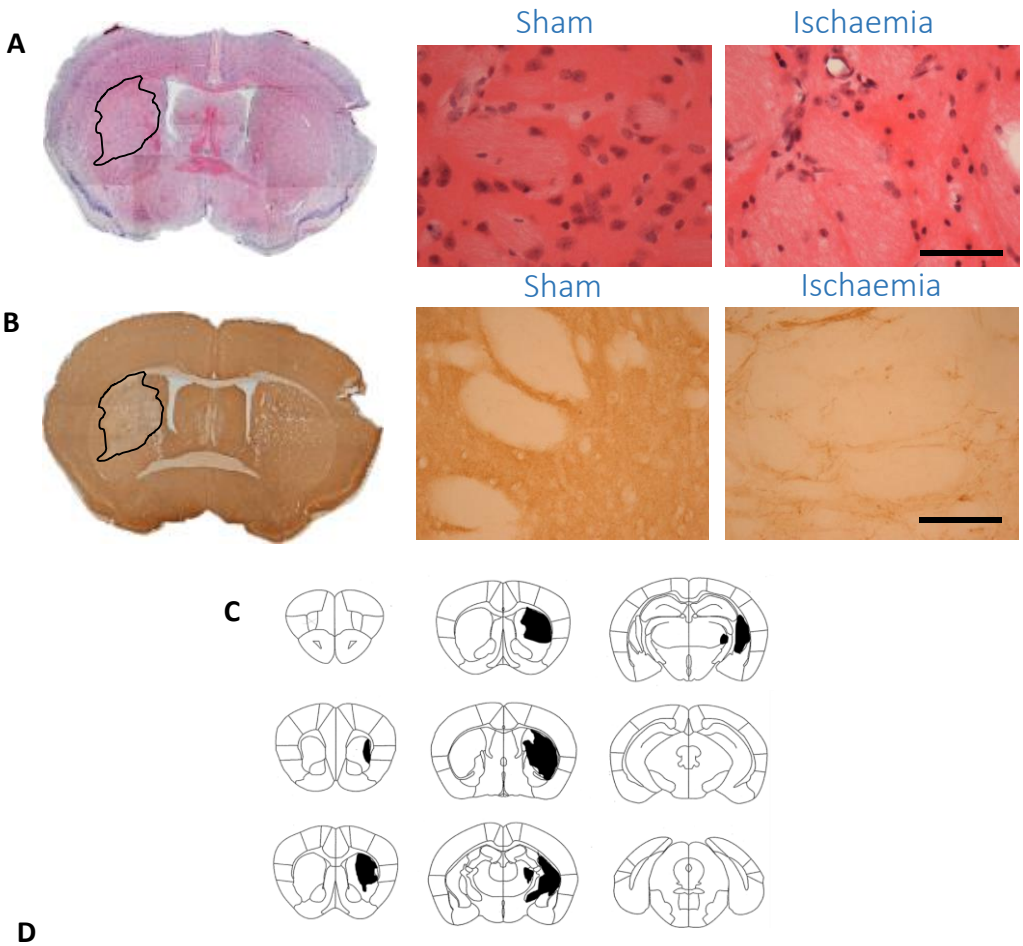

Figure 3-15 Ischaemia increases neuronal damage in the striatum but not the cortex 4 weeks after 15 minutes ischaemia.

(A) Representative image of neuronal damage outlined in black on haematoxylin and eosin staining (H & E) and high magnification images of H&E showed vacuolisation in the lesion and tissue was shrunken compared to the healthy tissue. Scale bar 100 µm.

(B) Representative image of neuronal damage outlined in black with microtubule-associated protein 2 (MAP2) and high magnification images of MAP2 immunostaining showed homogenous staining in the healthy tissue. After ischaemia, the lesion had reduced MAP2 immunostaining. Scale bar 100 µm.

(C) Representative line diagram with ischaemic neuronal damage in black from median animals (coordinates from Bregma +2.58; +1.54; +0.98; +0.74; -0.10; -1.06; -2.06; -2.92; -4.48 mm).

(D) Quantification of neuronal damage mapping revealed a significant difference between shams and 15-minute ischaemia in the total lesion ($t(14)=4.552$, $p=0.0005$) and the striatal lesion ($t(14)=5.046$, $p=0.0002$). There was no differences in the cortex when comparing shams and 15 minutes ischaemia ($t(14)=1.534$, $p=0.147$).

*Data presented as mean ± S.E.M. Student's t-test for gene expression study (N= 7 to 9 per group). ***p<0.001.*

3.4.2. Modest duration ischaemia increases the oxidative stress marker 3NT in the chronic phase

Oxidative stress, observed using 3NT immunostaining, was detected 4 weeks after 15 minutes of ischaemia whereas minimal immunostaining was detected in shams (Fig 3.16 A). Quantification of the volume of 3NT immunostaining showed that there was a significant increase in the total ipsilateral hemisphere and the striatum compared to the sham group ($t_{(14)}$=5.001, p=0.0002 and $t_{(14)}$=5.17, p=0.0001 respectively; Fig 3.16 B). In the cortex, 3NT expression was not significantly different from the sham ($t_{(14)}$=1.086, p=0.296; Fig 3.16 B).

The area of 3NT immunostaining was mapped and compared with the area of neuronal damage (Fig 3.16 C). Four weeks after the ischaemia, the area of 3NT immunostaining mirrored the lesion area (Fig 3.16 C). These results indicate that oxidative stress was still present at later time point; however, it was contained within the lesion.

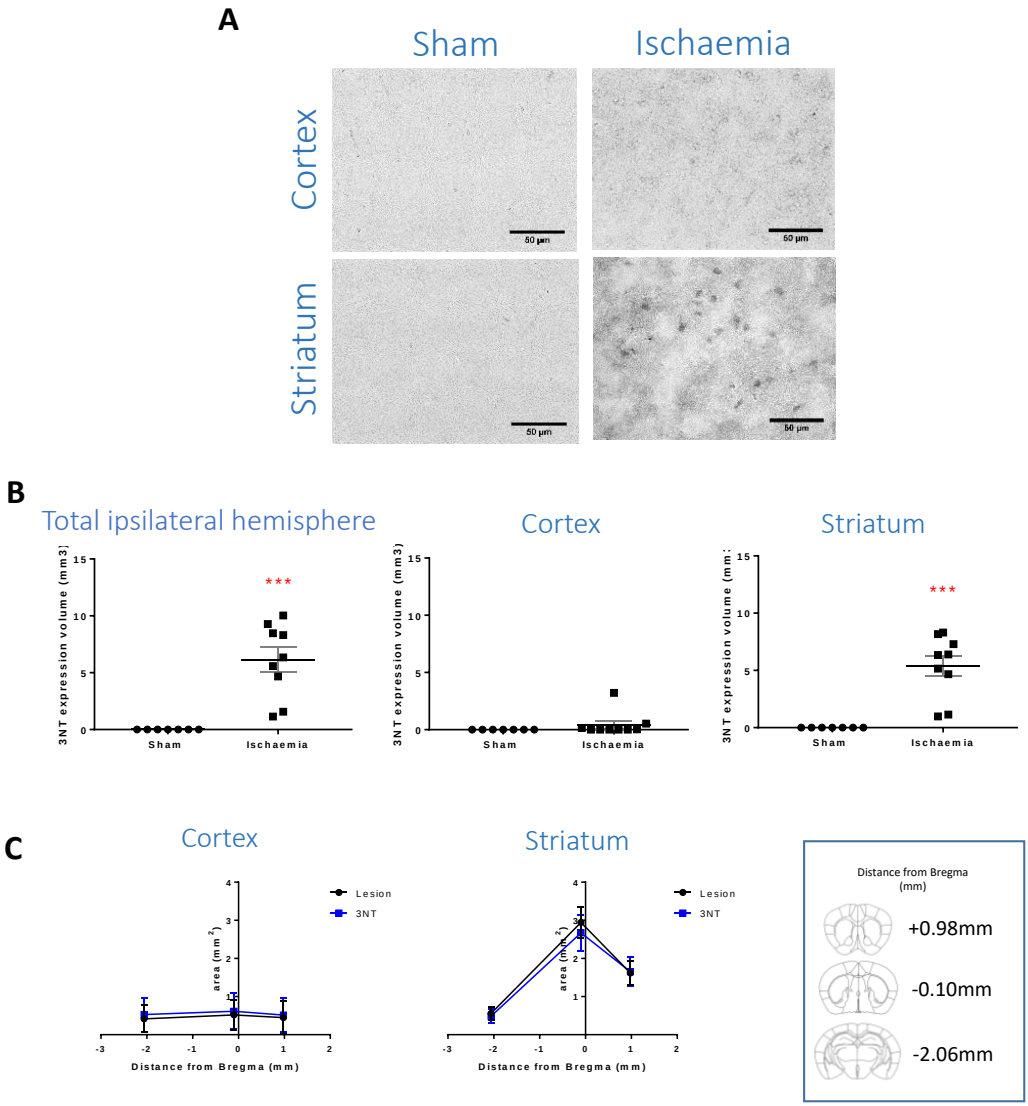

Figure 3-16 Modest duration ischaemia increases oxidative stress in the striatum but not the cortex 4 weeks after 15 minutes ischaemia.

(A) Representative images of 3-Nitrotyrosine (3NT) immunostaining showing peroxide nitrite generation in the striatum after ischaemia but not in the cortex or in shams four weeks after 15 minutes ischaemia. There was minimal 3NT immunostaining in shams and in the cortex after ischaemia.

(B) Quantification of 3NT staining by mapping the positive staining showed significant differences between shams and 15 minutes ischaemia in the total ipsilateral hemisphere ($t_{(14)}$=5.001, p=0.0002) and the striatum ($t_{(14)}$=5.17, p=0.0001). There was no differences in the cortex between shams and 15 minutes ischaemia ($t_{(14)}$=1.086, p=0.296).

(C) Profile of the staining area and the neuronal damage area in three coronal sections of the 15 minutes ischaemia group showed 3NT expression mirroring lesion area.

*Data presented as mean ± S.E.M. Student's t-test for gene expression study (N= 7 to 9 per group). ***p<0.001.*

3.4.3. Astrocytic response to chronic ischaemia

Reactive astrocytes were examined with GFAP immunostaining. There were minimal levels of GFAP immunostained cells in the cortex and striatum of sham controls. In this study, peri-infarct and core were homogenous and indistinguishable hence they gave the same results (see Appendix fig 8.1). Following ischaemia, there were increased levels of reactive astrocytes and individual cells were observed to be darker and more abundant in the ischaemic brains compared to shams in the cortex. In contrast, in the striatum there was a marked elevation of GFAP immunostaining however individual cells and their processes were no longer visible, and instead a glial scar was evident (Fig 3.17 A; Bush et al., 1999; Faulkner et al., 2004; Sofroniew, 2009).

Quantification of GFAP immunostaining by assessing %area revealed significant differences between shams and 15 minutes of ischaemia in the cortex ($t_{(14)}$=2.362, p=0.0332) and the striatum ($t_{(14)}$=4.116, p=0.0010; Fig 3.17 B).

To build on these findings, levels of GFAP gene were investigated. There was a significant difference between shams and ischaemia for *gfap* mRNA levels for both cortex ($t_{(9)}$=4.199, p=0.0009) and striatum ($t_{(9)}$=5.634, p<0.0001, Fig 3.17 C) 4 weeks after 15 minutes of ischaemia compared to shams. Taken together, these results showed that modest duration ischaemia upregulates GFAP at protein and gene levels in the chronic response to ischaemia and causes marked reactive gliosis.

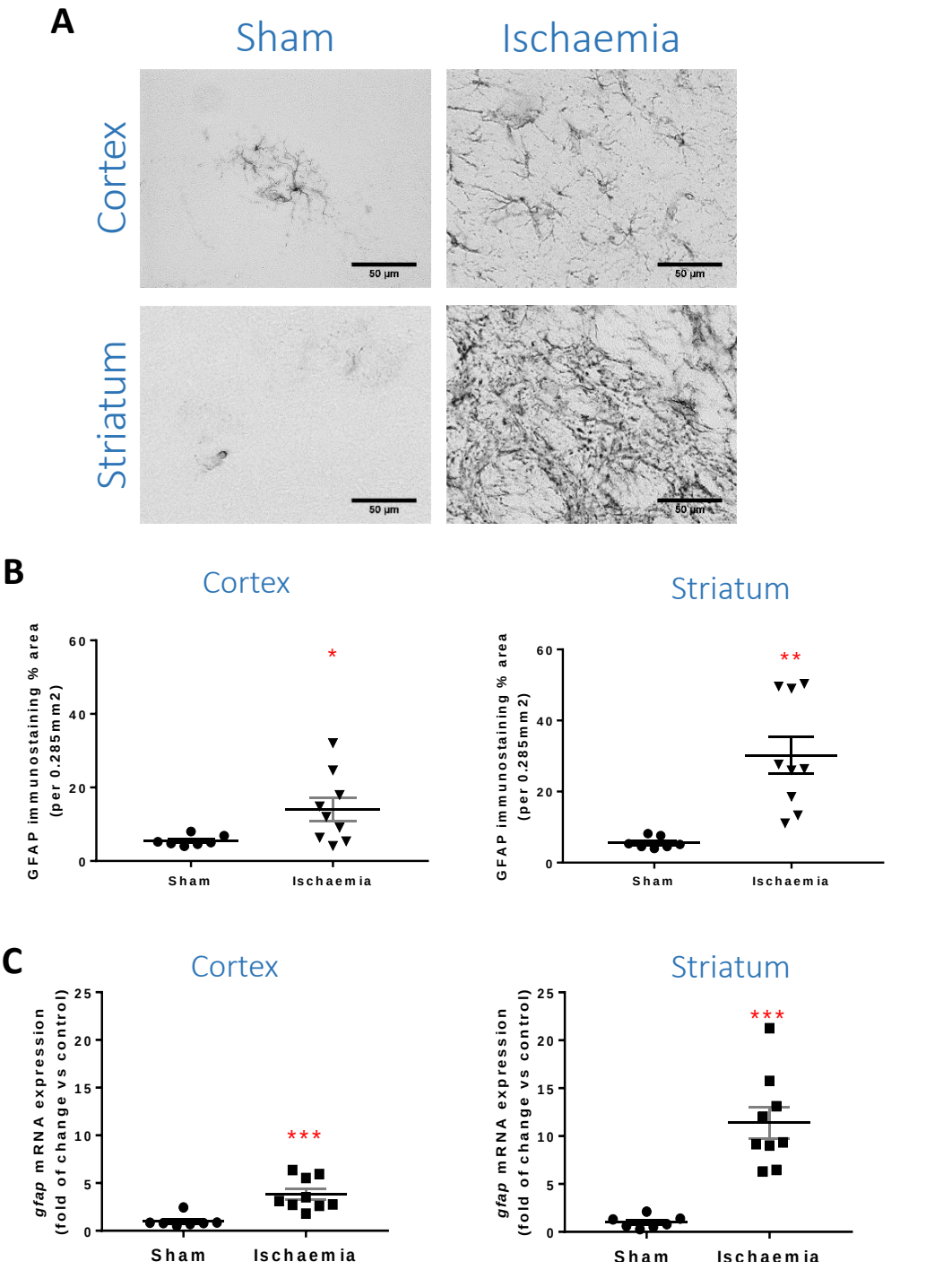

Figure 3-17 Astrocytic marker GFAP was increased in striatum and cortex 4 weeks after 15 minutes ischaemia.

(A) Representative images of GFAP immunostaining showing increased expression in the striatum and cortex after ischaemia compared to shams four weeks after 15 minutes ischaemia.

(B) Quantification of GFAP immunostaining by assessing %area revealed significant differences between shams and 15 minutes ischaemia in the cortex ($t_{(14)}$=2.362, p=0.0332) and the striatum ($t_{(14)}$=4.116, p=0.0010).

(C) There was a significant elevation of GFAP in mRNA both cortex ($t_{(9)}$=4.199, p=0.0009) and striatum ($t_{(9)}$=5.634, p<0.0001) 4 weeks after 15 minutes of ischaemia compared to shams.

*Data presented as mean ± S.E.M. Student's t-test (N= 7 to 9 per group). *p<0.05, **p<0.01, ***p<0.001.*

3.4.4. Microglia/macrophage response 4 weeks after ischaemia

Sham animals presented immunostaining of Iba1 similar to the shams in the 24-hour survival cohort, cell bodies were small, and processes were thin. After ischaemia, there was a similar pattern of immunostaining in the cortex compared to shams. In the striatum, Iba1-positive cells were darker, however they no longer had distinct processes and appeared amoeboid in the ischaemic brains compared to shams at 4 weeks (Fig 3.18 A).

Quantification of Iba1 immunostaining by investigating %area of immunostaining showed significant differences between shams and 15 minutes ischaemia in the striatum ($t_{(14)}$=2.677, p=0.0181) but not the cortex ($t_{(14)}$=1.751, p=0.1018; Fig 3.18 B).

Counting of Iba1-positive cells revealed that there was a significant increase in the striatum compared to shams ($t_{(14)}$=4.187, p=0.0009) but not in the cortex ($t_{(14)}$= 1.837, p=0.0875; Fig 3.18 C).

To further investigate alterations to Iba1, levels of the gene encoding Iba1, aif1 were determined. At 4 weeks, aif1 was increased in both cortex ($t_{(9)}$=2.218, p=0.0436) and striatum ($t_{(9)}$=3.363, p=0.0046) compared to shams (Fig 3.18 D).

Taken together, these results show that modest duration ischaemia causes a chronic upregulation of Iba1 protein and gene levels. Therefore, the increase in %area of Iba1 immunostaining sections was partly due to an increase in the number of microglia/macrophages and partly due to morphological alterations of microglia/macrophages.

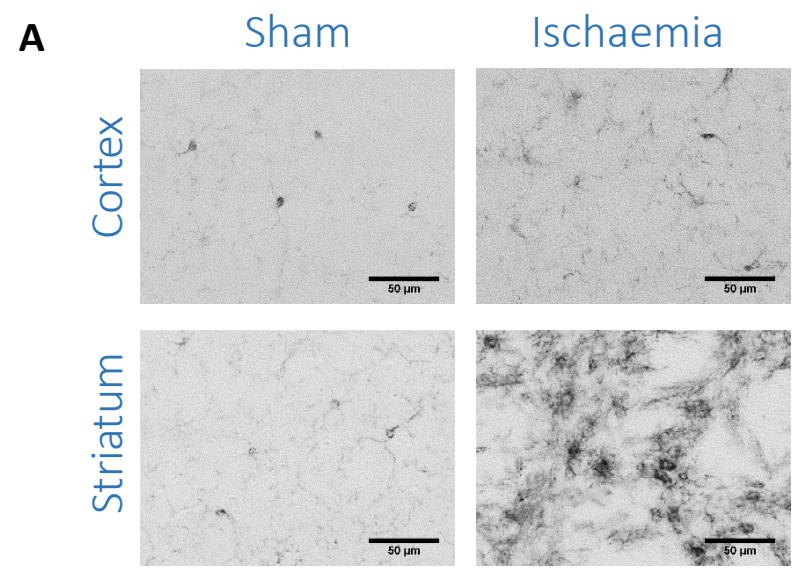
A
Sham
Ischaemia
Cortex
Striatum
50 µm
50 µm
50 µm
50 µm

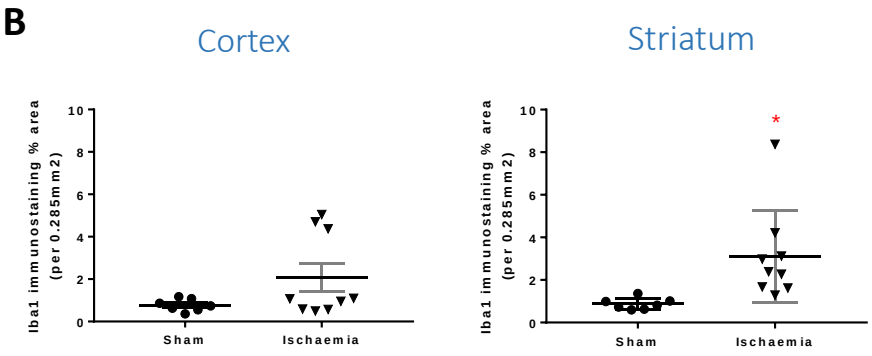
B
Cortex
Striatum
Iba1 immunostaining % area (per 0.285mm2)
Sham
Ischaemia
*

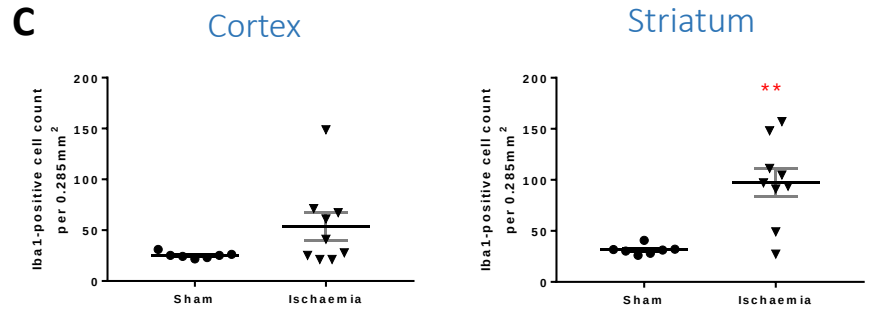
C
Cortex
Striatum
Iba1-positive cell count per 0.285mm2
Sham
Ischaemia
**

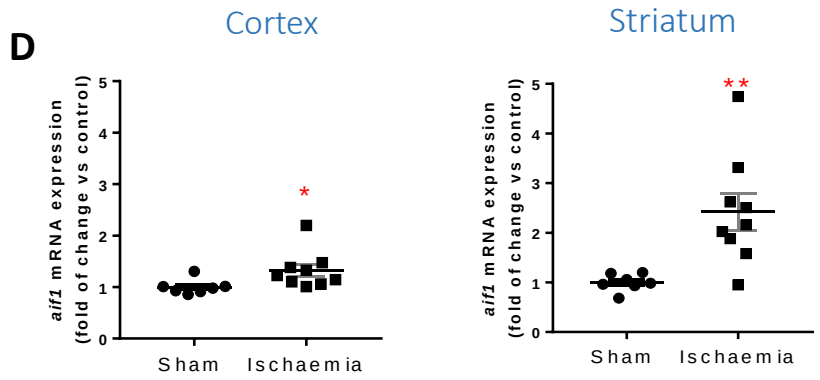
D
Cortex
Striatum
aif1 mRNA expression (fold of change vs control)
Sham
Ischaemia
*
**

← Figure 3-18 Modest duration ischaemia (15 minutes) increases microglia/macrophage marker Iba1 4 weeks post injury.

(A) Representative images of Iba1 immunostaining showing small cell bodies and thin processes in shams in the cortex after 15 minutes of ischaemia at 4 weeks. In the striatum after ischaemia, Iba1-positive cells were darker, bigger and overlapping with each other.

(B) Quantification of Iba1 immunostaining by %area showed significant differences between shams and 15 minutes ischaemia in the striatum ($t_{(14)}$=2.677, p=0.0181) but not the cortex ($t_{(14)}$=1.751, p=0.1018).

(C) There were significantly increased levels of Iba1 gene aif1 both cortex ($t_{(9)}$=2.218, p=0.0436) and striatum ($t_{(9)}$=3.363, p=0.0046) 4 weeks after 15 minutes of ischaemia compared to shams.

(D) Counting Iba1-positive cells revealed that there were significantly increased numbers of cells in the striatum ($t_{(14)}$=4.187, p=0.0009) but not the cortex ($t_{(14)}$= 1.837, p=0.0875).

*Data presented as mean ± S.E.M. Student's t-test (N= 7 to 9 per group). *p<0.05, **p<0.01.*

3.4.5. Genes il-1β and *cxcl10* were increased 4 weeks after modest duration of ischaemia

Interleukin 1 beta (Il-1β) and C-X-C motif chemokine 10 (CXCL10) are cytokines produced during inflammation (Chai et al., 2015; Hu et al., 2014; Rider et al., 2011). Genes encoding the cytokines *cxcl10* and *il-1β* were investigated at 4 weeks post injury. The data did not follow a normal distribution, thus statistical differences were investigated using Mann-Whitney test. In the cortex, there was a significant increase in *cxcl10* mRNA levels in ischaemic cortex (Mann–Whitney U=2, p=0.0007; Fig 3.19 A) compared to shams, but no significant difference for *il-1β* (Mann–Whitney U=13, p=0.0549; Fig 3.19 A). In the striatum, *cxcl10* mRNA expression was significantly increased compared to shams, (Mann–Whitney U=0, p=0.0002). Similarly, *il-1β* mRNA expression was significantly increased compared to shams (Mann–Whitney U=4, p=0.0021; Fig 3.19 B).

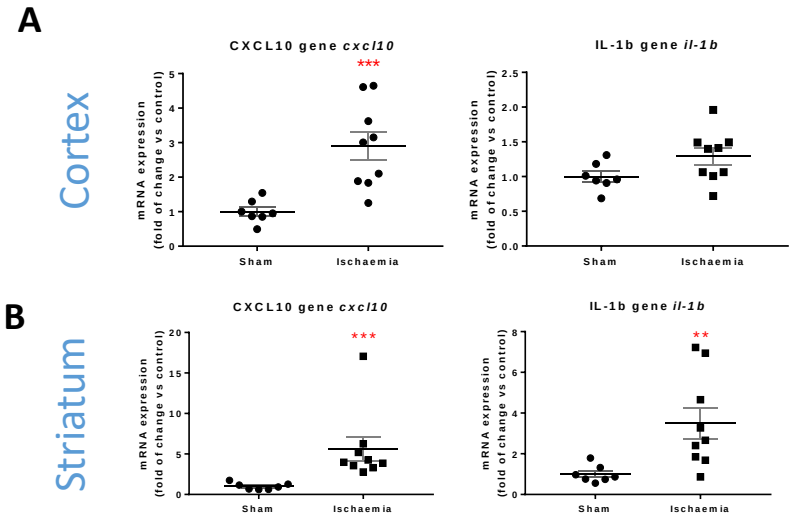

Figure 3-19 Inflammatory gene cxcl10 and il-1β were upregulated 4 weeks after 15 minutes of ischaemia.

(A) There was a significant increase in cxcl10 mRNA levels in ischaemic cortex (Mann–Whitney U=2, p=0.0007) compared to shams, but no significant difference for il-1β (Mann–Whitney U=13, p=0.0549). Genes of interest were normalised to 18S levels.

(B) In the striatum, cxcl10 mRNA expression was significantly increased compared to shams, as cxcl10 results did not follow normal distribution; Mann-Whitney test was used. (Mann–Whitney U = 0, p=0.0002). Similarly, il-1β mRNA expression was significantly increased compared to shams (Mann–Whitney U=4, p=0.0021).

*Dotted line indicates average sham level. Data presented as mean ± S.E.M. Student's t-test (N= 7 to 9 per group). **p<0.01, ***p<0.001.*

3.4.6. Peripheral immune cells infiltrate 4 weeks after modest duration ischaemia

Neutrophil infiltration was studied in this cohort of 4 weeks survival after 15 minutes ischaemia. Neutrophils were found in three ischaemic brains and one sham animal (Fig 3.20 A and B) and their presence was sparse as demonstrated in the striatum (Fig 3.20 A).

The probability of neutrophil infiltration occurring 4 weeks following 15 minutes ischaemia was unchanged in the ipsilateral hemisphere (p=0.585), unchanged in the cortex (p=0.475) and unchanged in the striatum (p=0.212), Fisher's exact test.

A

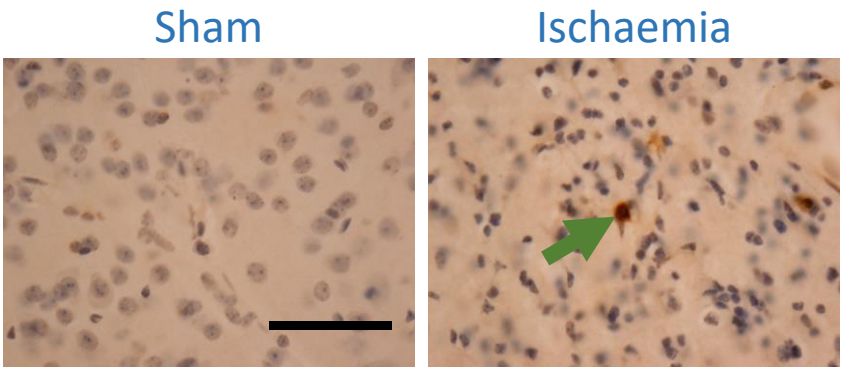

B

Anatomical Area	Sham	MCAo 4 weeks
Ispilateral	1 of 7	3 of 9
Cortex	0 of 7	2 of 9
Striatum	0 of 7	3 of 9

Figure 3-20 Modest duration ischaemia increases neutrophil infiltration 4 weeks after 15 minutes ischaemia.

(A) Representative images of neutrophil immunostaining after ischaemia but not in shams. Nuclei were counterstained with DAPI, in blue, and neutrophil in brown (green arrow). Scale bar 100 µm.

(B) Quantification of the presence of neutrophils revealed presence of neutrophils in the parenchyma in one sham animal and in 3 out of 9 animals of the 15-minute ischaemia group.

In order to evaluate macrophage infiltration and distinguish them from resident microglia, the microglia/macrophage marker Iba1 was co-stained with the microglia-specific marker TMEM 119. In sham animals, ba1-positive cells were co-labelled with TMEM 119 suggesting the presence of microglia but not macrophages (Fig 3.21 A and B). After ischaemia, cortical Iba1-positive cells were larger and had thicker processes. Furthermore, TMEM 119 staining was decreased and sometimes not detectable on some Iba1-positive cells (Fig 3.21 A). In the striatum, there was a marked increase in Iba1-positive cells that had an amoeboid shape and TMEM119 was reduced or not observable in many Iba1-positive cells.

Counting of $Iba1^{+}/TMEM^{-}$ cells (dots) revealed significant differences in the striatum ($t_{(14)}$=8.397, p<0.0001) but not the cortex ($t_{(14)}$=1,959, p=0.0704) between ischaemia and shams, four weeks after 15 minutes ischaemia (Fig 3.21 C).

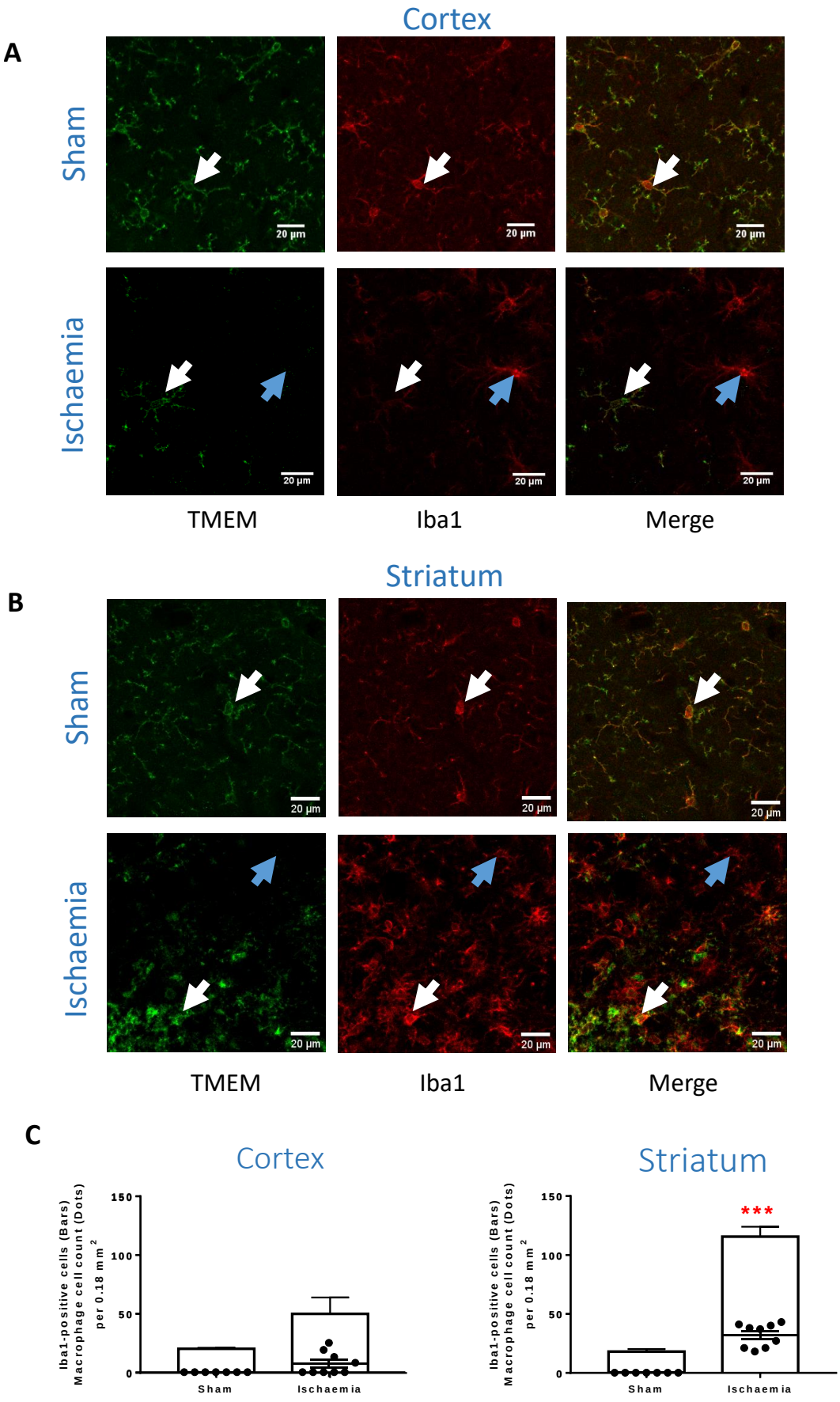
A
Cortex
Sham
Ischaemia
20 µm
TMEM
Iba1
Merge
B
Striatum
Sham
Ischaemia
20 µm
TMEM
Iba1
Merge
C
Cortex
Striatum
Iba1-positive cells (Bars)
Macrophage cell count (Dots)
per 0.18 mm 2
150
100
50
0
***
Sham
Ischaemia

← Figure 3-21 Ischaemia increases microglia/macrophage cells with reduced TMEM119 expression 4 weeks after 15 minutes ischaemia.

(A) Representative images of TMEM119 and Iba1 co-immunostaining in the cortex. In sham animals, both markers were expressed revealing resident microglia population (white arrows). Following ischaemia, Iba1-positive cells were bigger and had thicker processes; TMEM119 was reduced or not observable in some Iba1-positive cells (blue arrows).

(B) Representative images of TMEM119 and Iba1 co-immunostaining in the striatum. In sham animals, both markers were expressed revealing resident microglia population (white arrows). Following ischaemia, there was a marked increase of Iba1-positive TMEM119 was reduced or not observable in some Iba1-positive cells (blue arrows).

(C) Counting of Iba1-positive/TMEM-negative cells ($Iba1^+/TMEM^-$; dots) revealed significant differences in the striatum ($t_{(14)}=8.397$, $p<0.0001$) but not the cortex ($t_{(14)}=1,959$, $p=0.0704$) between ischaemia and shams, four weeks after 15 minutes ischaemia.

*Data presented as mean ± S.E.M. Student's t-test (N= 7 to 9 per group). ***p<0.001. comparing infiltrating macrophages ($Iba1^+/TMEM^-$; dots) for 15-minutes ischaemia to shams*

Taken together, these results suggest that 15 minutes of ischaemia has caused modest levels of neutrophil infiltration in a minority of animals, increased levels of Iba1-positive cells with possibly an infiltration of peripheral macrophages at 4 weeks after injury.

3.4.7. Nrf2 signalling was not activated in chronic ischaemia

HO1 immunostaining and Nrf2-related gene expression were investigated to assess Nrf2 signalling pathway activation. In both sham and ischaemic animals, HO1 staining was minimal (Fig 3.22 A). After quantification by %area, it was confirmed that HO1 staining was not significantly different from shams in the cortex and striatum ($t_{(14)}=0.7996$, $p=0.4373$ and $t_{(14)}=1.762$, $p=0.0999$ respectively; Fig 3.22 B).

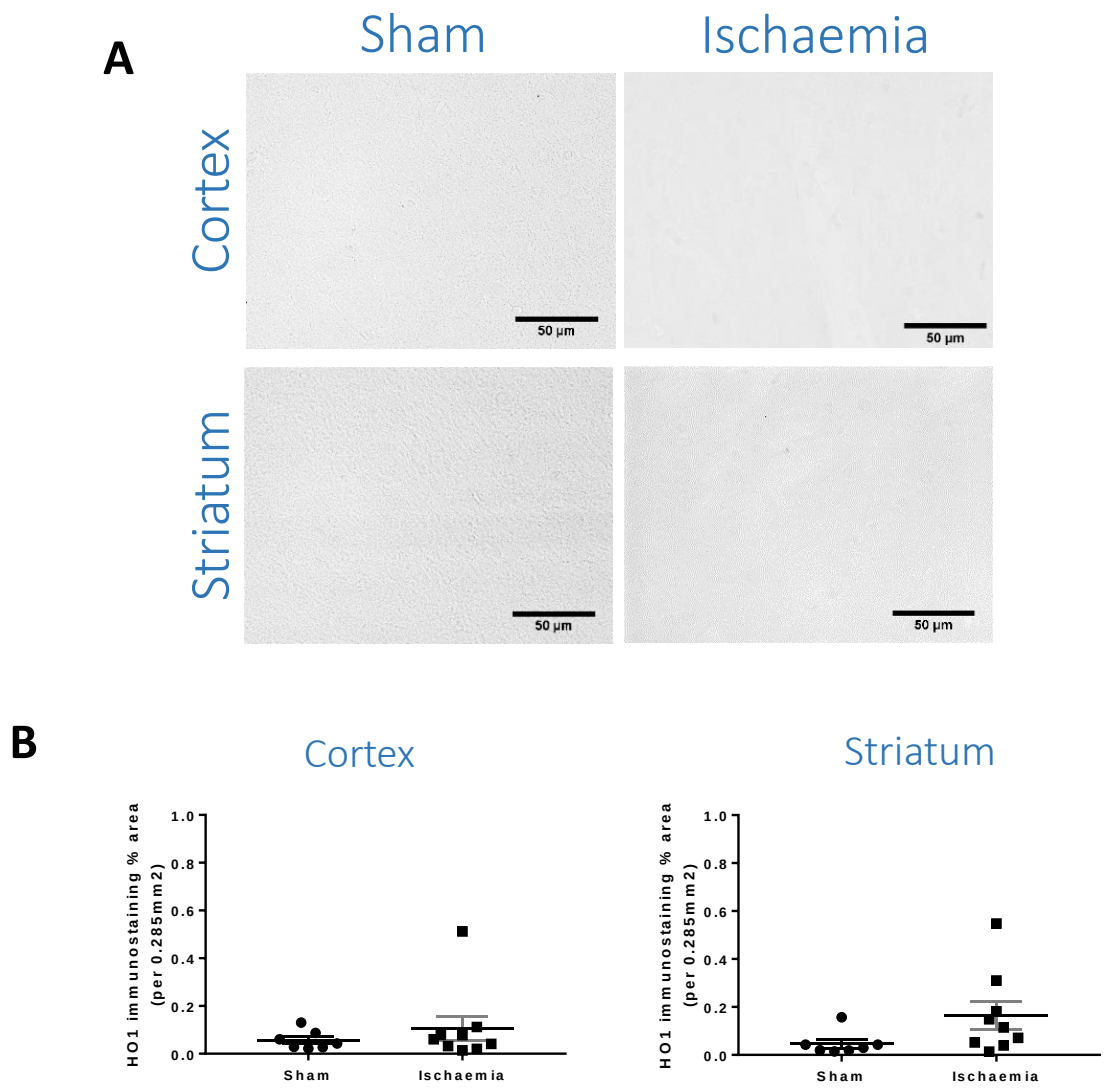

Figure 3-22 Modest duration ischaemia (15 minutes) does not modify heme oxygenase-1 four weeks post injury.

(A) Representative images of heme oxygenase-1 (HO1) immunostaining showing minimal staining in ischaemic animals and shams 4 weeks after 15 minutes ischaemia.

(B) Quantification of HO1 immunostaining by %area revealed that there were no significant differences between shams and 15 minutes ischaemia in the cortex ($t_{(14)}$=0.7996, p=0.4373) or the striatum ($t_{(14)}$=1.762, p=0.0999).

Data presented as mean ± S.E.M. Student's t-test (N= 7 to 9 per group).

Expression of *hmox1, nqo1, srxn1* and *Slc7a11* genes were not significantly altered in the cortex compared to shams 4 weeks after the ischaemia (*hmox1* ($t_{(14)}$=0.763, p=0.457), *nqo1* ($t_{(14)}$=0.479, p=0.638), *srxn1* ($t_{(14)}$=1.17, p=0.261) and xCT gene *slc7a11* ($t_{(14)}$=0.312, p=0.759.; Fig 3.23). However, Nrf2 gene *nfe2l2* was significantly upregulated at 4 weeks ($t_{(14)}$=2.247, p=0.0413).

In the striatum, *nfe2l2, hmox1, nqo1* and *slc7a11* gene expression was not altered (*nfe2l2* ($t_{(14)}$=1.717, p=0.1081), *hmox1* ($t_{(14)}$=0.211, p=0.835), *nqo1* ($t_{(14)}$=0.3895, p=0.702) and xCT gene *slc7a11* ($t_{(14)}$=0.5271, p=0.6064; Fig 3.23). However, *srxn1* expression was significantly downregulated compared to shams ($t_{(14)}$=3.693, p=0.0024). Interestingly the striatum results are more variable than the cortex results.

In conclusion Nrf2 signalling was not activated 4 weeks after 15 minutes of ischaemia. Furthermore, Nrf2 gene *nfe2l2* was upregulated in the cortex at 4 weeks.

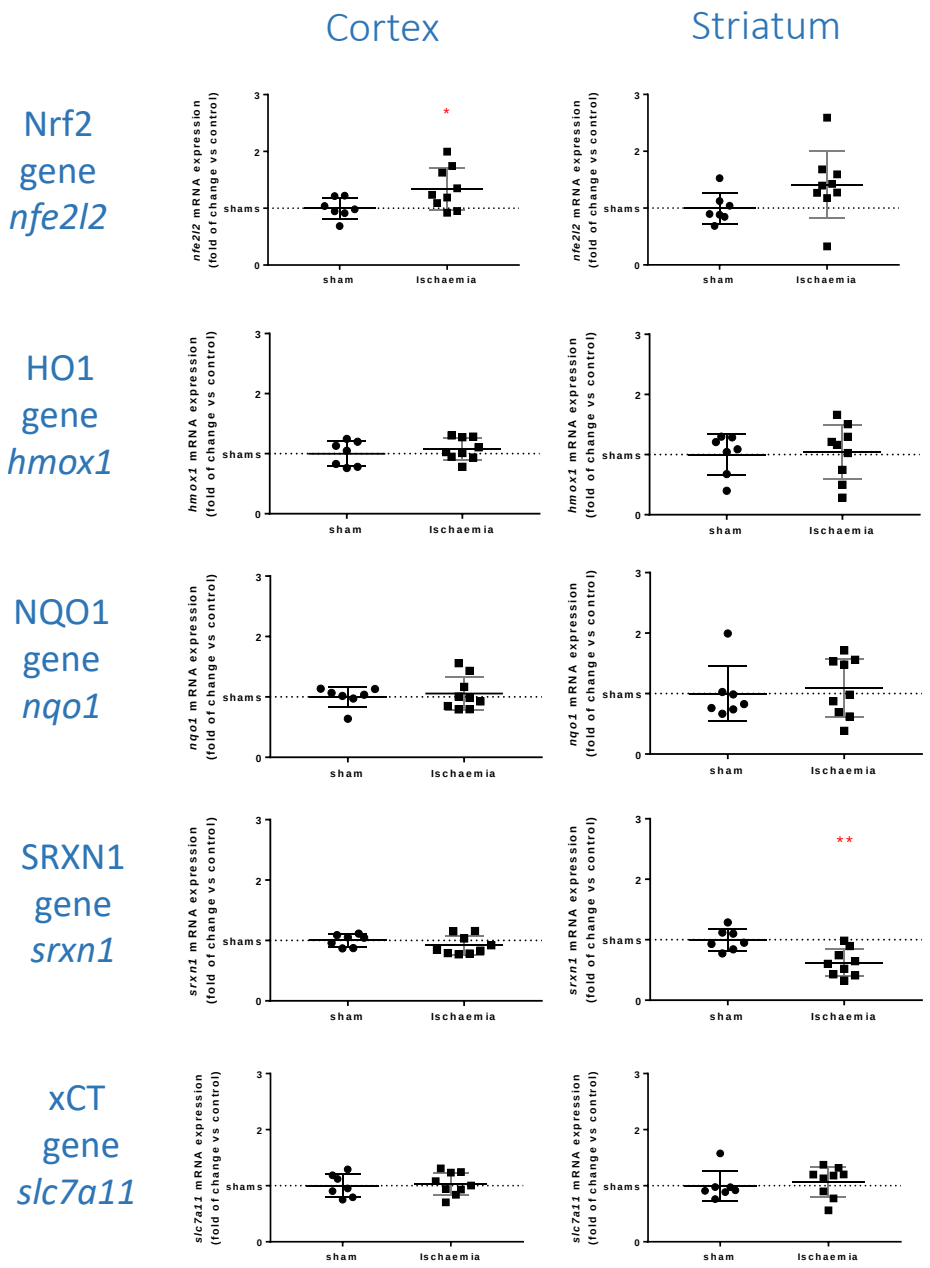

Figure 3-23 Nrf2 related genes were no longer upregulated 4 weeks after 15 minutes ischaemia.

There was a significant increase in Nrf2 mRNA levels (nfe2l2) in the cortex 4 weeks after 15-minute ischaemia ($t_{(14)}$=2.247, p=0.0413). Nrf2-related genes were not significantly altered when comparing ischaemia and shams animals in the cortex 4 weeks after the ischaemia with hmox1 ($t_{(14)}$=0.763, p=0.457), nqo1 ($t_{(14)}$=0.479, p=0.638), srxn1 ($t_{(14)}$=1.17, p=0.261) and xCT gene slc7a11 ($t_{(14)}$=0.312, p=0.759).

In the striatum there was no significant differences for nfe2l2 ($t_{(14)}$=1.717, p=0.1081), hmox1 ($t_{(14)}$=0.211, p=0.835), nqo1 ($t_{(14)}$=0.3895, p=0.702) and xCT gene slc7a11 ($t_{(14)}$=0.5271, p=0.6064) 4 weeks after 15 minutes of ischaemia compared to shams. Interestingly, there was a significant reduction of srxn1 compared to shams in the striatum ($t_{(14)}$=3.693, p=0.0024).

*Dotted line indicates average sham level. Data presented as mean ± S.E.M. Student's t-test for gene expression study (N= 7 to 9 per group). *p<0.05, **p<0.01.*

3.5. Discussion

To conclude, cellular oxidative stress and inflammation were detected at 24 hours after ischaemia and significantly increased with increasing duration of occlusion compared to shams. This was paralleled with a significant upregulation of the Nrf2-related genes *hmox1*, *nqo1, slc7a11* and *srxn1*. Four weeks following ischaemia, there was a significant increase in oxidative stress and inflammation; however, *hmox1, nqo1* and *slc7a11* were not significantly altered whereas *srxn1* was decreased compared to shams. This finding contradicts the initial hypothesis that Nrf2-signalling activation would be activated chronically after stroke and associated with oxidative stress and inflammation.

3.5.1. Cerebral ischaemia causes neuronal loss and increase duration of ischaemia increases the damaged area

Increased duration of ischaemia increases the volume of ischaemic neuronal damage. The lesion was mainly contained in the striatum after 15 minutes of ischaemia and was found in the cortex after 30 and 60 minutes of ischaemia (Fig 3.2) and as previously reported with 30 minutes ischaemia and longer (Popp et al., 2009). Neuronal damage was also observed in the thalamus and hypothalamus in the 60 minutes ischaemia group (Fig 3.2). This is consistent with the literature (Hata et al., 1998; Kanemitsu et al., 2002; McColl et al., 2004). Interestingly, these anatomical regions are not supplied by the MCA. This damage may be due to a direct ischaemia of these regions (Kanemitsu et al., 2002) caused by an incomplete circle of Willis (see Fig 3.24; McColl et al., 2004). Variability can be resolved by optimising the filament and by choosing a narrow range of animal age and weight to match the filament diameter (Hata et al., 1998; Tsuchiya et al., 2003). Overall, MCAo occlusion by insertion of a thread is still an adequate model to mimic ischaemic pathology from cell death to glial activation pattern and BBB breakdown (Howells et al., 2010; Kuraoka et al., 2009).

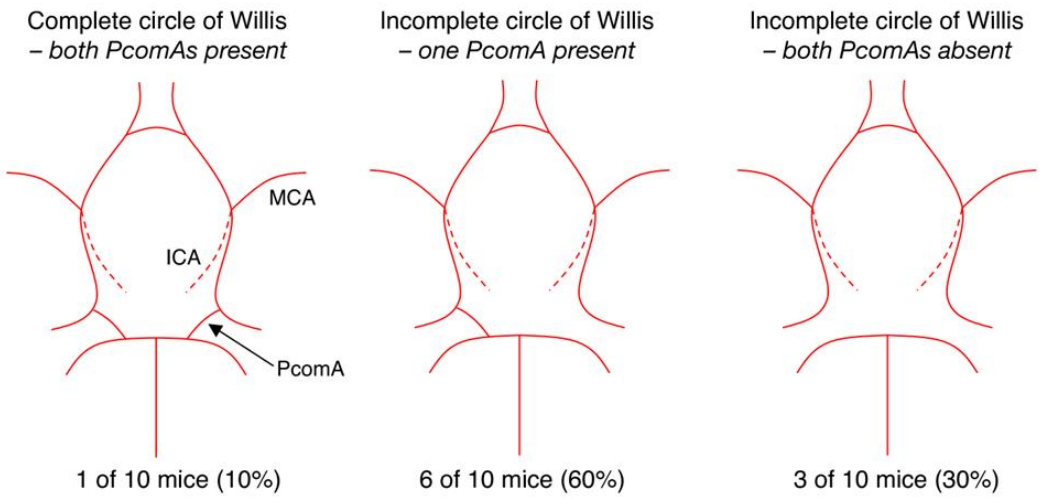

Figure 3-24 Incomplete circle of Willis in C57Bl/6J (from McColl et al., 2004).

In his study, McColl and colleagues found that lesion volume variability after MCAo in C57Bl/6J could be explained by a large variability in cerebro-vasculature of the circle of Willis. Out of 10 animals, only one presented a complete circle of Willis.

With abbreviated: ICA: internal carotid artery; MCA: middle cerebral artery; PcomA: posterior communicating artery.

The striatum and a part of the cortex are mainly perfused by the middle cerebral artery (MCA) in rodents (Feekes & Cassell, 2006; Scremin, 1995). In human anatomy, lenticulostriate arteries, a set of branches that supply important parts of the basal ganglia (striatum and lenticular nucleus notably), derive from the MCA and many branches perfusing the cortex in temporal, parietal and Rolandic areas mainly (Damasio, 1983). These areas have specific functions that are known to be impaired after a stroke:

- the temporal lobe is important for speech and memory; therefore, stroke patients might have aphasia and agnosia;
- the parietal lobe is associated with sensory inputs such as touch, hearing and vision;
- the Rolandic fissure (AKA the central sulcus) is surrounded by primary motor and somatosensory cortex, controlling movement outputs and receiving touch inputs respectively, stroke patients might show signs of apraxia, astereognosis and hemiparesis (Laurence, 2005).

Most ischaemic strokes are located in the middle cerebral artery due to a Y-shape origin with two small branches transformation from the internal carotid, but other important infarct

subtypes have to be considered for neurodegeneration such as transient ischaemic attack (TIA) and lacunar stroke. New methods are being developed to study these, such as cholesterol crystals or autologous blood clot injection, but they are less reproducible due to a large variability in areas covered. Other models exist such as electrocoagulation of the vessel that is permanent or application of endithelin-1 but this method cannot reproduce complete perfusion (Fan et al., 2017; Fluri et al., 2015).

Another limitation is that the model comprised transient MCAo and permanent unilateral common carotid artery occlusion (UCCAo; Hata et al., 1998), one focal and one global ischaemia model respectively (Liu & Mccullough, 2011). It has been reported that UCCAo decreased anti-inflammatory cytokines and increased pro-inflammatory cytokines with increased Iba1 staining (Yoshizaki et al., 2008); others have found increased %area and density for both Iba1 and GFAP with hypoperfusion in the short term (Zuloaga et al., 2016). A recent MRI study carried out by Lizi Hegarty and Jill Fowler revealed hypoperfusion in the sham UCCAo (Fig 3.25). However, their results suggest that the sham animals did not present a difference in levels of GFAP or Iba1 immunostaining when comparing the hemisphere ipsilateral to the stroke with the normally perfused, contralateral hemisphere. It would be interesting to add another control group which did not undergo UCCAo (i.e. a naïve group) or to repair the common carotid artery (Trotman-Lucas et al., 2017).

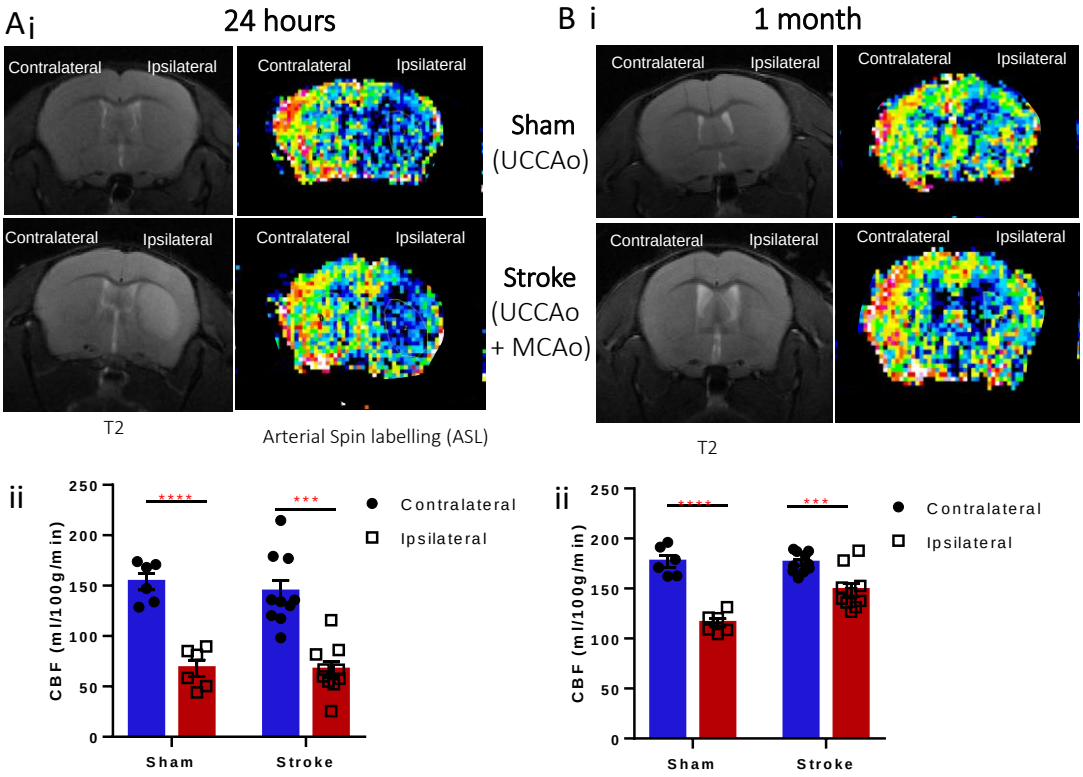

Figure 3-25 Magnetic resonance imaging used determine striatal cerebral blood flow.

*(A) Representative T2 and ASL images of sham and MCAo mice 24 hours after surgery. (ii) Ipsilateral striatal blood flow was reduced by ~56% 24 hours post-sham surgery, and ~59% post-MCAO surgery (B) Representative T2 and ASL images of sham and MCAO mice 1-month post stroke. (ii) Ipsilateral striatal blood flow was reduced by ~35% 1-month post-sham surgery and 16% post-MCAO surgery. Two-way ANOVA with post hoc Bonferroni ***p<0.001, ****p<0.0001.*

Today, most ischaemic stroke cases achieve reperfusion with emergency services improvements. Studying the intraluminal monofilament insertion is therefore very relevant as it mimics a new technique named thrombectomy that is used to remove the clot by stent retriever devices (Wardlaw & Bath, 2019; Zerna et al., 2018). This method is particularly of interest as it could extend the time window for treating patient (Baek et al., 2014; Jovin et al., 2015; Mokin et al., 2018).

3.5.2. Ischaemia produces oxidative stress environment that persist over time

Oxidative stress is a key pathophysiological mechanism of stroke-induced brain injury (Alexandrova & Bochev, 2005). It is associated with increased level of ROS and NO. Together, they form peroxynitrite "ONOO-" (Radi et al., 1991) that nitrates tyrosine residues in proteins

(Raina et al., 2000; Smith et al., 1997). This phenomenon is detected by 3-Nitrotyrosine (3NT; Giannessi et al., 2010) and was detected in the cortex and striatum at 24 hours for all durations of ischaemia (Fig 3.3). This is confirmed by other publications showing increased 3NT, 8-Hydroxydeoxyguanosine (8OHDG) that is formed by oxidative stress injury to nucleic acids hence DNA damage, malondialdehyde (MDA) that derives from ROS damage to polyunsaturated lipids and 4-Hydroxynonenal (4-HNE) produced by lipid peroxidation; and decreased antioxidant enzyme activities of superoxide dismutase (SOD) at 24 hours (Wu et al., 2017; Zhai et al., 2013). Oxidative stress can be found as early as 4 hours after the onset of a permanent MCAo with increased 8OHDG and 4HNE (Imai et al., 2003).

Immunostaining of 3NT was expressed beyond the lesion in the 15 minutes ischaemic group, notably in the cortex (Fig 3.3 C). This is confirmed by upregulation of Nrf2-pathway downstream genes *hmox1*, *nqo1*, *slc7a11*, *srxn1* (Fig 3.14). This might denote a modest hypoperfusion in the penumbra.

Finally, 3NT immunostaining was found at 4 weeks after 15 minutes ischaemia (Fig 3.16), but only within the lesion compared to the 24 hours-time point where it was present in the cortex without neuronal damage (Fig 3.3 C) suggesting that the penumbral regions recover from the oxidative stress observed at 24 hours, and this may be partly due to the activation of Nrf2 signalling. Previous publications showed oxidative stress until 16 weeks after modest duration ischaemia (Fujioka et al., 2003). A review from Alexandrova and Bochev (2005) showed there were many disturbances related to chronic oxidative stress in ischaemic patients several weeks to months after ischaemia: decrease of ascorbic acid (Hume et al., 1982) and SOD activity (Wehr et al., 2000), damage due to oxidative stress (Alexandrova et al., 2003) with long-lasting increased ROS (Mackensen et al., 2001).

One limitation of the work presented here was that only one indirect marker of oxidative stress was used. For detection of oxidative stress other markers could be used such as lipid peroxidation with 4-hydroxynonenal (4-HNE) and DNA damage with 8-OHDG. The antioxidant defences of the cell can also be studied by measuring Glutathione (GSH) / Glutathione disulphide (GSSG) ratio, but also tagging HO1 and SOD1 (Cherubini, et al., 2005). Antibodies targeting 4-HNE and 8OHDG markers were experimented but did not show results consistent with the literature.

3.5.3. Ischaemia creates an inflammatory environment *via* modification of glia and infiltration of peripheral immune cells

Twenty-four hours after ischaemia, two distinct regions of the lesion were observed: core and peri-infarct. In the chronic study, this distinction was not possible. The border of the glial scar was abrupt, peri-infarct and core were homogenous and indistinguishable hence they gave the same results and the peri-infarct was difficult to delineate (see appendix Fig 8.1 and 8.2). Images were taken for the peri-infarct but were not included in this final work.

3.2.1.2. Increased long-lasting astrocytosis

The modification of astrocyte morphology demonstrated in the present study such as hypertrophy denotes of their activation, known as reactive astrogliosis or astrocytosis, and was detected at 24 hours post-injury for 30 minutes ischaemia or longer (Fig 3.4 A). It explains the increase in the quantification of GFAP immunostaining found in the peri-infarct (Fig 3.4 B) Previous studies also indicate altered astrocyte morphology such as enlargement, with more and thicker processes (Lukaszevicz et al., 2002; Wagner et al., 2013).

The time course of astrocyte activation after ischaemia may depend on the model and duration of the CBF reductions: other studies have shown elevated levels of reactive astrocytes 3 hours after 30 minutes OGD (Shannon et al., 2007), 6 hours in the penumbra of permanent MCAo (Liu et al., 1999), 7 hours after the onset of a 3 hours transient MCAo (Dihné & Block, 2001). In the present study, it was demonstrated that 15 minutes of ischaemia does not modify astrocyte morphology at 24 hours (Fig 3.4). Interestingly astrocytosis was detected in the cortex 4 weeks after ischaemia despite minimal neuronal damage (Fig 3.17). The %area of GFAP immunostaining in the cortex core was not correlated with larger neuronal lesions (see Appendix 8.2.2, Fig 8.3) suggesting there is no relation between increased astrocytosis and lesion size. Other studies have suggested upregulation of reactive astrocytes at 3 days post-injury for the striatum and 6 days post-injury in the cortex under similar conditions (Hirayama, Ikeda-Matsuo, et al., 2015). Another publication found no reactivity of astrocytes before 48 hours after 30 minutes MCAo (Dirnagl et al., 1999). In rats, increased levels of reactive astrocytes were found at 5 days post-injury following 30 minutes of ischaemia but not following 15 minutes of ischaemia, however, no neuronal damage was observed under these conditions (Park et al., 2018). The increased

astrocytosis in the cortex of the present study, in the absence of neuronal damage might be due to waves of depolarisation in the peri-infarct (Hossmann, 1996; Umegaki et al., 2005). They have been linked to astrocyte activation, increased *gfap* expression (Rakers et al., 2017; Yamashita et al., 1996) and can be reproduced by cortical spreading depression that elicits astrocytic activation without causing any neuronal damage (Matsushima et al., 1998). Although glial activation is found in preconditioning protocols that exert no neuronal damage (Hirayama, Ikeda-Matsuo, et al., 2015).

With an injury, astrocytes become reactive; they exert morphological and transcriptomic changes. These changes have been classified in two main populations, one aggressive and potentially neurotoxic (named A1) and the other anti-inflammatory and neurotrophic (A2; Liddelow et al., 2017), although this classification is controversial. After ischaemia both phenotypes are reported to be found in the vicinity of the lesion (Liddelow & Barres, 2017; Zamanian et al., 2012; Rakers et al., 2018).

The massive activation of astrocytes and their entanglement in the lesion area in the striatum in the long term suggests that it has formed part of a glial scar. Associated with microglia, astrocytes then form a barrier thought to be protective (Bush et al., 1999; Wanner et al., 2013). It might avoid leakage of cytokines and thus limit the inflammation spreading as found with STAT3 deletion that impedes astrocyte activation and formation of the scar, leading to an expansion of inflammatory cell infiltration, increased lesion, demyelination, delayed and attenuated motor recovery (Herrmann et al., 2008; Okada et al., 2006; Wanner et al., 2013). However, the glial scar is permeable permitting oedema and neuronal damage beyond the scar. This is associated with clearance mechanisms such as drainage and phagocytosis at the border of the scar (Zbesko et al., 2018). Furthermore, astrocytes gain phagocytic functions and help the cleaning of debris (Koizumi et al., 2018; Morizawa et al., 2017). Reactive astrocytes can also develop a neurotoxic phenotype with age, inflammation and ischaemia (Clarke et al., 2018; Liddelow et al., 2017; Villarreal et al., 2016), these proliferate and migrate quickly but also induce activation of resting astrocytes (Villarreal et al., 2016). Several papers showed that ischaemia first leads to increased anti-inflammatory cytokines for the first hours/days and that later it declines, and pro-inflammatory cytokines were then increased (Amantea et al., 2018; Hu et al., 2012; Zhang et al., 2018). Taken together, it might suggest that during the chronic response to ischaemia, glia will produce pro-inflammatory cytokines and thus the population of astrocytes may be neurotoxic. In order to test this hypothesis,

astrocyte could be isolated and mixed with primary neuronal cultures to infer on their neurotoxicity by testing neuronal viability as previously done (Villarreal et al., 2016), or by sequencing their RNA to analyse their cytokines expression.

In the core of the lesion following 60 minutes of ischaemia, a loss of astrocyte staining was observed in the striatum, which is likely due to their death (Fig 3.4 A and B). Astrocytes have been shown to die quickly in ischaemic conditions, 1 hour after 30 minutes OGD or 3 hours after permanent MCAo (Liu et al., 1999 and Shannon et al., 2007 respectively). This was confirmed by structural alteration and severe degradation determined 1 hour after permanent MCAo revealed with electron microscopy (Lukaszevicz et al., 2002). For transient ischaemia, GFAP immunostaining was found decreased in the core of the lesion 5 days after 30 minutes of ischaemia (Park et al., 2018).

Gene expression of *gfap* was increased with 15 minutes ischaemia at 24 hours and 4 weeks (Fig 3.5 & 3.17). In a study by Liu et al., (1999), *gfap* mRNA was decreased in the cortex at 12 hours (Liu et al., 1999). This difference might be due to permanent MCAo model as they report an increase in both mRNA and protein of GFAP at the peri-infarct. Altogether, these findings suggest that astrocyte reactivity and death depend on the ischaemia duration and reperfusion. Astrocytes seem highly sensitive to death in anoxic conditions (complete depletion of oxygen level) and their reactivity requires hypoxia (reduction of oxygen level) or reperfusion after short anoxia. The increase of *gfap* mRNA might predict astrocytic changes found at later time point.

Complexity in the response of astrocytes might be due to a broad range of responses as explained here but also because of their heterogeneity. There are two different kinds of astrocytes: protoplasmic found in the grey matter and fibrous in the white matter (Miller & Raff, 1984). Fibrous astrocytes are more sensitive to injury than protoplasmic (Shannon et al., 2007) but were not studied here as the focus of this study was on cortex and striatum; thus it would be interesting to study their activation. Further studies carried out in Fowler lab by Lizi Hegarty revealed increased levels of reactive astrocytes in the substantia nigra and the internal capsule 4 weeks after ischaemia that were not present 24 hours after ischaemia (presented in a poster, 2019). It would be interesting also to count astrocytes in order to analyse migration or proliferation.

New studies show heterogeneity in astrocyte function at the synapse (Dallérac et al., 2018) but also in their diverse protein production in different anatomical regions, which is related to different functions (Lin et al., 2017; Morel et al., 2018). This phenomenon would imply on differential response to ischaemia, depending on the area of damage. Importantly, GFAP protein is not expressed by every astrocytes but only a subset of them; moreover, alterations to non-GFAP astrocytes are not well known and the use of a pan-astrocytic marker would be interesting such as ALDH1L1 (Cahoy et al., 2008).

3.2.1.3. Ischaemia triggers microglia/macrophage activation and recruitment

With ischaemia, Iba1 immunostaining was darker, stained cells became larger and the number of cell bodies was increased (Fig 3.6 A). The ischaemic lesion leads to activation of microglia, also named microgliosis, and was associated with morphological changes (Fumagalli et al, 2015; Morrison & Filosa, 2013). Other studies have reported microglia/macrophage activation as early as 3.5 hours after 1.5 hours MCAo (Ito et al., 2001).

Iba1 immunostaining was increased in the striatum 24 hours after 15 minutes or longer of ischaemia and in the cortex with 30 minutes or longer ischaemia as seen with %area quantification (Fig 3.6 B). This result mimics the neuronal damage result. This result agrees with previously published findings of microgliosis detected 24 hours after 15 minutes of MCAo in the striatum and not in the cortex (Hirayama, Ikeda-Matsuo, et al., 2015). In rats, microgliosis was detected 5 days after 30 minutes of ischaemia but not with 15 minutes ischaemia, however, no neuronal damage was observed in this condition (Park et al., 2018). No activation of microglia/macrophage was observed in the contralateral side in this chapter and later quantified by Lizi Hegarty finding no differences; however, a study has found microgliosis in the contralateral cortex and hippocampus 7 days after permanent MCAo and in the spinal cord at 5 weeks (Morioka et al., 1993).

Counting of Iba1-positive cell bodies showed an increase in the striatum peri-infarct with 15 minutes or longer ischaemia, and in the cortex peri-infarct with 30 minutes or longer ischaemia as found in the literature (Fig 3.7 A; Ito et al., 2001). In the core of the lesion, cell counts were increased only in the cortex with 30 minutes of ischaemia.

In the peri-infarct, Iba1 %area and Iba1-positive cell counts are both significantly increased for the same groups, suggesting that microglia/macrophages migrate to the lesion site (Fig 3.6 B and 3.7 A). However, in the core of the lesion, Iba1 %area increase is not paralleled with an increased number of positive cells (Fig 3.6 B and 3.7 A), suggesting that the morphology has changed in this area compared to shams. Images from this area showed shape modification as Iba1-positive cells were larger and thicker in the ischaemia (Fig 3.6 A). It has been reported that microglia/macrophage become modified at 3.5 hours and increase their cell number at the lesion at 48 hours (Ito et al., 2001). The increase in number can be explained by both recruitment and proliferation as reported in the literature (Lalancette-Hébert et al., 2007; Remington et al., 2007). However, these publications found proliferation at 48 and 72 hours after ischaemia (Lalancette-Hébert et al., 2007). It would have been interesting to study density as differences in the %area and the counting were reported in the current study (notably in the core of the lesion striatum) and could imply a different morphology of cells.

Iba1 gene *aif1* was unchanged 24 hours after 15 minutes ischaemia (Fig 3.7 B). This finding supports the idea that the number of microglia/macrophages is the same and that they do not proliferate at this early time point. Upregulation of the %area of Iba1 immunostaining but not of its gene at 24 hours suggests either a migration of the existing microglia/macrophages and/or morphological evolution of the microglia/macrophage in the lesion. As depicted in Fig 3.6 A, microglia/macrophages underwent morphological modification due to their activation (Fumagalli et al, 2015; Morrison & Filosa, 2013). And as seen in the counting result, there is an increase of the Iba1-positive cells at the lesion (Fig 3.7 A). Taken together, these results suggest that ischaemia triggers activation and recruitment of microglia/macrophages at 24 hours.

In the long term, alterations to Iba1 were maintained in the lesion. Iba1-positive cells were darker and larger in the lesion, and some had an ameboid shape devoid of processes. In contrast to the appearance of Iba1 stained cells from the 24-hour survival study, by 4 weeks some of the cells had overlapping processes (Fig 3.18 A). After 15 minutes of ischaemia, %area was increased in the striatum but not the cortex at 4 weeks (Fig 3.18 B). Interestingly, Iba1 immunostaining %area was correlated to the lesion volume in the cortex at 4 weeks (see Appendix 8.2.2, Fig 8.4). Counting also revealed an increase of Iba1-positive cells in the striatum but not the cortex at 4 weeks (Fig 3.18 C). At 4 weeks, the lesion area was atrophied,

and peri-infarct and core were homogenous, the lesion was abruptly delineated. Study of the peri-infarct images gave similar results to the core. A glial scar was formed as explained previously. As found in humans, the glial scar can impede neuronal growth and thus repair (Huang et al., 2014).

Counting microglia/macrophage in the core of the lesion at 4 weeks was difficult because of the morphological changes to the cells. An alternative that would overcome this problem is PU.1 marker that stains the nucleus of the microglia/macrophages (Smith et al., 2013).

Iba1 gene *aif1* was upregulated in the cortex and striatum 4 weeks after 15 minutes ischaemia (Fig 3.18 D). Iba1 is necessary for activation of microglia/macrophages (Imai & Kohsaka, 2002) and deletion of its gene *aif1* reduced multiple sclerosis onset, leukocyte infiltration and demyelination and gave resistance to acquired arthritis mouse model that is also an autoimmune condition (Casimiro et al., 2013; Chinnasamy et al., 2015). As *aif1* is upregulated following 4 weeks after ischaemia, it might be part of a defence mechanism that reinforces the glial scar and/or exacerbate deleterious pro-inflammatory conditions. A new model lacking microglia/macrophage has been developed and could be used to study the contribution of microglia/macrophages in the glial scar formation (Rojo et al., 2019).

Reactive glia can be protective due to the release of anti-inflammatory cytokines, thus limiting the extension of inflammation and upregulation antioxidant molecules. But it can also be deleterious by releasing pro-inflammatory cytokines, increasing peripheral infiltration, inhibiting repair, increasing ROS and NO production (Ekdahl et al., 2009; Lucas et al., 2006; Swanson et al., 2004).

There is a broad range of microglia and macrophages response and thus phenotypes. Furthermore, the distinction cannot be made by morphological studies (Boche et al., 2013; Minett et al., 2016). Immunohistology studies can however test different proteins that are linked to a function, for example CD68 is a marker of microglial lysosome study (Boche et al., 2013). Single-cell transcriptomic studies of the microglia revealed diverse responses to different injuries (Frigerio et al., 2019; Hammond et al., 2019).

A limitation of this study of microglia/macrophage is that only the cortex and striatum were studied. Further experiments carried out in the lab by Lizi Hegarty revealed increased microglia/macrophage activation in the internal capsule at 24 hours and in the substantia

nigra and internal capsule 4 weeks after ischaemia (presented in a poster at the ARUK conference, 2019).

3.2.1.4. Ischaemia increases pro-inflammatory cytokines cxcl10 and il-1ϐ

Expression levels of the *il-1ϐ* gene were not modified at 24 hours after 15 minutes of ischaemia however it was increased significantly in the striatum at 4 weeks compared with shams (Fig 3.8 and 3.19). This was in contradiction with publications finding *il-1ϐ* mRNA increased very early (15 minutes and 2 hours) after permanent MCAo in the rat (Buttini et al., 1994; Zhai et al., 1997). In a mouse model, IL-1β mRNA and protein were not detected at 4 hours but were significantly increased at 24 hours after 60 minutes ischaemia (Dénes et al., 2008). Collectively, it suggests that Il-1β is upregulated early after longer durations of ischaemia.

IL-1β is expressed by microglia and macrophages (Clausen et al., 2008) in a NFκB-dependant manner (White et al., 2017). After ischaemia, Il-1β is colocalised with astrocytes and the increase in IL-1β was dampened by CX3CR1 KO, a receptor for a chemokine that attract leukocytes and is important for microglia and macrophages activation (Dénes et al., 2008).

IL-1β promotes recruitment of macrophages in hypoxic conditions *in vitro* (Rider et al., 2011). IL-1β is not neurotoxic itself but it increases hypoxia-induced neuronal death (Fogal et al., 2005) and blocking its receptor IL-1ra reduces lesion volume in ischaemic conditions (Pradillo et al., 2012; Savard et al., 2013). Increase of il-1β at 4 weeks in the striatum denotes a pro-inflammatory environment. It would have been interesting to study protein level of IL-1β in these conditions and the cellular location of its expression.

Despite its key role in pro-inflammatory mechanisms, a few papers report a protective role for IL-1β. IL-1β treatment or combined with TNFα or C1q (both promoting neurotoxicity) upregulated A2 anti-inflammatory/neuroprotectant phenotype *in vitro* (Liddelow et al., 2017). Mesenchymal stem cells primed with IL-1 reduced LPS-induced inflammation (Redondo-Castro et al., 2017). Infusion of Il-1β onto human spinal cord astrocytes induced reactive astrocytosis and transcriptome analysis suggested a protective phenotype (Teh et al., 2017). In the case of ischaemia preconditioning, IL-1β is anti-inflammatory (Shin et al., 2009). In this paper, IL-1β protein level expression was greater following ischaemia than in

preconditioning. It supports the hypothesis that there might be a dose effect or a threshold which defined protective or detrimental effects of IL-1β.

Increased levels of *cxcl10* in the striatum at 24 hours and in the cortex and striatum at 4 weeks post-ischaemia might also predict astrocytic and microglial changes. This result was in accordance with the literature (Mcdonough et al., 2017). CXCL10 is produced by microglia, astrocytes, neurons, leukocytes, macrophages and T cells during inflammation (Chai et al., 2015; Harikumar et al., 2014; Klein et al., 2005; Nakamichi et al., 2004; Singh et al., 2008). Furthermore it is increased in pro-inflammatory conditions and following glial activation (Yu et al., 2018). Reactive astrocytes produce CXCL10 and it attracts microglia (Cross & Woodroofe, 1999; Rappert et al., 2004) but also macrophages and leukocytes through the CRCX3 receptor (Biber et al., 2002; Boztug et al., 2002; Klein et al., 2005; Rappert et al., 2002). However, the CXCR3 receptor is also present on astrocytes and neurons (Xia et al., 2000). CXCL10 KO mice have impaired migration of CD8-positive T cells after intratracheal instillation (Campanella et al., 2006) and in a multiple sclerosis model it diminished the accumulation CD4-positive lymphocytes and mildly reduced demyelination and clinical deficits (Mills Ko et al., 2014). It would be interesting to study CXCL10 protein level to assess precisely their role and colocalization with different cell markers would be important in order to understand its activity.

Several papers showed that ischaemia first increased anti-inflammatory cytokines for the first hours/days and that they later it decline, followed by elevations of pro-inflammatory cytokines (Amantea et al., 2018; Hu et al., 2012; Zhang et al., 2018). Furthermore, a different spatial distribution of diverse microglia/macrophage inflammatory phenotypes for the same time point after ischaemia was observed (Hu et al., 2012; Perego et al., 2011). Some have found upregulated M2 markers at the core and M1 markers at the peri-infarct (Perego et al., 2011). Others found upregulated M2 markers in the peri-infarct from 1 to 7 days, then these markers decreased and M1 markers were upregulated (from 5 days up to 14 days; Hu et al., 2012). However, this study is limited by the method, as most cytokines are produced by diverse cells, and their modulation only partly support this theory. RNA sequencing is a much superior method in this regard.

Upregulation of *il-1β*, *cxcl10* and *aif1* suggests an upregulation of pro-inflammatory pathways and may be part of the mechanism that mediates peripheral immune cell infiltration. Neutrophil immunostaining showed infiltration in all groups apart from the shams and only in one animal at 24 hours after 15 minutes ischaemia (Fig 3.9 and 3.20). Previous studies report neutrophil infiltration at 48 and 72 hours following 60-minutes of ischaemia and following 30-minutes of ischaemia animals that resulted in cortical damage. Furthermore, this paper found that neutrophils were surrounded by Iba1-cells suggesting phagocytosis (Denes et al., 2007). Another paper found neutrophil infiltration in the parenchyma from 24 hours after 60 minutes ischaemia and detected increased level of circulating neutrophils from 1.5 hours in both ischaemic animals and shams (Vaas et al., 2017). Knowing the harm that neutrophils can do, their detection in the parenchyma has been pinpointed as extremely harmful and may increase neuronal death (Iadecola & Alexander, 2001).

A recent review from Enzmann and collaborators (2018) warned of possible misunderstandings made due to the detection of neutrophil in the parenchyma. Indeed, after ischaemia in rodent or human, neutrophils tend to stay in the neurovascular unit and the subarachnoid space. The glia surrounding the neurovascular unit might prevent any harm creating a barrier called the *glia limitans* (Enzmann et al., 2018). Thus, labelling neutrophil now require co-staining with glial cells or vascular staining to locate them more precisely.

The neutrophil infiltration and chemokine upregulation raised the possibility of macrophage infiltration in the parenchyma after ischaemia. Iba1 is a protein expressed by resident microglia and infiltrated macrophages. The distinction of these two cells is important regarding inflammation, BBB breakdown and neurotoxicity. Macrophages were observed from day 2 to day 14 after 30 minutes ischaemia but it was impossible to distinguish them by their morphology (Schilling et al., 2003). In order to do so, labelling one or the other by genetic modification seems to be the most reliable technique way so far using CD163, expressed by microglia but not macrophages, or CD169 and lysozyme M locus that are expressed in macrophages but not microglia (Butovsky & Weiner, 2018; Zarruk et al., 2017). Others have created chimeric mice with GFP-tagged bone marrow derived macrophages injected in the blood of animals, and they perceived macrophages infiltrated the brain

following ischaemic injury, and were distinguished from resident microglia (Schilling et al., 2003).

A specific marker of microglia only (TMEM 119) was chosen in order to assess possible macrophages infiltration. TMEM 119 is expressed by resident microglia but not peripheral macrophages (Bennett et al., 2016; Satoh et al., 2016). TMEM 119 was decreased with ischaemia suggesting that a population of the Iba1 stained cells are peripheral macrophages (Fig 3.10, 3.11, 3.12 and 3.21). However, recent findings suggested that there is decreased TMEM119 expression in microglia after ischaemia (Rajan et al., 2018). Thus, the result observed could be due to macrophage infiltration or changes to the phenotype of resident microglia. It has been reported that there is no macrophage infiltration on the three first days following 30 or 60 minutes of ischaemia (Denes et al., 2007). However, others had observed macrophages in the parenchyma 7 days after ischaemia (Kokovay et al., 2006; Schilling et al., 2003, 2005; Tanaka et al., 2003; Yamagami et al., 1999). Labelling microglia or macrophages by genetic modification is the best technique so far to distinguish them and should be done in future studies.

3.5.4. Ischaemia modifies Nrf2 signalling at acute but not chronic response to 15 minutes ischaemia

HO1 immunostaining was upregulated with 30- and 60-minutes ischaemia in the peri-infarct and core of the 60-minutes ischaemia group (Fig 3.13). Other studies confirmed upregulation of HO1 protein in the acute response to ischaemia (Bergeron et al., 1997; Zeynalov et al., 2009). HO1 protein was increased from 3 and 4 hours after ischaemia in rats and mice respectively (Alfieri et al., 2013; Yang et al., 2009). HO1 is expressed by astrocytes and microglia (Alfieri et al., 2013; Bergeron et al., 1997; Min et al., 2006), that would explain its upregulation at the peri-infarct where microglia and astrocytes are activated and recruited (Alfieri et al., 2013). Furthermore, oxidative stress was detected beyond the lesion and notably in the cortex during the acute phase (Fig 3.3). Oxidative stress activates Nrf2 signalling by releasing Nrf2 from Keap1 and thus upregulates its downstream genes (Itoh et al., 1997). Furthermore, Keap1 was reduced 2 hours and up to 72 hours after 60 minutes occlusion in both peri-infarct and core of the lesion (Tanaka et al., 2010).

In the acute response to 15 minutes of ischaemia several Nrf2-related genes were upregulated (Fig 3.14). In the cortex, *hmox1* and *srnx1* were upregulated 4 hours after the injury and *nqo1*, *srxn1* and *slc7a11* were upregulated at 24 hours. In the striatum, *hmox1, srxn1* and *slc7a11* were upregulated at 24 hours. Other publications have found *hmox1*, *srxn1* and *slc7a11* upregulated from 4 hours after 15 minutes ischaemia (Bell et al., 2011; Bell et al., 2011b). Interestingly *nqo1* gene was not upregulated in the striatum. One study revealed that DMF, an activator of Nrf2-signalling pathway, used with inflammatory LPS on human monocytes reduced NQO1 and OSGIN1 (another Nrf2-related gene) mRNA levels (Michell-Robinson et al., 2016). This mechanism is not well understood so far, post-transcriptional changes should be studied and Nrf2 protein translocation to the nucleus is key to new studies in that scope. Importantly, the shams in this experiment had 4 hours survival after ischaemia. This experiment could be further analysed adding a sham group for each survival time point.

Nrf2-signalling was no longer upregulated 4 weeks after ischaemia despite persistent elevation of oxidative stress and inflammatory conditions (Fig 3.23). Interestingly, *srxn1* was downregulated in the striatum. Since *srxn1* is mainly expressed in neurons (Zhang et al., 2014), the loss of neuron at 4 weeks in the striatum could lead to a reduction of *srxn1*. Furthermore, *srxn1* is regulated by other pathway such as AP-1 and NF-kB (Jeong et al., 2012). AP-1 is induced by inflammation and cellular stress (Ameyar et al., 2003) and is upregulated following ischaemia notably by its transcription factor c-Fos and c-Jun, themselves upregulated following ischaemia (Akaji et al., 2003; Dai et al., 1999). Of note, AP-1 is inhibited by Nrf2 inducers Curcumin (Dong et al., 2009).

Nrf2 gene *nfe2l2* was not altered in the cortex and was upregulated in the striatum with 15 minutes ischaemia in the acute phase. This is consistent with the literature, upregulation of Nrf2 protein and mRNA in the ischaemic lesion 24 hours after reperfusion (Zhai et al., 2013). On the other hand, Nrf2 gene *nfe2l2* was upregulated in the cortex and not the striatum at 4 weeks (Fig 3.23). Nrf2 is mainly expressed by glia (Zhang et al., 2014). Our results indicate an increase of Iba1 and GFAP that thus might cause an upregulation of Nrf2. At 24 hours, *nfe2l2* was upregulated in the striatum, where *gfap* was upregulated and Iba1 %area was increased. Nrf2 gene upregulation was significantly upregulated 4 weeks after ischaemia in the cortex, in both cases, *gfap* gene was upregulated and hence might be linked to *nfe2l2* upregulation. However, since *gfap* was also upregulated in the striatum and *nfe2l2* was not, the link between the two might be more complex. The upregulation of Nrf2 gene *nfe2l2* expression

can be due to the activation of Nrf2-signalling pathway activity as *nfe2l2* gene has itself an ARE sequence (Kwak et al., 2002; Raghunath et al., 2018).

Nrf2-signalling activity mainly returned to baseline 4 weeks after modest duration ischaemia despite elevations of oxidative stress and inflammation (Fig 3.23). This result has not been reported previously. Sustained activation of Nrf2 can be detrimental as it promotes cancer (Kensler & Wakabayashi, 2010) and cancer therapy resistance (Hayes & McMahon, 2009); hence the pathway is likely to restore to homeostasis. It would be interesting to study whether Nrf2-signalling is robust in response to new oxidative stress challenges and whether it could still be activated in the chronic response to ischaemia. So far, there are reports in the literature of other age-related mechanisms inhibiting or downregulating Nrf2 signalling *via* c-Myc and Bach 1 (Zhang et al., 2012). Ageing tends to result in increased oxidative stress and decreased nuclear Nrf2 and responsiveness in the nervous system but an increase in several peripheral organs such as liver and spleen (Suh et al., 2004; Zhang et al., 2015).

Alternatively, Nrf2-signalling activation could have been more comprehensively studied using an Nrf2 biochemical-assay (Atef et al., 2018; Huang et al., 2018), cloning the promoter of the ARE sequence on a luciferase vector (Moehlenkamp & Johnson, 1999; Shih et al., 2003), by studying the fraction of Nrf2 in the nucleus (Chen et al., 2016; Lei et al., 2016), or by pre-treating the sections with N-ethylmaleimide to permit the detection of reduced glutathione (Miller et al., 2009; Won et al., 2015).

Another limitation to this work is the that Nrf2 activation was not studied after 30 or 60 minutes of ischaemia and this could be carried out in the future.

3.5.5. Conclusion

Following ischaemia, oxidative stress and inflammation were detected 24 hours after the injury. Lesion volume, oxidative stress and the glial response were increased with increasing duration of occlusion compared to shams. This was paralleled with a significant upregulation of the Nrf2-related genes *hmox1*, *nqo1, slc7a11* and *srxn1*. Interestingly, following 15 minutes ischaemia with 24 hours survival group there was oxidative stress, increased *gfap* and Nrf2-related genes in the cortex despite minimal neuronal damage. It suggests that the cortex underwent hypoperfusion and peri-infarct depolarisation waves. Altogether this acute

study confirms that Nrf2-signalling activation was associated with oxidative stress and inflammation.

In the chronic phase, 4 weeks following ischaemia, there was a significant increase in oxidative stress and glial response; however, *hmox1, nqo1* and *slc7a11* were not significantly altered, whereas *srxn1* was decreased compared to shams. This might indicate a lack of responsiveness or activation of Nrf2-signalling for long-lasting oxidative injury. In this group of 15 minutes ischaemia and 4 weeks survival, there was minimal neuronal damage or oxidative stress in the cortex, but *aif1*, *cxcl10* and *gfap* genes and GFAP protein were upregulated. Altogether, these results demonstrated long-term changes with activation of astrocytes and possibly modification of the microglia transcriptome in an area that underwent acute oxidative stress. Lastly, the upregulation of *nfe2l2* at 24 hours in the striatum and at 4 weeks in the cortex suggests that ischaemia modified Nrf2 gene permanently and differently throughout the cascade of event following ischaemia. This finding contradicts the hypothesis that Nrf2-signalling activation was associated with oxidative stress and inflammation and thus is still activated in the long term after an injury.

To conclude, we have demonstrated that a modest duration of focal ischaemia triggers long lasting oxidative stress and inflammation however Nrf2 was only altered in the acute response to ischaemia. Therefore, in the next chapter, it was hypothesised that overexpressing Nrf2 would prevent neuronal damage.

4. Protective effect of Nrf2 overexpression in the acute response to ischaemia in mice

4.1. Introduction

Nrf2 is a transcription factor and master regulator of a battery of antioxidant and anti-inflammatory genes such as heme oxygenase-1 (HO1), NAD(P)H dehydrogenase quinone 1 (NQO1), sulfiredoxin 1 (SRXN1) and glutamate-cystine antiporter (xCT; gene *slc7a11*). In physiological conditions, Nrf2 is sequestrated by Keap1 and continuously degraded. As seen in the previous chapter, Nrf2-signalling is upregulated in the acute response to ischaemia but not at 4 weeks. Its upregulation was found in the striatum and cortex and several papers localised it in the peri-infarct (Alfieri et al., 2013; Dang et al., 2012; Srivastava et al., 2013; Tanaka et al., 2010). Despite its upregulation in the acute response to ischaemia, oxidative stress and glial activation were detected beyond the lesion.

Nrf2-signalling activators reduce oxidative stress following ischaemia (Alfieri et al., 2013; Li et al., 2016; Yao et al., 2016; Jakel et al., 2007; Lin et al., 2016; Scannevin et al., 2012; Zhao et al., 2007; Kunze, 2017; Kunze et al., 2015; Liu et al., 2019; Bynum et al., 2015). Furthermore, Nrf2-signalling has anti-inflammatory properties, notably through HO1 that alters the phenotype of macrophages to anti-inflammatory (Naito et al., 2014). It has also been reported that Nrf2 represses the expression of many pro-inflammatory cytokines during an inflammatory challenge (Kobayashi et al., 2016). This effect was independent of its antioxidant properties as Nrf2 interferes with the transcriptional upregulation of these genes by binding directly to their upstream sequence, notably for IL-6 and IL-1β.

Astrocytes have an important role in the production of antioxidant to protect neurons and microglia (Bronstein et al., 1995; Desagher et al. 1996; McNaught & Jenner, 1999; Min et al., 2006; Tanaka et al., 1999) notably through the glutathione system (Dringen et al., 1999; Drukarch et al., 1997; Gegg et al., 2005). Furthermore, Nrf2-signalling is preferentially activated in astrocytes (Ahlgren-Beckendorf et al., 1999; Murphy et al., 2001), Nrf2 adenovirus is selectively taken up by astrocytes and not neurons (Kraft et al., 2004) and Nrf2 is stable in astrocytes compared to neurons where it is epigenetically repressed (Bell et al., 2015; Habas et al., 2013; Jimenez-Blasco et al., 2015). Finally, astrocytes are necessary for the neuroprotective effect of Nrf2 (Kraft et al., 2004; Lee et al., 2003; Shih et al., 2003).

Nrf2 activation in astrocytes had previously been shown to confer protection in mouse models of neurodegeneration. Overexpression of Nrf2 in GFAP-positive astrocytes by genetic mutation (GFAP-Nrf2 model) has been shown to be protective in a model of Parkinson's disease by reducing glial cell activation (Chen et al., 2009) and can prevent neurodegeneration in mouse model of amyotrophic lateral sclerosis (Vargas et al., 2008). Interestingly, in models related to ischaemic conditions such as mitochondrial dysfunction and cerebral hypoperfusion there was a protection of neurons, white matter and a reduction of the glial cell response and inflammatory cytokines in GFAP-Nrf2 mice (Gan et al., 2012; Sigfridsson et al., 2018).

However, this it is unclear whether overexpression of astrocytes can confer protective effects following *in vivo* ischaemia. Therefore, it is hypothesised that overexpression of Nrf2, selectively in astrocytes, attenuates neuronal damage following *in vivo* ischaemia by reducing oxidative stress and inflammation.

4.1.1. Aims

The aim of the current study was to determine if overexpression of Nrf2 in GFAP expressing astrocytes is neuroprotective during the acute response to 60 minutes of ischaemia compared with wild-type littermates by reducing oxidative stress, inflammation and modifying glial cell activation.

- To determine potential effect of Nrf2 overexpression in astrocytes after ischaemia in the acute phase.
    a. To quantify lesion volume and oxidative stress following ischaemia in GFAP-Nrf2 model and wild-type.
    b. To investigate possible modulation of inflammation and glial activation/phenotype with astrocytic overexpression of Nrf2 after ischaemia.
    c. To determine if Nrf2-related gene expression is increased in the GFAP-Nrf2 model in response to ischaemia compared to wild-type.

4.2. Materials & Methods

4.2.1. Mice and experimental groups

GFAP-Nrf2 male mice and C57Bl/6J (wild-type; WT) littermates underwent ischaemia with transient middle cerebral artery occlusion (MCAo) for 60 minutes (n=7-15/group) or sham surgery and brains were collected at 24 hours for immunohistochemistry and biochemical analysis. Group size was chosen based on power calculation performed on previous results (presented in chapter 3) to achieve $p<0.05$ with a 20% effect. All analyses were carried out with the experimenter blinded to groups/genotype and mice were allocated to groups in a randomised fashion.

Four animals were excluded from the histological cohort and 4 from the biochemistry cohort. These mice were culled early due to a poor response to the surgery.

			24 hours survival			
			Histology cohort		Biochemistry cohort	
		Genotype	Initial size	Final size	Initial size	Final size
Occlusion duration or sham surgery	sham	WT	8	8	8	7
		GFAP-Nrf2	8	7	7	7
	60 minutes	WT	15	13	12	10
		GFAP-Nrf2	16	15	12	11

Table 4-1 Summary of the group size of each group for histologic and biochemistry cohorts.

Histologic cohorts and the biochemistry cohorts depending on the surgery and the duration of occlusion and the survival (time between the ischaemia and the sacrifice) and the genotypes.

4.2.2. Focal cerebral ischaemia

As previously explained in section 2.2 of the Materials & Methods chapter, a monofilament was introduced into the CCA via a small incision and advanced 10mm distal to the carotid bifurcation to occlude the MCA (Monofilament 6-0 medium A MCAO suture L34 PK10; Doccol). Shams underwent the same procedure without the insertion of the thread. To withdraw the thread, mice were re-anaesthetised with isoflurane anaesthesia. Mice received 0.5ml saline (0.9%) subcutaneously by injection and were transferred to an incubator (30 °C) for 2 hours. The mice were monitored carefully for the 24 hours survival. All ischaemia surgery was undertaken by Dr Jill Fowler. Aseptic techniques were used.

4.2.3. Histology and immunohistochemistry

Histology and immunohistochemistry techniques used were performed as described in section 2.3 of the Material & Methods. Lesion volume was assessed by drawing areas of ischaemic neuronal death observed in Haematoxylin and Eosin stained sections. Oxidative stress was detected using 3-nitrotyrosine antibody and then mapped at three coronal levels as described in section 2.3, microglia/macrophages and reactive astrocytes were studied using Iba1 and GFAP immunostaining respectively and quantified by assessing %area of immunostaining in Image J (Fiji, NIH) as described in section 2.3. 3NT mapping, GFAP and Iba1 immunohistochemistry images were captured by Katharina Nagassima Rodrigues dos Reis. Finally, HO1 immunostaining was used to assess HO1 upregulation and as an index of Nrf2 activation and the immunostaining was quantified as described in section 2.3.

After observation and analysis of the different markers, the results in the core of the lesion were similar between ischaemic wild-type and GFAP-Nrf2 animals. However, a few differences were found in the peri-infarct areas. Thus, the results presented in the histologic sections are from the peri-infarct analysis.

4.2.4. qRT-PCR

To study gene expression, qRT-PCR was performed as explained in the Methods section 2.4. The animals received 60 minutes ischaemia and survived for a further 23 hours. The results of the immunostaining experiments suggested that modification of oxidative stress occurred in the peri-infarct area, therefore this area was used for qRT-PCR experiments. Observation of the lesion revealed that the striatum was almost completely damaged after 60 minutes ischaemia at 24 hours. Thus, only the cortex peri-infarct samples were analysed.

For this study, glial cell responses were assessed by *gfap* and *aif1* gene analysis. For Nrf2-related gene expression, *nfe2l2*, *hmox1*, *nqo1* and *slc7a11* genes were performed. To study the inflammatory environment, *il-1β*, *cxcl10* and *il-6* genes were analysed to assess the pro-inflammatory environment and *IL-4rα* for the anti-inflammatory environment. Furthermore, complement component 3 (*C3*) and *amigo2* genes were analysed for pro-inflammatory (A1) astrocytes and *stat3* for anti-inflammatory (A2). The *il-1β, il-4ra, c3, amigo2, il-6, stat3, keap1* qRT-PCR were experiments were undertaken by Lizi Hegarty under my supervision. For each

animal, the level of gene expression was normalised to the expression of a housekeeping gene, *18S*.

4.2.5. Statistics

Data were expressed mean ± S.E.M. using GraphPad Prism software. For parametric analysis, two-way analysis of variance (ANOVA) followed by *post-hoc* Bonferroni test were performed to correct for multiple comparisons. $P<0.05$ was deemed statistically significant.

4.3. Results

4.3.1. Overexpression of Nrf2 gene in GFAP-Nrf2 mice

In order to confirm the overexpression of Nrf2 in the GFAP-Nrf2 model, levels of the Nrf2 gene *nfe2l2* was performed with qRT-PCR in the cortex and striatum of naïve, uninjured mice. There was a 2.5-fold increased expression of Nrf2 gene in this model compared to wild-type littermate mice (Fig 4.1).

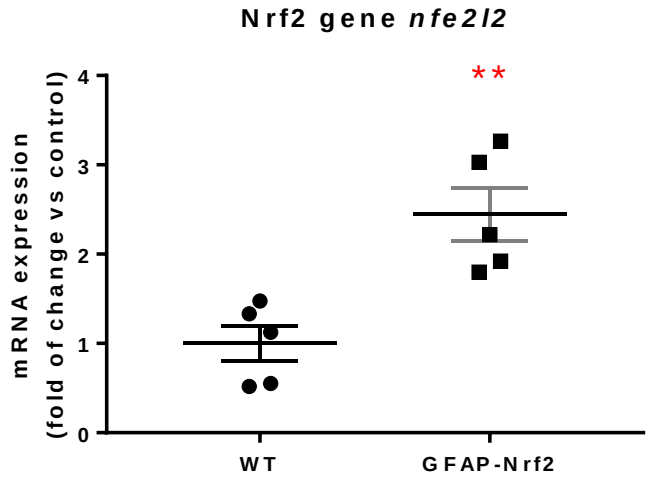

Figure 4-1 Mice overexpressing Nrf2 in astrocytes (GFAP-Nrf2 mice) have over two-fold increase of Nrf2 gene nfe2l2 mRNA expression compared to wild-type (WT).

There was a significant increase in levels of Nrf2 gene (nfe2l2) in the GFAP-Nrf2 mice compared to wild-type ($t_{(8)}$=4.059, p=0.0036). Samples collected from both cortex and striatum. Animals were 2 to 4-month old.

*Data presented as mean ± S.E.M. Student's t-test for gene expression study (N= 5 per group). **p<0.01.*

4.3.2. Neuroprotection in mice overexpressing Nrf2 in astrocytes

The lesion volume after 60 minutes ischaemia was reduced in the GFAP-Nrf2 mice compared with wild-type (WT) at 24 hours. No neuronal damage was observed in the shams of both genotypes.

For the total lesion volume, there was a significant effect of surgery ($F_{(1, 39)}$=162.9, p<0.0001) but no effect of genotype or an interaction between surgery and genotype (both $F_{(1, 39)}$=1.917, p=0.1740). Post hoc comparison revealed a reduction in the lesion volume of GFAP-Nrf2 mice ischaemic mice when compared with wild-type ischaemic mice (p=0.0486; Fig 4.2 B).

In the cortex and striatum, there was a significant effect of surgery ($F_{(1, 39)}$=159, p<0.0001 and $F_{(1, 39)}$=12259, p<0.0001 respectively) but no effect of genotype and no interaction between surgery and genotype (both $F_{(1, 39)}$=1.176, p=0.284 for the cortex and both $F_{(1, 39)}$=0.952, p=0.335 for the striatum). Post hoc tests revealed there was no alteration between wild type and GFAP-Nrf2 mice following ischaemia.

In other regions comprising hippocampus, thalamus and hypothalamus there was a significant effect of surgery ($F_{(1, 39)}$=67.26, p<0.0001). However there was no genotype effect or interaction between surgery and genotype, both $F_{(1, 39)}$=3.43, p=0.0716. Post hoc comparison revealed a reduction in ischaemic neuronal damage between GFAP-Nrf2 mice compared to ischaemic wild-type (p=0.0065; Fig 4.2 B). Profiling the lesion throughout the 9 coronal sections observed revealed that the difference between wild-type and GFAP-Nrf2 area was mainly observed in the caudal part of the brain, the area comprising the thalamus and hypothalamus (Fig 4.2 C).

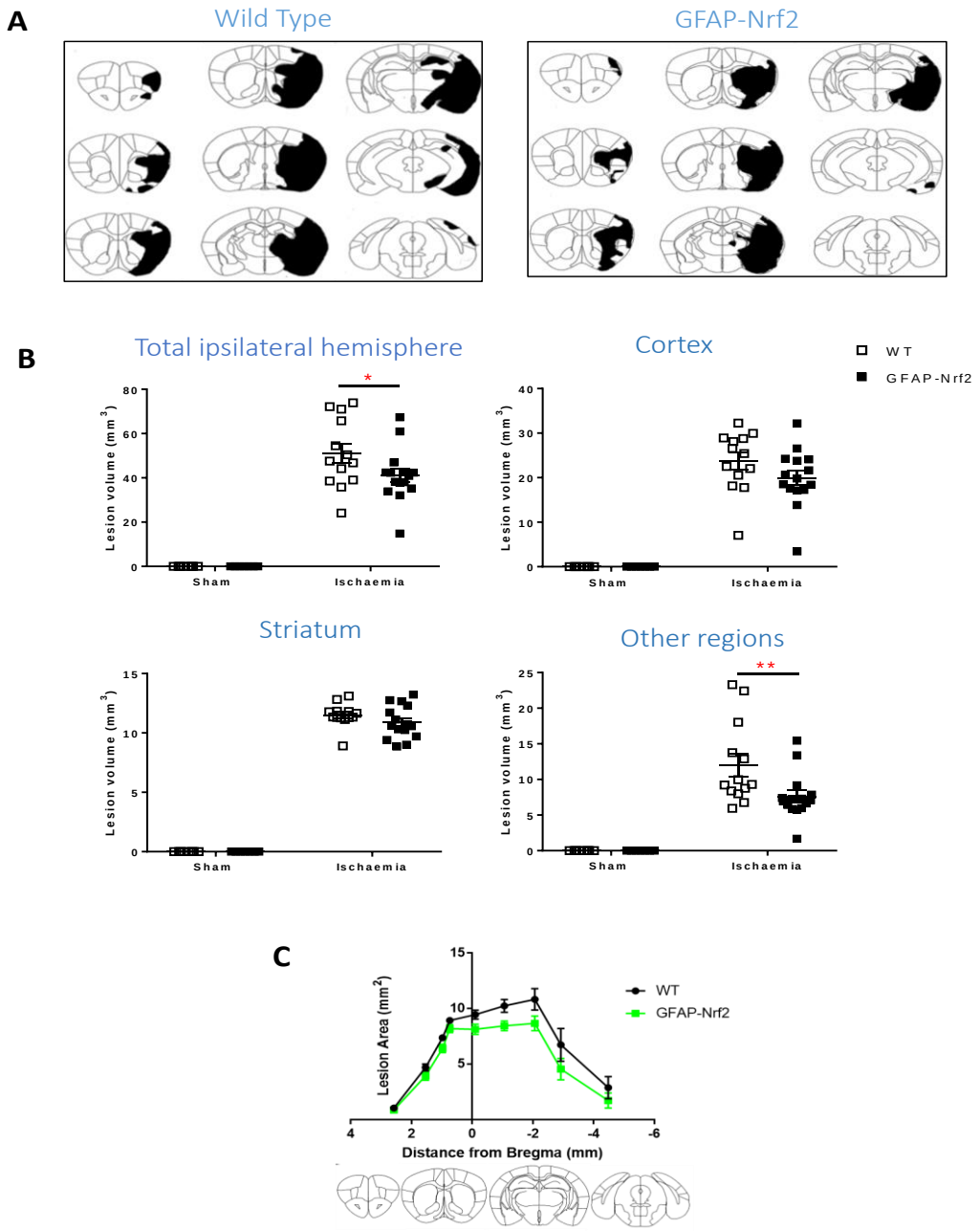

Figure 4-2 Nrf2 overexpression in astrocytes reduced neuronal damage 24 hours after 60 minutes ischaemia.

(A) Representative coronal line diagrams with neuronal damage in black for the median animals of GFAP-Nrf2 or wild-type (WT) genotype. The lesion was mainly comprised in cortex, striatum, thalamus and hypothalamus.

(B) Quantification of neuronal damage mapping showed a significant effect of the surgery for each region ($p<0.0001$). Post hoc comparison revealed there was a significant reduction of the total lesion in GFAP-Nrf2 mice compared to wild-type ($p=0.0486$). Study of the cortical and striatal lesion showed no differences between GFAP-Nrf2 and wild-type mice ($p=0.148$ and $p=0.213$ respectively). The protective effect of Nrf2 overexpression in astrocytes was found in other regions such as thalamus and hypothalamus were the lesion was reduced compared to wild-type ($p=0.0065$).

(C) Profile of the lesion area in nine coronal sections 24 hours after 60 minutes ischaemia showed the reduction was mainly found in the caudal part of the brain, where thalamus and hypothalamus are located.

*Data presented as mean ± S.E.M. Two-way ANOVA followed by post hoc comparisons with Bonferroni (N= 7 to 15 per group). *$p<0.05$, **$p<0.01$.*

4.3.3. Astrocytic overexpression of Nrf2 reduced oxidative stress

Oxidative stress was studied with 3NT immunostaining. There was increased 3NT immunostaining in the cortex and striatum of the ischaemic animals for both genotypes and there was minimal immunostaining observed in shams (Fig 4.3 A). By mapping the area of 3NT immunostaining on three coronal sections for each animal, quantification revealed a reduction of oxidative stress in the GFAP-Nrf2 ischaemic animals compared to ischaemic wild-type (WT) animals. For each region observed, there was significant effect of surgery (total ipsilateral hemisphere $F_{(38)}$=128.9, p<0.0001; cortex $F_{(1,38)}$=100, p<0.0001; striatum $F_{(1,38)}$=233, p<0.0001; other regions $F_{(1,39)}$=81.78, p<0.0001; Fig 4.3 B). There was also a significant effect of genotype and an interaction between surgery and genotype for the total ipsilateral hemisphere (both $F_{(1,38)}$=4.13, p=0.0492) and other regions (comprising thalamus, hypothalamus and white matter; both $F_{(1,39)}$=5.54, p=0.0237). There was no effect of the genotype or interaction for cortex (both $F_{(1,38)}$=2.535, p=0.1197) and striatum (both $F_{(38)}$=1.893, p=0.176 respectively; Fig 4.3 B).

After comparing ischaemic wild-type (WT) to ischaemic GFAP-Nrf2 with post hoc tests, a significant reduction was found in the GFAP-Nrf2 group compared to the wild-type group in the total ipsilateral hemisphere (p=0.0032), the cortex (p=0.0224) and other regions (p=0.0006). No significant differences were detected in the striatum (p=0.0535; Fig 4.3 B).

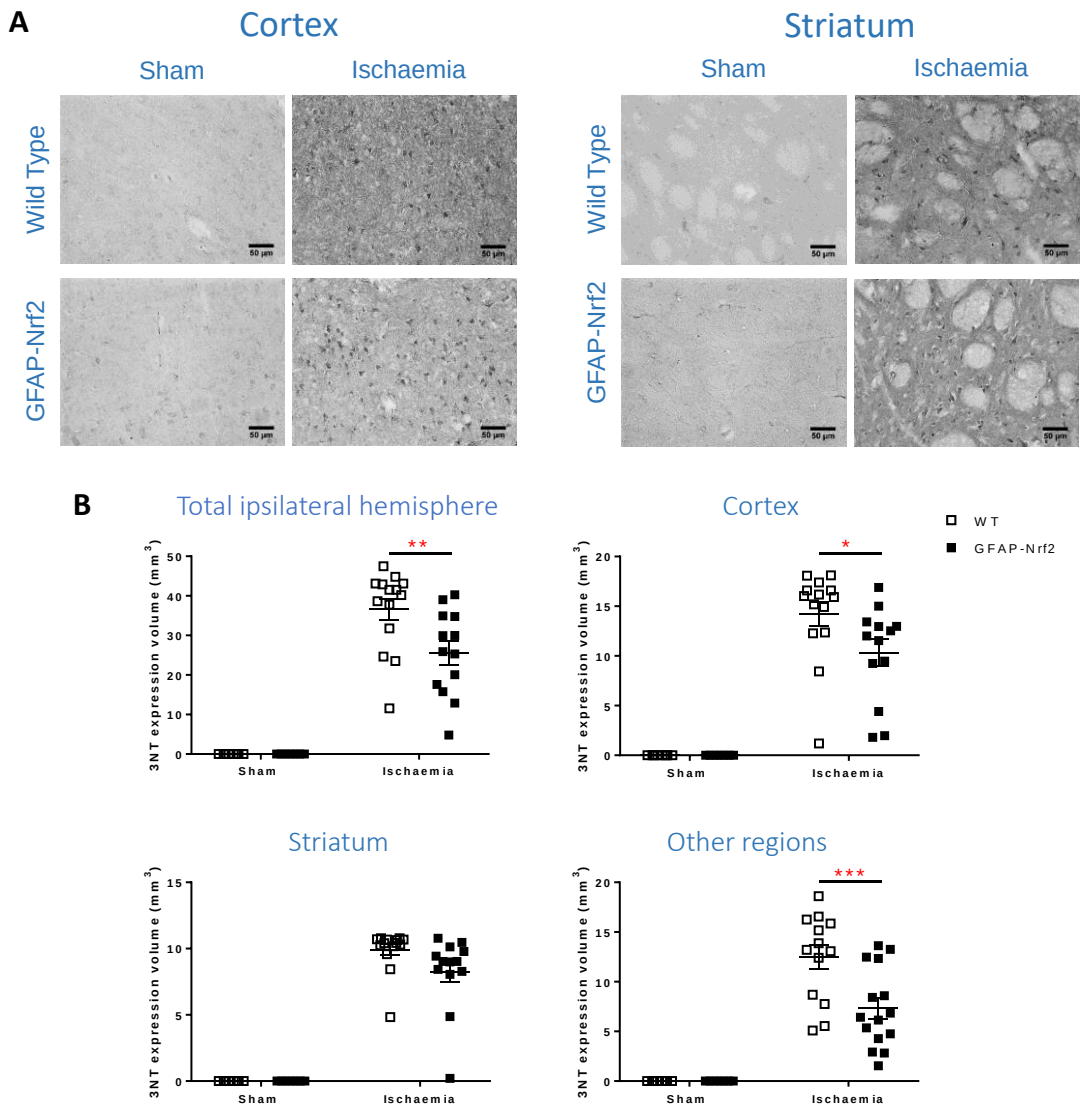

Figure 4-3 Nrf2 overexpression in astrocytes reduced oxidative stress 24 hours after 60 minutes ischaemia.

(A) Representative images of 3-Nitrotyrosine (3NT) immunostaining showing peroxide nitrite generation in cortex and striatum after ischaemia but not in shams.

(B) Quantification of 3NT immunostaining by mapping the positive staining showed a significant increase of the staining with the surgery for each region (total ipsilateral hemisphere $F_{(38)}$=128.9, p<0.0001; cortex $F_{(1,38)}$=100, p<0.0001; striatum $F_{(1,38)}$=233, p<0.0001; other regions $F_{(1,39)}$=81.78, p<0.0001). There was also a significant effect of genotype and interaction for the total ipsilateral hemisphere (both $F_{(1,38)}$=4.13, p=0.0492) and other regions (comprising thalamus, hypothalamus and white matter; both $F_{(1,39)}$=5.54, p=0.0237). There was no effect of the genotype or interaction for cortex (both $F_{(1,38)}$=2.535, p=0.1197) and striatum (both $F_{(38)}$=1.893, p=0.176 respectively). There was a significant reduction of the 3NT immunostaining in the GFAP-Nrf2 mice compared to shams in the total ipsilateral hemisphere (p=0.0032), the cortex (p=0.022) and other regions (p=0.0006), but not the striatum (p=0.0535).

*Data presented as mean ± S.E.M. Two-way ANOVA followed by post hoc comparisons with Bonferroni (N= 7 to 15 per group). *p<0.05, **p<0.01, ***p<0.001.*

After comparing the area of neuronal damage and oxidative stress on three coronal sections, it was found that oxidative stress extended beyond the area of neuronal damage in the wild-type animals but not the GFAP-Nrf2 animals (Fig 4.4 A). Two-way ANOVA with repeated measures revealed no differences between 3NT-immunostained area and neuronal damage area ($F_{(1,26)}$=2.599, p=0.119), there was a significant effect of the genotype ($F_{(1,26)}$=11.525, p=0.002) and a significant interaction between the marker (oxidative stress and neuronal damage) and the genotype ($F_{(1,26)}$=5.339, p=0.029). Post hoc comparisons revealed a significant increase of oxidative stress compared to lesion in the wild-type (p=0.013) but not in the GFAP-Nrf2 mice (p=0.613; Fig 4.4 A); in detail for the three regions of the wild-types (+0.98 mm: p=0.034, -0.10 mm: p=0.073; -2.06 mm: p=0.016). Oxidative stress was significantly increased in the wild-types compared with GFAP-Nrf2 animals in the three regions (+0.98 mm: p=0.003, -0.10 mm: p=0.026; -2.06 mm: p=0.007). These results taken together proved that the GFAP-Nrf2 animals had oxidative stress in the lesion only in contrast to wild-type animals where the oxidative stress was found in an area greater than the lesion (Fig 4.4 B).

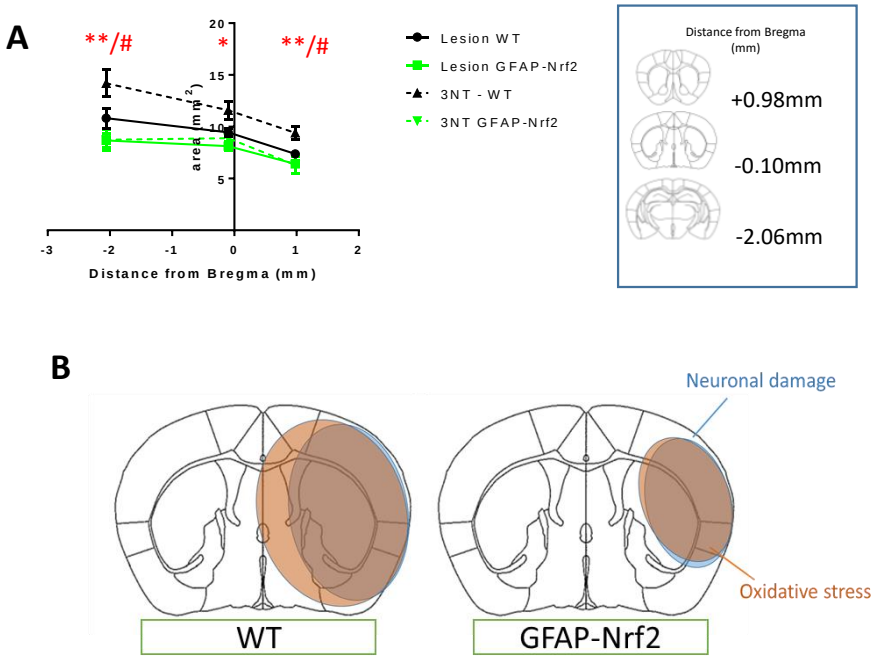

Figure 4-4 Nrf2 overexpression in astrocytes reduced oxidative stress spread out beyond the lesion 24 hours after 60 minutes ischaemia.

(A) Profile of the staining area and the neuronal damage area in three coronal sections of the ischaemic group showed 3NT expression beyond lesion site in wild-type (WT). In the GFAP-Nrf2 mice, 3NT immunostaining was not found beyond the lesion. Two-way ANOVA revealed an effect of the genotype ($F_{(1,26)}$=11.525, p=0.002) and post hoc comparisons revealed increased oxidative stress area in wild-types compared to GFAP-Nrf2 (+0.98 mm: p=0.003, -0.10 mm: p=0.026; -2.06 mm: p=0.007). Furthermore, oxidative stress area was bigger than lesion area for the wild-types but not for the GFAP-Nrf2 animals (+0.98 mm: p=0.034, -0.10 mm: p=0.073; -2.06 mm: p=0.016).

(B) Schematic of the comparison oxidative stress (by 3NT mapping) and lesion. Oxidative stress was found beyond the lesion in the wild-type but not in the GFAP-Nrf2 animals.

*Data presented as mean ± S.E.M. N= 12 to 13 per group. *p<0.05 and **p<0.01 for the comparison of oxidative stress between the two genotypes and #p<0.05 for the comparison of lesion area and oxidative stress area in the wild-types.*

4.3.4. Nrf2 signalling was boosted in mice that overexpress Nrf2 in astrocytes

Nrf2 detection using immunohistochemistry is limited at present due to a lack of specificity of the commercially available antibodies (Kemmerer et al., 2015). Consequently, to assess Nrf2-pathway activation, downstream genes or proteins of this pathway were studied. The following immunohistochemical study is based on heme oxygenase-1 (HO1), one of the most upregulated protein of Nrf2-pathway activation, previously shown to be upregulated with ischaemia (Alfieri et al., 2013) and in response to 60 minutes of ischaemia in the previous chapter.

There was minimal staining of HO-1 in shams of both GFAP-Nrf2 and wild-type genotypes (Fig 4.5 B). In ischaemic animals for both genotypes, HO1 immunostaining was increased and mainly detected at the border of the lesion (Fig 4.5 A). HO1 immunostaining was present in the soma of cells that had the appearance of glial cells including processes (Fig 4.5 B).

In order to quantify this upregulation throughout the brain, mapping of the positive immunostaining was transcribed onto coronal line diagrams to allow quantification of the area and volume of immunostaining. There was a significant effect of the surgery for the total lesion volume and in every brain region (total ipsilateral hemisphere $F_{(1,37)}$=31.23, p<0.0001; cortex $F_{(1,35)}$=16.83, p=0.0002; striatum $F_{(1,35)}$=20.89, p<0.0001; other regions $F_{(1,36)}$=35.99, p<0.0001; Fig 4.5 B). There was a significant effect of genotype in the total ipsilateral hemisphere ($F_{(1,37)}$=8.926, p=0.0050), striatum ($F_{(1,35)}$=6.565, p=0.0149) and other regions ($F_{(1,36)}$=9.958, p=0.0032) but not in the cortex ($F_{(1,35)}$=3.159, p=0.0842) and a significant interaction was detected in every region apart from the cortex (total ipsilateral hemisphere $F_{(1,37)}$=9.097, p=0.0046; cortex $F_{(1,35)}$=3.159, p=0.0842; striatum $F_{(1,35)}$=7.439, p=0.0099; other regions $F_{(1,36)}$=9.958, p=0.0032; Fig 4.5 B). Post hoc comparisons revealed a significant increase of HO1 immunostaining was found in every region of ischaemic GFAP-Nrf2 mice compared to ischaemic wild-type mice (total ipsilateral hemisphere p<0.0001, cortex p=0.0147, striatum p=0.0003 and other regions p<0.0001).

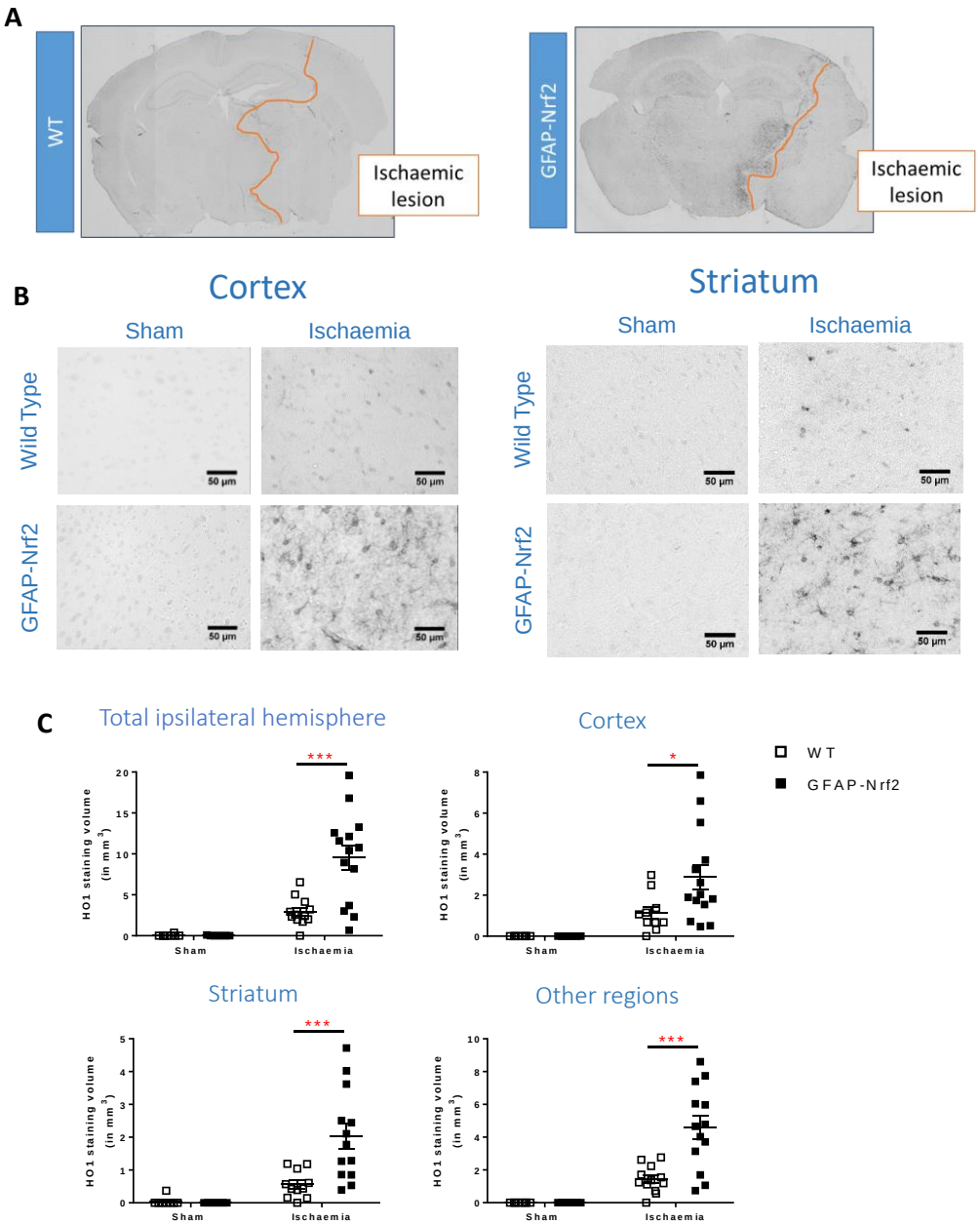

Figure 4-5 Nrf2 overexpression in astrocyte increased HO1 expression, 24 hours after 60 minutes ischaemia.

(A) Representative images of HO1 immunostaining sections showed an increase in staining with ischaemia at the boundary of the lesion particularly on GFAP-Nrf2 animals. Lesion outlined with an orange line.

(B) Representative images of HO1 immunostaining in the cortex and striatum. HO1 staining was increased with ischaemia and further increased with the GFAP-Nrf2 genotype.

(C) Quantification of HO1 immunostaining by mapping the positive staining revealed a significant increase with ischaemia in every region observed ($p<0.001$). Furthermore, there was a significant increase of HO1 area in GFAP-Nrf2 animals after ischaemia compared to shams in the total ipsilateral hemisphere ($p<0.0001$), in the cortex ($p=0.0147$), in the striatum ($p=0.0003$) and other regions comprising the thalamus and hypothalamus ($p<0.0001$).

*Data presented as mean ± S.E.M. Two-way ANOVA followed by post hoc comparisons with Bonferroni (N= 7 to 15 per group). *$p<0.05$, ***$p<0.001$.*

Therefore, there was a striking upregulation was observed in the GFAP-Nrf2 mice compared with wild-type mice, especially in the peri-infarct area (Fig 4.5 A). GFAP-Nrf2 mice showed increased HO1 immunostaining in both cortex and striatum (Fig 4.5 B).

Activation of Nrf2-signalling leads to upregulation of Nrf2 downstream genes. Quantification of mRNA levels of *slc7a11*, *hmox1* and *nqo1* genes revealed no differences between sham WT and GFAP-Nrf2 groups.

Comparing levels of the *nfe2l2* gene revealed a significant effect of surgery, genotype and an interaction ($F_{(1,31)}$=19.91, p<0.0001, $F_{(1,31)}$=54.2, p<0.0001 and $F_{(1,31)}$=22.9, p<0.0001 respectively). Post hoc comparisons revealed a significant increase following ischaemia GFAP-Nrf2 mice compared with wild type littermates (p<0.0001; Fig 4.6).

For Nrf2-signalling genes, there was a significant effect of surgery (*slc7a11* $F_{(1,31)}$=36.27, p<0.0001; *hmox1* $F_{(1,31)}$=19.52, p=0.0001 and *nqo1* $F_{(1,31)}$=9.962, p=0.0035), a significant effect of genotype (*slc7a11* $F_{(1,31)}$=25.92, p<0.0001; *hmox1* $F_{(1,31)}$=7.593, p=0.0097 and *nqo1* $F_{(1,31)}$=21.97, p<0.0001) and an interaction (*slc7a11* $F_{(1,31)}$=21.96, p<0.0001; *hmox1* $F_{(1,31)}$=14.45, p=0.0006 and *nqo1* $F_{(1,31)}$=13.2, p=0.0010; Fig 4.6). Post hoc comparison of ischaemic GFAP-Nrf2 with ischaemic wild-type mice revealed a significant increase for these three genes (*slc7a11* p<0.0001; *hmox1* p<0.0001 and *nqo1* p<0.0001; Fig 4.6).

Interestingly, in this area (cortex peri-infarct), there were no significant differences between wild-type shams and wild-type ischaemia (*slc7a11* p>0.999; *hmox1* p>0.999 and *nqo1* p>0.999). Furthermore, there was no differences between shams and ischaemic GFAP-Nrf2 animals (*slc7a11* p>0.999; *hmox1* p>0.999 and *nqo1* p>0.999; Fig 4.6).

Keap1 gene expression was not modified, there was no effect of the surgery, genotype and interaction ($F_{(1,31)}$=0.018, p=0.89, $F_{(1,31)}$=0.112, p=0.73 and $F_{(1,31)}$=1.47, p=0.23 respectively; Fig 4.6).

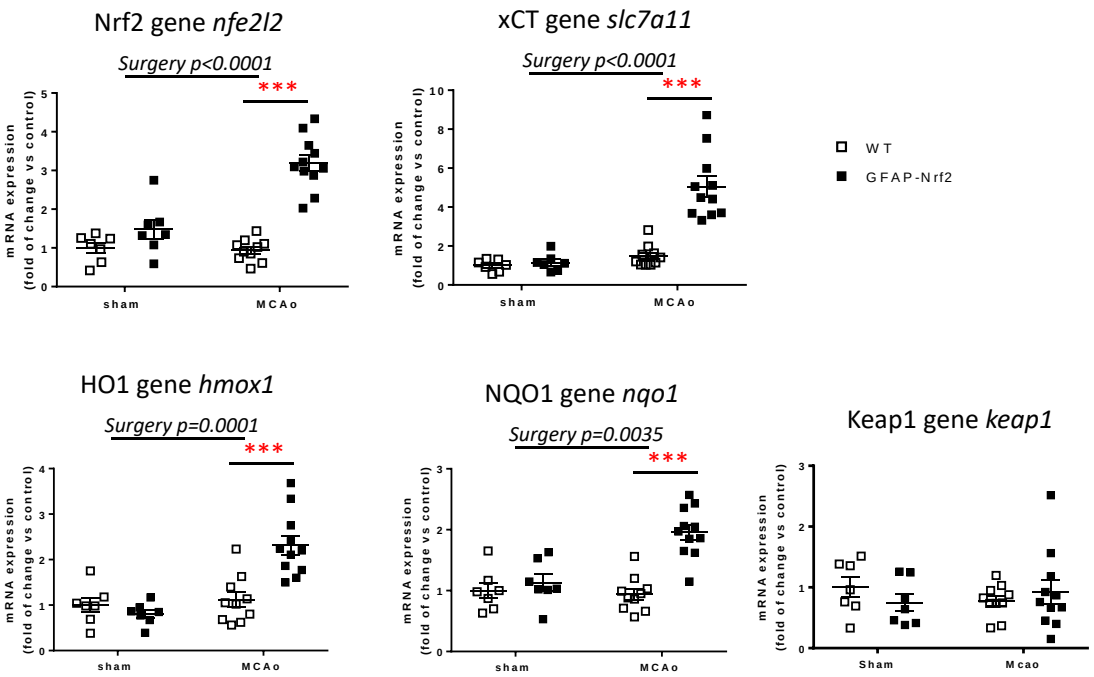

Figure 4-6 Nrf2 overexpression in astrocyte increased Nrf2-related genes 24 hours after 60 minutes ischaemia in the cortex peri-infarct.

Comparing levels of the Nrf2 gene nfe2l2 and its downstream genes hmox1, nqo1 and slc7a11 revealed an effect of the surgery (nfe2l2 $F_{(1,31)}$=19.91, p<0.0001; hmox1 $F_{(1,31)}$=19.52, p=0.0001; nqo1 $F_{(1,31)}$=9.962, p=0.0035; slc7a11 $F_{(1,31)}$=36.27, p<0.0001), a significant effect of the genotype (nfe2l2 $F_{(1,31)}$=54.2, p<0.0001; hmox1 $F_{(1,31)}$=7.593, p=0.0097; nqo1 $F_{(1,31)}$=21.97, p<0.0001 slc7a11 $F_{(1,31)}$=25.92, p<0.0001) and an interaction (nfe2l2 $F_{(1,31)}$=22.9, p<0.0001; hmox1 $F_{(1,31)}$=14.45, p=0.0006; nqo1 $F_{(1,31)}$=13.2, p=0.0010; slc7a11 $F_{(1,31)}$=21.96, p<0.0001). Bonferroni post-hoc comparison revealed a significant difference between wild-type (WT) and GFAP-Nrf2 after ischaemia for each gene (nfe2l2 p<0.0001; hmox1 p<0.0001; nqo1 p<0.0001; slc7a11 p<0.0001;). However, Keap1 gene expression was not modified, there was no effect of the surgery, genotype and interaction ($F_{(1,31)}$=0.018, p=0.89, $F_{(1,31)}$=0.112, p=0.73 and $F_{(1,31)}$=1.47, p=0.23 respectively).

*Data presented as mean ± S.E.M. Two-way ANOVA followed by post hoc comparisons with Bonferroni (N= 7 to 11 per group). ***p<0.001.*

4.3.5. Reactive astrocytosis was modified with astrocyte specific Nrf2 overexpression

Astrocyte reactivity was investigated using GFAP immunostaining. In the wild-type shams, astrocytes had small cell bodies and long and clear processes with many branches (Fig. 4.7 A). After ischaemia, GFAP immunostaining was increased, more reactive astrocytes were detected, and some astrocytes had disintegrated processes (Fig 4.7 A). Quantification of %area of GFAP immunostaining revealed an effect of surgery for the cortex and striatum ($F_{(1,39)}$=29.68, p<0.0001 and $F_{(1,38)}$=12.83, p=0.0010 respectively; Fig 4.7 B). Interestingly, there was an effect of genotype in the cortex ($F_{(1,39)}$=20.47, p<0.0001) but not the striatum ($F_{(1,38)}$=0.002, p=0.9629; Fig 4.7 B). There was no effect of interaction for the cortex and striatum ($F_{(1,39)}$=0.015, p=0.9012 and $F_{(1,38)}$=2.802, p=0.1024 respectively; Fig 4.7 B). With post

hoc tests, a significant increase was detected in levels of reactive astrocytes in the cortex of GFAP-Nrf2 shams compared to wild-type (WT) shams (p=0.0191) and in ischaemic GFAP-Nrf2 compared to ischaemic wild-type mice (p=0.0007). However, there was no interaction in either the cortex or striatum ($F_{(1,39)}$=0.015, p=0.90 and $F_{(1,38)}$=2.802, p=0.102 respectively; Fig 4.7 B). Gene expression for *gfap* was increased with surgery but was not modified by genotype ($F_{(1,31)}$=73.1, p<0.0001 and $F_{(1,31)}$=0.019, p=0.89 respectively; Fig 4.7 C) and there was no interaction between surgery and genotype ($F_{(1,31)}$=0.044, p=0.835).

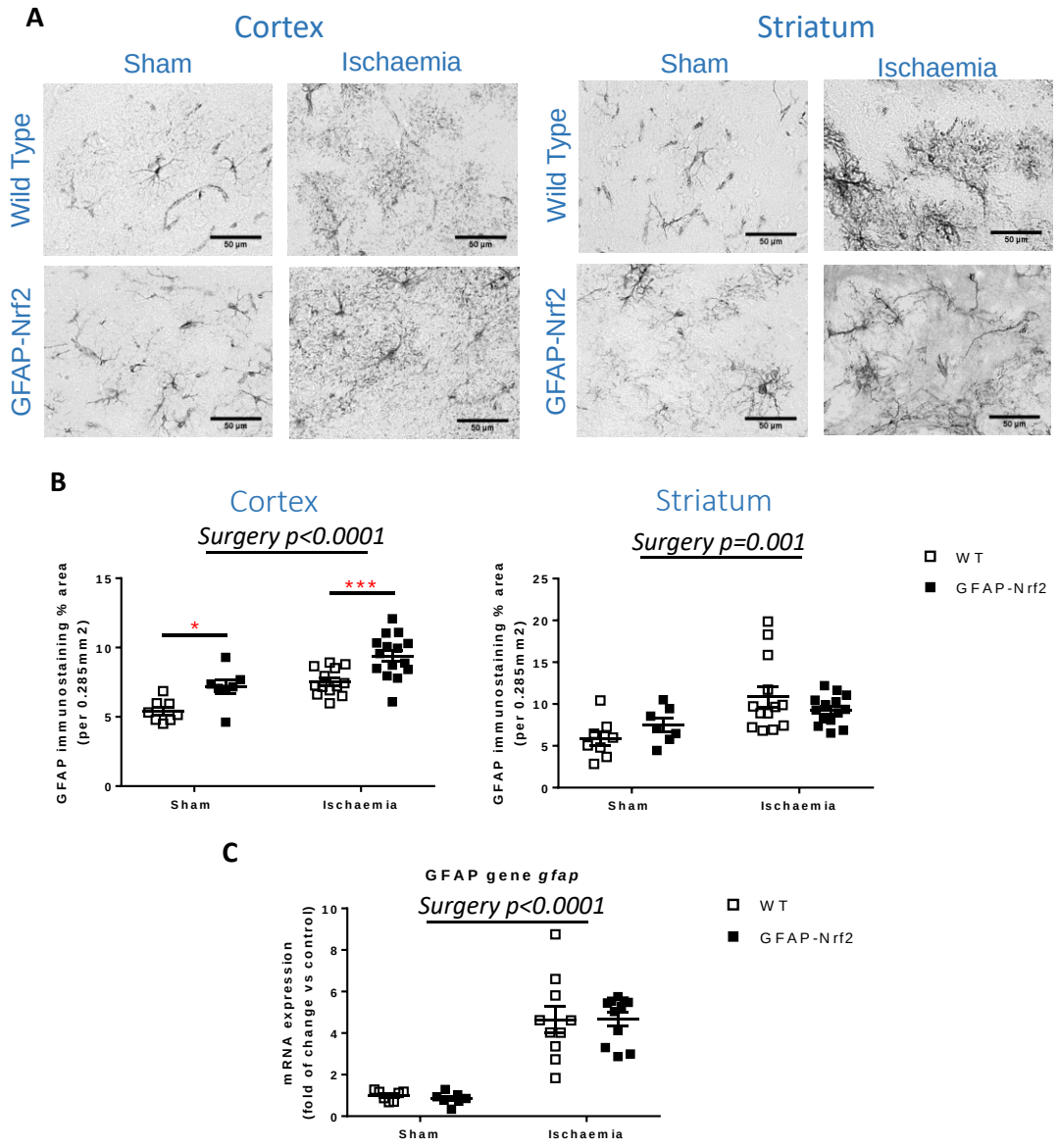

Figure 4-7 GFAP immunostaining was increased at 24 hours after 60 minutes ischaemia in both cortex and striatum and GFAP-Nrf2 sham animals had increased GFAP immunostaining in the cortex.

(A) Representative images of GFAP immunostaining showed an increase with the ischaemia in the cortex and the striatum after ischaemia compared to shams. Some astrocytes had disintegrated processes and swelling and vacuolisation of the cell body; they are named clasmatodendrocytes.

(B) Quantification of GFAP staining by %area in the peri-infarct showed significant increase of surgery for cortex and striatum ($F_{(1, 39)}$=29.68, p<0.0001 and $F_{(1, 38)}$=12.83, p=0.0010). There was also an effect of genotype in the cortex ($F_{(1, 39)}$=20.47, p<0.0001) with an increase of GFAP %area between the sham groups (p=0.019) and between the ischaemic groups (p=0.0007).

(C) Study of the mRNA expression of GFAP gene gfap showed significant increase with surgery ($F_{(1, 31)}$=73.1, p<0.0001) but no effect of the genotype ($F_{(1, 31)}$=0.019, p=0.89) in the cortex peri-infarct.

*Data presented as mean ± S.E.M. Two-way ANOVA followed by post hoc comparisons with Bonferroni (N= 7 to 15 per group for the immunostaining study and N= 7 to 11 per group for gene expression study). *p<0.05, ***p<0.001.*

4.3.6. Microglial/macrophage response after ischaemia was not altered with astrocyte-specific overexpression of Nrf2

Microglial/macrophage reactivity was investigated with Iba1 immunostaining. After ischaemia, microglial/macrophage cell bodies were larger, darker and had thicker processes (Fig 4.8 A). Quantification of %area revealed an effect of the surgery for the cortex and striatum ($F_{(1,39)}$=161.6, p<0.0001 and $F_{(1,39)}$=21.19, p=0.0010 respectively; Fig 4.8 B). There was no effect of the genotype in the cortex and striatum ($F_{(1,39)}$=0.075, p=0.78 and $F_{(1,39)}$=2.206, p=0.145 respectively; Fig 4.8 B) and no interaction in both cortex and striatum ($F_{(1,39)}$=0.049, p=0.82 and $F_{(1,39)}$=0.038, p=0.845 respectively; Fig 4.8 B). Post hoc tests revealed there was no alteration between wild type and GFAP-Nrf2 mice following ischaemia. suggesting that overexpression of Nrf2 in astrocytes does not modulate levels of microglia/macrophage. Iba1 gene *aif1* was not altered with surgery or genotype ($F_{(1,31)}$=0.59, p=0.44 and $F_{(1,31)}$=0.29, p=0.59 respectively; Fig 4.8 C).

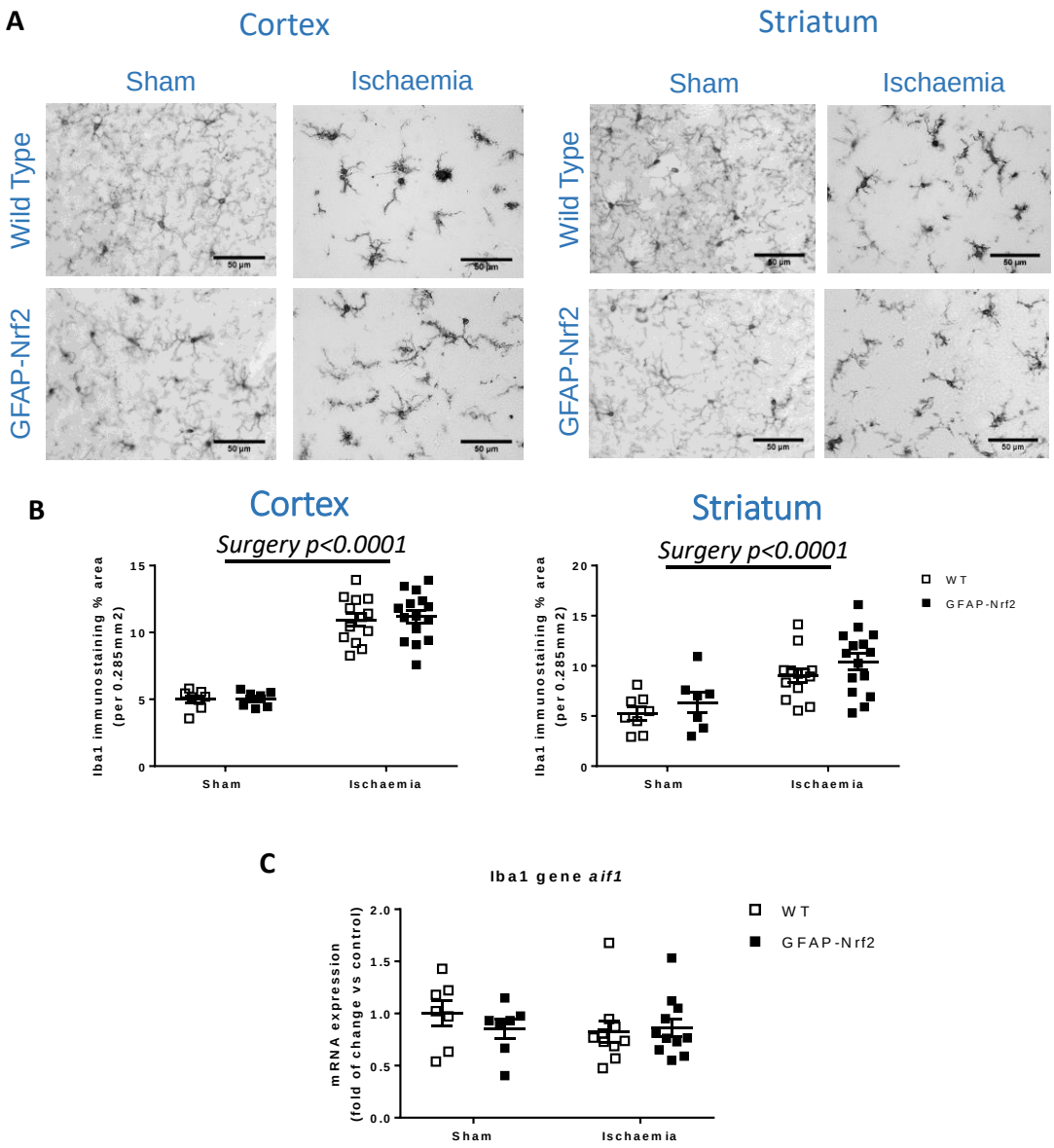

Figure 4-8 Nrf2 overexpression in astrocytes did not alter levels of the microglia/macrophage marker Iba1, 24 hours after 60 minutes ischaemia.

(A) Representative images of Iba1 immunostaining showed an increase morphological alteration to the microglia/macrophages following ischaemia in the cortex and the striatum compared to shams. The cells had larger cell bodies and thicker processes after ischaemia compared to the cells found in shams.

(B) Quantification of %area of Iba1 staining in the peri-infarct showed significant increase with surgery for cortex and striatum ($F_{(1, 38)}$=161.6, p<0.0001 and $F_{(1, 39)}$=21.19, p<0.0001). There was no effect of the genotype in the cortex ($F_{(1, 38)}$=0.0755, p=0.784) or the striatum ($F_{(1, 39)}$=2.206, p=0.1455).

(C) Iba1 gene aif1 mRNA expression was not altered by surgery ($F_{(1, 31)}$=0.595, p=0.446) or genotype ($F_{(1, 31)}$=0.291, p=0.59) in the peri-infarct of the cortex.

Data presented as mean ± S.E.M. Two-way ANOVA followed by post hoc comparisons with Bonferroni (N= 7 to 15 per group for the immunostaining study and N= 7 to 11 per group for gene expression study).

4.3.7. Increase of *IL-4rα* and *cxcl10* genes with astrocyte-specific overexpression of Nrf2

Through genetic or pharmacological approaches, it has been demonstrated that activation of the Nrf2-signalling pathway modulates inflammation. Nrf2 genetic global knockout was found to increase pro-inflammatory cytokines, decrease anti-inflammatory cytokines and increase glial reactivity in a Parkinson's disease model (Rojo et al., 2010). On the other hand, HO1 shifts the phenotype of macrophages to an anti-inflammatory phenotype (Naito et al., 2014).

To explain this effect, it has been reported that Nrf2 represses many pro-inflammatory cytokines during an inflammatory challenge by interfering with the transcriptional upregulation of these genes by binding directly to their upstream sequence, notably for IL-6 and IL-1β (Kobayashi et al., 2016). There was a significant increase with surgery of the pro-inflammatory cytokines, *il-1β* and *il-6* ($F_{(1, 31)}$=39.31, p<0.0001 and $F_{(1, 31)}$=15.34, p=0.0005 respectively) but there was no effect of genotype ($F_{(1, 31)}$=0.54, p=0.46 and $F_{(1, 31)}$=1.65, p=0.207 respectively; Fig 4.9 A) and post hoc tests revealed there was no alteration between wild type and GFAP-Nrf2 mice.

IL-4 cytokine is a key modulator of the anti-inflammatory microglia/macrophage phenotype. Mainly produced by monocytes, microglia and macrophages, it binds to its receptor IL-4rα and promotes the M2 anti-inflammatory phenotype (Fenn et al.,2014; Fenn et al., 2012; Liu et al., 2016). Interestingly, cells expressing the M2 phenotype upregulate IL-4 and IL-4rα genes (Norden et al., 2014). *IL-4rα* was upregulated with ischaemia surgery ($F_{(1, 31)}$=9.783, p=0.0038). There was no genotype effect ($F_{(1, 31)}$=1.298, p=0.26) however post hoc tests showed that there was a significant increase of IL-4rα mRNA levels in the GFAP-Nrf2 ischaemic mice compared to ischaemic wild-type (p=0.025; Fig 4.9 B).

cxcl10 is increased in inflammatory environments and is expressed by reactive astrocytes amongst other cell types. *cxcl10* mRNA levels were significantly increased with surgery ($F_{(1, 31)}$=27.61, p<0.0001) and there was also an effect of genotype ($F_{(1, 31)}$=6.621, p=0.0151). Together, two-way ANOVA revealed an interaction ($F_{(1, 31)}$=9.53, p=0.0042). Post hoc comparison between ischaemic groups revealed a significant increase in the GFAP-Nrf2 animals compared to wild-type (p=0.0002; Fig 4.9 C).

Reactive astrocytes show transcriptomic changes that can be classified as either neurotoxic (named A1) or neuroprotective (named A2; Clarke et al., 2018; Liddelow & Barres, 2017; Liddelow et al., 2017). To study pro-inflammatory (A1) astrocyte phenotype, *amigo2* and complement component 3 (*c3*) genes were analysed. For these two genes there was a significant effect of surgery (*c3*: $F_{(1, 31)}$=8.424, p=0.0068 and *amigo2* $F_{(1, 31)}$=8.451, p=0.0067) but no effect of genotype (*c3*: $F_{(1, 31)}$=0.99, p=0.32 and *amigo2* $F_{(1, 31)}$=0.15, p=0.70; Fig 4.9 D). Post hoc tests revealed there was no alteration between wild type and GFAP-Nrf2 mice following ischaemia (amigo2: p=0.453 and c3: p=0.455).

Stat3 gene *stat3* is highly upregulated in A2 protective astrocytes and not expressed in A1 astrocytes, furthermore it is an important gene for glial scar formation. There was a significant effect of surgery ($F_{(1, 31)}$=50.33, p<0.0001) but no effect of the genotype ($F_{(1, 31)}$=0.104, p=0.74; Fig 4.9 E). Post hoc tests revealed there was no alteration between wild type and GFAP-Nrf2 mice following ischaemia (p=0.841).

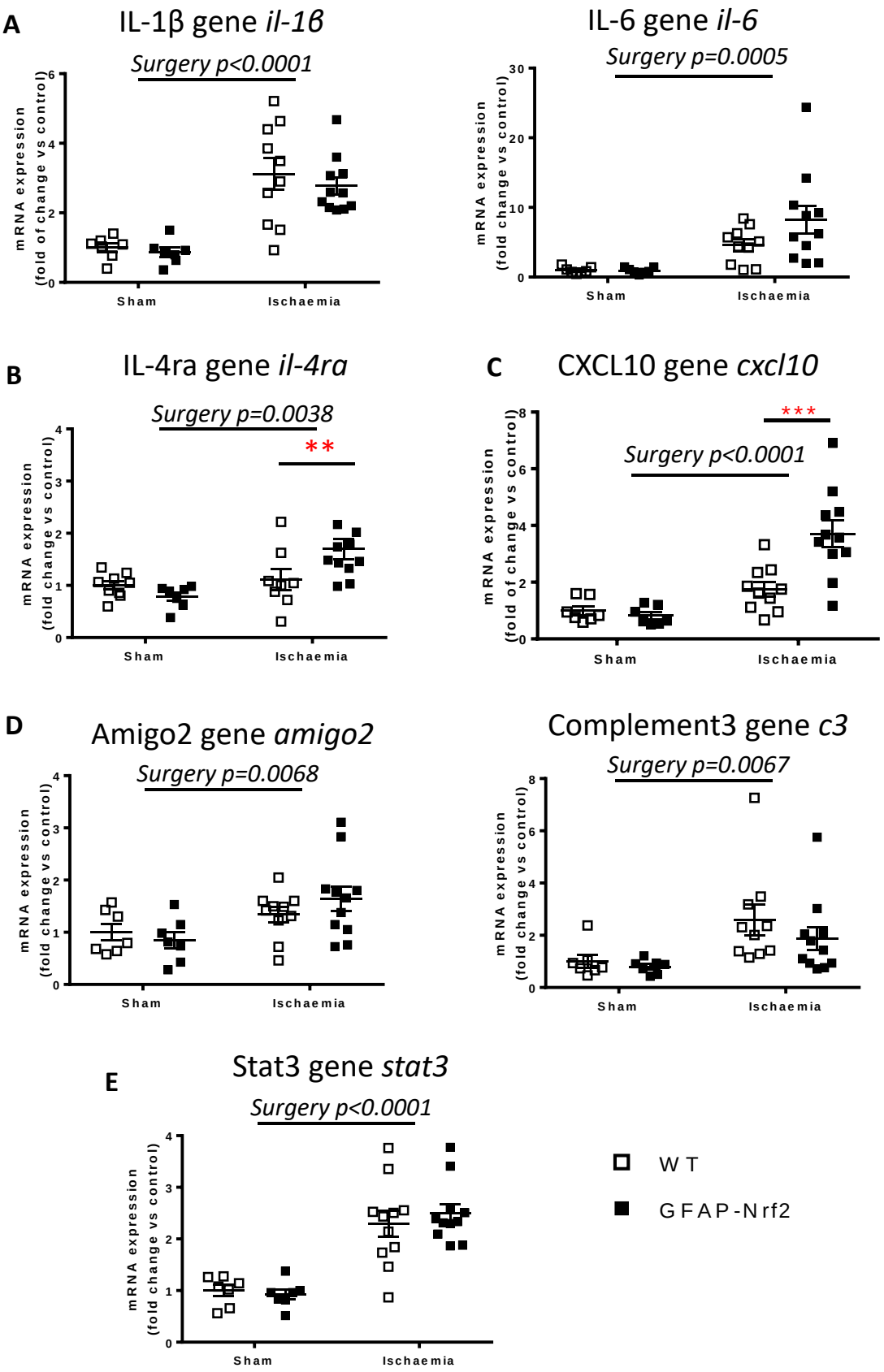
A
IL-1β gene il-1β
Surgery p<0.0001
mRNA expression (fold of change vs control)
Sham
Ischaemia
IL-6 gene il-6
Surgery p=0.0005
B
IL-4ra gene il-4ra
Surgery p=0.0038
**
C
CXCL10 gene cxcl10
***
Surgery p<0.0001
D
Amigo2 gene amigo2
Surgery p=0.0068
Complement3 gene c3
Surgery p=0.0067
E
Stat3 gene stat3
Surgery p<0.0001
WT
GFAP-Nrf2

← Figure 4-9 Nrf2 overexpression in astrocyte increases cxcl10 and IL-4rα genes 24 hours after 60 minutes ischaemia in the peri-infract of the cortex.

(A & B) Levels of pro-inflammatory genes il-1β and il-6 were significantly increased with ischaemia ($F_{(1, 31)}$=39.31, p<0.0001 and $F_{(1, 31)}$=15.34, p=0.0005 respectively) but not modified in GFAP-Nrf2 mice compared with wild type mice (p=0.806 and p=0.092 respectively).

(C) The anti-inflammatory gene IL-4rα was significantly increased with ischaemia ($F_{(1, 31)}$=9.783, p=0.0038) and post hoc comparisons showed a further increase by Nrf2 overexpression in astrocytes (p=0.025).

(D) Reactive astrocytes express cxcl10, this gene was increased with ischaemia ($F_{(1, 31)}$=27.61, p<0.0001) and post hoc test revealed that cxcl10 was further increased by Nrf2 overexpression in astrocytes (p=0.0002).

(E & F) Levels of amigo2 and complement 3 gene c3 were significantly increased with ischaemia ($F_{(1, 31)}$=8.424, p=0.0068 and $F_{(1, 31)}$=8.451, p=0.0067 respectively). Post hoc tests revealed there was no alteration between wild type and GFAP-Nrf2 mice following ischaemia (amigo2: p=0.453 and c3: p=0.455).

(G) A2 protective astrocytes gene stat3 was significantly increased with ischaemia ($F_{(1, 31)}$=50.33, p<0.0001 Post hoc tests revealed there was no alteration between wild type and GFAP-Nrf2 mice following ischaemia. (p=0.841).

*Data presented as mean ± S.E.M. Two-way ANOVA followed by post hoc comparisons with Bonferroni (N= 7 to 11 per group). **p<0.01, ***p<0.001.*

4.4. Discussion

There was a significant reduction in ischaemic neuronal damage in mice that overexpressed Nrf2 in astrocytes compared to wild-type littermates, and this neuroprotection was associated with reduced oxidative stress, increased Nrf2 signalling, increased levels of reactive astrocytes and increased *il-4rα* and *cxcl10* gene expression. Altogether, these finding provide support for the initial hypothesis that the Nrf2 overexpression in GFAP-positive astrocytes is neuroprotective as it reduces oxidative stress and inflammation.

4.4.1. Nrf2 overexpression in astrocytes reduces lesion and oxidative stress induced by ischaemia

Neuronal damage was reduced in the GFAP-Nrf2 animals compared to wild-type littermates; however, the reduction was modest (Fig 4.2). This result is supported by other studies that show there is an increased infarct volume in Nrf2 deficient mice (Liu et al., 2019; Shah et al., 2007; Shih et al., 2005; Wang et al., 2012), in addition to worsened ischaemic-induced neurological deficits (Liu et al., 2019; Shah et al., 2007). Conversely pharmacological activation of Nrf2-signalling reduced infarct volume, improve neurological deficits and reduce oxidative stress and oedema (Kunze et al., 2015; Liu et al., 2019; Mao et al., 2018; Shih et al., 2005a; Wang et al., 2012; Yao et al., 2016; Zeynalov et al., 2009). Furthermore, astrocytes are recognised as the cell that conveys Nrf2 neuroprotective effect as seen in OGD challenges and ischaemia (Bell et al., 2011; Kraft et al., 2004; Lee et al., 2003; Shih et al., 2003). In contrast, Narayanan et al. (2015) did not report increased infarct volume in Nrf2 knockout mice whereas Wang et al. (2012) did not observe an exacerbation of ischaemia-induced neurological deficits (Narayanan et al., 2015; Wang et al., 2012). Also mitochondrial inhibition is a feature of ischaemia (Schulz et al., 1998; Wojtovich & Brookes, 2008) and neuronal damage was also reported to be reduced in GFAP-Nrf2 mice following mitochondrial inhibition driven by injection of malonate (Calkins et al., 2010).

The reduction of neuronal damage in GFAP-Nrf2 mice in the present study was associated with reduced oxidative stress (Fig 4.3). Furthermore, oxidative stress spread beyond the lesion in the wild-type whereas it was contained in the lesion in GFAP-Nrf2 mice after ischaemia (Fig 4.4). This result was confirmed by upregulation of antioxidant Nrf2-related genes (Fig 4.6). As found in the literature, Nrf2 is a master regulator of a battery of

antioxidant genes and its activation in ischaemic models reduces oxidative stress (Alfieri et al., 2013; Li et al., 2016; Yao et al., 2016). With ischaemia and oxidative stress, glial-cells such as microglia and astrocytes showed an upregulation of their anti-oxidant defences, notably Nrf2 and glutathione (Shih et al., 2003; Vargas et al., 2008; Won et al., 2015). Some glial-like cells were immunostained with 3NT, it would have been interesting to counterstain them and assess the proportion of astrocytes and microglia/macrophages that underwent oxidative stress in both wild-type and GFAP-Nrf2 ischaemic groups.

The lesion seems to spread from the striatum to cortex and then hypothalamus and thalamus as seen with increased duration of ischaemia (Chapter 3 and McColl et al., 2004) or studying acute temporal evolution of ischaemia (Yoon et al., 2018). Thus, the results suggest that Nrf2 overexpression might reduce oxidative stress imbalance and hinder the normal spreading of the lesion.

In the present study a 2.5-fold increase in Nrf2 levels was reported in naïve, uninjured GFAP-Nrf2 mice and these levels were lower than the 3 to 8-fold increase reported by other groups using GFAP-Nrf2 mice (Calkins et al., 2010; LaPash Daniels et al., 2012; Sigfridsson et al., 2018; Vargas et al., 2008). However, Nrf2 overexpression was in GFAP-expressing astrocytes only and the tissue collected was from a 2 mm thick portion of the cortex or striatum with limited number of astrocytes whereas the cited papers used whole brain or the entire striatum or region of interest. Astrocytic overexpression of Nrf2 could be analysed by selectively sorting astrocytes before measuring Nrf2 gene mRNA levels. This discrepancy can also be due to a difference in the background of the strain. In this study, GFAP-Nrf2 mice were obtained from a C57Bl/6j background whereas in these papers, GFAP-Nrf2 mice had FVB background.

Astrocytic Nrf2 overexpression did not modify Nrf2-related gene expression in shams (Fig 4.6) contrary to the first check on Nrf2 level of expression in unoperated mice (Fig 4.1). One potential explanation is the difference of anatomical regions sampled between the two figures; cortex peri-infarct after sham or ischaemia surgery in contrast to a 2 mm slice from cortex, corpus callosum and striatum for the naïve mice. These two regions have different amounts of GFAP-positive cells and this region was quite small compared to the areas collected for the naïve animals that include corpus callosum which is enriched in GFAP-expressing cells. Importantly, Nrf2 levels do not inform on the activation of Nrf2-signalling. Alternatively, the distinction of nuclear or cytoplasmic location of Nrf2 by western blot could

have informed more about the activation of Nrf2-signalling (Chen et al., 2016; Lei et al., 2016).

Nrf2 is known for its antioxidant master regulator role, and it was found that overexpression of Nrf2 in astrocytes increased Nrf2 and Nrf2-dependent gene expression after ischaemia (Fig 4.5 and 4.6). Increased levels of Nrf2-related genes were reported in other studies that used GFAP-Nrf2 mice (Calkins et al., 2010; Gan et al., 2012; Sigfridsson et al., 2018). Interestingly, in the cortex peri-infarct, there was no increase or very little in Nrf2-related gene expression in wild type mice in response to ischaemia (Fig 4.6). Also, HO1 immunostaining was upregulated in the rim of the lesion in ischaemic wild-type animals but it did not extend too much further (Fig 4.5). This suggests that in the cortex peri-infarct there was minimal upregulation of Nrf2-related genes in wild-type animals after 60-minutes ischaemia, despite finding increased oxidative stress beyond the lesion. It could be that studying an earlier timepoint such as 2 or 4 hours may have revealed a difference in levels of Nrf2 genes between ischaemic and sham animals. Using the same procedure, a paper showed upregulation of Nrf2-related proteins in the peri-infarct (Tanaka et al., 2010). However, this paper did not give details on the analysed area (cortex or striatum? at the frontier or outside the lesion?) and counted cells were positive for thioredoxins, glutathione and HO1 immunostaining. These results also suggest that in GFAP-Nrf2 mice, levels of Nrf2-related gene expression were minimally altered compared with wild-type mice in the cortex peri-infarct of sham mice (Fig 4.6). It would be interesting to use ARE-hPAP reporter to localise Nrf2-signalling activity (Calkins et al., 2010; Chen et al., 2009; Vargas et al., 2008).

In physiological conditions, Nrf2 is sequestered by Keap1 and constantly degraded (Itoh et al., 1997). Some papers uses Keap1 knockout to upregulate Nrf2-signalling activation (Itoh et al., 2004; Kobayashi et al., 2016). Interestingly, Keap1 was neither changed with ischaemia compared to shams nor with astrocytic Nrf2-overexpression compared with wild-type (Fig 4.6). This was contrary to findings that Keap1 is reduced from 2 hours to 72 hours after 60 minutes of ischaemia (Ling et al., 2015; Tanaka et al., 2010). However, these papers analysed the core of the lesion where cells were lost and different timepoint to the present study. It would be interesting to study the expression of Nrf2-related genes in the striatum in the current study and at different time points after ischaemia.

4.4.2. Nrf2 overexpression and the effects on reactive astrocytes and microglia/macrophages after ischaemia

3.2.1.6. Increased astrocyte marker GFAP after ischaemia and in GFAP-Nrf2 mice

As seen in chapter 3, 60 minutes of ischaemia increased the %area of GFAP immunostaining and this was likely due increased levels of reactive astrocytes (Fig 4.7). Astrocytosis was also increased in the cortex peri-infarct of GFAP-Nrf2 compared to wild-type mice after ischaemia (Fig 4.7). Increased GFAP immunostaining can be due to morphological changes or increased cell number. Morphological changes are often linked to activation, but in that case, GFAP immunostaining was also increased in GFAP-Nrf2 shams compared to wild-type shams. Astrocytosis is caused by increased cytokines produced by injured neurons and activated microglia but also oxidative stress (Liddelow et al., 2017; Sofroniew, 2009; Swanson et al., 2004). This result has not been reported previously. Other papers using this model found no differences between wild-type and GFAP-Nrf2 sham control for their GFAP protein level or %area (Calkins et al., 2010; Gan et al., 2012; Sigfridsson et al., 2018). Interestingly a number of disease models of mitochondrial dysfunction, Parkinson's disease and cerebral hypoperfusion model all show increased levels of reactive astrocytes detected with GFAP that were dampened by astrocytic overexpression of Nrf2 (Calkins et al., 2010; Gan et al., 2012; Sigfridsson et al., 2018). However, of pertinence to the current study, one paper found that following knockout of Nrf2 mice there were decreased GFAP-positive cell number 24 hours after ischaemia compared to wild-type and that pharmacological activation of Nrf2 with Ginseng or DMF increased GFAP-positive cells in a Nrf2-dependent manner (Liu et al., 2019). They conclude that Nrf2 activation might play a role in the activation and proliferation of astrocytes.

A count of GFAP positive cell bodies (Dr Jill Fowler, personal communication) revealed a similar trend to %area, there was increased number of GFAP-positive cells in GFAP-Nrf2 mice compared with wild-type in both shams and ischaemia. Ischaemia increases the number of astrocytes by proliferation, however this is effect is reported to occur during the first week following the injury and not at 24 hours (Bardehle et al., 2013; Barreto et al., 2011; Oki et al., 2010). This result raises the hypothesis that GFAP-Nrf2 model increases GFAP-cells by promoting their production of GFAP and thus increasing their reactivity or that Nrf2 promotes astrocyte survival.

In the recent years, the concept of clasmatodendrocytosis has re-emerged with growing interests in astrocytes and their key role in brain pathology. Clasmatodendrocytosis was observed with *in vitro* models of ischaemia such as anaerobic glycolysis (Friede & Van Houten, 1961); acidic Ringer's solution coupled with mitochondrial inhibition (Hulse et al., 2001); with *in vivo* models of ischaemia (Davies et al., 1998), hypoperfusion (Hase et al., 2017) and was found in post-stroke AD post mortem (Chen et al., 2016). Counting of clasmatodendrocytes had been performed by Jill Fowler. No clasmatodendrocytes had been found in shams. For the wild-type ischaemic animals, 10 out of 13 animals presented clasmatodendrocytes whereas only 4 out of 15 GFAP-Nrf2 ischaemic animals had clasmatodendrocytosis. Nrf2 impact on clasmatodendrocytosis has not been reported previously. Altogether, these results suggest that astrocytic overexpression of Nrf2 might increase the survival of astrocytes.

Many papers highlight a protective role of astrocytes after an injury (Bhatia et al., 2019; Liu et al., 2017; Shinozaki et al., 2017; Zamanian et al., 2012). Astrocytes have many protective roles during ischaemia (Barreto et al., 2011; Becerra-Calixto & Cardona-Gómez, 2017; Takano et al., 2009) notably by modulating inflammation (Cekanaviciute & Buckwalter, 2016; Trendelenburg & Dirnagl, 2005) reducing oedema (Thrane et al., 2014), upregulating neurotrophic genes (Zamanian et al., 2012), gaining phagocytic function (Morizawa et al., 2017) and upregulating antioxidants (Bronstein et al., 1995; Desagher et al. 1996; MCNaught & Jenner, 1999; Min et al., 2006; Tanaka et al., 1999). More specifically, reduced astrocyte reactivity is associated with increased lesion volume in IL-4 knockout mice (Xiong et al., 2011). Altogether, these papers and reviews stress the idea that reactive astrocytes have a protective role following ischaemia and that their survival is beneficial.

3.2.1.7. UCCAo model might initiate early changes in astrocytes after ischaemia

An increased in the %area of GFAP immunostaining in sham GFAP-Nrf2 animals compared with wild-type mice was also detected in the present study. One possible explanation is that the sham procedure used in this work, known as unilateral common carotid artery occlusion (UCCAo) will reduce CBF and has been used as a vascular cognitive impairment model (Zuloaga et al., 2015). It has been reported that UCCAo decreased anti-inflammatory cytokines and increased pro-inflammatory cytokines with increased Iba1 staining, however

one limitation of this paper is that Iba1 levels were not quantified (Yoshizaki et al., 2008); others have found increased %area and density for both Iba1 and GFAP (Zuloaga et al., 2016). However, these results were found at 30 days and 3.5 months and it is unclear if this occurs at an earlier time point. No increase in levels of reactive astrocytes were detected between the contralateral and ipsilateral hemispheres of sham mice in the previous chapter as quantified by Lizi Hegarty of Jill Fowler's lab. Importantly, a study of the astrocyte transcriptome has found changes in the contralateral side of ischaemic animals compared with shams without seeing any differences in their GFAP immunostaining (Rakers et al., 2018). Furthermore, there was an upregulation of IL-1β, TNFα and CXCL10 protein levels 24 hours after 15 mins of UCCAo. However, this paper reported ischaemic damage in the cortex and hippocampus whereas we do not detect neuronal damage in sham UCCAo mice (Silva et al., 2015). Another paper found an upregulation of *il-1β* at 1 and 3 days, *il-6* at 2 hours and 2 months, and a downregulation of *il-4* at 1 and 3 days and *il-10* at 1 day, without neuronal damage following cerebral hypoperfusion model UCCAo, the model used for the sham of the present study (Yoshizaki et al., 2008).

Taken together, these results suggest that UCCAo procedure may modify astrocytes and cytokine production. It is possible that these changes could occur as early as 24 hours and were not detectable by immunohistology. Possibly, astrocytic Nrf2-overexpression might exacerbate these early modifications leading to an upregulation of GFAP immunostaining. It would be interesting to further study GFAP-Nrf2 mice astrocyte and inflammation following UCCAo and compare it to naïve animals.

3.2.1.8. Microglia/macrophages were increased with ischaemia but not altered by overexpression of Nrf2 in astrocytes.

Ischaemia caused an increase in the %area of Iba1 immunostaining that was not modified by astrocytic overexpression of Nrf2 (Fig 4.8). Similarly, other disease models that report protective effects in GFAP-Nrf2 mice did cause differences in Iba1 protein level or %area (Calkins et al., 2010; Sigfridsson et al., 2018). However, an increase of Iba1 mRNA in a model of Parkinson's disease was dampened by astrocytic overexpression of Nrf2 (Gan et al., 2012).

Ginseng or DMF dampened ischaemia-induced microgliosis at 6 and 24 hours after ischaemia compared to vehicle treated ischaemia controls (Liu et al., 2019), an effect that was lost in Nrf2 knockout mice. In another paper, DMF modestly reduced the microglia/macrophage marker Iba1 in a model of chronic cerebral hypoperfusion (Fowler et al., 2017). Conversely, Nrf2-signalling activator sulforaphane increased Iba1-positive cells in the peri-infarct but not in the core after ischaemia (Pekna et al., 2012).

As discussed previously in the chapter 3, ischaemia induced an increase in %area of Iba1 immunostaining that was due to possible morphological changes and increased cell number. Further investigation of these changes would be interesting such as counting Iba1-positive cells, co-labelling them with TMEM 119 or studying broad transcriptomic changes by using RNA-sequencing in a single-cell study.

3.2.1.9. Cytokine expression modified with Nrf2-overexpression in astrocytes

Inflammation after ischaemia is mainly driven by glial cells and infiltrating immune cells. In the past few years new concepts have emerged of diverse or polarised phenotypes for astrocytes and neutrophils paralleled to microglia. A discreet communication between these cells by second messenger cytokines contributes to the inflammatory state and gives direction to the immune response. Microglia activation can modify astrocytes at a transcriptomic level (Liddelow et al., 2017; Rothhammer et al., 2018; Shigemoto-Mogami et al., 2018) and vice versa (Min et al., 2006; Norden et al., 2014; Ovanesov et al., 2008). These changes were operated by means of microglia-astrocyte interactions (for review Jha et al., 2018). To distinguish the phenotypes, plethora of markers were developed, and methods have been refined, notably analysing transcriptomic changes on multi-cells samples or on single cell. It would be interesting to study alterations to transcriptomic changes of these cell types in the current study using RNA-sequencing.

IL-4 signalling, found on monocytes, microglia and macrophages (Zhang et al., 2014) is a key player in the anti-inflammatory response. There is increased neuronal damage in IL-4 knockout mice together with increased pro-inflammatory cytokine production and decreased anti-inflammatory responses, leading to increased cognitive impairment compared to wild-type mice (Liu et al., 2016). Furthermore, IL-4 knockout also reduces levels

of reactive astrocytes following ischaemia (Xiong et al., 2011). IL-4rα KO reduced IL-4 production (Lee et al., 2018; Noben-Trauth et al., 1997). Following ischaemia, IL-4 and its receptor IL-4rα are both upregulated at acute and chronic stage (Lee et al., 2018; Liu et al., 2016). IL-4 KO is associated with reduced anti-inflammatory responses and impaired behavioural recovery after ischaemia (Liu et al., 2016). The KO of IL-4rα increases apoptosis and reduces cell viability following ischaemia (Lee et al., 2018). In the present study, astrocytic overexpression of Nrf2 increased levels of *il-4rα*. Other studies report that Nrf2 and HO1 alter microglia phenotype from pro-inflammatory to anti-inflammatory using Nrf2 pharmacological activators or oxidative challenge (Han et al., 2016; Kadl et al., 2010; Min et al., 2006; Naito et al., 2014; Wang et al., 2018). Upregulation of *il-4rα* is in accordance with papers showing that Nrf2 activation by DMF increases IL-4 levels (Han et al., 2016) and that Nrf2 KO decreases IL-4 in a Parkinson's disease model (Rojo et al., 2010). Altogether, these results uphold the idea of microglia-astrocyte interactions and confirm the possible anti-inflammatory effect of Nrf2. However, it should be noted that the upregulation of IL-4ra in the present study was modest and anti-inflammatory effect could be further investigated by analysing microglial transcriptome.

Reactive astrocytes show transcriptomic changes that can be classified as either neurotoxic with upregulation of pro-inflammatory complement cascade (named A1) or neuroprotective (named A2; Clarke et al., 2018; Liddelow & Barres, 2017; Liddelow et al., 2017). There were no changes in astrocytic A1 or A2 specific genes *amigo2*, *C3* and s*tat3* in the present study. An increase in *cxcl10* (a 'pan reactive' gene present in both neurotoxic and neuroprotective astrocytes in Liddelow et al, 2017) was observed after ischaemia and further increased in ischaemic GFAP-Nrf2 mice (Fig 4.9). This result could reflect the increased astrocyte activation also reported in the present study; however, *cxcl10* is also expressed in many other cells such as microglia, astrocytes, neurons, leukocytes, macrophages and T cells (Chai et al., 2015; Harikumar et al., 2014; Klein et al., 2005; Nakamichi et al., 2004; Singh et al., 2008). Recent studies show increased CXCL10 in the inflammatory environment (triggered with LPS) due to the presence of activated microglia and astrocytes, however there was very little CXCL10 within activated microglia alone suggesting a major role of reactive astrocyte in this production of CXCL10 (Shigemoto-Mogami et al., 2018). This paper also found that the presence of astrocytes did not modify IL-1β or TNFα levels. Therefore, this result associated with increased GFAP immunostaining might hence denote increased levels of reactive astrocytes with Nrf2 overexpression. It would have been interesting to further study

astrocyte phenotype and transcriptome by using RNA-sequencing on isolated astrocyte and microglial populations. Another interesting study would have been to study their morphology by creating 2D or 3D models of their shape and measure the length and thickness of their processes as this reveal different subclasses (Clark et al., 2019; Wagner et al., 2013).

Upregulation of *cxcl10* in our GFAP-Nrf2 model was surprising as some reported CXCL10 levels were decreased with pharmacological activators of Nrf2 (Cheng et al., 2018; Kang & Lee, 2012) and unchanged with Keap1 KO (Draheim et al., 2016). CXCL10 is expressed in the pro-inflammatory environment and Nrf2 is known to increase anti-inflammatory and dampen pro-inflammatory cytokines. CXCL10 is expressed by reactive astrocytes and can attract microglia (Cross & Woodroofe, 1999; Rappert et al., 2004). This was not confirmed in the present study as Nrf2 overexpression in astrocytes increased *cxcl10* mRNA levels but did not modify %area of the microglia/macrophage marker Iba1. As explained previously, increased CXCL10 was found with LPS-reactive astrocytes (Shigemoto-Mogami et al., 2018) and after ischaemia (Zamanian et al., 2012). For GFAP-Nrf2 animals, astrocyte activation is increased by Nrf2 overexpression and CXCL10 increase can either be due to increased astrocyte levels or by a direct effect of Nrf2 overexpression.

Nrf2 is reported to repress IL-6 and IL-1β cytokine expression during an inflammatory challenge by binding directly to their upstream sequence and repressing their transcription (Kobayashi et al., 2016). This finding was not in accordance with our results. However, the model we used had an overexpression of Nrf2 in the astrocytes, whereas Kobayashi et al (2016) were using a myeloid-cell specific Keap1 knockout. Furthermore, IL-1β is mainly produced by microglia and IL-6 is mainly produced by endothelial cells (Zhang et al., 2014).

To distinguish the glial cell phenotype, a plethora of markers have been developed, and methods have been refined, notably analysing transcriptomic changes on multi-cell samples or on single cells. The current study is limited by the number of genes investigated; most papers studying astrocyte or microglia transcriptomic phenotype use RNA-sequencing as the heterogeneity of this activated population is a range of diverse response (Anderson et al., 2014; Boisvert et al., 2018). This heterogeneity can be defined with regional (Lanjakornsiripan et al., 2018) and injury specificities (Lin et al., 2017) but also with aging (Boisvert et al., 2018). Furthermore, the sample analysed in the present study comprises a mix of microglia,

astrocytes and many other cell types, bringing a difficult conclusion to which cell is being modified.

4.4.3. Other possible protective effects of Nrf2 overexpression in astrocytes

4.4.3.1. BBB leakage and oedema reduced by Nrf2

Nrf2 activators such as DMF, sulforaphane or Curcumin reduce BBB breakdown or oedema after ischaemia (Alfieri et al., 2013; Kunze et al., 2015; Li et al., 2016; Liu et al., 2019; Yang et al., 2009; Yao et al., 2016). Only two of these publications used Nrf2 KO to determine if these drugs acted via an Nrf2 dependent mechanism (Liu et al., 2019; Yao et al., 2016). It would have been interesting to investigate BBB integrity and leakage by mapping IGg or HRP immunostaining after ischaemia with the GFAP-Nrf2 model or by staining aquaporin4 or by measuring the expression of tight junction markers such as claudin1, occludin or ZO1.

4.4.3.2. Infiltration of peripheral immune cells

Because other studies report that Nrf2 reduces BBB breakdown and modifies inflammation (Alfieri et al., 2013; Kunze et al., 2015; Li et al., 2016; Liu et al., 2019; Yang et al., 2009; Yao et al., 2016), it has been suggested that it would reduce peripheral immune cell infiltration. One paper shows reduced neutrophil and T-cell infiltration 14 days after ischaemia with DMF treatment, along with infarct reduction and decreased neurological deficits (Lin et al., 2016). However, this paper did not challenge their protective effects with silencing or knock down of Nrf2. It would be interesting to study levels of peripheral immune cell infiltration in the currently study by using microglia specific marker TMEM 119, neutrophil or another peripheral immune cell marker.

4.4.4. Other limitations

4.4.4.1. Modest neuroprotection of Nrf2-overexpression in astrocytes

In this work, neuronal damage was modestly reduced in the GFAP-Nrf2 mice compared to their wild-type littermates after ischaemia (Fig 4.2). This model is developed in accordance with previous research showing an astrocytic specific protective effect of Nrf2 (Kraft et al.,

2004; Lee et al., 2003; Shih et al., 2003) and the GFAP-Nrf2 model attenuates neuronal damage and neurodegeneration after mitochondrial dysfunction and in Parkinson's and amyotrophic lateral sclerosis models (Calkins et al., 2010; Chen et al., 2009; Gan et al., 2012; Vargas et al., 2008). Despite the use of different disease models, these studies were undertaken on mice with a FVB background, whereas the present study was undertaken on mice with a C57Bl/6J background; FVB mice show more potent overexpression of Nrf2 and important gliosis reduction.

Knockout of the same gene in different mouse strains and sub-strains can exert different physiological effects (Doetschman, 2009; Linder, 2006). Notably in ischaemia research, different behavioural outcomes and infarct size have been reported in different mice strains (Rosell et al., 2013; Zhao et al., 2017). Finally, Nrf2 knockout showed lower antioxidant expression in female and old male compared to young male (Pellegrini et al., 2017).

Models overexpressing Nrf2 in endothelial or microglial cells, cell types also known to contain higher levels of Nrf2 would be useful to study in the context of ischaemia.

New research emerged developing cocktails of treatments. For ischaemia notably, overexpression of Nrf2 coupled with the overexpression of an astrocytic glutamate reuptake agent and of a catalyser for glutamate degradation led to drastic improvement and recovery of the motor functions after ischaemia (Molcho et al., 2018).

4.4.4.2. Research on ischaemia and aging

Ischaemia occurs mainly in elderly patients that present with comorbidities. Most preclinical research is carried out on young animals, limiting translation to clinical trials. Many differences in the cellular response to ischaemia are notable in aged compared to young animals (Popa-Wagner et al., 2007). Aged animals have increased oxidative stress and decreased antioxidant (Buga et al., 2008; Li et al., 2005; Roberts et al., 1997; Sieber et al., 2014; Zhang et al., 2018). Furthermore, Nrf2 signalling and its responsiveness is decreased with age (Suh et al., 2004; Zhang et al., 2015). However, no papers have studied the potential beneficial effect of Nrf2 activation following ischaemia with aged animals. It would be very interesting to test whether GFAP-Nrf2 aged animals have reduced ischaemic-induced damage compared to aged wild-type.

4.4.5. Conclusions

This study suggests that Nrf2-overexpression in astrocytes is potentially neuroprotective through an increase in reactivity and survival of GFAP-positive cells, but also by boosting antioxidant pathways and upregulating *il-4rα* and *cxcl10* genes it may reduce the spread of the lesion. It confirms our hypothesis that Nrf2-overexpression in GFAP-cells attenuates neuronal damage following ischaemia by reducing oxidative stress and inflammation.

In order to improve this study, more genes could be analysed, but also a single-cell approach would greatly reduce possible confusion as most cytokines are produced by a multitude of cells.

To conclude, we have demonstrated that Nrf2 overexpression in astrocytes decreased ischaemia-induced oxidative stress and neuronal damage, but also modified astrocytes and inflammatory response. Therefore, in the next chapter, the potential protective effect of astrocytic overexpression of Nrf2 in a chronic model of ischaemia was investigated along its effect on cognition and neurological function.

5. Astrocytic overexpression of Nrf2 does not protect neurons and does not alter neurological function or cognitive deficits in the chronic response to a modest duration of ischaemia

5.1. Introduction

In the previous chapter, boosting Nrf2 specifically in astrocytes protected neurons 24 hours after 60 minutes of focal cerebral ischaemia. The neuroprotective effect of boosting Nrf2 was paralleled by reduced oxidative stress, increased levels of reactive astrocytes and increased *il-4rα* and *cxcl10* mRNA expression.

Neurological deficits have been reported following hours or days after focal cerebral ischaemia, however neurological function has been shown to improve at later time points (7 to 28 days; Macrez et al., 2011; Omura et al., 2006; Titova et al., 2011; Yang et al., 2011; Yao et al., 2016). Neurological deficits at 3 and 7 days after focal cerebral ischaemia can be improved with by boosting Nrf2 signalling pharmacologically with DMF (Yao et al., 2016). Nrf2 activation *in vivo* decreases inflammation and improves spatial memory in a mouse model of Alzheimer's disease (Dumont et al., 2011; Kanninen et al., 2009). In a model of chronic cerebral hypoperfusion, spatial working memory assessed by an 8 arm radial arm maze was impaired compared with sham mice, however overexpressing Nrf2 specifically in astrocytes protected against these cognitive deficits (Sigfridsson et al., 2018).

Novel object recognition (NOR) is a sensitive test to detect cognitive deficits in the first weeks after focal cerebral ischaemia (Wang et al., 2012; White et al., 2012; Yabuki & Fukunaga, 2013; Zhu et al., 2015). This test has two phases, familiarisation of the mouse with two objects followed by a retention test with one novel object and one familiar. Naïve or sham animals spent more time exploring the novel object whereas ischaemic animals do not prefer the novel object. Glutathione treatment improves cognitive NOR memory in ischaemic animals (Yabuki & Fukunaga, 2013). Although the protective effects of boosting Nrf2 *in vitro* (Shih et al., 2003; Kraft et al., 2004; Murphy et al., 2002) and *in vivo* (Kraft et al., 2004) have been reported to occur via an astrocytic dependent mechanism, the effects of boosting astrocytic Nrf2 on cognitive and neurological deficits after focal cerebral ischaemia have not been studied.

5.1.1. Aims

It is hypothesised that overexpression of Nrf2 in the GFAP-positive astrocytes could attenuate neurological deficits, neuronal damage and improve cognitive function 4 weeks following modest duration of ischaemia by reducing oxidative stress and inflammation.

The specific aims are:

- To investigate the potential protective effects of Nrf2 overexpression in astrocytes after ischaemia in the chronic response (4 weeks recovery).
    a. To determine if ischaemia induces deficits in neurological function and novel object recognition memory and to determine whether Nrf2 overexpression in astrocytes modifies these behavioural deficits.
    b. To determine if boosting Nrf2 in astrocytes can protect neurons and reduce oxidative stress 4 weeks after ischaemia.
    c. To investigate possible modulation of inflammation and glial activation/phenotype with astrocytic overexpression of Nrf2 after ischaemia.
    d. To verify Nrf2-related gene expression is increased in the GFAP-Nrf2 model in response to ischaemia compared to wild-type mice.

5.2. Materiel & Methods

5.2.1. Mice and experimental groups

Male GFAP-Nrf2 mice and C57Bl/6J (wild-type; WT) littermates underwent ischaemia (transient middle cerebral artery occlusion for 15 minutes) (n=12-15/group for histology cohort and n=6-10/group for biochemistry cohort) or sham surgery and brains were collected at 4 weeks (see table 5.1). In order to study behaviour and cognition after ischaemia, a period of 4 weeks of survival after the ischaemia was chosen. As 60 minutes of focal cerebral ischaemia is severe, it induces a large area of neuronal damage in the hemisphere and mice can often recover poorly. However, the characterisation in chapter 3 demonstrated elevated oxidative stress and inflammation following a more modest duration of ischaemia (15-minutes) in the acute and chronic response. Thus, in the current experiments, 15 minutes of ischaemia with 4 weeks survival was investigated. Group sizes were determined using power calculations performed on previous result (presented in chapter 4): 15 animals per group are needed to achieve $p<0.05$ with a 20% effect (total lesion volume reduced of 19.576% in the GFAP-Nrf2 mice compared wild-types).

Two criteria of exclusion throughout the thesis has been used: (1) Lack of damage in the striatum following MCAo and (2) presence of infarction (pan necrosis of cells) defined as cluster of infiltrated cells and glia in the core of very large lesion. In this study, 3 animals of the histology cohort were excluded: 2 wild-type MCAo (1 infarcted and 1 with no lesion in the striatum) and 1 GFAP-Nrf2 MCAo (infarcted). Additionally, 5 animals in the histological cohort had to be culled early as they had a poor response to the surgery, or they exceeded 20% weight loss, and 2 for other non-ischaemia related health problems. In the biochemistry cohort, 3 animals had to be culled due to poor response to the procedure and 1 animal exceeded 20% weight loss.

All analyses were carried out with the experimenter blinded to groups and mice were allocated to groups in a randomised fashion.

			4 weeks survival			
			Histology cohort		Biochemistry cohort	
		Genotype	Initial size	Final size	Initial size	Final size
Occlusion duration or sham surgery	sham	WT	15	14	7	7
		GFAP-Nrf2	12	12	6	6
	15 minutes	WT	19	15	12	10
		GFAP-Nrf2	16	11	11	9

Table 5-1 Summary of the group size of each group after exclusion for histologic and biochemistry cohorts.

Histologic cohorts and the biochemistry cohorts depending on the surgery and the duration of occlusion and the survival (time between the ischaemia and the sacrifice) and the genotypes.

5.2.2. Focal cerebral ischaemia

As previously explained in section 2.2 of the Materials & Methods chapters, a monofilament was introduced into the CCA via a small incision and advanced 10mm distal to the carotid bifurcation to occlude the MCA (Monofilament 6-0 medium A MCAO suture L34 PK10; Doccol). Shams underwent the same procedure without the insertion of the thread. To withdraw the thread, mice were re-anaesthetised with isoflurane anaesthesia. Mice received 0.5ml saline (0.9%) subcutaneously by injection and were transferred to an incubator (30 °C) for 2 hours. The mice were weighed daily and monitored at least twice a day for the first 72 hours, and then daily, in order to assess the severity of the ischaemia injury. All ischaemia surgery was undertaken by Dr Jill Fowler. Aseptic techniques were used.

5.2.3. Sensorimotor and cognitive function tests

The methods used for assessing behaviour are described in section 2.5 of the materials and methods. Neurological deficits were assessed at 1, 3, 7, 10, 14, 21 and 28 days post-ischaemia using a neuroscore test based on a protocol from De Simoni et al., 2003 and Orsini et al., 2012. Scores range from 0 to 36, with a score of 0 indicating no deficit and a score of 36 indicating maximal impairment (See table 2.4). The score represents the sum of the results obtained in diverse categories.

Novel Object Recognition (NOR) was performed in a modified rat Y-Maze to minimize stress caused by open apparatus as detailed in section 2.5. Briefly, the animal was habituated to the maze by using the “starting arm” that was closed to the rest of the maze (see Fig. 2.4).

During the familiarisation and retention phases, the maze was opened, and two objects were placed in the two other arms. The trial began by placing the mouse in the "starting arm" and let free to explore the rest of the maze and the two objects. Each trial was 10 minutes long and video recorded. A pilot test showed that the animals were interested in the object mainly during the 3 first minutes. As a result, the 3 first minutes of exploration were used. The analysis was based on the time spent exploring the objects. A discrimination index (DI) was used to normalise the time spent on the novel object compared to the total time spent in the apparatus. An animal that spent less than 10 seconds to explore each object during the 10 minutes of familiarisation would be excluded. In the study, no animals were excluded following this rule. One animal was excluded as it did not explore the object during the first 3 minutes during the 4th week experiment.

$$DI = \frac{(\text{Time on Novel object} - \text{Time on Familiarised Object})}{(\text{Time on Novel object} + \text{Time on Familiarised Object})}$$

5.2.4. Histology

Histology and immunohistochemistry techniques used were performed as detailed in section 2.3 of the Methods. Lesion volume was assessed by drawing areas of neuronal death and tissue damage after assessing Haematoxylin and eosin staining, NeuN and MAP2 immunostaining. Oxidative stress was detected using 3-nitrotyrosine immunostaining and then mapped as undertaken for the lesion but using only 3 coronal levels, Microglia/macrophages and reactive astrocytes were studied using Iba1 and GFAP immunostaining respectively and quantified assessing %area in Image J (Fiji, NIH). After 4 weeks, the peri-infarct boundary was less obvious, therefore all the results presented in this section are from the core of the lesion. GFAP and Iba1 immunohistochemistry were undertaken by Lizi Hegarty.

5.2.5. qRT-PCR

To study Nrf2 related and inflammatory related gene expression, qRT-PCR was performed as explained in the Methods section 2.4. Because 15 minutes of ischaemia caused neuronal damage that mainly affected the striatum, the samples analysed in this section are from the

striatum. For this study, *cxcl10*, *il-1β*, *il-4rα* and *c3* genes were analysed to study inflammation. For Nrf2-related gene expression, *nfe2l2*, *hmox1*, *nqo1* and *slc7a11* genes were performed. For each animal, the level of expression was normalised compared with the housekeeping gene *18S*.

5.2.6. Statistics

Data were expressed mean ± S.E.M. using GraphPad Prism software. For parametric analysis, two-way analysis of variance (ANOVA) followed by *post-hoc* Bonferroni test was performed to correct for multiple comparisons. To analyse neuroscore, two-way ANOVA with repeated measures were performed with SPSS (v24.0). To analyse discrimination and preference for the novel object in the NOR test, one-sample *t*-test was used to compare the results to zero, (i.e. no preference). $P<0.05$ was deemed statistically significant.

5.3. Results

5.3.1. Nrf2 overexpression in astrocytes impaired cognitive functions and did not modify neurological function

Ischaemia impairs sensorimotor functions. To assess recovery from ischaemia and the potential effect of Nrf2 overexpression in astrocytes, a neuroscore scaling from 0 to 36, with 0 no deficit to 36, maximal impairment, was performed at different time points throughout the experiment. Different categories regrouped essential sensorimotor tests: grooming (hair, eyes and coat), sensorial response (whisker stimulation), posture and gait, spontaneous activity, symmetry, circling and gripping.

For each mouse, even shams, the score was different from 0 on the first days after the surgical procedure (Fig 5.1). Overall, ischaemic animals had significant increased neuroscore compared to shams ($F_{(1, 56)}$=16.729, p<0.0001). There was no effect of the genotype ($F_{(1, 56)}$=0.062 p=0.805; Fig. 5.1) and no interaction ($F_{(1, 56)}$=0.941, p=0.336), however, post hoc comparisons revealed a significant decrease of the neuroscore for the GFAP-Nrf2 ischaemic animals compared to ischaemic wild-types at 7 days (p=0.046). No significant differences were detected between the groups at other timepoint.

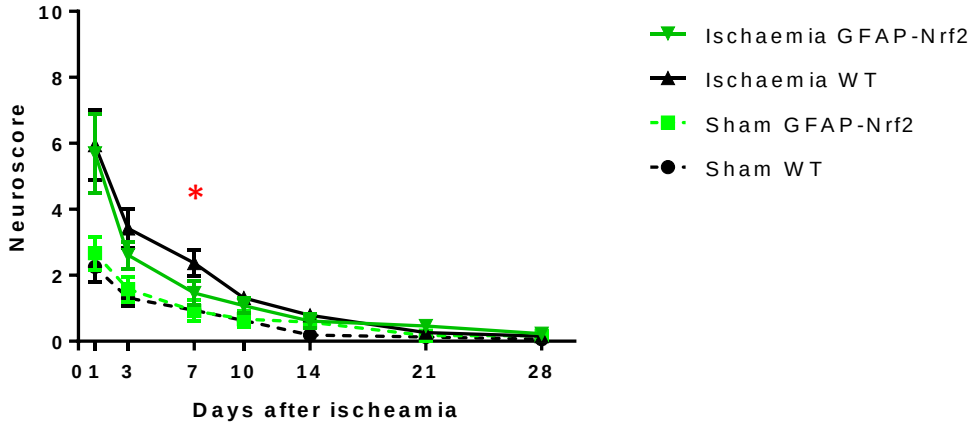

Figure 5-1 After modest duration (15 minutes) ischaemia, animals present neurological deficits and recovered quickly.

Neurological deficits were assessed at 1, 3, 7, 10, 14, 21- and 28-days post-ischaemia. Scores range from 0 to 36, with a score of 0 indicating no deficit and a score of 36 indicating maximal impairment.

Ischaemia caused a significant increase in neuroscore compared to shams ($F_{(1, 56)}$=16.729, p<0.0001). There was no effect of the genotype ($F_{(1, 56)}$=0.062 p=0.805) and no interaction ($F_{(1, 56)}$=0.941, p=0.336). Comparison of the different time points showed a significant difference between wild-types (WT) and GFAP-Nrf2 animals after ischaemia at day 7 (p=0.046). There was no significant difference between the groups at any other time point.

*Data presented as mean ± S.E.M. Two-way ANOVA with repeated measures followed post hoc comparisons with Bonferroni (N= 11 to 15 per group). *p<0.05.*

To test the cognitive function of the animals after ischaemia, novel object recognition (NOR) memory was assessed. This test has previously been used to detect cognitive deficits after ischaemia (Wang et al., 2012; White et al., 2012; Zhu et al., 2015). It assesses the ability of an animal to recognise a novel and remember a familiar object and thus assesses learning and memory (Leger et al., 2013). The 10-minutes trials of familiarisation and retention were 24 hours apart therefore assessing long term memory (Dudai, 2002; Montarolo et al., 1986). Quantification of the object preference was based on the time spent exploring the objects, using a discrimination index (DI) to measure the time spent on the novel object (N) compared to the time exploring the familiar object (F) and normalised on the total time exploring: DI = (N - F)/(N + F).

In a pilot experiment designed to test different durations of retention wild-type naïve animals tested showed a preference for the novel object with a DI close to 0.2, meaning 60% of the time spent exploring the novel object, and 40% on the familiar (pre-test on 5 wild-types: mean 0.195±0.081; Fig. 5.2) which is expected performance from naïve mice (Alachkar et al., 2019; Becerril-Ortega et al., 2014; Dong et al., 2019; Yabuki & Fukunaga, 2013).

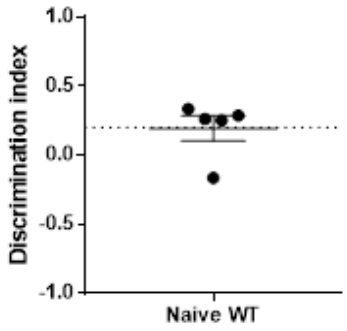

Figure 5-2 Novel object recognition on wild-types mice.

The novel object recognition task was designed to test the ability of the animal to remember an object. The animal was free to explore an object and its twin during a familiarisation trial. After a 24-hour retention period, the animal was free to explore the familiar object or a novel object. As animals naturally prefer novelty, the animal spent more time exploring the novel object. The analysis was based on the time spent exploring the objects, using a discrimination index (DI) to measure the time spent on the novel object (N) compared to the time exploring the familiar object (F) and normalised on the total time exploring: DI = (N - F)/(N + F). Animals were 2 to 4-month old.

On the first week after ischaemia, mice had recovered from the surgery and no animals were excluded for lack of exploration. Analysis of the DI with two-way ANOVA revealed no

significant effect of surgery ($F_{(1, 48)}$=0.309, p=0.581) nor of genotype ($F_{(1, 48)}$=1.799, p=0.186) or an interaction ($F_{(1, 48)}$=0.426, p=0.517; Fig 5.3).

At the end of the experiment, 4 weeks after ischaemia, analysis of the differences between groups revealed a significant effect of the surgery ($F_{(1, 47)}$=5.541, p=0.0228) but there was no effect of the genotype ($F_{(1, 47)}$=3.806, p=0.057) nor an interaction between surgery and genotype ($F_{(1, 47)}$=1.538, p=0.221). Post hoc comparisons revealed no differences between the two genotypes following ischaemia (p=0.056).

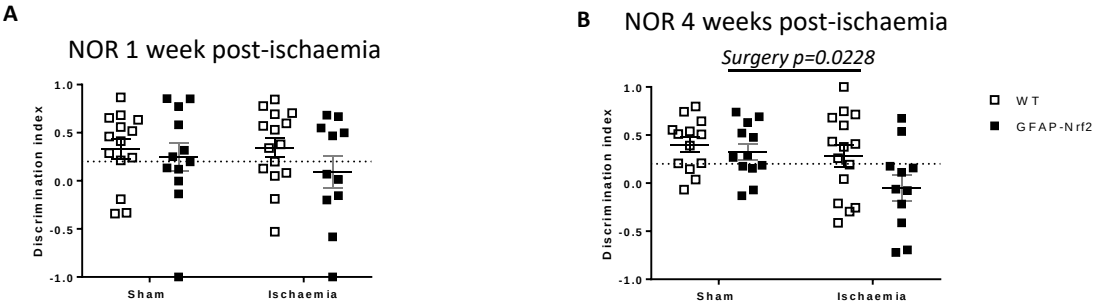

Figure 5-3 Cognitive deficit was observed 4 weeks after 15 minutes ischaemia compared to sham controls.

(A) There was no effect of surgery $F_{(1, 48)}$=0.309, p=0.581 nor of genotype $F_{(1, 48)}$=1.799, p=0.186 1 week after the ischaemia.

(B) There was an effect of the surgery $F_{(1, 47)}$=5.541, p=0.0228 but there was no effect of the genotype $F_{(1, 47)}$=3.806, p=0.057 at 4 weeks after the ischaemia.

Results above the dotted line represent a discrimination of the two objects with a preference for the novel object. Data presented as mean ± S.E.M. Two-way ANOVA followed by post hoc comparisons with Bonferroni (N= 11 to 15 per group).

The performance of both sham and ischaemic GFAP-Nrf2 mice seemed impaired on the NOR. A group of naïve animals, uninjured wild-type and GFAP-Nrf2 animals (n=3 to 7) were tested with 3 weeks apart to reproduce the experimental procedure (Fig 5.4). No differences were found between wild-types and GFAP-Nrf2 animals at both time points (baseline: p=0.58; 3 weeks later: 0.24).

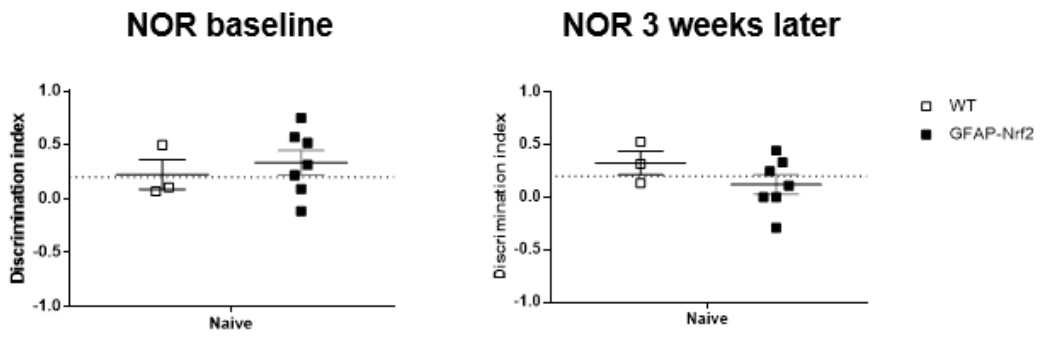

Figure 5-4 Discrimination of the novel object compared to the familiar was performed twice on naïve animals of both genotype with three weeks apart.

Results above the dotted line represent a discrimination of the two objects with a preference for the novel object. Data presented as mean ± S.E.M. (N= 3 to 7 per group). One-sample t-test to test the difference from zero (i.e. no preference for any object) with #p<0.05. Animals were 2 to 4-month old.

5.3.2. Neuronal damage was not altered by astrocytic overexpression of Nrf2

As described in Chapter 3, 15 minutes of ischaemia caused neuronal damage that was mainly detected in the striatum (Fig 5.5 A). Lesion volume was assessed by mapping the lesion onto coronal line diagrams. Quantification with two-way ANOVA showed that there was a significant effect of surgery, ischaemia increasing neuronal damage in each region (Total lesion $F_{(1, 48)}$=74.05, p<0.0001; cortex $F_{(1, 48)}$=8.653, p<0.0001; striatum $F_{(1, 48)}$=134.4, p<0.0001; other regions $F_{(1, 48)}$=14.96, p=0.0003). There was no effect of genotype (Total lesion $F_{(1, 48)}$=0.08, p=0.77; cortex $F_{(1, 48)}$=0.14, p=0.70; striatum $F_{(1, 48)}$=0.77, p=0.38; other regions $F_{(1, 48)}$=1.80, p=0.18) nor an interaction effect (Total lesion $F_{(1, 48)}$=0.12, p=0.72; cortex $F_{(1, 48)}$=0.14, p=0.70; striatum $F_{(1, 48)}$=0.77, p=0.38; other regions $F_{(1, 48)}$=1.80, p=0.18; Fig. 5.5). Post-hoc comparisons showed no differences between GFAP-Nrf2 and wild-type ischaemic animals in the total lesion (p>0.99), the lesion in the cortex (p>0.99), in the striatum (p=0.44) or the other anatomical regions (p=0.130; Fig. 5.5).

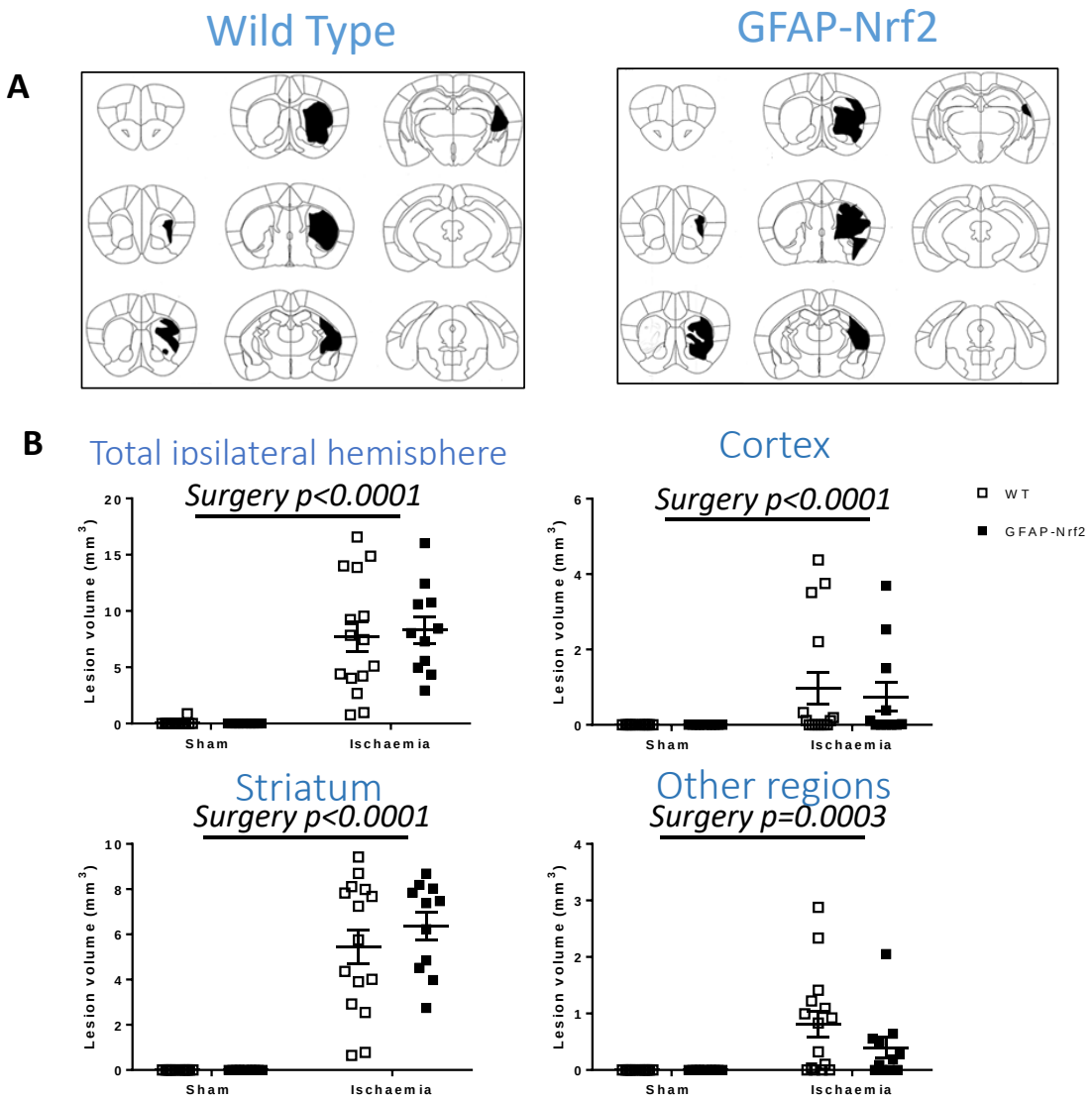

Figure 5-5 Nrf2 overexpression in astrocytes did not modify neuronal damage 4 weeks after modest duration of ischaemia (15 minutes).

(A) Representative line diagram with neuronal damage in black from the median animal of GFAP-Nrf2 and wild-type (WT) genotype. The lesion was mainly comprised in the striatum.

(B) Quantification of neuronal damage mapping showed a significant effect of the surgery for each region ($p<0.0001$). Nrf2-overexpression did not modify the total lesion ($p>0.99$), the lesion in the cortex ($p>0.99$), in the striatum ($p=0.44$) or the other regions ($p=0.130$).

Data presented as mean ± S.E.M. Two-way ANOVA followed by post hoc comparisons with Bonferroni (N= 11 to 15 per group).

5.3.3. Oxidative stress in response to ischaemia was unchanged in Nrf2 overexpressing mice compared to wild-type controls

Oxidative stress was assessed using 3NT immunostaining and mapped on line diagrams. The staining was mainly found in the striatum and only rarely in the cortex (Fig 5.6 A and B). Quantification revealed an effect of the surgery for each region (total ipsilateral hemisphere $F_{(1, 48)}$=61.47, p<0.0001; cortex $F_{(1, 48)}$=7.388, p=0.0091; striatum $F_{(1, 48)}$=79.34, p<0.0001), no effect of the genotype (total ipsilateral hemisphere $F_{(1, 48)}$=0.13, p=0.72; cortex $F_{(1, 48)}$=0.12, p=0.73; striatum $F_{(1, 48)}$=0.296, p=0.59) and no interaction (total ipsilateral hemisphere $F_{(1, 48)}$=0.13, p=0.72; cortex $F_{(1, 48)}$=0.11, p=0.75; striatum $F_{(1, 48)}$=0.296, p=0.59; Fig 5.6 B).

After mapping the lesion and 3NT areas of 3 coronal sections it was possible to compare the genotype (wild-type *versus* GFAP-Nrf2), marker (3NT area of expression *versus* neuronal lesion area) and the regions (+0.98, -0.10, -2.06 mm to Bregma). Using a two-way ANOVA with repeated measure by implementing the region variable, there was no effect of the genotype ($F_{(1, 52)}$=0.983, p0.326), nor of the marker ($F_{(1, 52)}$=0.507, p=0.480), however there was a significant interaction between genotype and marker ($F_{(1, 52)}$=145.622, p<0.001; Fig 5.6 C). Interestingly, there was an effect of the region ($F_{(1, 52)}$=111.283, p<0.001) and an interaction between region and genotype ($F_{(1, 52)}$=6.027, p=0.005; Fig 5.6 C). Post hoc analysis indicated that there was no difference between wild-types and GFAP-Nrf2 in oxidative stress (p=0.568) or in the lesion (p=0.412) but also for each region (Fig 5.6 C). Therefore, it means that the difference was dependant on the interaction of all factors without any factor being the main cause for this difference.

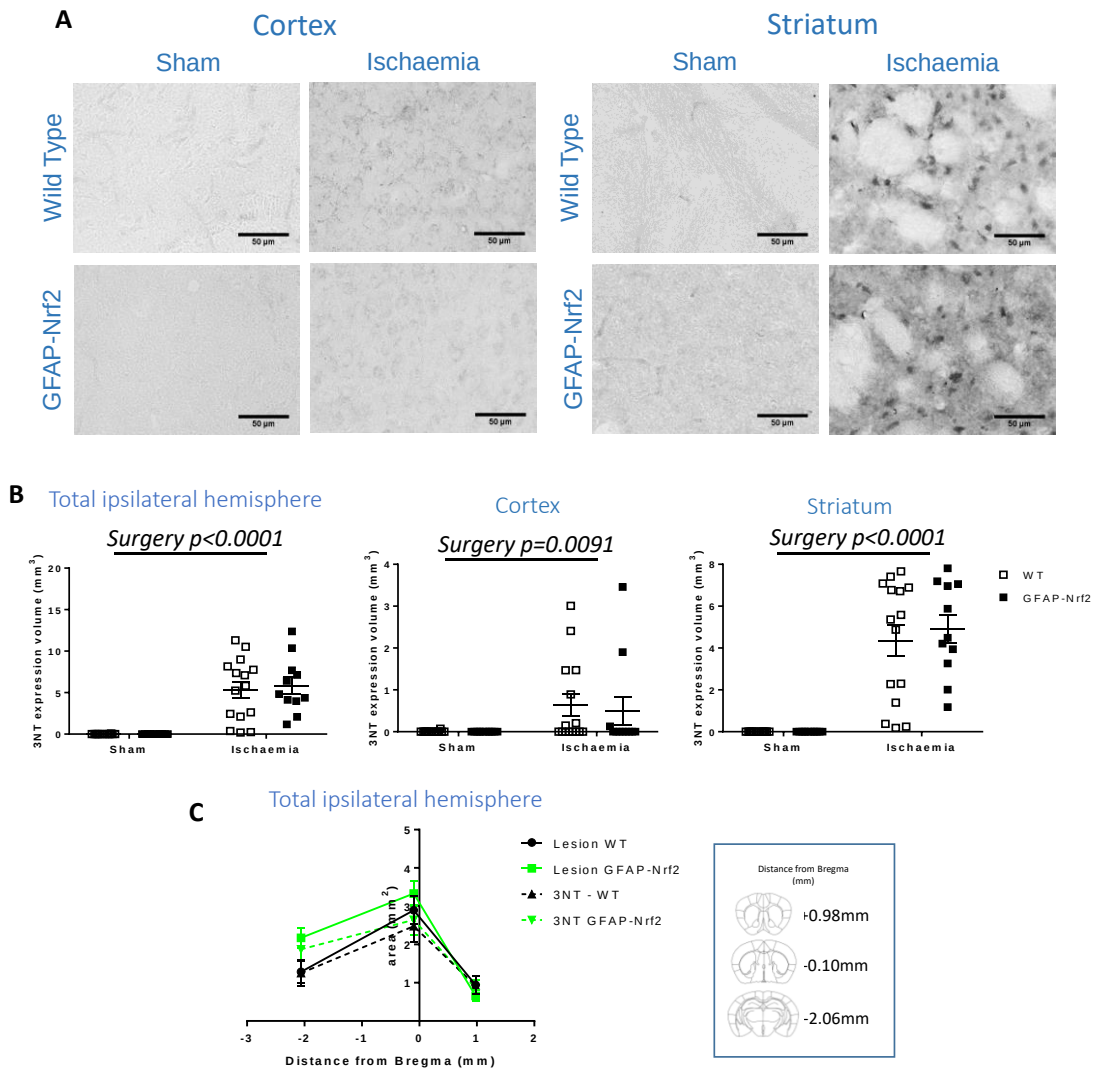

Figure 5-6 Nrf2 overexpression in astrocytes does not modify oxidative stress marker 3NT 4 weeks after 15 minutes ischaemia.

(A) Representative images of 3-Nitrotyrosine (3NT) immunostaining showed peroxide nitrite generation in the striatum after ischaemia but not in shams.

(B) Quantification of 3NT immunostaining by mapping the positive staining showed a significant increase of the staining with the surgery for each region (total ipsilateral hemisphere $F_{(1, 48)}$=61.47, p<0.0001; cortex $F_{(1, 48)}$=7.388, p=0.0091; striatum $F_{(1, 48)}$=79.34, p<0.0001), no effect of the genotype (total ipsilateral hemisphere $F_{(1, 48)}$=0.13, p=0.72; cortex $F_{(1, 48)}$=0.12, p=0.73; striatum $F_{(1, 48)}$=0.296, p=0.59) and no interaction (total ipsilateral hemisphere $F_{(1, 48)}$=0.13, p=0.72; cortex $F_{(1, 48)}$=0.11, p=0.75; striatum $F_{(1, 48)}$=0.296, p=0.59).

(C) Profile of the staining area and the neuronal damage area in three coronal sections of the ischaemic groups showed 3NT expression mirroring lesion area and slightly more elevated oxidative stress and neuronal damage in caudal brain for the GFAP-Nrf2 mice compared to wild-types. Using Two-way ANOVA with repeated measure, there was no effect of the genotype ($F_{(1, 52)}$=0.983, p0.326), nor of the marker ($F_{(1, 52)}$=0.507, p=0.480), however an interaction between genotype and marker was found significant ($F_{(1, 52)}$=145.622).

Data presented as mean ± S.E.M. Two-way ANOVA followed by post hoc comparisons with Bonferroni (N= 7 to 15 per group).

5.3.4. Nrf2-signalling was increased in the GFAP-Nrf2 mice

To determine if Nrf2-signalling was boosted in GFAP-Nrf2 mice and in response to ischaemia, Nrf2 gene *nfe2l2* and downstream genes *hmox1*, *nqo1* and xCT gene *slc7a11* were studied with qRT-PCR in the striatum. For each gene, there was no effect of surgery (*nfe2l2* $F_{(1, 28)}$=0.92, p=0.34; *hmox1* $F_{(1, 28)}$=0.17, p=0.68; *nqo1* $F_{(1, 28)}$=1.77, p=0.19; *slc7a11* $F_{(1, 28)}$=3.959, p=0.0565) and no interaction (*nfe2l2* $F_{(1, 28)}$=0.522, p=0.476; *hmox1* $F_{(1, 28)}$=1.094, p=0.304; *nqo1* $F_{(1, 28)}$=1.044, p=0.316; *slc7a11* $F_{(1, 28)}$=0.325, p=0.573; Fig 5.7). However, for each gene there was an effect of genotype (*nfe2l2* $F_{(1, 28)}$=54.46, p<0.0001; *hmox1* $F_{(1, 28)}$=12.12, p=0.0017; *nqo1* $F_{(1, 28)}$=46.15, p<0.0001; *slc7a11* $F_{(1, 28)}$=44.79, p<0.0001), with a significant increase in the GFAP-Nrf2 animals compared to wild-types (Fig 5.7). Bonferroni post-hoc corrections revealed a significant difference between wild-type and GFAP-Nrf2 in shams (*nfe2l2* p<0.0001; *hmox1* p=0.0127; *nqo1* p=0.0016; *slc7a11* p=0.0009), and after ischaemia for *nfe2l2*, *nqo1* and *slc7a11* (p<0.0001), but not for *hmox1* (p=0.135; Fig. 5.7).

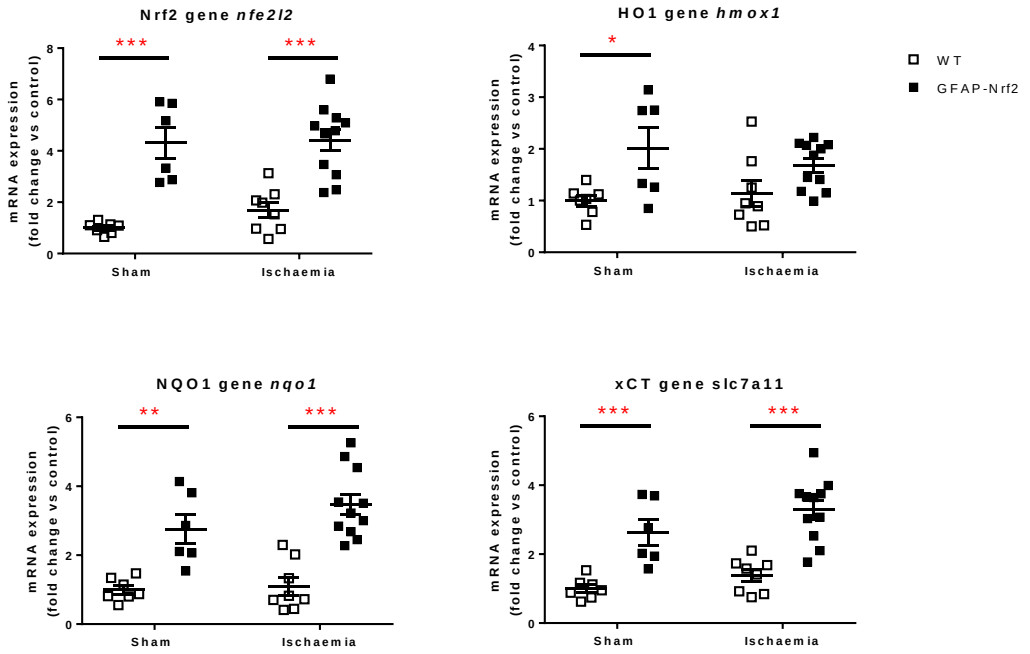

Figure 5-7 Nrf2 overexpression in astrocyte increases Nrf2-related genes in the striatum 4 weeks after 15 minutes ischaemia.

Nrf2 gene nfe2l2 mRNA levels and downstream genes hmox1, nqo1 and slc7a11 were not altered by surgery (nfe2l2 F(1, 28)=0.92, p=0.34; hmox1 F(1, 28)=0.17, p=0.68; nqo1 F(1, 28)=1.77, p=0.19; slc7a11 F(1, 28)=3.959, p=0.0565). However, for each gene there was an effect of the genotype (nfe2l2 F(1, 28)=54.46, p<0.0001; hmox1 F(1, 28)=12.12, p=0.0017; nqo1 F(1, 28)=46.15, p<0.0001; slc7a11 F(1, 28)=44.79, p<0.0001). There was no interaction (nfe2l2 F(1, 28)=0.522, p=0.476; hmox1 F(1, 28)=1.094, p=0.304; nqo1 F(1, 28)=1.044, p=0.316; slc7a11 F(1, 28)=0.325, p=0.573).

*Data presented as mean ± S.E.M. Two-way ANOVA followed by post hoc comparisons with Bonferroni (N= 6 to 10 per group). *p<0.05, **p<0.01, ***p<0.001.*

5.3.5. Nrf2 overexpression did not alter levels of reactive astrocytes 4 weeks after modest duration ischaemia (15 minutes)

Astrocytosis was studied with GFAP immunostaining. GFAP staining was present on shams, showing sparsely distributed astrocyte cell bodies and processes (Fig. 5.8 A). Ischaemic animals presented increased GFAP staining; in the cortex, more cell bodies were visible, and in the striatum, a maelstrom of processes and cell bodies were seen in the core of the lesion (Fig. 5.8 A). Quantification of the staining was undertaken with %area; it revealed a significant effect of surgery with increased staining after ischaemia (cortex $F_{(1, 48)}$=17.41, p=0.0001; striatum $F_{(1, 48)}$=306.1, p<0.0001; Fig. 5.8 B). There was no effect of the genotype (cortex $F_{(1, 48)}$=0.014, p=0.905; striatum $F_{(1, 48)}$=0.196, p=0.659) and no interaction (cortex $F_{(1, 48)}$=0.085, p=0.772; striatum $F_{(1, 48)}$=0.788, p=0.379; Fig. 5.8 B). Post hoc tests revealed there was no alteration between wild type and GFAP-Nrf2 mice following ischaemia.

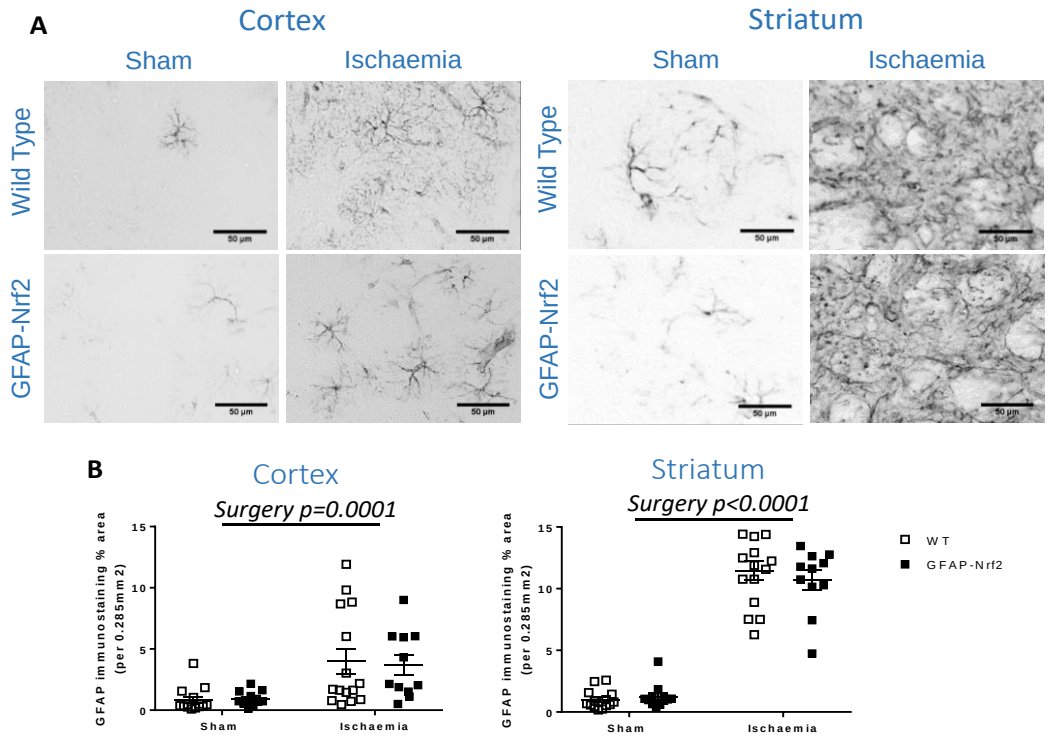

Figure 5-8 Astrocytic Nrf2-overexpression does not modify astrocyte reactivity after 15 minutes ischaemia 4 weeks post-injury.

(A) Representative images of GFAP immunostaining showing an increase with the ischaemia in the cortex and the striatum after ischaemia compared to shams. Some clasmatodendrocytes were observed in the lesion.

(B) Quantification of reactive astrocytes (%area of GFAP immunostaining) showed that there was a significant increase in reactive astrocytes with ischaemia surgery for cortex and striatum ($F_{(1, 48)}$=17.41, p=0.0001 and $F_{(1, 48)}$=306.1, p<0.0001). There was no effect of the genotype in the cortex or striatum ($F_{(1, 48)}$=0.014, p=0.905 and $F_{(1, 48)}$=0.196, p=0.659 respectively) and no interaction (cortex $F_{(1, 48)}$=0.085, p=0.772; striatum $F_{(1, 48)}$=0.788, p=0.379).

Data presented as mean ± S.E.M. Two-way ANOVA followed by post hoc comparisons with Bonferroni (N= 7 to 15 per group for the immunostaining study and N= 7 to 11 per group for gene expression study).

5.3.6. Astrocytic overexpression of Nrf2 increased microglia/macrophages response 4 weeks after mild ischaemia

In order to study microglia/macrophage activation, Iba1 immunostaining was used. Iba1 staining was present on sham and ischaemic animals with cell bodies and processes covering the parenchyma (Fig. 5.9 A). Ischaemic animals presented increased Iba1 staining in the striatum, where most of the neuronal damage was, processes and cell bodies were thicker and darker (Fig. 5.9 A). Quantification of the staining of % area immunostaining was undertaken. There was a significant effect of surgery with increased staining after ischaemia (cortex $F_{(1, 48)}$=6.225, p=0.0161; striatum $F_{(1, 48)}$=37.05, p<0.0001; Fig. 5.9 B). Interestingly, there was an effect of the genotype in striatum ($F_{(1, 48)}$=7.169, p=0.0101) with a significant increase in GFAP-Nrf2 animals compared to wild-types after ischaemia (p=0.0005), and an interaction ($F_{(1, 48)}$=8.742, p=0.0048). There was no effect of the genotype in the cortex ($F_{(1, 48)}$=0.0002, p=0.988) and no interaction ($F_{(1, 48)}$=0.016, p=0.898; Fig. 5.9 B).

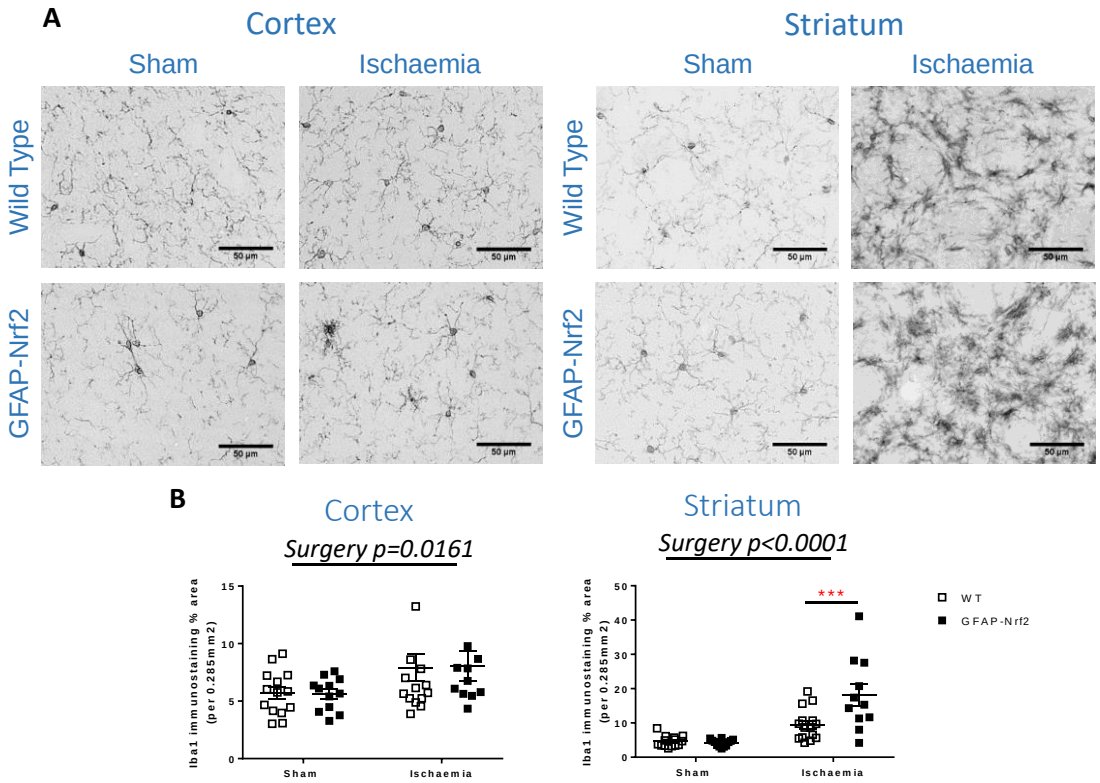

Figure 5-9 Nrf2 overexpression in astrocytes modifies microglia/macrophage levels 4 weeks after modest duration ischaemia (15 minutes).

(A) Representative images of Iba1 immunostaining showing an increase with ischaemia in the striatum.

(B) Quantification of Iba1 immunostaining by analysing %area of immunostaining showed a significant increase with surgery in the cortex and striatum ($F_{(1, 48)}$=6.225, p=0.0161 and $F_{(1, 48)}$=37.05, p<0.0001). There was an effect of the genotype in striatum ($F_{(1, 48)}$=7.169, p=0.0101) with a significant increase in GFAP-Nrf2 animals compared to wild-types (WT) after ischaemia (p=0.0005) and an interaction ($F_{(1, 48)}$=8.742, p=0.0048). There was no effect of the genotype in the cortex ($F_{(1, 48)}$=0.0002, p=0.988) and no interaction ($F_{(1, 48)}$=0.016, p=0.898).

*Data presented as mean ± S.E.M. Two-way ANOVA followed by post hoc comparisons with Bonferroni (N= 7 to 15 per group for the immunostaining study and N= 7 to 11 per group for gene expression study). ***p<0.001.*

5.3.7. Nrf2 overexpression in astrocytes reduced *c3* gene expression after ischaemia but did not modify the expression of *cxcl10*, *il-1β* or *il-4rα* genes

A few relevant markers of inflammation, known to be modulated by Nrf2, were investigated. Pro-inflammatory gene *il-1β* was significantly increased 4 weeks after ischaemia ($F_{(1,28)}$=15.71, p=0.0005), but there was no significant effect of the genotype or interaction ($F_{(1,28)}$=0.66, p=0.42 and $F_{(1,28)}$=0.605 p=0.44 respectively; Fig 5.10). IL-4rα is a key player of the anti-inflammatory response; its gene expression was significantly increased with ischaemia ($F_{(1,28)}$=23.61, p<0.0001), but there was no significant effect of the genotype or interaction ($F_{(1,28)}$=0.08, p=0.78 and $F_{(1,28)}$=0.177, p=0.677 respectively; Fig 5.10). CXCL10 is produced mainly by reactive astrocytes in an inflammatory environment. *Cxcl10* gene expression was significantly increased 4 weeks after ischaemia ($F_{(1,28)}$=22.28, p<0.0001), but there was no significant effect of the genotype or interaction ($F_{(1,28)}$=0.39, p=0.54 and $F_{(1,28)}$=2.933, p=0.097 respectively; Fig 5.10). Reactive astrocytes with a neurotoxic phenotype (A1) produce complement component 3 gene *c3*; analysis of its expression revealed a significant increase with ischaemia 4 weeks after the injury ($F_{(1,28)}$=10.34, p=0.0033). Furthermore, there was a significant effect of genotype ($F_{(1,28)}$=4.955, p=0.034) and an significant effect of the interaction between surgery and genotype ($F_{(1,28)}$=5, p=0.0335). Post hoc tests revealed there was a significant reduction in *c3* mRNA levels the GFAP-Nrf2 compared to wild-type animals after ischaemia (p=0.0033; Fig. 5.10).

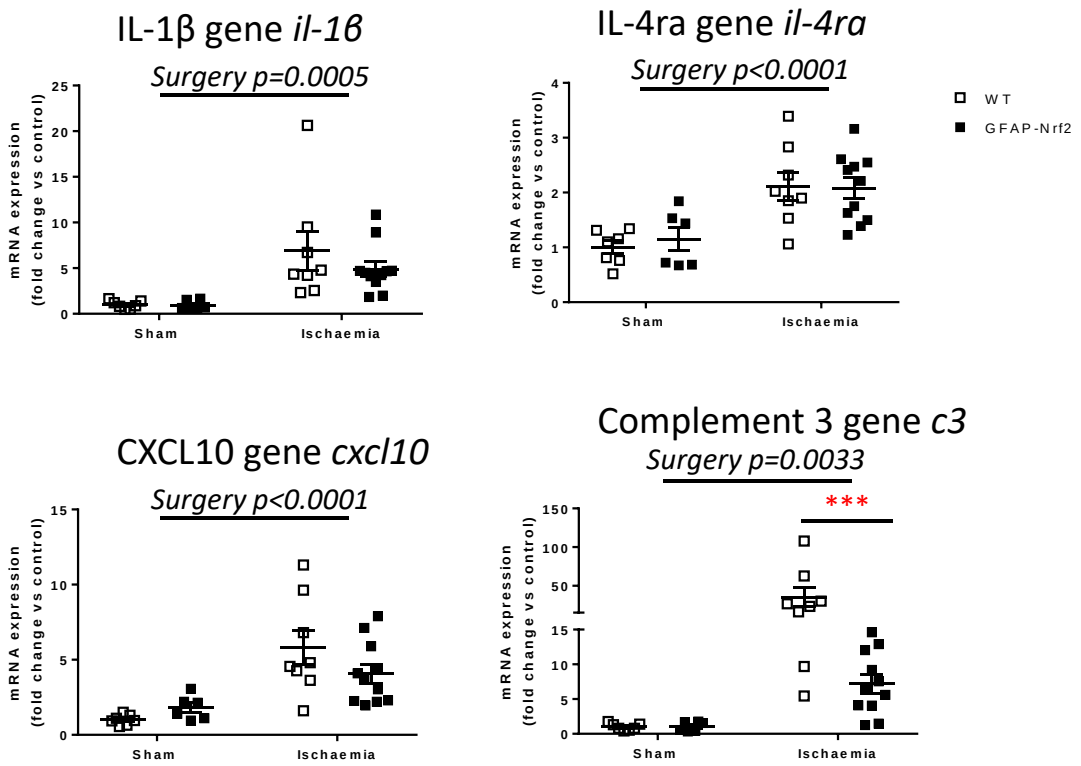

Figure 5-10 Nrf2 overexpression in astrocyte decreases complement 3 (c3) gene but not cxcl10, il-1β or il-4rα in the striatum 4 weeks after 15 minutes ischaemia.

There was a significant increase in mRNA levels of pro-inflammatory gene il-1b, anti-inflammatory gene IL-4rα , reactive astrocytes gene cxcl10 and A1 specific gene complement 3 gene c3 4 weeks after ischaemia (il-1β $F_{(1,28)}$=15.71, p=0.0005; il-4rα $F_{(1,28)}$=23.61, p<0.0001; cxcl10 $F_{(1,28)}$=22.28, p<0.0001; c3 $F_{(1,28)}$=10.34, p=0.0033). There was an effect of the genotype for c3 ($F_{(1,28)}$=4.955, p=0.034) with a significant reduction in the GFAP-Nrf2 compared to wild-type (WT) animals after ischaemia (p=0.0033), but no effect for the other genes (il-1β $F_{(1,28)}$=0.66, p=0.42; il-4rα $F_{(1,28)}$=0.08, p=0.78; cxcl10 $F_{(1,28)}$=0.39, p=0.54).

*Data presented as mean ± S.E.M. Two-way ANOVA followed by post hoc comparisons with Bonferroni (N= 6 to 10 per group). ***p<0.001.*

5.4. Discussion

In conclusion, Nrf2 overexpression in astrocytes did not modify neuronal damage and oxidative stress in the chronic response to a modest duration of focal cerebral ischaemia. However, GFAP-Nrf2 mice had decreased neurological deficits at 7 days after ischaemia, pro-inflammatory *c3* gene expression was decreased and microglia/macrophages reactivity was increased at 4 weeks when compared with wild type mice. Importantly, cognitive deficits seemed increased in GFAP-Nrf2 animals.

Altogether, these findings refute the original hypothesis that Nrf2-overexpression in astrocytes would be neuroprotective and improve cognition in the chronic response following ischaemia as it failed to reduce neuronal damage and oxidative stress but also further impaired discrimination of the novel object; however, it had other beneficial effects, it reduced inflammatory related *c3* expression and neurological deficits.

5.4.1. Neurological deficits improved at 7 days in the GFAP-Nrf2 animals

In this chapter, it was determined that there were early deficits in neurological function assessed with neuroscore. The first day following the surgery, shams and ischaemic animals had neurological deficits however it was very mild for shams and they recovered within a few days, whereas it took more than a week for ischaemic animals to recover (Fig. 5.1). This is supported by other research; ischaemic animals presented general sensorimotor impairments following the injury but then recovered after the first week (Deng et al., 2016; Macrez et al., 2011; Omura et al., 2006; Orset et al., 2007; Titova et al., 2011). Interestingly, these papers reported results for long duration of ischaemia (from 50 minutes to permanent) apart from one that showed locomotor activity recovery 48 hours after thrombin injection (Orset et al., 2007). Specific unilateral sensorimotor functions are impaired for much longer and possibly permanently due to the presence of striatal and/or cortical lesion (Yang et al., 2011).

Quantification of the neuroscore data did not show an overall effect of the genotype, however at day 7 GFAP-Nrf2 ischaemic animals had reduced neurological deficits than their ischaemic wild-type littermates (Fig 5.1). Other studies have shown that Nrf2 activation by pharmacological or transgenic means is beneficial as it can decrease neurological deficits (Lin

et al., 2016; Shih et al., 2005; Yamauchi et al., 2016; Yao et al., 2016). With the present data, the protection at 7 days cannot be explained as no data have been collected on oxidative stress, inflammation, neuronal damage at this time point. To investigate this effect, a new experiment must be designed with 15 minutes ischaemia and 7 days survival.

5.4.2. Novel object recognition (NOR) to test cognitive function

The result of the NOR showed no effect of the surgery after the first week but an effect at 4 weeks (Fig. 5.3) suggesting that cognitive functions were impaired in the longer term after ischaemia. Others reports cognitive impairment at 7 days (Doyle et al., 2015; Wang et al., 2012; White et al., 2012), with improvement at 21 days (Wang et al., 2012) or at later time points (1 month; Zhu et al., 2015) for novel object recognition memory impairments after ischaemia. These papers have severe ischaemia procedures and it can cause chronic impairments on cognitive function from 7 days to 2 months (Ryan et al., 2006). Concomitant with our findings, Guégan and colleagues performed permanent distal MCAo and showed impairments on the Morris water maze at 5 weeks but not during the first week (Guégan et al., 2006). The severity is thus an important discrepancy regarding the lesion location and thus the impact on cognitive function. Our findings indicate that the lesion is present in the striatum, however pathology was present in the cortex for a few animals. These papers described above all have cortical and striatal lesions, with only one of the papers stating that the lesion impacted the hippocampus (Wang et al., 2012). Contrary to the previous cited literature, ischaemic wild-type animals were able to discriminate the novel object compared to the familiar object at 4 weeks (Fig. 5.3). This might be due to either the time point, as other publications found cognitive impairment after ischaemia at 7 to 12 weeks (Doyle et al., 2015). Therefore, if a later timepoint had been examined, there may have been an increased memory impairment. The lack of impairment following ischaemia wild type mice at 4 weeks could also be related to the difficulty of the task. The mice had 10 minutes during the familiarisation to observe the familiar object as recommended by other papers (Leger et al., 2013; Yabuki & Fukunaga, 2013). However, a few others investigated 5 minutes of familiarisation and were still able to have mice discriminate (Wang et al., 2012; Zhu et al., 2015). By decreasing the duration of the familiarisation, it increases the difficulty of the task and possibly its sensitivity. Another alternative is to remove the mouse from the apparatus after 20 to 38 seconds exploring the objects (Leger et al., 2013; White et al., 2012). It also

exists other protocols that complexify the task by putting two different objects during the familiarisation or by doing two habituation sessions with different objects (Asiminas et al., 2019).

It is interesting to note that GFAP-Nrf2 animals had better neurological scores at 7 days than the wild-types after ischaemia and that is paralleled with decreased discrimination of the novel object at the same time point for GFAP-Nrf2 compared to wild-types despite the surgery. In summary, Nrf2-overexpression in astrocytes causes worsened cognition for both focal (MCAo) and global (UCCAo) ischaemia at 7 days and improving neurological outcomes at 7 days of ischaemia. Together, these findings suggest both detrimental and beneficial effect, with unclear mechanism. In order to investigate this effect, a study of the synaptic proteins at 7 days after ischaemia and UCCAo should be conducted on the different region underlying these functions.

It has been reported that cognitive deficits after ischaemia are attenuated following pharmacological activation of Nrf2 (Mao et al., 2018). Another paper showed improvements on the NOR with glutathione treatment after ischaemia (Yabuki & Fukunaga, 2013). However, our results showed impaired recognition for GFAP-Nrf2 animals after ischaemia at 1 and 4 weeks (Fig 5.3). Sustained activation of Nrf2-signalling can be detrimental for cancer and diabetes, cardiac myopathy and obesity (Kensler & Wakabayashi, 2010; Dodson et al., 2015; Kannan et al., 2013; Loboda et al., 2016; Seo & Lee, 2013). However, none of these publications explain a possible modification of the cognition by Nrf2. Nrf2 is repressed early in cortical neurons and this is key to their development and synaptogenesis, as otherwise, forced Nrf2 expression in neurons during the early days of development lead to reduced synapses, retarded electrophysiological maturation and outgrowth of dendritic arborescence (Bell et al., 2015). This mechanism is interesting but not relevant for the present work, as Nrf2 was overexpressed in GFAP-positive astrocytes only. Of the different Nrf2-related genes expressed when Nrf2 is activated, some reports identified detrimental effect of HO1. Like Nrf2, HO1 is linked to tumour aggressiveness and cell proliferation in cancer (Alaoui-Jamali et al., 2009; Deininger et al., 2000; Hara et al., 1996). A recent review outlined the detrimental effects of HO1 (Schipper et al., 2019). For example, repeated or sustained production of HO1 could modify mitochondrial iron uptake, permeability and lead to mitochondrial damage (Schipper et al., 2019). Blockage of HO1 in an AD model led to decreased inflammation and improved learning (Gupta et al., 2014). Importantly, a few

studies conducted on a suppressor of HO1 activity found there was reduced trauma-induced neuronal damage, decreased necrosis and oedema in cerebral hypoperfusion model (Kadoya et al., 1995; Panizzon et al., 1996). In terms of cognition, two papers have found that HO1 overexpression was linked to learning and memory deficits via synapse protein reduction and increased Amyloid-β and Tau (Li et al., 2015; Si et al., 2018). However, in the present study HO1 was found increased in GFAP-Nrf2 shams compared to wild-type shams but not increased when comparing GFAP-Nrf2 ischaemic animals to wild-types animals; and learning abilities were reduced in GFAP-Nrf2 ischaemic animals and not GFAP-Nrf2 shams. In a mouse model of chronic cerebral hypoperfusion, GFAP-Nrf2 animals presented less impairment in the radial arm maze at 8 weeks compared to wild-type hypoperfused mice (Sigfridsson et al., 2018). However, in this paper, control groups of sham operated GFAP-Nrf2 animals and wild-type animals had differences in their learning patterns as it appeared that GFAP-Nrf2 mice made more re-visiting errors in the second part of the trial. In this paper they suggested that this effect was due to overwhelming antioxidant production as basal level maintenance of ROS is important for homeostasis (Angelova & Abramov, 2018; Ye et al., 2015). Particularly fine tuning of ROS production and regulation is critical as both high and low ROS levels impact at different time point the physiological development of nervous system cells (Olguín-Albuerne & Morán, 2018; Schippers et al., 2012) notably neurons (Kennedy et al., 2012). As reductive stress is detrimental for cells (Kornienko et al., 2019; Pérez-Torres et al., 2017), we can infer that severe inhibition of ROS might be detrimental for cognition. There is very few researches conducted on this subject, but it has been demonstrated that overexpression of antioxidant SOD was detrimental for long-term memory (Hu et al., 2006; Lee et al., 2014; Thiels et al., 2000) as it inhibited hydrogen peroxide elevation, required for long-term potentiation. Furthermore, ROS are essential for vascular homeostasis and function, immune response, haematopoiesis (Vara & Pula, 2014). In order to investigate this possibility, an investigation of synaptic protein expression could be conducted after ischaemia in GFAP-Nrf2 mice.

5.4.3. Neuronal damage unaltered with overexpression of Nrf2 in astrocytes

Infarct volume was similar between wild-type and GFAP-Nrf2 animals (Fig. 5.5), suggesting no neuroprotective effect of Nrf2-overexpression in astrocytes at 4 weeks after modest duration ischaemia. This result is contradicted by the previous chapter and other studies that

reported improved survival, reduced neuronal loss and reduced lesion after mitochondrial dysfunction with Nrf2 overexpression in astrocytes (Calkins et al., 2010; Chen et al., 2009; Gan et al., 2012; Vargas et al., 2008).

Interestingly, as the lesion was comparable for GFAP-Nrf2 mice and their wild-type littermates, the cognitive impairment seen in GFAP-Nrf2 mice 4 weeks after ischaemia cannot be explained a worsening of neuronal damage. Thus, any impairment that was observed in the novel object recognition was not due to neuro-motor deficits but caused by cognitive impairment.

Nrf2-signalling activation by pharmacological approach or genetic modification of Nrf2 expression have been shown to exert protective effects on ischaemic neuronal death in numerous papers, however a few papers did not find a protective effect (Kunze et al., 2015; Narayanan et al., 2015). These papers investigated the protective effect of two pharmacological compounds and used Nrf2 knockout model to test whether these compounds had Nrf2-dependant protective effect. Narayanan and colleagues found that untreated Nrf2 knockout had similar lesion volume and oxidative stress levels than the wild-types (Narayanan et al., 2015). This result contradicts others showing a worsening of neuronal damage with Nrf2 knockout and thus suggesting a neuroprotective effect of Nrf2 following ischaemia (Liu et al., 2019; Shih, et al., 2005a; Wang et al., 2012; Wu et al., 2017; Yao et al., 2016). Kunze and colleagues failed to find a reduction of the lesion using DMF, however DMF reduced the oedema. Using Nrf2 siRNA towards endothelial cells, the protective effects of DMF on oedema were lost, suggesting an Nrf2-dependant mechanism (Kunze et al., 2015). However other publications reported that DMF reduced neuronal damage (Lin et al., 2016; Liu et al., 2019; Yao et al., 2016) and this may be related to dose as neuroprotective effects are reported for using 45 mg/kg or more, compared to Kunze et al. using only 15 mg/kg.

In chapter 3, it was demonstrated that lesion volume observed at 24 hours and 4 weeks after 15-minutes of ischaemia was comparable in wild type mice, suggesting that there is no progression of the lesion, although it should be noted that this was not compared in a contemporaneous, randomised manner. In the previous chapter, it was shown that astrocytic overexpression of Nrf2 was neuroprotective, and it was suggested that this neuroprotective effect concerned the hypothalamus and thalamus, regions that have damage only after 60-

minutes or longer ischaemia. Of all the literature cited previously that demonstrated neuroprotective effects of boosting Nrf2, ischaemic models were either permanent or 60-minutes or longer ischaemia that contrast with our 15-minutes long ischaemia in current chapter. It raised the hypothesis that Nrf2-overexpression in astrocytes is protective after severe ischaemia as it reduced the spreading of the lesion. The lesion is reported to be developed in the first 18 hours after the onset (Hartings et al., 2003; Heiss, 2000), thus it is salvageable in that time.

Another hypothesis is that Nrf2 may have differential effect depending on the anatomical area, as neurons and astrocytes are very heterogeneous through the different part of the brain (astrocytes: Lin et al., 2017; Morel et al., 2018; Lanjakornsiripan et al., 2018; neurons: Watakabe et al., 2006; Zeng et al., 2018). The previous chapter showed a neuroprotective effect that seemed to affect the hypothalamic and thalamic regions (Fig 4.2). This would imply that the neuroprotective effect Nrf2-overexpression in astrocytes is not found in striatum but in these regions, however the hypothalamus and thalamus are mainly unaffected by a modest duration (15 mins) of focal cerebral ischaemia. However, Nrf2 overexpression in astrocytes had proven beneficial effects in the striatum following mitochondrial inhibition (Calkins et al., 2010).

Another possibility is insufficient Nrf2 activation (Fig. 5.7). HO1 immunostaining, as an index of Nrf2 activation, is only modestly increased by 15-minutes of ischaemia with 24 hours and 4 weeks survival (Fig 3.14 and 3.23). Also, the effect of 15 mins of ischaemia on Nrf2-signalling activation for GFAP-Nrf2 mice at acute timepoints such as 4 and 24 hours has not been investigated. As seen in chapter 3, in wild-type mice only *hmox1* and *srxn1* were upregulated at 4 hours after modest duration ischaemia and this was in the cortex, spared from neuronal damage and not in the striatum that was the core of the damage in this model. It would be interesting to use alternative methods to study spatial and temporal alterations to Nrf2-signalling activation after 15 minutes of ischaemia, such as luciferase tagging of Nrf2-signalling activation or *in situ* hybridation of Nrf2-related genes.

One interesting difference between 15- and 60-minutes ischaemia at 24 hours was that GFAP immunostaining was increased in the severe model but not following the modest duration of ischaemia (Fig 3.4). Since Nrf2 overexpression depends on a GFAP promoter in the GFAP-Nrf2 mice, this difference suggests the possible need of astrocytic reactivity and/or astrocytic

oxidative stress for a beneficial effect of Nrf2-overexpression. However, two results contradict this hypothesis. First increased *gfap* mRNA was observed 24 hours after 15-minutes ischaemia (Fig 3.5). However, there can be discrepancies between protein and mRNA levels (Vogel & Marcotte, 2012) and GFAP is prone to many post-translational modification (Yang & Wang, 2015). Importantly, a paper reported that the Nrf2-inducer Curcumin reduces GFAP protein level but not mRNA levels (Bachetti et al., 2012). Second, the oxidative stress marker 3NT was found in a broader area than the lesion, extending to the undamaged cortex at 24 hours after 15 minutes of ischaemia (Fig 3.3 B and C). Oxidative stress would certainly induce Nrf2-signalling in that case. Co-staining GFAP with oxidative stress marker 3NT would potentially elucidate this question, but also studying the effects of 15-minutes ischaemia on GFAP-Nrf2 animals that survive for 24 hours would help to understand potential early activation of Nrf2-signalling in astrocytes.

In the present study, Nrf2 gene expression was only 4-fold higher than Nrf2 levels in wild-type mice. Previous work on this model found very strong Nrf2-signalling activation in primary astrocytes cultures and in different brain regions (cortex, brain stem, spinal cord) using luciferase luminescence or by measuring 8-fold increase in GFAP-Nrf2 mRNA levels in spinal cord astrocytes compared to wild-types (Johnson et al., 2008; Vargas et al., 2008). Nrf2 overexpression was specific to GFAP-positive astrocytes that were very few and scattered in the cortex and striatum of shams or 15-minutes ischaemia. That would explain such a small Nrf2 gene expression rate in the mRNA of the multi-cell sample from the parenchyma. Areas with increased astrocytic GFAP such as in 60-minutes ischaemia will benefit of the Nrf2 overexpression to protect from neuronal damage. The GFAP-Nrf2 mice used were heterozygous. It would be possible that homozygous model would present further increased Nrf2 overexpression and thus increase potential beneficial effects and reduced variability, however it remains uncertain if this would alter neuronal damage after a modest duration of focal ischaemia (15 minutes).

5.4.4. Increased Nrf2-signalling in GFAP-Nrf2 animals compared to wild-type animals

Antioxidant genes *nqo1* and *slc7a11* were both upregulated in the GFAP-Nrf2 animals with or without ischaemia (Fig. 5.7). For each Nrf2-related gene, there was no effect of the surgery confirming previous results in chapter 3 in the chronic state, that although wild-type

ischaemic animals had oxidative stress, Nrf2-related genes were equals to shams (Fig. 3.23). For each gene, there was an effect of the genotype with increased gene expression in Nrf2-overexpressing mice, confirming the validity of the model.

Interestingly, *hmox1* was upregulated in GFAP-Nrf2 sham animals and unchanged with ischaemia, but Bonferroni post-hoc corrections revealed no differences between GFAP-Nrf2 and wild-type animals comparing ischaemic groups. HO1 is slightly downregulated after ischaemia in the GFAP-Nrf2 animals and that could be due to homeostatic regulation of its production as HO1 can be detrimental as previously explained (Schipper et al., 2019; Gupta et al., 2014; Kadoya et al., 1995; Panizzon et al., 1996; Li et al., 2015; Si et al., 2018).

5.4.5. Oxidative stress was unchanged in GFAP-Nrf2 animals compared to wild-type littermates after modest duration ischaemia

In this chapter, the oxidative stress marker 3NT was observed 4 weeks after ischaemia and unchanged with Nrf2-overexpression in astrocytes (Fig 5.6). There was no difference between GFAP-Nrf2 animals and wild-types when comparing the lesion or the genotype following ischaemia (Fig 5.6 C). Many papers showed efficiency of Nrf2 in reducing oxidative stress during acute time points. Chronic studies of the response to ischaemia are rarely carried out. It is even so the case for the impact of boosting Nrf2 signalling on chronic ischaemia. Two papers showed a neuroprotective effect of Nrf2 activation paralleled with increased antioxidant activity and decreased free radicals at 7 and 11 days post-ischaemia (Yabuki & Fukunaga, 2013; Yao et al., 2016).

5.4.6. Astrocyte reactivity unchanged in GFAP-Nrf2 animals compared to their wild-type littermates

In this chapter, astrocytes immunostained with the GFAP antibody were increased with ischaemia and formed a glial scar 4 weeks after ischaemia (Fig. 3.17). However, there was no alteration in levels of reactive astrocytes when comparing GFAP-Nrf2 mice with wild-type controls 4 weeks after ischaemia (Fig. 5.8). This contrasts with previous findings where 60 minutes ischaemia led to increased astrocytosis in GFAP-Nrf2 animals at 24 hours (Fig. 4.7). This discrepancy could be due to many possible factors that varied between this chapter and

the previous one. In the acute response to 60 minutes ischaemia, neuronal damage and astrocytosis were observed in the cortex (Fig. 3.2 and 3.4), however there was markedly less neuronal damage in the cortex after 15 minutes ischaemia at the same time point (Fig. 3.2 and 4). This suggest that early astrocytosis due to severe ischaemia can be modified by Nrf2-overexpression in astrocytes, but that long term astrocytosis is not impacted as it lacks the early effect on reactive astrocytes.

Furthermore, in chapter 4 the peri-infarct was investigated whereas in the present chapter, the core of the lesion has been quantified. This potentially explains the discrepancy. As previously explained, the peri-infarct and core were homogenous, and it was difficult to distinguish them at 4 weeks. In chapter 3, peri-infarct and core analysis of GFAP and Iba1 markers gave the same results at 4 weeks and thus it suggests the discrepancies were not due to this difference (see Appendix 8.2.1, Fig 8.1).

As discussed in chapter 4, other studies have reported that reactive astrocytosis induced in neurodegenerative disease models was dampened with Nrf2-overexpression in astrocytes (Calkins et al., 2010; Gan et al., 2012; Sigfridsson et al., 2018). It is possible that overexpression of Nrf2-in astrocytes modified astrocytosis before 4 weeks and that GFAP levels went back to wild-type levels after that. To test this hypothesis, a longitudinal study of astrocytes should be designed, using for example *in vivo* multi-photon techniques that allow for temporal, longitudinal studies of cellular modification in the same animals.

Using GFAP immunostaining is the best technique to study reactive astrocytes as this protein is linked to their morphology (Lebkuechner et al., 2015; Pekny & Nilsson, 2005). However, GFAP-astrocytes constitute only a subpopulation of astrocytes and new markers are emerging such as ALDH1L1, a pan-astrocytic marker (Cahoy et al., 2008). In this paper, they tested other markers, and found that S100β, commonly reported as an astrocytic marker, was found in a wide range of astrocytes, however, it is not specific for astrocytes, as it was expressed in oligodendrocytes.

5.4.7. Microglia/macrophages increased in the striatum of the GFAP-Nrf2 animals compared to wild-types

After 4 weeks of survival, ischaemic animals have increased Iba1 staining that was further increased in GFAP-Nrf2 animals compared to ischaemic wild-types (Fig. 5.9). In both cases, the staining was found within the glial scar as previously seen in chapter 3 (Fig. 3.18). To model multiple sclerosis, cuprizone causes oligodendrocyte loss, demyelination and microgliosis. Draheim et al. (2016) boosted Nrf2 by knocking out Keap1 in GFAP-expressing astrocytes in this model (Draheim et al., 2016). They found that Nrf2-signalling was increased and microgliosis was drastically reduced along with oligodendrocyte rescue and reduced axonal damage. They believe that Nrf2-signalling had an impact on microglia reactivity and diversification.

An increase of Iba1 staining in GFAP-Nrf2 ischaemic animals could potentially be linked to increased CXCL10 gene expression in GFAP-Nrf2 ischaemic animals found in the acute phase (Fig. 4.9) as CXCL10 is known to attract microglia (Cross & Woodroofe, 1999; Rappert et al., 2004). However, *cxcl10* gene expression was increased with ischaemia but unchanged with Nrf2 overexpression in astrocytes compared to wild-types 4 weeks after ischaemia (Fig. 5.10).

5.4.8. Inflammatory-related genes expression

Pro-inflammatory astrocyte gene *c3* was upregulated in ischaemic animals but GFAP-Nrf2 animals had drastic reduction of this gene expression compared to wild-type (Fig. 5.10). C3 is part of the complement cascade that promote phagocytosis (Veerhuis et al., 2011). Using GFAP-Nrf2 mice, Sigfridsson and colleagues found increased complement cascade component C1q and C4 after hypoperfusion and it was dampened with Nrf2-overexpression in astrocytes (Sigfridsson et al., 2018). Inhibition or lack of C3 was protective in AD mouse models, reducing synapse loss and in ischaemic models reducing neuronal loss (Alawieh et al., 2018; Hong et al., 2016; Shi et al., 2017). Importantly, one limitation of this marker is that C3 is also produced by microglia (Zhang et al., 2014). Fluorescent-associated cell sorting of astrocytes revealed that the production of C3 was specific to neurotoxic and pro-inflammatory reactive astrocytes (Liddelow et al., 2017).

In this chapter, *cxcl10*, *il-4rα* and *il-1b* genes were still increased 4 weeks after ischaemia (Fig. 5.10). Decreased *c3* gene expression with Nrf2 overexpression in astrocytes after ischaemia

suggests an anti-inflammatory effect. However, *cxcl10*, *il-4rα* and *il-1b* were comparable between ischaemia GFAP-Nrf2 mice and ischaemic wild-types. Several papers showed that ischaemia first increased anti-inflammatory cytokines for the first hours/days and that they later it decline, followed by elevations of pro-inflammatory cytokines (Amantea et al., 2018; Hu et al., 2012; Zhang et al., 2018). *IL-4rα* is increased 4 weeks following ischaemia compared to shams. But these papers suggest that anti-inflammatory cytokines peaked early and decline which we cannot prove with this work as it requires an analysis of the different time point in the same cohort. Interestingly, lack of anti-inflammatory IL-4 worsens cognitive functions following ischaemia (Liu et al., 2016). Furthermore, two inhibitors of M1 polarisation improved cognitive function and reduced infarction (Qin et al., 2017; Zhang et al., 2019). But in our case, decreased c3 levels were not paralleled with improved cognitive functions. This result is limited as a wide range of genes should be used to assess inflammation.

Results presented in the current chapter contradict known inhibitory effect of Nrf2 towards il-1β gene expression (Kobayashi et al., 2016). In the first chapter, il-1β was unchanged at 24 hours after 15 minutes ischaemia (Fig. 3.10). In the Kobayashi paper, il-1β expression was inhibited by Nrf2 after LPS treatment. It is possible that Nrf2 inhibition on this gene expression appears only early after a very large increase of this aforementioned gene. However, no effects of boosting Nrf2 signalling on il-1β were reported after 60 minutes of ischaemia in chapter 4. Interestingly, LPS and ischaemia are known to confer polarised effects on the transcriptome of reactive astrogliosis (Zamanian et al., 2012). Furthermore, Kobayashi uses Keap1-Knockout in myeloid cells. However, many papers argue that astrocytes can modify microglia activation at a transcriptomic level (Min et al., 2006; Norden et al., 2014; Ovanesov et al., 2008). Additionally, Min and colleagues found that reactive astrocytes boosted Nrf2-signalling in microglia and notably *hmox1* gene (Min et al., 2006). These results were observed *in vitro* and thus might be limited compared to *in vivo* conditions.

Severe ischaemia led to increased level of *il-4rα* at 24 hours and it was further increased with Nrf2 overexpression in astrocytes (Fig. 4.9). Modulation of *il-4rα* in early phase of modest duration of ischaemia is however unknown. It would be interesting to study this gene in the GFAP-Nrf2 mice 24 hours after 15 minutes ischaemia.

Importantly, *cxcl10* gene is increased in the striatum of the 15 minutes ischaemia at 24 hours (Fig. 3.8) and after 60 minutes ischaemia in the wild-type (Fig. 4.9). Nrf2-overexpression in astrocytes further increased *cxcl10* levels at that time point. But this gene had comparable increase in GFAP-Nrf2 mice compared with wild-types 4 weeks after 15 minutes ischaemia.

In summary, Nrf2 overexpression in astrocytes caused further increases in *cxcl10* and *il-4rα* at 24 hours after 60 minutes of ischaemia but not 4 weeks after 15 minutes of ischaemia. Either or both, severity or analysed time point can explain this discrepancy. Thus, two hypotheses can be produced: Nrf2 overexpression in astrocytes can modulate cytokine gene expression following severe ischaemia but not with modest duration of ischaemia; or Nrf2 overexpression in astrocytes can modulate cytokine gene at early time point but not in their chronic upregulation. To test these, two studies must be designed: cytokine gene expression has to be analysed in GFAP-Nrf2 mice compared to wild-types at 24 hours after 15 minutes ischaemia, and at 4 weeks after 60 minutes ischaemia.

5.4.9. Conclusions

In this chapter, Nrf2 overexpression in GFAP-expressing astrocytes reduced learning and memory performance compared to wild-types, at 1 week in both shams and after ischaemia, and at 4 weeks after ischaemia. This result contradicts the initial hypothesis that Nrf2 overexpression in astrocytes would improve cognitive decline observed in the chronic phase of ischaemia. Unexpectedly, the genotype did not impact on oxidative stress or neuronal damage at 4 weeks. However, this finding does not explain the worsening of the cognitive function observed in GFAP-Nrf2 mice. Of interest, GFAP-Nrf2 ischaemic animals had increased microglia/macrophage staining in the striatum and *c3* gene expression was reduced compared to ischaemic wild-types. This result supports the hypothesis that Nrf2 overexpression in astrocytes would modulate inflammation. Finally, neurological deficits were decreased with Nrf2-overexpression in astrocytes 7 days after ischaemia.

Taken together, this chapter showed that the effect of Nrf2 overexpression in astrocytes were different from the previous chapter. The severity of the ischaemia, as well as the different time point study may explain these discrepancies. To conclude, Nrf2 overexpression in astrocytes have diverse beneficial and detrimental effects depending on the injury.

Limitations of this work must be addressed, such as the use of a mild ischaemic model with possible variability and later cellular changes notably of astrocytes that may have driven the potential beneficial effect of Nrf2 as seen in chapter 4. Furthermore, there is a potential detrimental effect of continuous Nrf2 activation as seen in reductive stress, diabetes, cardiac myopathy and obesity research in the past. The use of young mice is an important limitation to translation, especially for neurodegenerative diseases. Comorbidities must be analysed and carefully included for future therapeutic trials. Finally, further studies should be conducted to understand Nrf2 modulation mechanisms involved in cytokines modulation, glial activation and cognition.

6. Discussion

6.1. Summary and implications

Ischaemic stroke is an important health condition and a leading cause of death, disability and persistent cognitive deficits. Neuronal damage occurs in two waves with the lack of oxygen and nutrients at first, and a second wave of oxidative stress and inflammation build-up that threatens to extend the primary lesion. There is a vast amount of literature on Nrf2-signalling pathway showing beneficial effects in inflammation, oxidative stress and ischaemic conditions.

The first chapter characterised the modifications triggered by ischaemia. It laid a ground of knowledge on inflammation and oxidative stress and their effects on Nrf2-signalling activation, particularly useful for the next chapters. Results of different occlusion duration gave a basis for understanding the lesion spreading. The lesion was contained in the striatum following 15 minutes ischaemia, and extended to cortex with 30 minutes ischaemia, and further to the thalamus, hypothalamus and hippocampus following 60 minutes occlusion. Modest duration of ischaemia (15 minutes) was sufficient to increase oxidative stress, astrocytic *gfap* gene expression and microglia reactivity; and increasing durations of ischaemia led to increased neuronal damage, oxidative stress and inflammation.

Interestingly, areas with no neuronal damage showed signs of inflammation and oxidative stress, both in the acute and chronic phase of ischaemia. As this MCAo model is known for mimicking penumbra, these modifications are probably an observation of it. Going further, these modifications are similar to ischaemic preconditioning in which astrocytes and antioxidants (notably Nrf2) are imperative for its neuroprotective effect (Bell et al., 2011a & b; Hirayama et al., 2015; Xue et al., 2016). Here was found antioxidant upregulation and astrocytic gene *gfap* upregulated at 1 day. Furthermore, long-lasting changes in those areas appear at 4 weeks but not at 1 day such as upregulation of GFAP immunostaining %area, *cxcl10* gene and microglial/macrophage gene *aif1*.

Studying different time points revealed an evolution of Nrf2-signalling upregulation. Nrf2-signalling was upregulated in the acute phase of ischaemia; however, there was a lack of responsiveness in the chronic phase despite maintained oxidative stress and inflammation. This effect is possibly due to an auto-regulation mechanism that bring back Nrf2 levels to

homeostatic levels. This hypothesis is supported by known detrimental effect of Nrf2 upregulation on reductive stress (Kennedy et al., 2012; Olguín-Albuerne & Morán, 2018; Schippers et al., 2012; Vara & Pula, 2014), carcinogenesis (Kensler & Wakabayashi, 2010) and insulin resistance (Fu et al., 2016).

Nrf2 activators have off-target effects. In this regard, the model used in this thesis can inform on the effects of Nrf2 effect exclusively It has been suggested in the literature that the protective effects of boosting Nrf2 signalling seem to depend mainly on astrocytes and their activation. The creation of a model that induces astrocytic overexpression of Nrf2 (GFAP-Nrf2) *in vivo* has been central to addressing these questions and interesting protective effects have been demonstrated in a number of different neurodegenerative diseases (Calkins et al., 2010; Chen et al., 2009; Gan et al., 2012; LaPash Daniels et al., 2012; Sigfridsson et al., 2018; Vargas et al., 2008).

In the second chapter, astrocytic overexpression of Nrf2 caused a reduction of oxidative stress, increased astrocyte reactivity and a modification of inflammation with notably *il-4rα* gene expression increased. These changes were paralleled with a modest reduction of neuronal damage, suggesting a neuroprotective effect of these modifications. However, the modest nature of the neuroprotection would suggest that Nrf2 may need to be targeted in other cell types (Liddell, 2017) or in combinations with other neuroprotective targets for a more effective stroke treatment (Molcho et al., 2018).

The neuroprotective effects of Nrf2 are mainly observed in thalamus, hypothalamus and hippocampus. From the data collected in the previous chapter, these regions were injured following 60 minutes of occlusion but not 30 minutes ischaemia. Taken together, it suggests a role of Nrf2 overexpression in astrocytes in the containment of the lesion extension via a modification of inflammation/glial response and a reduction of oxidative stress.

In the third chapter, Nrf2 overexpression in astrocytes did not modify neuronal damage and oxidative stress in the chronic response to ischaemia. The neuroprotective effect of Nrf2 after ischaemia reported in the literature was mostly achieved using pharmacological activators with off-target effects (Abed et al., 2015; Magesh et al., 2012) and with a global effect on different cells. It appears that Nrf2 activation in astrocytes is known and thought as sufficient to induce neuroprotection (Shih et al., 2003). However, in regard of the findings of this chapter, boosting Nrf2 in other cells may be key. Nrf2 has protectant and anti-inflammatory

effects on endothelial cells notably (Chen et al., 2006; Jyrkkänen et al., 2008; Zakkar et al., 2009) and a statement about modulating microglial phenotype by boosting microglial Nrf2.

Interestingly, GFAP-Nrf2 mice had decreased discrimination at 4 weeks after ischaemia compared to their wild-type littermates, and this finding was not associated with increased neuronal damage. This discrepancy can be explained by different part of the brain underlying this behaviour. Other tests could be developed to encompass the spectrum of behavioural disorders observed after ischaemia such as nest building used to assess executive functions (Hase et al., 2017). It exists other protocols to the NOR that complexify the task by putting two different objects during the familiarisation or by doing two habituation sessions with different objects (Asiminas et al., 2019).

There is potential detrimental role of Nrf2 and its activation notably for cancer, cardiomyopathy and reductive stress (Kensler & Wakabayashi, 2010; Hayes & McMahon, 2009; Dodson et al., 2015; Kannan et al., 2013; Loboda et al., 2016). In the brain, HO1 expression can be linked to mitochondrial damage (Schipper et al., 2019); inflammation and impaired learning in an AD model (Li et al., 2015; Si et al., 2018; Gupta et al., 2014); and trauma-induced neuronal damage, decreased necrosis and oedema in a cerebral hypoperfusion model (Kadoya et al., 1995; Panizzon et al., 1996). However, in chapter 5, HO1 is not significantly upregulated in GFAP-Nrf2 mice compared to wild-types after ischaemia, suggesting that the detrimental effect of Nrf2 is somewhere else. Nrf2 is repressed early in cortical neurons because redox signalling pathways are critical for their development and synaptogenesis. Forced Nrf2 expression in neurons during the early days of development led to reduced synapses, retarded electrophysiological maturation and outgrowth of dendritic arborescence (Bell et al., 2015). This result suggests a homeostatic mechanism that regulates Nrf2. Detrimental effect of Nrf2 overexpression in astrocytes observed in the NOR could be explained by an overwhelming antioxidant production as basal level maintenance of ROS is important for homeostasis (Angelova & Abramov, 2018; Ye et al., 2015). Furthermore, ROS are essential for vascular homeostasis and function, immune response, haematopoiesis (Vara & Pula, 2014). These results are a reminder that redox signalling pathways play critical biological functions and that sustained activation of the Nrf2 pathway may have detrimental effects.

Ischaemia	Survival/ reperfusion	Genotype	Lesion	Oxidative Stress	Astrocytes	Microglia	Cytokines/ Chemokines	Nrf2-signalling
60 min	24 hours	WT	Striatum/Cortex	130% of lesion	Astrocytosis	Microgliosis	Every studied genes upregulated	HO1 prot. upregulated, genes to baseline (cortex peri-infarct)
		GFAP-Nrf2	Reduction	103% of lesion	+	Equal to WT	*cxcl10* and *il-4ra* further upregulated	HO1 prot. further upregulated and genes upregulated
15 min	4 weeks	WT	Striatum	~ 100%	Glial Scar	Glial Scar	Every studied genes upregulated	Genes to baseline (striatum)
		GFAP-Nrf2	Equal to WT	Equal to WT	Equal to WT	+	*c3* gene downregulated	Genes upregulated (striatum)

Table 6-1 Main results from chapter 4 and chapter 5 following ischaemia for wild-type and GFAP-Nrf2 animals.

Furthermore, this study of astrocytic overexpression of Nrf2 showed interaction of astrocytes with microglia and neurons. In the chapter 4, astrocytic overexpression in astrocytes reduced neuronal damage. In the chapter 5, astrocytic overexpression in astrocytes increased microglia/macrophage marker Iba1. This interaction also impacts on inflammatory modulation. In chapter 4, *cxcl10* and *il-4rα* were upregulated in GFAP-Nrf2 animals compared to wild-types following ischaemia. In chapter 5, pro-inflammatory *c3* gene expression was decreased and microglia/macrophages reactivity was increased. It was previously shown that Nrf2 had anti-inflammatory properties, notably by modulating cytokines and leading microglial phenotypes transformation (Kadl et al., 2010; Kobayashi et al., 2016; Liu et al., 2019; Liu et al., 2017; Naito et al., 2014; Peng et al., 2016). This thesis reinforced that theory with opening new understanding in which astrocytes interact with their neighbouring cells and on Nrf2 modulation of inflammation.

The protocol used in this thesis required an occlusion of the common carotid artery (UCCAo), mixing global and focal ischaemia (Liu & Mccullough, 2011). Therefore, the sham procedure underwent permanent UCCAo. In the chapter 4, sham model UCCAo on GFAP-Nrf2 mice had increased astrocyte marker GFAP immunostaining %area compared to sham wild-types. In chapter 5, GFAP-Nrf2 animals with UCCAo performed poorly on cognitive task compared to their wild-type littermates. In the last decade, growing interest on this method linked it to vascular cognitive impairment (Nishino et al., 2016; Silva et al., 2015; Zhao et al., 2014; Zuloaga et al., 2015). This model induces a reduction in blood flow (Tajima et al., 2014; Urushihata et al., 2018; Zuloaga et al., 2015) and that potentially lead to astrocytic response that was exacerbated in GFAP-Nrf2 mice, and to reduced performance on the NOR.

The results in chapter 4 and 5 showed an important discrepancy (Table 6.1). The severity of the injury as well as the survival times are the possible main causes to these discrepancies.

The mechanism underlying this difference could be guided by the heterogeneity of astrocytes and microglia observed in differential disease models, anatomical areas and injuries (astrocytes: Anderson et al., 2014; Lin et al., 2017; Liddelow & Barres, 2017; Pekny et al., 2016; Zamanian et al., 2012; microglia: Böttcher et al., 2019; Masuda et al., 2019). As glia and their response can differ depending on the area observed or the injury caused, it might have led to differential response in these chapters.

Interestingly, the literature on insulin resistance and carcinogenesis open a controversy as different methods lead to different conclusions on the account of protective or detrimental effects of Nrf2. Nrf2 knockout had the same beneficial effect as Nrf2 activation in insulin resistance (Fu et al., 2016; Seo & Lee, 2013). In the same way, Nrf2 inhibition and Nrf2 hyperactivation were both detrimental for carcinogenesis (Jiang et al., 2010; Kensler & Wakabayashi, 2010; Zhang et al., 2010). These discrepancies were born from diverse methods, and thus a simple conclusion is difficult to draw. These results first suggest that boosting or activating Nrf2-signalling require a control as an excessive upregulation could be detrimental. Secondly, that Nrf2 results may produce discrepancies between methods, and that a clearer understanding is needed in this regard.

MCAo duration	**60 minutes**	**15 minutes**
Survival	**24 hours**	**4 weeks**
neuroprotection	modest	none
oxidative stress	reduced	equal
GFAP expression	increased	equal
Iba1 expression	equal	increased
IL-4ra mRNA	increased	equal
CXCL10 mRNA	increased	equal
C3 mRNA	equal	decreased

Table 6-2 Main discrepancies between chapter 4 and chapter 5 following ischaemia comparing GFAP-Nrf2 to wild-type animals.

For each experiment, the result is the comparison of Nrf2 overexpression in astrocytes with wild-type animals following ischaemia. In black is shown that GFAP-Nrf2 animals had similar results to the wild-types. In red are noted the significant differences between GFAP-Nrf2 animals and wild-types.

6.2. Limitations and future directions

The different pieces of work of this thesis have highlighted several limitations of the experiments.

For most of this study, cortex and striatum were studied but further studies should be focused on the white matter, thalamus, hypothalamus and hippocampus. These brain regions are especially important because the neuroprotective effects found in the chapter 4 seemed to occur in the caudal part of the brain with thalamus and hypothalamus. A study designed to include these additional anatomical regions of interest could inform on the heterogeneity of neurons, microglia and astrocytes throughout the brain, with the impact of Nrf2 beneficial effect depending on this heterogeneity.

In this work, spatial differences were found (peri-infarct *versus* core) for a same time point. *In situ* hybridisation could be developed to get further insight of the inflammatory modulation and of the Nrf2-signalling activation that is better studied looking at downstream gene expression. An alternative could be to collect and analyse the different areas underlying ischaemic pathology. Furthermore, histology techniques are now developed to gain sensitivity, looking for more specific markers for the different function of microglia, for the different subtypes of astrocytes, for the different pro- and anti-inflammatory phenotypes (Cahoy et al., 2008; Franco-Bocanegra et al., 2019; Hammond et al., 2019). It could be hypothesised that Nrf2 can modify glial phenotypes in different ways depending on the area of the lesion, or the anatomical region involved.

Inflammation was characterised using a few markers and these genes were not analysed with cell-specific methods. In the same way, oxidative stress was analysed using only one antibody. Due to the heterogeneity of astrocytes and microglia, more genes could be analysed, but also a single-cell approach would greatly reduce possible confusion as most cytokines are produced by a multitude of cells. Ideally, RNA-sequencing of fluorescent-associated cell sorting are to date the best techniques to give more detailed overview of inflammation (Frigerio et al., 2019; Liddelow et al., 2017; Anderson et al., 2014; Boisvert et al., 2018). The Nrf2/HO1 pathway is related to an anti-inflammatory response (Rojo et al., 2010; Kobayashi et al., 2016; Liu et al., 2017; Peng et al., 2016; Liu et al., 2019) and linked to specific modulation of microglia/macrophage phenotypes but their transcriptional signature has not been defined yet (Boyle et al., 2012; Kadl et al., 2010; Naito et al., 2014).

The magnitude of difference between chapter 4 and 5 in the result is of importance. It would be interesting to study GFAP-Nrf2 mice 24 hours after 15 minutes ischaemia and 4 weeks after 60 minutes ischaemia. Furthermore, there was an improvement in the neuroscore for GFAP-Nrf2 mice at 7 days after 15 minutes ischaemia compared to wild-types. It would be interesting to further study this time point by collecting some brains and analyse cellular and molecular differences in between these genotypes. There is potentially an effect of both the severity and the survival, but also of the area. As seen in chapter 3, increased duration led to increased pathology features. Furthermore, ischaemia unfolds a cascade of many features that evolve through time.

Finally, new techniques in magnetic resonance imaging (MRI) and positron-emission tomography (PET) have provided important *in vivo* insight and allow for temporal follow up of inflammation, blood flow, lesion and penumbra. In addition, *in vivo* imaging using multi-photon microscopy is an important research field and provide increasing studies on temporal evolution of any disease model and cellular response (Wu et al., 2017).

Cerebral ischaemia occurs for 95% of cases in individuals aged 45-years old or older (Grau et al., 2001). However, aged animals are frail and following severe procedures like ischaemia there are increased levels of mortality and technical difficulties, furthermore maintenance and care of these animals is expensive. Thus, research on elder animals is difficult and mainly done on young animals. This bias limit translations from preclinical to clinical research. Aged animals have reduced Nrf2 signalling (Suh et al., 2004; Zhang et al., 2015) and in case of ischaemia have increased oxidative stress (Buga et al., 2008; Li et al., 2005; Roberts et al., 1997; Sieber et al., 2014; Zhang et al., 2018) and inflammation (Badan et al., 2003; DiNapoli et al., 2008; Manwani et al., 2011; Popa-Wagner et al., 2007; Sieber et al., 2011; Sieber et al., 2014; Titova et al., 2011) worsening ischaemic damage in most cases (DiNapoli et al., 2008; Doyle et al., 2012; Manwani et al., 2011; Nguyen et al., 2018; Popa-Wagner et al., 2007). In this scope, Nrf2 activation following ischaemia on older animals may have a potential beneficial effect. However, it is limited by the long list of comorbidities found on old ischaemic patient, such as diabetes, cancer, coronary diseases, hypertension, obesity and cardiac diseases. As explained previously, Nrf2 is potentially detrimental in diabetes and cardiac myopathy. Thus, therapeutic use of Nrf2-signalling pathway activation for ischaemic patient will have to be controlled and reviewed with comorbidity cases. Pharmacological compounds that target Nrf2 in the brain will have effects on all organs in the body.

Interestingly, Nrf2-overexpression in astrocytes caused increased levels of the microglia/macrophage marker Iba1 at 4 weeks. This result suggests a possible interplay between the different glial cells. New studies have emerged with the single-cell dimension, giving cell-specific modification (Frigerio et al., 2019; Hammond et al., 2019; Liddelow et al., 2017). As this piece of work gave differential effect of Nrf2-overexpression in astrocytes, the next step would be to gain further understanding in the cell mechanisms at stake using these single-cell methods such as fluorescent-associated cell sorting.

In order to further study the modulation of inflammation seen in this piece of work, cell-specific analysis could be done using fluorescent-associated cell sorting (FACs) method or by tagging and sorting cells using TRAP-BAC mice models. As many genes are modified by ischaemia, in the inflammation cascade or around the Nrf2-signalling pathway, RNA-sequencing method would give a better understanding of the molecular pathways involved.

Nrf2 overexpression in astrocytes is known for its protective effects on diverse neurodegenerative conditions (Calkins et al., 2010; Chen et al., 2009; Gan et al., 2012; LaPash Daniels et al., 2012; Sigfridsson et al., 2018; Vargas et al., 2008). However, Nrf2 activation in multiple cell types seems to be important to achieve protection for other pathologies (Liddell, 2017). This would explain that the neuroprotective effect found in the chapter 4 was modest and that there was no neuroprotection in the chapter 5. Beneficial effects of Nrf2-signalling activation after ischaemia have been demonstrated using pharmacological compounds that possibly have Nrf2-independent effects on are on a global multi-cells scale (Thomas W Kensler & Wakabayashi, 2010; O'Mealey et al., 2017; Schulze-Topphoff et al., 2016; Zagorski et al., 2017). Coupling Nrf2-signalling activation with other drugs targeting other protective pathways might be key to achieving a drastic reduction of neuronal damage (Molcho et al., 2018).

7. References

Abbott, A. L., Silvestrini, M., Topakian, R., Golledge, J., Brunser, A. M., de Borst, G. J., … Wardlaw, J. M. (2017). Optimizing the Definitions of Stroke, Transient Ischemic Attack, and Infarction for Research and Application in Clinical Practice. *Frontiers in Neurology*, *8*, 537. https://doi.org/10.3389/fneur.2017.00537

Abed, D. A., Goldstein, M., Albanyan, H., Jin, H., & Hu, L. (2015). Discovery of direct inhibitors of Keap1-Nrf2 protein-protein interaction as potential therapeutic and preventive agents. *Acta Pharmaceutica Sinica B*, *5*(4), 285–299. https://doi.org/10.1016/j.apsb.2015.05.008

Abiko, Y., Miura, T., Phuc, B. H., Shinkai, Y., & Kumagai, Y. (2011). Participation of covalent modification of Keap1 in the activation of Nrf2 by tert-butylbenzoquinone, an electrophilic metabolite of butylated hydroxyanisole. *Toxicology and Applied Pharmacology*, *255*(1), 32–39. https://doi.org/10.1016/J.TAAP.2011.05.013

Aguilar-Navarro, S. G., Mimenza-Alvarado, A. J., Anaya-Escamilla, A., & Gutiérrez-Robledo, L. M. (2016). Frailty and Vascular Cognitive Impairment: Mechanisms Behind the Link. *Revista de Investigacion Clinica; Organo Del Hospital de Enfermedades de La Nutricion*, *68*(1), 25–32.

Ahlgren-Beckendorf, J. A., Reising, A. M., Schander, M. A., Herdler, J. W., & Johnson, J. A. (1999). Coordinate regulation of NAD(P)H:Quinone oxidoreductase and glutathione-S-transferases in primary cultures of rat neurons and glia: Role of the antioxidant/electrophile responsive element. *Glia*, *25*(2), 131–142. https://doi.org/10.1002/(SICI)1098-1136(19990115)25:2<131::AID-GLIA4>3.0.CO;2-6

Ahuja, X. M., Kaidery, N. A., Yang, L., Calingasan, N., Smirnova, N., Gaisin, A., … Thomas, B. (2016). Distinct Nrf2 Signaling Mechanisms of Fumaric Acid Esters and Their Role in Neuroprotection against 1-Methyl-4- Parkinson ' s-Like Disease. *The Journal of Neuroscience*, *36*(23), 6332–6351. https://doi.org/10.1523/JNEUROSCI.0426-16.2016

Akaji, K., Suga, S., Fujino, T., Mayanagi, K., Inamasu, J., Horiguchi, T., … Kawase, T. (2003). Effect of intra-ischemic hypothermia on the expression of c-Fos and c-Jun, and DNA binding activity of AP-1 after focal cerebral ischemia in rat brain. *Brain Research*, *975*(1–2), 149–157. Retrieved from http://www.ncbi.nlm.nih.gov/pubmed/12763603

Akbar, M., Essa, M. M., Daradkeh, G., Abdelmegeed, M. A., Choi, Y., Mahmood, L., & Song, B.-J. (2016). Mitochondrial dysfunction and cell death in neurodegenerative diseases through nitroxidative stress. *Brain Research*, *1637*, 34–55. https://doi.org/10.1016/J.BRAINRES.2016.02.016

Akinyemi, R. O., Owolabi, M. O., Ihara, M., Damasceno, A., Ogunniyi, A., Dotchin, C., … Kalaria, R. N. (2019). Stroke, cerebrovascular diseases and vascular cognitive impairment in Africa. *Brain Research Bulletin*, *145*(April 2018), 97–108. https://doi.org/10.1016/j.brainresbull.2018.05.018

Alachkar, A., Khan, N., Łażewska, D., Kieć-Kononowicz, K., & Sadek, B. (2019). Histamine H3 receptor antagonist E177 attenuates amnesia induced by dizocilpine without modulation of anxiety-like behaviors in rats. *Neuropsychiatric Disease and Treatment*, *15*, 531–542. https://doi.org/10.2147/NDT.S193125

Alam, J., Stewart, D., Touchard, C., Boinapally, S., Choi, A. M., & Cook, J. L. (1999). Nrf2, a Cap'n'Collar transcription factor, regulates induction of the heme oxygenase-1 gene. *The Journal of Biological Chemistry*, *274*(37), 26071–26078. https://doi.org/10.1074/JBC.274.37.26071

Alaoui-Jamali, M. A., Bismar, T. A., Gupta, A., Szarek, W. A., Su, J., Song, W., … Schipper, H. M. (2009). A novel experimental heme oxygenase-1-targeted therapy for hormone-

refractory prostate cancer. *Cancer Research*, *69*(20), 8017–8024. https://doi.org/10.1158/0008-5472.CAN-09-0419

Alawieh, A., Elvington, A., Zhu, H., Yu, J., Kindy, M. S., Atkinson, C., & Tomlinson, S. (2015). Modulation of post-stroke degenerative and regenerative processes and subacute protection by site-targeted inhibition of the alternative pathway of complement. *Journal of Neuroinflammation*, *12*(1), 247. https://doi.org/10.1186/s12974-015-0464-8

Alawieh, A., Farris Langley, E., & Tomlinson, S. (2018). Targeted complement inhibition salvages stressed neurons and inhibits neuroinflammation after stroke in mice. *Science Translational Medicine*, *10*(441), 1–14. https://doi.org/10.1126/scitranslmed.aao6459

Albers, G. W., Marks, M. P., Kemp, S., Christensen, S., Tsai, J. P., Ortega-Gutierrez, S., … Lansberg, M. G. (2018). Thrombectomy for Stroke at 6 to 16 Hours with Selection by Perfusion Imaging. *New England Journal of Medicine*, *378*(8), 708–718. https://doi.org/10.1056/NEJMoa1713973

Alexandrova, M. L., & Bochev, P. G. (2005). Oxidative stress during the chronic phase after stroke. *Free Radical Biology and Medicine*, *39*(3), 297–316. https://doi.org/10.1016/j.freeradbiomed.2005.04.017

Alexandrova, M. L., Bochev, P. G., Markova, V. I., Bechev, B. G., Popova, M. A., Danovska, M. P., & Simeonova, V. K. (2003). Oxidative stress in the chronic phase after stroke. *Redox Report*, *8*(3), 169–176. https://doi.org/10.1179/135100003225001548

Alfieri, A., Srivastava, S., Siow, R. C. M., Cash, D., Modo, M., Duchen, M. R., … Mann, G. E. (2013). Sulforaphane preconditioning of the Nrf2/HO-1 defense pathway protects the cerebral vasculature against blood-brain barrier disruption and neurological deficits in stroke. *Free Radical Biology and Medicine*, *65*, 1012–1022. https://doi.org/10.1016/j.freeradbiomed.2013.08.190

Allen, C. L., & Bayraktutan, U. Risk for Ischaemic stroke, 3 International Journal of Stroke § (2008). SAGE PublicationsSage UK: London, England. https://doi.org/10.1111/j.1747-4949.2008.00187.x

Alzheimer, A. (1910). Die diagnostischen Schwierigkeiten in der Psychiatric. *Zeitschrift Für Die Gesamte Neurologie Und Psychiatrie*, *1*(1), 1–19. https://doi.org/10.1007/BF02895916

Amantea, D., Greco, R., Micieli, G., & Bagetta, G. (2018). Paradigm Shift to Neuroimmunomodulation for Translational Neuroprotection in Stroke. *Frontiers in Neuroscience*, *12*, 241. https://doi.org/10.3389/fnins.2018.00241

Amantea, D., Micieli, G., Tassorelli, C., Cuartero, M. I., Ballesteros, I., Certo, M., … Bagetta, G. (2015). Rational modulation of the innate immune system for neuroprotection in ischemic stroke. *Frontiers in Neuroscience*, *9*, 147. https://doi.org/10.3389/fnins.2015.00147

Amaro, S., Llull, L., Renú, A., Laredo, C., Perez, B., Vila, E., … Chamorro, Á. (2015). Uric acid improves glucose-driven oxidative stress in human ischemic stroke. *Annals of Neurology*, *77*(5), 775–783. https://doi.org/10.1002/ana.24378

Ameyar, M., Wisniewska, M., & Weitzman, J. B. (2003). A role for AP-1 in apoptosis: the case for and against. *Biochimie*, *85*(8), 747–752. https://doi.org/10.1016/j.biochi.2003.09.006

Andersen, K. K., Andersen, Z. J., & Olsen, T. S. (2010). Age- and gender-specific prevalence of cardiovascular risk factors in 40 102 patients with first-ever ischemic stroke: A Nationwide Danish Study. *Stroke*, *41*(12), 2768–2774. https://doi.org/10.1161/STROKEAHA.110.595785

Anderson, M. A., Ao, Y., & Sofroniew, M. V. (2014). Heterogeneity of reactive astrocytes. *Neuroscience Letters*, *565*, 23–29. https://doi.org/10.1016/j.neulet.2013.12.030

Anderson, M. A., Burda, J. E., Ren, Y., Ao, Y., O'Shea, T. M., Kawaguchi, R., … Sofroniew, M. V. (2016). Astrocyte scar formation aids central nervous system axon regeneration.

Nature, *532*(7598), 195–200. https://doi.org/10.1038/nature17623

Angelova, P. R., & Abramov, A. Y. (2018). Role of mitochondrial ROS in the brain: from physiology to neurodegeneration. *FEBS Letters*, *592*(5), 692–702. https://doi.org/10.1002/1873-3468.12964

Anrather, J., & Iadecola, C. (2016). Inflammation and Stroke: An Overview. *Neurotherapeutics*, *13*(4), 661–670. https://doi.org/10.1007/s13311-016-0483-x

Antunes, M., & Biala, G. (2012). The novel object recognition memory: neurobiology, test procedure, and its modifications. *Cognitive Processing*, *13*(2), 93–110. https://doi.org/10.1007/s10339-011-0430-z

Aroor, S., Singh, R., & Goldstein, L. B. (2017). BE-FAST (Balance, Eyes, Face, Arm, Speech, Time): Reducing the Proportion of Strokes Missed Using the FAST Mnemonic. *Stroke*, *48*(2), 479–481. https://doi.org/10.1161/STROKEAHA.116.015169

Asiminas, A., Jackson, A. D., Louros, S. R., Till, S. M., Spano, T., Dando, O., … Kind, P. C. (2019). Sustained correction of associative learning deficits after brief, early treatment in a rat model of Fragile X Syndrome. *Science Translational Medicine*, *11*(494), eaao0498. https://doi.org/10.1126/scitranslmed.aao0498

Association, S. (2018). *State of the nation: Stroke statistics - Februrary 2018*. Retrieved from https://www.stroke.org.uk/system/files/sotn_2018.pdf

Astrup, J., Siesjö, B. K., & Symon, L. (1981). Thresholds in cerebral ischemia - the ischemic penumbra. *Stroke*, *12*(6), 723–725. https://doi.org/10.1161/01.STR.12.6.723

Atef, R. M., Agha, A. M., Abdel-Rhaman, A.-R. A., & Nassar, N. N. (2018). The Ying and Yang of Adenosine A1 and A2A Receptors on ERK1/2 Activation in a Rat Model of Global Cerebral Ischemia Reperfusion Injury. *Molecular Neurobiology*, *55*(2), 1284–1298. https://doi.org/10.1007/s12035-017-0401-1

Avila-Muñoz, E., & Arias, C. (2014). When astrocytes become harmful: Functional and inflammatory responses that contribute to Alzheimer's disease. *Ageing Research Reviews*, *18*, 29–40. https://doi.org/10.1016/j.arr.2014.07.004

Bachetti, T., Di Zanni, E., Balbi, P., Ravazzolo, R., Sechi, G., & Ceccherini, I. (2012). Beneficial effects of curcumin on GFAP filament organization and down-regulation of GFAP expression in an in vitro model of Alexander disease. *Experimental Cell Research*, *318*(15), 1844–1854. https://doi.org/10.1016/J.YEXCR.2012.06.008

Bachiller, S., Jiménez-Ferrer, I., Paulus, A., Yang, Y., Swanberg, M., Deierborg, T., & Boza-Serrano, A. (2018). Microglia in Neurological Diseases: A Road Map to Brain-Disease Dependent-Inflammatory Response. *Frontiers in Cellular Neuroscience*, *12*, 488. https://doi.org/10.3389/fncel.2018.00488

Badan, I., Buchhold, B., Hamm, A., Gratz, M., Walker, L. C., Platt, D., … Popa-Wagner, A. (2003). Accelerated Glial Reactivity to Stroke in Aged Rats Correlates With Reduced Functional Recovery. *Journal of Cerebral Blood Flow & Metabolism*, *23*, 845–854. https://doi.org/10.1097/01.WCB.0000071883.63724.A7

Baek, J. M., Yoon, W., Kim, S. K., Jung, M. Y., Park, M. S., Kim, J. T., & Kang, H. K. (2014). Acute basilar artery occlusion: outcome of mechanical thrombectomy with Solitaire stent within 8 hours of stroke onset. *AJNR. American Journal of Neuroradiology*, *35*(5), 989–993. https://doi.org/10.3174/ajnr.A3813

Balkaya, M., Kröber, J. M., Rex, A., Endres, M., Krö Ber, J. M., Rex, A., … Endres, M. (2013). Assessing post-stroke behavior in mouse models of focal ischemia. *Journal of Cerebral Blood Flow and Metabolism : Official Journal of the International Society of Cerebral Blood Flow and Metabolism*, *33*(3), 330–338. https://doi.org/10.1038/jcbfm.2012.185

Banjac, A., Perisic, T., Sato, H., Seiler, A., Bannai, S., Weiss, N., … Bornkamm, G. W. (2008). The cystine/cysteine cycle: a redox cycle regulating susceptibility versus resistance to cell death. *Oncogene*, *27*(11), 1618–1628. https://doi.org/10.1038/sj.onc.1210796

Bano, D., & Ankarcrona, M. (2018). Beyond the critical point: An overview of excitotoxicity, calcium overload and the downstream consequences. *Neuroscience Letters*, *663*, 79–85. Retrieved from https://www.sciencedirect.com/science/article/pii/S030439401730695X?via%3Dihub#fig0010

Barbay, M., Taillia, H., Nédélec-Ciceri, C., Bompaire, F., Bonnin, C., Varvat, J., … GRECOG-VASC Study Group. (2018). Prevalence of Poststroke Neurocognitive Disorders Using National Institute of Neurological Disorders and Stroke-Canadian Stroke Network, VASCOG Criteria (Vascular Behavioral and Cognitive Disorders), and Optimized Criteria of Cognitive Deficit. *Stroke*, *49*(5), 1141–1147. https://doi.org/10.1161/STROKEAHA.117.018889

Barcellos-Hoff, M. H., & Dix, T. A. (1996). Redox-mediated activation of latent transforming growth factor-beta 1. *Molecular Endocrinology*, *10*(9), 1077–1083. https://doi.org/10.1210/mend.10.9.8885242

Bardehle, S., Krüger, M., Buggenthin, F., Schwausch, J., Ninkovic, J., Clevers, H., … Götz, M. (2013). Live imaging of astrocyte responses to acute injury reveals selective juxtavascular proliferation. *Nature Neuroscience*, *16*(5), 580–586. https://doi.org/10.1038/nn.3371

Baron, J.-C. (2018). Protecting the ischaemic penumbra as an adjunct to thrombectomy for acute stroke. *Nature Reviews Neurology 2018*, *14*, 325–337. https://doi.org/10.1038/s41582-018-0002-2

Barone, F. C., Knudsen, D. J., Nelson, a H., Feuerstein, G. Z., & Willette, R. N. (1993). Mouse strain differences in susceptibility to cerebral ischemia are related to cerebral vascular anatomy. *Journal of Cerebral Blood Flow and Metabolism : Official Journal of the International Society of Cerebral Blood Flow and Metabolism*, *13*(4), 683–692. https://doi.org/10.1038/jcbfm.1993.87

Barreto, G. E., Sun, X., Xu, L., & Giffard, R. G. (2011). Astrocyte proliferation following stroke in the mouse depends on distance from the infarct. *PloS One*, *6*(11), e27881. https://doi.org/10.1371/journal.pone.0027881

Barreto, G. E., White, R. E., Ouyang, Y., Xu, L., & Giffard, R. G. (2011). Astrocytes: targets for neuroprotection in stroke. *Central Nervous System Agents in Medicinal Chemistry*, *11*(2), 164–173. https://doi.org/10.2174/187152411796011303

Baxter, P. S., & Hardingham, G. E. (2016a). Adaptive regulation of the brain's antioxidant defences by neurons and astrocytes. *Free Radical Biology and Medicine*, *100*, 147–152. https://doi.org/10.1016/j.freeradbiomed.2016.06.027

Baxter, P. S., & Hardingham, G. E. (2016b). Adaptive regulation of the brain's antioxidant defences by neurons and astrocytes. *Free Radical Biology and Medicine*, *100*, 147–152. https://doi.org/10.1016/j.freeradbiomed.2016.06.027

Becerra-Calixto, A., & Cardona-Gómez, G. P. (2017). The Role of Astrocytes in Neuroprotection after Brain Stroke: Potential in Cell Therapy. *Frontiers in Molecular Neuroscience*, *10*(April), 1–12. https://doi.org/10.3389/fnmol.2017.00088

Becerril-Ortega, J., Bordji, K., Fréret, T., Rush, T., & Buisson, A. (2014). Iron overload accelerates neuronal amyloid-β production and cognitive impairment in transgenic mice model of Alzheimer's disease. *Neurobiology of Aging*, *35*(10), 2288–2301. https://doi.org/10.1016/J.NEUROBIOLAGING.2014.04.019

Beckman, J. S. (1991). The double-edged role of nitric oxide in brain function and superoxide-mediated injury. *Journal of Developmental Physiology*, *15*(1), 53–59. Retrieved from http://www.ncbi.nlm.nih.gov/pubmed/1678755

Béjot, Y., & Giroud, M. Stroke in diabetic patients, 36 Diabetes & Metabolism § (2010). https://doi.org/10.1016/S1262-3636(10)70472-9

Bell, K. F., Al-Mubarak, B., Fowler, J. H., Baxter, P. S., Gupta, K., Tsujita, T., … Hardingham, G. E. (2011). Mild oxidative stress activates Nrf2 in astrocytes, which contributes to neuroprotective ischemic preconditioning. *Proceedings of the National Academy of Sciences of the United States of America*, *108*(1), E1-2; author reply E3-4. https://doi.org/10.1073/pnas.1015229108

Bell, K. F., Al-Mubarak, B., Martel, M.-A., McKay, S., Wheelan, N., Hasel, P., … Hardingham, G. E. (2015). Neuronal development is promoted by weakened intrinsic antioxidant defences due to epigenetic repression of Nrf2. *Nature Communications*, *6*(May), 7066. https://doi.org/10.1038/ncomms8066

Bell, K. F. S., Fowler, J. H., Al-Mubarak, B., Horsburgh, K., & Hardingham, G. E. (2011). Activation of Nrf2-regulated glutathione pathway genes by ischemic preconditioning. *Oxidative Medicine and Cellular Longevity*, *2011*. https://doi.org/10.1155/2011/689524

Benakis, C., Garcia-Bonilla, L., Iadecola, C., & Anrather, J. (2015). The role of microglia and myeloid immune cells in acute cerebral ischemia. *Frontiers in Cellular Neuroscience*, *8*(January), 1–16. https://doi.org/10.3389/fncel.2014.00461

Bennett, M. L., Bennett, F. C., Liddelow, S. A., Ajami, B., Zamanian, J. L., Fernhoff, N. B., … Barres, B. A. (2016). New tools for studying microglia in the mouse and human CNS. *Proceedings of the National Academy of Sciences of the United States of America*, *113*(12), E1738-46. https://doi.org/10.1073/pnas.1525528113

Bennett, S., Grant, M. M., & Aldred, S. (2008). Oxidative Stress in Vascular Dementia and Alzheimer's Disease: A Common Pathology. *Journal of Alzheimer's Disease*, *17*(2), 245–257. https://doi.org/10.3233/JAD-2009-1041

Bergeron, M., Ferriero, D. M., Vreman, H. J., Stevenson, D. K., & Sharp, F. R. (1997). Hypoxia-ischemia, but not hypoxia alone, induces the expression of heme oxygenase-1 (HSP32) in newborn rat brain. *Journal of Cerebral Blood Flow and Metabolism : Official Journal of the International Society of Cerebral Blood Flow and Metabolism*, *17*(6), 647–658. https://doi.org/10.1097/00004647-199706000-00006

Berlyne, D. E. (1950). Novelty and curiosity as determinants of exploratory behaviour. *British Journal of Psychology. General Section*, *41*(1–2), 68–80. https://doi.org/10.1111/j.2044-8295.1950.tb00262.x

Bhatia, T. N., Pant, D. B., Eckhoff, E. A., Gongaware, R. N., Do, T., Hutchison, D. F., … Leak, R. K. (2019). Astrocytes Do Not Forfeit Their Neuroprotective Roles After Surviving Intense Oxidative Stress. *Frontiers in Molecular Neuroscience*, *12*, 87. https://doi.org/10.3389/fnmol.2019.00087

Biber, K., Dijkstra, I., Trebst, C., De Groot, C. J. ., Ransohoff, R. ., & Boddeke, H. W. G. . (2002). Functional expression of CXCR3 in cultured mouse and human astrocytes and microglia. *Neuroscience*, *112*(3), 487–497. https://doi.org/10.1016/S0306-4522(02)00114-8

Boche, D., Perry, V. H., & Nicoll, J. A. R. (2013). Review: Activation patterns of microglia and their identification in the human brain. *Neuropathology and Applied Neurobiology*, *39*(1), 3–18. https://doi.org/10.1111/nan.12011

Boehme, A. K., Esenwa, C., Elkind, M. S. V, Fisher, M., Iadecola, C., & Sacco, R. (2017). Stroke Risk Factors, Genetics, and Prevention. *Circulation Research*, *120*(3), 472–495. https://doi.org/10.1161/CIRCRESAHA.116.308398

Bogaert, L., Scheller, D., Moonen, J., Sarre, S., Smolders, I., Ebinger, G., & Michotte, Y. (2000). Neurochemical changes and laser Doppler flowmetry in the endothelin-1 rat model for focal cerebral ischemia. *Brain Research*, *887*(2), 266–275. Retrieved from http://www.ncbi.nlm.nih.gov/pubmed/11134615

Boisvert, M. M., Erikson, G. A., Shokhirev, M. N., Allen, N. J., Correspondence, N. J. A., Allen, N. J., & Correspondence, N. J. A. (2018). The Aging Astrocyte Transcriptome from Multiple Regions of the Mouse Brain. *Cell Reports*, *22*(1), 269–285.

https://doi.org/10.1016/j.celrep.2017.12.039
Bolaños, J. P., Heales, S. J. R., Peuchen, S., Barker, J. E., Land, J. M., & Clark, J. B. (1996). Nitric oxide-mediated mitochondrial damage: A potential neuroprotective role for glutathione. *Free Radical Biology and Medicine*, *21*(7), 995–1001. https://doi.org/10.1016/S0891-5849(96)00240-7
Böttcher, C., Schlickeiser, S., Sneeboer, M. A. M., Kunkel, D., Knop, A., Paza, E., … Priller, J. (2019). Human microglia regional heterogeneity and phenotypes determined by multiplexed single-cell mass cytometry. *Nature Neuroscience*, *22*(1), 78–90. https://doi.org/10.1038/s41593-018-0290-2
Boyko, M., Zlotnik, A., Gruenbaum, B. F., Gruenbaum, S. E., Ohayon, S., Goldsmith, T., … Teichberg, V. I. (2010). An experimental model of focal ischemia using an internal carotid artery approach. *Journal of Neuroscience Methods*, *193*(2), 246–253. https://doi.org/10.1016/J.JNEUMETH.2010.08.026
Boyle, J. J., Johns, M., Kampfer, T., Nguyen, A. T., Game, L., Schaer, D. J., … Haskard, D. O. (2012). Activating Transcription Factor 1 Directs Mhem Atheroprotective Macrophages Through Coordinated Iron Handling and Foam Cell Protection. *Circ Res*, *110*, 20–33. https://doi.org/10.1161/CIRCRESAHA.111.247577
Boztug, K., Carson, M. J., Pham-Mitchell, N., Asensio, V. C., DeMartino, J., & Campbell, I. L. (2002). Leukocyte infiltration, but not neurodegeneration, in the CNS of transgenic mice with astrocyte production of the CXC chemokine ligand 10. *Journal of Immunology (Baltimore, Md. : 1950)*, *169*(3), 1505–1515. https://doi.org/10.4049/JIMMUNOL.169.3.1505
Branston, N. M., Strong, A. J., & Symon, L. (1977). *Extracellular Potassium Activity, Evoked Potential And Tissue Blood Flow Relationships During Progressive Ischaemia in Baboon Cerebral Coltex*. *Journal of the Neurological Sciences* (Vol. 32). Elsevier. https://doi.org/10.1016/0022-510X(77)90014-4
Brenner, M., Johnson, A. B., Boespflug-Tanguy, O., Rodriguez, D., Goldman, J. E., & Messing, A. (2001). Mutations in GFAP, encoding glial fibrillary acidic protein, are associated with Alexander disease. *Nature Genetics*, *27*(1), 117–120. https://doi.org/10.1038/83679
Bronstein, D. M., Perez-Otano, I., Sun, V., Mullis Sawin, S. B., Chan, J., Wu, G.-C., … McMillian, M. K. (1995). Glia-dependent neurotoxicity and neuroprotection in mesencephalic cultures. *Brain Research*, *704*(1), 112–116. https://doi.org/10.1016/0006-8993(95)01189-7
Buchan, A. M., Xue, D., & Slivka, A. (1992). A new model of temporary focal neocortical ischemia in the rat. *Stroke*, *23*(2), 273–279. Retrieved from http://www.ncbi.nlm.nih.gov/pubmed/1561658
Buga, A.-M., Sascau, M., Pisoschi, C., Herndon, J. G., Kessler, C., & Popa-Wagner, A. (2008). The genomic response of the ipsilateral and contralateral cortex to stroke in aged rats. *Journal of Cellular and Molecular Medicine*, *12*(6b), 2731–2753. https://doi.org/10.1111/j.1582-4934.2008.00252.x
Burda, J. E., & Sofroniew, M. V. (2014). Reactive gliosis and the multicellular response to CNS damage and disease. *Neuron*, *81*(2), 229–248. https://doi.org/10.1016/j.neuron.2013.12.034
Bush, T. G., Puvanachandra, N., Horner, C. H., Polito, A., Ostenfeld, T., Svendsen, C. N., … Sofroniew, M. V. (1999). Leukocyte Infiltration, Neuronal Degeneration, and Neurite Outgrowth after Ablation of Scar-Forming, Reactive Astrocytes in Adult Transgenic Mice. *Neuron*, *23*(2), 297–308. https://doi.org/10.1016/S0896-6273(00)80781-3
Butovsky, O., & Weiner, H. L. (2018). Microglial signatures and their role in health and disease. *Nature Reviews Neuroscience*, *19*(10), 622–635. https://doi.org/10.1038/s41583-018-0057-5

Buttini, M., Sauter, A., & Boddeke, H. W. G. M. (1994). Induction of interleukin-1β mRNA after focal cerebral ischaemia in the rat. *Molecular Brain Research*, *23*(1–2), 126–134. https://doi.org/10.1016/0169-328X(94)90218-6

Bynum, J. A., Bowman, P. D., Rastogi, A., & Stavchansky, S. A. (2015). Cytoprotection of Human Endothelial Cells from Oxidant Stress with CDDO Derivatives : Network Analysis of Genes Responsible for Cytoprotection. *Pharmacology*, 181–192. https://doi.org/10.1159/000381188

Cahoy, J. D., Emery, B., Kaushal, A., Foo, L. C., Zamanian, J. L., Christopherson, K. S., … Barres, B. A. (2008). A Transcriptome Database for Astrocytes, Neurons, and Oligodendrocytes: A New Resource for Understanding Brain Development and Function. *Journal of Neuroscience*, *28*(1), 264–278. https://doi.org/10.1523/JNEUROSCI.4178-07.2008

Calabrese, V., Giordano, J., Signorile, A., Laura Ontario, M., Castorina, S., De Pasquale, C., … Calabrese, E. J. (2016). Major pathogenic mechanisms in vascular dementia: Roles of cellular stress response and hormesis in neuroprotection. *Journal of Neuroscience Research*, *94*(12), 1588–1603. https://doi.org/10.1002/jnr.23925

Calkins, M. J., Jakel, R. J., Johnson, D. A., Chan, K., Kan, Y. W., & Johnson, J. A. (2005). Protection from mitochondrial complex II inhibition in vitro and in vivo by Nrf2-mediated transcription. *Proceedings of the National Academy of Sciences*, *102*(1), 244–249. https://doi.org/10.1073/pnas.0408487101

Calkins, M. J., Vargas, M. R., Johnson, D. A., & Johnson, J. A. (2010). Astrocyte-Specific Overexpression of Nrf2 Protects Striatal Neurons from Mitochondrial Complex II Inhibition. *Toxicological Sciences*, *115*(2), 557–568. https://doi.org/10.1093/toxsci/kfq072

Campanella, G. S. V., Grimm, J., Manice, L. A., Colvin, R. A., Medoff, B. D., Wojtkiewicz, G. R., … Luster, A. D. (2006). Oligomerization of CXCL10 Is Necessary for Endothelial Cell Presentation and In Vivo Activity. *The Journal of Immunology*, *177*(10), 6991–6998. https://doi.org/10.4049/JIMMUNOL.177.10.6991

Caprio, S., Daniels, S. R., Drewnowski, A., Kaufman, F. R., Palinkas, L. A., Rosenbloom, A. L., & Schwimmer, J. B. (2008). Influence of race, ethnicity, and culture on childhood obesity: implications for prevention and treatment: a consensus statement of Shaping America's Health and the Obesity Society. *Diabetes Care*, *31*(11), 2211–2221. https://doi.org/10.2337/dc08-9024

Casimiro, I., Chinnasamy, P., & Sibinga, N. E. S. (2013). Genetic inactivation of the allograft inflammatory factor-1 locus. *Genesis (New York, N.Y. : 2000)*, *51*(10), 734–740. https://doi.org/10.1002/DVG.22424

Catorce, M. N., & Gevorkian, G. (2016). LPS-induced Murine Neuroinflammation Model: Main Features and Suitability for Pre-clinical Assessment of Nutraceuticals. *Current Neuropharmacology*, *14*(2), 155–164. Retrieved from http://www.ncbi.nlm.nih.gov/pubmed/26639457

Cekanaviciute, E., & Buckwalter, M. S. (2016). Astrocytes: Integrative Regulators of Neuroinflammation in Stroke and Other Neurological Diseases. *Neurotherapeutics*, *13*(4), 685–701. https://doi.org/10.1007/s13311-016-0477-8

Centers for Disease Control and Prevention (CDC). (2001). Prevalence of disabilities and associated health conditions among adults--United States, 1999. *MMWR. Morbidity and Mortality Weekly Report*, *50*(7), 120–125. Retrieved from http://www.ncbi.nlm.nih.gov/pubmed/11393491

Chai, Q., She, R., Huang, Y., & Fu, Z. F. (2015). Expression of Neuronal CXCL10 Induced by Rabies Virus Infection Initiates Infiltration of Inflammatory Cells, Production of Chemokines and Cytokines, and Enhancement of Blood-Brain Barrier Permeability. *Journal of Virology*, *89*(1), 870–876. https://doi.org/10.1128/JVI.02154-14

Chan, J. Y., & Paolo, M. C. (1995). Chromosomal localization of the human NF-E2 family of bZIP transcription factors by fluorescence in situ hybridization, 265–269.

Chen, A., Akinyemi, R. O., Hase, Y., Firbank, M. J., Ndung', M. N., Foster, V., … Kalaria, R. N. (2016). Frontal white matter hyperintensities, clasmatodendrosis and gliovascular abnormalities in ageing and post-stroke dementia. *Brain*, *139*, 242–258. https://doi.org/10.1093/brain/awv328

Chen, B., Cao, H., Chen, L., Yang, X., Tian, X., Li, R., & Cheng, O. (2016). Rifampicin Attenuated Global Cerebral Ischemia Injury via Activating the Nuclear Factor Erythroid 2-Related Factor Pathway. *Frontiers in Cellular Neuroscience*, *10*, 273. https://doi.org/10.3389/fncel.2016.00273

Chen, P., Vargas, M. R., Pani, A. K., Smeyne, R. J., Johnson, D. A., Wai, Y., & Johnson, J. A. (2009). Nrf2-mediated neuroprotection in the MPTP mouse model of Parkinson ' s disease : Critical role for the astrocyte. *PNAS*, *106*(8), 2933–2938.

Chen, X.-L., Dodd, G., Thomas, S., Zhang, X., Wasserman, M. A., Rovin, B. H., & Kunsch, C. (2006). Activation of Nrf2/ARE pathway protects endothelial cells from oxidant injury and inhibits inflammatory gene expression. *American Journal of Physiology-Heart and Circulatory Physiology*, *290*(5), H1862–H1870. https://doi.org/10.1152/ajpheart.00651.2005

Chen, X., Varner, S. E., Rao, A. S., Grey, J. Y., Thomas, S., Cook, C. K., … Kunsch, C. (2003). Laminar Flow Induction of Antioxidant Response Element-mediated Genes in Endothelial Cells, *278*(2), 703–711. https://doi.org/10.1074/jbc.M203161200

Chen, Z., & Trapp, B. D. (2016). Microglia and neuroprotection. *Journal of Neurochemistry*, *136*, 10–17. https://doi.org/10.1111/jnc.13062

Cheng, Y., Yang, C., Luo, D., Li, X., Le, X. C., & Rong, J. (2018). N-Propargyl Caffeamide Skews Macrophages Towards a Resolving M2-Like Phenotype Against Myocardial Ischemic Injury via Activating Nrf2/HO-1 Pathway and Inhibiting NF-κB Pathway. *Cellular Physiology and Biochemistry : International Journal of Experimental Cellular Physiology, Biochemistry, and Pharmacology*, *47*(6), 2544–2557. https://doi.org/10.1159/000491651

Cherry, J. D., Olschowka, J. A., Banion, M. K. O., & O'Banion, M. (2014). Neuroinflammation and M2 microglia: the good, the bad, and the inflamed. *Journal of Neuroinflammation*, *11*(1), 1–15. https://doi.org/10.1186/1742-2094-11-98

Cherubini, A., Polidori, M. C., Bregnocchi, M., Pezzuto, S., Cecchetti, R., Ingegni, T., … Mecocci, P. (2000). Antioxidant profile and early outcome in stroke patients. *Stroke*, *31*(10), 2295–2300. https://doi.org/10.1161/01.STR.31.10.2295

Cherubini, A., Ruggiero, C., Polidori, M. C., & Mecocci, P. (2005). Potential markers of oxidative stress in stroke. *Free Radical Biology and Medicine*, *39*(7), 841–852. https://doi.org/10.1016/J.FREERADBIOMED.2005.06.025

Chinnasamy, P., Lutz, S. E., Riascos-Bernal, D. F., Jeganathan, V., Casimiro, I., Brosnan, C. F., & Sibinga, N. E. (2015). Loss of Allograft Inflammatory Factor-1 Ameliorates Experimental Autoimmune Encephalomyelitis by Limiting Encephalitogenic CD4 T-Cell Expansion. *Molecular Medicine*, *21*(1), 233. https://doi.org/10.2119/MOLMED.2014.00264

Choi, D. H., & Lee, J. (2017). A mini-review of the NADPH oxidases in vascular dementia: Correlation with NOXs and risk factors for VaD. *International Journal of Molecular Sciences*, *18*(11), 1–16. https://doi.org/10.3390/ijms18112500

Choi, D. W. (1988). Glutamate neurotoxicity and diseases of the nervous system. *Neuron*, *1*(8), 623–634. https://doi.org/10.1016/0896-6273(88)90162-6

Chowdhury, I., Mo, Y., Gao, L., Kazi, A., Fisher, A. B., & Feinstein, S. I. (2009). Oxidant stress stimulates expression of the human peroxiredoxin 6 gene by a transcriptional

mechanism involving an antioxidant response element. *Free Radical Biology and Medicine*, *46*(2), 146–153. https://doi.org/10.1016/j.freeradbiomed.2008.09.027

Cipolla, M. J., Liebeskind, D. S., & Chan, S.-L. (2018). The importance of comorbidities in ischemic stroke: Impact of hypertension on the cerebral circulation. *Journal of Cerebral Blood Flow & Metabolism*, *38*(12), 2129–2149. https://doi.org/10.1177/0271678X18800589

Clark, D. P. Q., Perreau, V. M., Shultz, S. R., Brady, R. D., Lei, E., Dixit, S., … Boon, W. C. (2019). Inflammation in Traumatic Brain Injury: Roles for Toxic A1 Astrocytes and Microglial–Astrocytic Crosstalk. *Neurochemical Research*, 1–15. https://doi.org/10.1007/s11064-019-02721-8

Clark, W., Lessov, N., Dixon, M., & Eckenstein, F. (1997). Monofilament intraluminal middle cerebral artery occlusion in the mouse. *Neurological Research*, *19*(6), 641–648. https://doi.org/10.1080/01616412.1997.11740874

Clarke, L. E., Liddelow, S. A., Chakraborty, C., Münch, A. E., Heiman, M., & Barres, B. A. (2018). Normal aging induces A1-like astrocyte reactivity. *PNAS*, *115*(8), 1896–1905. https://doi.org/10.1073/pnas.1800165115

Clausen, Bettina H, Lambertsen, K. L., Babcock, A. A., Holm, T. H., Dagnaes-Hansen, F., & Finsen, B. (2008). Interleukin-1beta and tumor necrosis factor-alpha are expressed by different subsets of microglia and macrophages after ischemic stroke in mice. *Journal of Neuroinflammation*, *5*(1), 46. https://doi.org/10.1186/1742-2094-5-46

Clausen, Bettina Hjelm, Lundberg, L., Yli-Karjanmaa, M., Martin, N. A., Svensson, M., Alfsen, M. Z., … Lambertsen, K. L. (2017). Fumarate decreases edema volume and improves functional outcome after experimental stroke. *Experimental Neurology*, *295*, 144–154. https://doi.org/10.1016/j.expneurol.2017.06.011

Cleeter, M. W. J., Cooper, J. M., Darley-Usmar, V. M., Moncada, S., & Schapira, A. H. V. (1994). Reversible inhibition of cytochrome c oxidase, the terminal enzyme of the mitochondrial respiratory chain, by nitric oxide: implications for neurodegenerative diseases. *FEBS Letter*, *345*, 50–54. https://doi.org/10.1016/0014-5793(94)00424-2

Coutts, S. B. (2017, February 1). Diagnosis and Management of Transient Ischemic Attack. *CONTINUUM Lifelong Learning in Neurology*. Lippincott Williams and Wilkins. https://doi.org/10.1212/CON.0000000000000424

Cross, A. K., & Woodroofe, M. N. (1999). Chemokines induce migration and changes in actin polymerization in adult rat brain microglia and a human fetal microglial cell line in vitro. *Journal of Neuroscience Research*, *55*(1), 17–23. https://doi.org/10.1002/(SICI)1097-4547(19990101)55:1<17::AID-JNR3>3.0.CO;2-J

Cuartero, M. I., Ballesteros, I., Moraga, A., Nombela, F., Vivancos, J., Hamilton, J. A., … Moro, M. A. (2013). N2 Neutrophils, Novel Players in Brain Inflammation After Stroke. *Stroke*, *44*(12), 3498–3508. Retrieved from https://www.ahajournals.org/doi/10.1161/STROKEAHA.113.002470

Cullen, J. M. (2010). Histologic Patterns of Hepatotoxic Injury. *Comprehensive Toxicology*, 141–173. https://doi.org/10.1016/B978-0-08-046884-6.01007-1

Dai, W. J., Funk, A., Herdegen, T., Unger, T., & Culman, J. (1999). Blockade of central angiotensin AT(1) receptors improves neurological outcome and reduces expression of AP-1 transcription factors after focal brain ischemia in rats. *Stroke*, *30*(11), 2391–2398; discussion 2398-9. Retrieved from http://www.ncbi.nlm.nih.gov/pubmed/10548676

Dai, Y., Zhang, H., Zhang, J., & Yan, M. (2018). Isoquercetin attenuates oxidative stress and neuronal apoptosis after ischemia/reperfusion injury via Nrf2-mediated inhibition of the NOX4/ROS/NF-κB pathway. *Chemico-Biological Interactions*, *284*, 32–40. https://doi.org/10.1016/J.CBI.2018.02.017

Dallérac, G., Zapata, J., & Rouach, N. (2018). Versatile control of synaptic circuits by

astrocytes: where, when and how? *Nature Reviews Neuroscience*, *19*(12), 729–743. https://doi.org/10.1038/s41583-018-0080-6

Damasio, H. (1983). A computed tomographic guide to the identification of cerebral vascular territories. *Archives of Neurology*, *40*(3), 138–142. Retrieved from http://www.ncbi.nlm.nih.gov/pubmed/6830451

Dang, J., Brandenburg, L. O., Rosen, C., Fragoulis, A., Kipp, M., Pufe, T., … Wruck, C. J. (2012). Nrf2 expression by neurons, astroglia, and microglia in the cerebral cortical penumbra of ischemic rats. *Journal of Molecular Neuroscience*, *46*(3), 578–584. https://doi.org/10.1007/s12031-011-9645-9

Daulatzai, M. A. (2016). Fundamental role of pan-inflammation and oxidative-nitrosative pathways in neuropathogenesis of Alzheimer's disease in focal cerebral ischemic rats. *American Journal of Neurodegenerative Disease*, *5*(2), 102–130. Retrieved from http://www.ncbi.nlm.nih.gov/pubmed/27335702

Davies, C. A., Loddick, S. A., Stroemer, R. P., Hunt, J., & Rothwell, N. J. (1998). An Integrated Analysis of the Progression of Cell Responses Induced by Permanent Focal Middle Cerebral Artery Occlusion in the Rat. *Experimental Neurology*, *154*(1), 199–212. https://doi.org/10.1006/EXNR.1998.6891

Dawson, D. A., & Hallenbeck, J. M. (1996). *Utilization as a Marker for Volumetric Assessment of Acute Brain Injury*. *Journal of Cerebral Blood Flow and Metabolism* (Vol. 16). Retrieved from https://journals.sagepub.com/doi/pdf/10.1097/00004647-199601000-00020

De Simoni, M. G., Storini, C., Barba, M., Catapano, L., Arabia, A. M., Rossi, E., & Bergamaschini, L. (2003). Neuroprotection by Complement (C1) Inhibitor in Mouse Transient Brain Ischemia. *Journal of Cerebral Blood Flow & Metabolism*, *23*(2), 232–239. https://doi.org/10.1097/01.WCB.0000046146.31247.A1

De Strooper, B., & Karran, E. (2016). The Cellular Phase of Alzheimer's Disease. *Cell*, *164*, 603–615. https://doi.org/10.1016/j.cell.2015.12.056

Deininger, M. H., Meyermann, R., Trautmann, K., Duffner, F., Grote, E. H., Wickboldt, J., & Schluesener, H. J. (2000). Heme oxygenase (HO)-1 expressing macrophages/microglial cells accumulate during oligodendroglioma progression. *Brain Research*, *882*(1–2), 1–8. Retrieved from http://www.ncbi.nlm.nih.gov/pubmed/11056178

Del Zoppo, G. J., & Mabuchi, T. (2003). Cerebral Microvessel Responses to Focal Ischemia. *Journal of Cerebral Blood Flow & Metabolism*, *23*(8), 879–894. https://doi.org/10.1097/01.WCB.0000078322.96027.78

Dénes, Á., Ferenczi, S., Halász, J., Környei, Z., Kovács, K. J., Dénes, A., … Kovács, K. J. (2008). Role of CX3CR1 (fractalkine receptor) in brain damage and inflammation induced by focal cerebral ischemia in mouse. *Journal of Cerebral Blood Flow & Metabolism*, *28*(10), 1707–1721. https://doi.org/10.1038/jcbfm.2008.64

Denes, A., Vidyasagar, R., Feng, J., Narvainen, J., Mccoll, B. W., Kauppinen, R. A., & Allan, S. M. (2007). Proliferating resident microglia after focal cerebral ischaemia in mice. *Journal of Cerebral Blood Flow & Metabolism*, *27*(12), 1941–1953. https://doi.org/10.1038/sj.jcbfm.9600495

Deng, Y., He, H., Yang, L., & Zhang, P. (2016). Dynamic changes in neuronal autophagy and apoptosis in the ischemic penumbra following permanent ischemic stroke. *Neural Regeneration Research*, *11*(7), 1108. https://doi.org/10.4103/1673-5374.187045

Desagher, S., Glowinski, J., & Premont, J. (1996). Astrocytes protect neurons from hydrogen peroxide toxicity. *The Journal of Neuroscience : The Official Journal of the Society for Neuroscience*, *16*(8), 2553–2562. https://doi.org/10.1523/JNEUROSCI.16-08-02553.1996

Desestret, V., Riou, A., Chauveau, F., Cho, T.-H., Devillard, E., Marinescu, M., … Wiart, M.

(2013). In Vitro and In Vivo Models of Cerebral Ischemia Show Discrepancy in Therapeutic Effects of M2 Macrophages. *PLoS ONE*, *8*(6), e67063. https://doi.org/10.1371/journal.pone.0067063

Dihné, M., & Block, F. (2001). Focal ischemia induces transient expression of IL-6 in the substantia nigra pars reticulata. *Brain Research*, *889*(1–2), 165–173. Retrieved from http://www.ncbi.nlm.nih.gov/pubmed/11166700

Dimmock, J. R., Elias, D. W., Beazely, M. A., & Kandepu, N. M. (1999). Bioactivities of chalcones. *Current Medicinal Chemistry*, *6*(12), 1125–1149. Retrieved from http://www.ncbi.nlm.nih.gov/pubmed/10519918

DiNapoli, V. A., Huber, J. D., Houser, K., Li, X., & Rosen, C. L. (2008). Early disruptions of the blood–brain barrier may contribute to exacerbated neuronal damage and prolonged functional recovery following stroke in aged rats. *Neurobiology of Aging*, *29*(5), 753–764. https://doi.org/10.1016/J.NEUROBIOLAGING.2006.12.007

Ding, S. (2014). Dynamic reactive astrocytes after focal ischemia. *NEURAL REGENERATION RESEARCH*, *9*(23), 2048–2052. https://doi.org/10.4103/1673-5374.147929

Ding, Y., Chen, M., Wang, M., Wang, M., Zhang, T., Park, J., … Wen, A. (2014). Neuroprotection by Acetyl-11-Keto-β-Boswellic Acid, in Ischemic Brain Injury Involves the Nrf2/HO-1 defense Pathway. *Scientific Reports*, *4*, 7002. https://doi.org/10.1038/srep07002

Dinkova-Kostova, A. T., & Talalay, P. (2010). NAD(P)H:quinone acceptor oxidoreductase 1 (NQO1), a multifunctional antioxidant enzyme and exceptionally versatile cytoprotector. *Archives of Biochemistry and Biophysics*, *501*(1), 116–123. https://doi.org/10.1016/j.abb.2010.03.019

Dirnagl, U., Iadecola, C., & Moskowitz, M. A. (1999). Pathology of ischaemic stroke: an integrated view. *Trends in Neurosciences*, *22*(9), 391–397. https://doi.org/10.1016/S0166-2236(99)01401-0

Dittmar, M., Spruss, T., Schuierer, G., & Horn, M. (2003). External Carotid Artery Territory Ischemia Impairs Outcome in the Endovascular Filament Model of Middle Cerebral Artery Occlusion in Rats. *Stroke*, *34*(9), 2252–2257. https://doi.org/10.1161/01.STR.0000083625.54851.9A

Dodson, M., Redmann, M., Rajasekaran, N. S., Darley-Usmar, V., & Zhang, J. (2015). KEAP1-NRF2 signalling and autophagy in protection against oxidative and reductive proteotoxicity. *The Biochemical Journal*, *469*(3), 347–355. https://doi.org/10.1042/BJ20150568

Doetschman, T. (2009). Influence of Genetic Background on Genetically Engineered Mouse Phenotypes. In *Gene Knockout Protocols: Second Edition, vol. 530* (pp. 423–433). Humana Press. https://doi.org/10.1007/978-1-59745-471-1_23

Dolmans, L. S., Rutten, F. H., Koenen, N. C. T., Bartelink, M. L. E. L., Reitsma, J. B., Kappelle, L. J., & Hoes, A. W. (2019, September 1). Candidate Biomarkers for the Diagnosis of Transient Ischemic Attack: A Systematic Review. *Cerebrovascular Diseases*. S. Karger AG. https://doi.org/10.1159/000502449

Domínguez, C., Delgado, P., Vilches, A., Martín-Gallán, P., Ribó, M., Santamarina, E., … Montaner, J. (2010). Oxidative stress after thrombolysis-induced reperfusion in human stroke. *Stroke*, *41*(4), 653–660. https://doi.org/10.1161/STROKEAHA.109.571935

Dong, L., Wang, Y., Lv, J., Zhang, H., Jiang, N., Lu, C., … Liu, X. (2019). Memory enhancement of fresh ginseng on deficits induced by chronic restraint stress in mice. *Nutritional Neuroscience*, *22*(4), 235–242. https://doi.org/10.1080/1028415X.2017.1373928

Dong, Y., Liu, H. D., Zhao, R., Yang, C. Z., Chen, X. Q., Wang, X. H., … Yu, A. C. H. (2009). Ischemia activates JNK/c-Jun/AP-1 pathway to up-regulate 14-3-3γ in astrocyte. *Journal of Neurochemistry*, *109*, 182–188. https://doi.org/10.1111/j.1471-4159.2009.05974.x

Dowell, J. A., & Johnson, J. A. (2013). Mechanisms of Nrf2 Protection in Astrocytes as Identified by Quantitative Proteomics and siRNA Screening. *PLoS ONE*, *8*(7), e70163. https://doi.org/10.1371/journal.pone.0070163

Doyle, K. P., Fathali, N., Siddiqui, M. R., & Buckwalter, M. S. (2012). Distal hypoxic stroke: A new mouse model of stroke with high throughput, low variability and a quantifiable functional deficit. *Journal of Neuroscience Methods*, *207*(1), 31–40. https://doi.org/10.1016/J.JNEUMETH.2012.03.003

Doyle, K. P., Quach, L. N., Solé, X. M., Axtell, R. C., Nguyen, T.-V. V, Soler-Llavina, G. J., … Buckwalter, S. (2015). B-Lymphocyte-Mediated Delayed Cognitive Impairment following Stroke. *Journal of Neuroscience*, *35*(5), 2133–2145. https://doi.org/10.1523/JNEUROSCI.4098-14.2015

Draheim, T., Liessem, A., Scheld, M., Wilms, F., Weißflog, M., Denecke, B., … Clarner, T. (2016). Activation of the astrocytic Nrf2/ARE system ameliorates the formation of demyelinating lesions in a multiple sclerosis animal model. *Glia*, *64*(12), 2219–2230. https://doi.org/10.1002/glia.23058

Dringen, R., Pfeiffer, B., & Hamprecht, B. (1999). Synthesis of the Antioxidant Glutathione in Neurons: Supply by Astrocytes of CysGly as Precursor for Neuronal Glutathione. *Journal of Neuroscience*, *19*(2), 562–569. https://doi.org/10.1523/JNEUROSCI.19-02-00562.1999

Drukarch, B, Schepens, E., Jongenelen, C. A. ., Stoof, J. ., & Langeveld, C. . (1997). Astrocyte-mediated enhancement of neuronal survival is abolished by glutathione deficiency. *Brain Research*, *770*(1–2), 123–130. https://doi.org/10.1016/S0006-8993(97)00790-7

Drukarch, Benjamin, Schepens, E., Stoof, J. C., Langeveld, C. H., & Van Muiswinkel, F. L. (1998). Astrocyte-Enhanced Neuronal Survival is Mediated by Scavenging of Extracellular Reactive Oxygen Species. *Free Radical Biology and Medicine*, *25*(2), 217–220. https://doi.org/10.1016/S0891-5849(98)00050-1

Dudai, Y. (2002). Molecular bases of long-term memories: A question of persistence. *Current Opinion in Neurobiology*, *12*(2), 211–216. https://doi.org/10.1016/S0959-4388(02)00305-7

Dumont, M., Wille, E., Calingasan, N. Y., Tampellini, D., Williams, C., Gouras, G. K., … Lin, M. T. (2011). Triterpenoid CDDO–methylamide improves memory and decreases amyloid plaques in a transgenic mouse model of Alzheimer's disease. *Journal of Neurochemistry*, *109*(2), 502–512. https://doi.org/10.1111/j.1471-4159.2009.05970.x.Triterpenoid

Duverger, D., & MacKenzie, E. T. (1988). The Quantification of Cerebral Infarction following Focal Ischemia in the Rat: Influence of Strain, Arterial Pressure, Blood Glucose Concentration, and Age. *Journal of Cerebral Blood Flow & Metabolism*, *8*(4), 449–461. https://doi.org/10.1038/jcbfm.1988.86

Easton, J. D., Saver, J. L., Albers, G. W., Alberts, M. J., Chaturvedi, S., Feldmann, E., … Sacco, R. L. (2009, June 1). Definition and evaluation of transient ischemic attack: A scientific statement for healthcare professionals from the American heart association/American stroke association stroke council; council on cardiovascular surgery and anesthesia; council on cardiovascular radiology and intervention; council on cardiovascular nursing; and the interdisciplinary council on peripheral vascular disease. *Stroke*. https://doi.org/10.1161/STROKEAHA.108.192218

Eftekharpour, E., Holmgren, A., & Juurlink, B. H. (2000). Thioredoxin reductase and glutathione synthesis is upregulated by t-butylhydroquinone in cortical astrocytes but not in cortical neurons. *Glia*, *31*(3), 241–248. Retrieved from http://www.ncbi.nlm.nih.gov/pubmed/10941150

Eggler, A. L., Gay, K. A., & Mesecar, A. D. (2008). Molecular mechanisms of natural products in chemoprevention: Induction of cytoprotective enzymes by Nrf2. *Molecular Nutrition*

and Food Research, *52*, 84–94. https://doi.org/10.1002/mnfr.200700249

Ekdahl, C. T., Kokaia, Z., & Lindvall, O. (2009). Brain inflammation and adult neurogenesis: The dual role of microglia. *Neuroscience*, *158*(3), 1021–1029. https://doi.org/10.1016/j.neuroscience.2008.06.052

El-Brolosy, M. A., & Stainier, D. Y. R. (2017). Genetic compensation: A phenomenon in search of mechanisms. *PLoS Genetics*, *13*(7), e1006780. https://doi.org/10.1371/journal.pgen.1006780

Engelhardt, S., Huang, S.-F., Patkar, S., Gassmann, M., & Ogunshola, O. O. (2015). Differential responses of blood-brain barrier associated cells to hypoxia and ischemia: a comparative study. *Fluids and Barriers of the CNS*, *12*(1), 4. https://doi.org/10.1186/2045-8118-12-4

Ennaceur, A., & Delacour, J. (1988). A new one-trial test for neurobiological studies of memory in rats. 1: Behavioral data. *Behavioural Brain Research*, *31*(1), 47–59. https://doi.org/10.1016/0166-4328(88)90157-X

Enzmann, G., Kargaran, S., & Engelhardt, B. (2018). Ischemia-reperfusion injury in stroke: impact of the brain barriers and brain immune privilege on neutrophil function. *Therapeutic Advances in Neurological Disorders*, *11*, 1–15. https://doi.org/10.1177/1756286418794184

Erbsloh, F., Bernsmeier, A., & Hillesheim, H. (1958). The glucose consumption of the brain; its dependence on the liver. *Archiv Fur Psychiatrie Und Nervenkrankheiten, Vereinigt Mit Zeitschrift Fur Die Gesamte Neurologie Und Psychiatrie*, *196*(6), 611–626. Retrieved from http://www.ncbi.nlm.nih.gov/pubmed/13534602

Fagerberg, L., Hallström, B. M., Oksvold, P., Kampf, C., Djureinovic, D., Odeberg, J., … Uhlén, M. (2014). Analysis of the human tissue-specific expression by genome-wide integration of transcriptomics and antibody-based proteomics. *Molecular & Cellular Proteomics : MCP*, *13*(2), 397–406. https://doi.org/10.1074/mcp.M113.035600

Fan, J., Li, Y., Fu, X., Li, L., Hao, X., & Li, S. (2017). Nonhuman primate models of focal cerebral ischemia. *Neural Regeneration Research*, *12*(2), 321–328. https://doi.org/10.4103/1673-5374.200815

Faulkner, J. R., Herrmann, J. E., Woo, M. J., Tansey, K. E., Doan, N. B., & Sofroniew, M. V. (2004). Reactive astrocytes protect tissue and preserve function after spinal cord injury. *The Journal of Neuroscience : The Official Journal of the Society for Neuroscience*, *24*(9), 2143–2155. https://doi.org/10.1523/JNEUROSCI.3547-03.2004

Feekes, J. A., & Cassell, M. D. (2006). The vascular supply of the functional compartments of the human striatum. *Brain*, *129*, 2189–2201. https://doi.org/10.1093/brain/awl158

Fenn, A. M., Hall, J. C. E., Gensel, J. C., Popovich, P. G., & Godbout, J. P. (2014). IL-4 signaling drives a unique arginase+/IL-1β+ microglia phenotype and recruits macrophages to the inflammatory CNS: consequences of age-related deficits in IL-4Rα after traumatic spinal cord injury. *The Journal of Neuroscience : The Official Journal of the Society for Neuroscience*, *34*(26), 8904–8917. https://doi.org/10.1523/JNEUROSCI.1146-14.2014

Fenn, A. M., Henry, C. J., Huang, Y., Dugan, A., & Godbout, J. P. (2012). Lipopolysaccharide-induced interleukin (IL)-4 receptor-α expression and corresponding sensitivity to the M2 promoting effects of IL-4 are impaired in microglia of aged mice. *Brain, Behavior, and Immunity*, *26*(5), 766–777. https://doi.org/10.1016/j.bbi.2011.10.003

Ferro, D. A., van den Brink, H., Exalto, L. G., Boomsma, J. M. F., Barkhof, F., Prins, N. D., … TRACE-VCI study group, on behalf of the T.-V. study. (2019). Clinical relevance of acute cerebral microinfarcts in vascular cognitive impairment. *Neurology*, 10.1212/WNL.0000000000007250. https://doi.org/10.1212/WNL.0000000000007250

Fluri, F., Schuhmann, M. K., & Kleinschnitz, C. (2015). Animal models of ischemic stroke and their application in clinical research. *Drug Design, Development and Therapy*, *9*, 3445–

3454. https://doi.org/10.2147/DDDT.S56071

Fogal, B., Hewett, J. A., & Hewett, S. J. (2005). Interleukin-1beta potentiates neuronal injury in a variety of injury models involving energy deprivation. *Journal of Neuroimmunology*, *161*(1–2), 93–100. https://doi.org/10.1016/j.jneuroim.2004.12.007

Fowler, J. H., Mcqueen, J., Holland, P. R., Manso, Y., Marangoni, M., Scott, F., … Horsburgh, K. (2017). Dimethyl fumarate improves white matter function following severe hypoperfusion: Involvement of microglia/macrophages and inflammatory mediators. *Journal of Cerebral Blood Flow & Metabolism*, 0271678X1771310. https://doi.org/10.1177/0271678X17713105

Francis, A., & Baynosa, R. (2017). Ischaemia-reperfusion injury and hyperbaric oxygen pathways: a review of cellular mechanisms. *Diving and Hyperbaric Medicine*, *47*(2), 110–117. https://doi.org/10.28920/DHM47.2.110-117

Franco-Bocanegra, D. K., McAuley, C., Nicoll, J. A. R., Boche, D., Franco-Bocanegra, D. K., McAuley, C., … Boche, D. (2019). Molecular Mechanisms of Microglial Motility: Changes in Ageing and Alzheimer's Disease. *Cells*, *8*(6), 639. https://doi.org/10.3390/cells8060639

Freitas-Andrade, M., Bechberger, J. F., MacVicar, B. A., Viau, V., & Naus, C. C. (2017). Pannexin1 knockout and blockade reduces ischemic stroke injury in female, but not in male mice. *Oncotarget*, *8*(23), 36973–36983. https://doi.org/10.18632/oncotarget.16937

Friede, R. L., & Van Houten, W. H. (1961). Relations between Post-Mortem Alterations and Glycolytic Metabolism in the Brain. *Experimental Neurology*, *4*, 197–2014. Retrieved from https://deepblue.lib.umich.edu/bitstream/handle/2027.42/32354/0000425.pdf?sequence=1&isAllowed=y

Frigerio, C. S., Wolfs, L., Fattorelli, N., Perry, V. H., Fiers, M., Strooper, B. De, … Schmidt, I. (2019). The Major Risk Factors for Alzheimer ' s Disease : Age , Sex , and Genes Modulate the Microglia Response to A b Plaques Resource The Major Risk Factors for Alzheimer ' s Disease : Age , Sex , and Genes Modulate the Microglia Response to A b Plaques. *Cell Reports*, *27*, 1293–1306. https://doi.org/10.1016/j.celrep.2019.03.099

Fu, J., Hou, Y., Xue, P., Wang, H., Xu, Y., Qu, W., … Pi, J. (2016). Nrf2 in Type 2 diabetes and diabetic complications: Yin and Yang. *Current Opinion in Toxicology*, *1*, 9–19. https://doi.org/10.1016/J.COTOX.2016.08.001

Fujioka, M., Taoka, T., Matsuo, Y., Mishima, K., Ogoshi, K., Kondo, Y., … Siesjö, B. K. (2003). Magnetic resonance imaging shows delayed ischemic striatal neurodegeneration. *Annals of Neurology*, *54*(6), 732–747. https://doi.org/10.1002/ana.10751

Fumagalli, S., Perego, C., Pischiutta, F., Zanier, E. R., & Simoni, M. De. (2015). The ischemic environment drives microglia and macrophage function, *6*(April), 1–19. https://doi.org/10.3389/fneur.2015.00081

Gallacher, K. I., Mcqueenie, R., Nicholl, B., Jani, B. D., Lee, D., & Mair, F. S. (2018). Risk factors and mortality associated with multimorbidity in people with stroke or transient ischaemic attack: a study of 8,751 UK Biobank participants. *Journal of Comorbidity*, *8*(1), 1–8. https://doi.org/10.15256/joc.2018.8.129

Gan, L., Vargas, M. R., Johnson, D. A., & Johnson, J. A. (2012). Astrocyte-specific Overexpression of Nrf2 Delays Motor Pathology and Synuclein Aggregation throughout the CNS in the Alpha-synuclein Mutant (A53T) Mouse Model. *Journal of Neuroscience*, *32*(49), 17775–17787. https://doi.org/10.1523/JNEUROSCI.3049-12.2012

Geden, M. J., Romero, S. E., & Deshmukh, M. (2019). Apoptosis versus axon pruning: Molecular intersection of two distinct pathways for axon degeneration. *Neuroscience Research*, *139*, 3–8. https://doi.org/10.1016/J.NEURES.2018.11.007

Gegg, M. E., Clark, J. B., & Heales, S. J. R. (2005). Co-culture of neurones with glutathione deficient astrocytes leads to increased neuronal susceptibility to nitric oxide and increased glutamate-cysteine ligase activity. *Brain Research*, *1036*(1–2), 1–6. https://doi.org/10.1016/J.BRAINRES.2004.11.064

Giannessi, F., Ursino, F., Fattori, B., Giambelluca, M. A., Scavuzzo, M. C., Nacci, A., … Ruffoli, R. (2010). Expression of 3-nitrotyrosine , a marker for peroxynitrite , in nasal polyps of nonatopic patients, *16*(4), 172–179.

Gille, J. J., & Joenje, H. (1992). Cell culture models for oxidative stress: superoxide and hydrogen peroxide versus normobaric hyperoxia. *Mutation Research*, *275*(3–6), 405–414. Retrieved from http://www.ncbi.nlm.nih.gov/pubmed/1383781

Girouard, H., & Iadecola, C. (2006). Neurovascular coupling in the normal brain and in hypertension, stroke, and Alzheimer disease. *Journal of Applied Physiology*, *100*(1), 328–335. https://doi.org/10.1152/japplphysiol.00966.2005

Giulian, D. (1987). Ameboid microglia as effectors of inflammation in the central nervous system. *Journal of Neuroscience Research*, *18*(1), 155–171. https://doi.org/10.1002/jnr.490180123

Gorelick, P. B., Counts, S. E., & Nyenhuis, D. (2016). Vascular cognitive impairment and dementia. *Biochimica et Biophysica Acta (BBA) - Molecular Basis of Disease*, *1862*(5), 860–868. https://doi.org/10.1016/j.bbadis.2015.12.015

Gorelick, P. B., Scuteri, A., Black, S. E., Decarli, C., Greenberg, S. M., Iadecola, C., … Seshadri, S. (2011). Vascular contributions to cognitive impairment and dementia: A statement for healthcare professionals from the American Heart Association/American Stroke Association. *Stroke*, *42*(9), 2672–2713. https://doi.org/10.1161/STR.0b013e3182299496

Grau, A J, Weimar, C., Buggle, F., Heinrich, A., Goertler, M., Neumaier, S., … Diener, H. C. (2001). The German Stroke Data Bank. *Stroke*, *32*(11), 2559–2566. https://doi.org/10.1161/hs1101.098524

Grau, Armin J, Weimar, C., Buggle, F., Heinrich, A., Goertler, M., Neumaier, S., … Brandt, T. (2001). The German Stroke Data Bank. *Journal of the American Heart Association. Stroke*, *32*, 2559–2566. https://doi.org/10.1161/hs1101.098524

Grilo, A. L., & Mantalaris, A. (2019). Apoptosis: A mammalian cell bioprocessing perspective. *Biotechnology Advances*, *37*(3), 459–475. https://doi.org/10.1016/J.BIOTECHADV.2019.02.012

Grønberg, N. V., Johansen, F. F., Kristiansen, U., & Hasseldam, H. (2013). Leukocyte infiltration in experimental stroke. *Journal of Neuroinflammation*, *10*(1), 1–9. https://doi.org/10.1186/1742-2094-10-115

Guégan, C., Braudeau, J., Couriaud, C., Dietz, G. P. H., Lacombe, P., Bähr, M., … Onténiente, B. (2006). PTD–XIAP protects against cerebral ischemia by anti-apoptotic and transcriptional regulatory mechanisms. *Neurobiology of Disease*, *22*(1), 177–186. https://doi.org/10.1016/J.NBD.2005.10.014

Gupta, A., Lacoste, B., Pistel, P. J., Ingram, D. K., Hamel, E., Alaoui-Jamali, M. A., … Schipper, H. M. (2014). Neurotherapeutic effects of novel HO-1 inhibitors *in vitro* and in a transgenic mouse model of Alzheimer's disease. *Journal of Neurochemistry*, *131*(6), 778–790. https://doi.org/10.1111/jnc.12927

Habas, A., Hahn, J., Wang, X., & Margeta, M. (2013). Neuronal activity regulates astrocytic Nrf2 signaling. *PNAS*, *110*(45), 18291–18296. https://doi.org/10.1073/pnas.1208764110

Hachinski, V., Petersen, R. C., Breteler, M. M., Nyenhuis, D. L., Black, S. E., Powers, W. J., … Leblanc, G. G. (2006). National Institute of Neurological Disorders and Stroke-Canadian Stroke Network Vascular Cognitive Impairment Harmonization Standards. *Stroke*, *37*,

2220–2241. https://doi.org/10.1161/01.STR.0000237236.88823.47
Hacke, W., Donnan, G., Fieschi, C., Kaste, M., von Kummer, R., Broderick, J., … ATLANTIS Trials Investigators; ECASS Trials Investigators; NINDS rt-PA Study. (2004). Association of outcome with early stroke treatment: pooled analysis of ATLANTIS, ECASS, and NINDS rt-PA stroke trials. *Lancet*, *363*(9411), 768–774. https://doi.org/10.1016/S0140-6736(04)15692-4
Hammond, T. R., Dufort, C., Dissing-Olesen, L., Giera, S., Young, A., Wysoker, A., … Stevens, B. (2019). Single-Cell RNA Sequencing of Microglia throughout the Mouse Lifespan and in the Injured Brain Reveals Complex Cell-State Changes. *Immunity*, *0*(0), 1–19. https://doi.org/10.1016/J.IMMUNI.2018.11.004
Hammond, T. R., Robinton, D., & Stevens, B. (2018). Microglia and the Brain: Complementary Partners in Development and Disease. *Annual Review of Cell and Developmental Biology*, *34*(1), 523–544. https://doi.org/10.1146/annurev-cellbio-100616
Han, R., Xiao, J., Zhai, H., & Hao, J. (2016). Dimethyl fumarate attenuates experimental autoimmune neuritis through the nuclear factor erythroid-derived 2-related factor 2/hemoxygenase-1 pathway by altering the balance of M1/M2 macrophages. *Journal of Neuroinflammation*, *13*(1), 97. https://doi.org/10.1186/s12974-016-0559-x
Hankey, G J. (1999). Smoking and risk of stroke. *Journal of Cardiovascular Risk*, *6*(4), 207–211. Retrieved from http://www.ncbi.nlm.nih.gov/pubmed/10501270
Hankey, Graeme J. (2017). Stroke. *The Lancet*, *389*. https://doi.org/10.1016/S0140-6736(16)30962-X
Hao, E., Lang, F., Chen, Y., Zhang, H., Cong, X., Shen, X., & Su, G. (2013). Resveratrol Alleviates Endotoxin-Induced Myocardial Toxicity via the Nrf2 Transcription Factor. *PLoS ONE*, *8*(7). https://doi.org/10.1371/journal.pone.0069452
Hara, E., Takahashi, K., Tominaga, T., Kumabe, T., Kayama, T., Suzuki, H., … Shibahara, S. (1996). Expression of heme oxygenase and inducible nitric oxide synthase mRNA in human brain tumors. *Biochemical and Biophysical Research Communications*, *224*(1), 153–158. https://doi.org/10.1006/bbrc.1996.0999
Harbison, J., Hossain, O., Jenkinson, D., Davis, J., Louw, S. J., & Ford, G. A. (2003). Diagnostic accuracy of stroke referrals from primary care, emergency room physicians, and ambulance staff using the face arm speech test. *Stroke*, *34*(1), 71–76. https://doi.org/10.1161/01.STR.0000044170.46643.5E
Hardingham, G. E., & Do, K. Q. (2016). Linking early-life NMDAR hypofunction and oxidative stress in schizophrenia pathogenesis. *Nature Reviews Neuroscience*, 1–9. https://doi.org/10.1017/CBO9781107415324.004
Harikumar, K. B., Yester, J. W., Surace, M. J., Oyeniran, C., Price, M. M., Huang, W.-C., … Kordula, T. (2014). K63-linked polyubiquitination of transcription factor IRF1 is essential for IL-1-induced production of chemokines CXCL10 and CCL5. *Nature Immunology*, *15*(3), 231–238. https://doi.org/10.1038/ni.2810
Hartings, J. A., Rolli, M. L., Lu, X.-C. M., & Tortella, F. C. (2003). Development/Plasticity/Repair Delayed Secondary Phase of Peri-Infarct Depolarizations after Focal Cerebral Ischemia: Relation to Infarct Growth and Neuroprotection. *J Neuroscience*, *23*(37), 11602–11610. Retrieved from http://www.jneurosci.org/content/jneuro/23/37/11602.full.pdf
Hase, Y., Craggs, L., Hase, M., Stevenson, W., Slade, J., Lopez, D., … Kalaria, R. N. (2017). Effects of environmental enrichment on white matter glial responses in a mouse model of chronic cerebral hypoperfusion, 1–14. https://doi.org/10.1186/s12974-017-0850-5
Hase, Y. Y., Horsburgh, K., Ihara, M., & Kalaria, R. N. (2017). White matter degeneration in vascular and other ageing-related dementias. *Journal of Neurochemistry*, *144*(5), 617–633. https://doi.org/10.1111/ijlh.12426
Hata, R., Mies, G., Wiessner, C., Fritze, K., Hesselbarth, D., Brinker, G., & Hossmann, K.-A.

(1998). *A Reproducible Model of Middle Cerebral Artery Occlusion in Mice: Hemodynamic, Biochemical, and Magnetic Resonance Imaging*. *Journal of Cerebral Blood Flow and Metabolism* (Vol. 18). Retrieved from https://journals.sagepub.com/doi/pdf/10.1097/00004647-199804000-00004

Hayes, J. D., & McMahon, M. (2009). NRF2 and KEAP1 mutations: permanent activation of an adaptive response in cancer. *Trends in Biochemical Sciences*, *34*(4), 176–188. https://doi.org/10.1016/J.TIBS.2008.12.008

Heiss, W.-D. (2000). Ischemic Penumbra: Evidence From Functional Imaging in Man. *Journal of Cerehral Blood Flow and Metaholism*, *20*, 1276–1293. Retrieved from http://journals.sagepub.com/doi/pdf/10.1097/00004647-200009000-00002

Hellwig, S., Heinrich, A., & Biber, K. (2013). The brain's best friend: microglial neurotoxicity revisited. *Frontiers in Cellular Neuroscience*, *7*, 71. https://doi.org/10.3389/fncel.2013.00071

Herrmann, J. E., Imura, T., Song, B., Qi, J., Ao, Y., Nguyen, T. K., … Sofroniew, M. V. (2008). STAT3 is a Critical Regulator of Astrogliosis and Scar Formation after Spinal Cord Injury. *Journal of Neuroscience*, *28*(28), 7231–7243. https://doi.org/10.1523/JNEUROSCI.1709-08.2008

Hirayama, Y., Ikeda-Matsuo, Y., Notomi, S., Enaida, H., Kinouchi, H., & Koizumi, S. (2015). Astrocyte-mediated ischemic tolerance. *The Journal of Neuroscience : The Official Journal of the Society for Neuroscience*, *35*(9), 3794–3805. https://doi.org/10.1523/JNEUROSCI.4218-14.2015

Hirayama, Y., Ikeda-matsuo, Y., Notomi, S., Enaida, H., Kinouchi, H., & Koizumi, X. (2015). Astrocyte-Mediated Ischemic Tolerance. *Journal of Neuroscience*, *35*(9), 3794–3805. https://doi.org/10.1523/JNEUROSCI.4218-14.2015

Hirbec, H. E., Noristani, H. N., & Perrin, F. E. (2017). Microglia responses in acute and chronic neurological diseases: What microglia-specific transcriptomic studies taught (and did not teach) Us. *Frontiers in Aging Neuroscience*, *9*(JUL). https://doi.org/10.3389/fnagi.2017.00227

Honarpisheh, P., & McCullough, L. D. (2019). Sex as a biological variable in the pathology and pharmacology of neurodegenerative and neurovascular diseases. *British Journal of Pharmacology*, bph.14675. https://doi.org/10.1111/bph.14675

Hong, F., Freeman, M. L., & Liebler, D. C. (2005). Identification of Sensor Cysteines in Human Keap1 Modified by the Cancer Chemopreventive Agent Sulforaphane. *Chemical Research in Toxicology*, *18*(12), 1917–1926. https://doi.org/10.1021/tx0502138

Hong, S., Beja-Glasser, V. F., Nfonoyim, B. M., Frouin, A., Li, S., Ramakrishnan, S., … Stevens, B. (2016). Complement and microglia mediate early synapse loss in Alzheimer mouse models. *Science (New York, N.Y.)*, *352*(6286), 712–716. https://doi.org/10.1126/science.aad8373

Hoogland, I. C. M., Houbolt, C., van Westerloo, D. J., van Gool, W. A., & van de Beek, D. (2015). Systemic inflammation and microglial activation: systematic review of animal experiments. *Journal of Neuroinflammation*, *12*(1), 114. https://doi.org/10.1186/s12974-015-0332-6

Hossmann, K.-A. (1994). Viability thresholds and the penumbra of focal ischemia. *Annals of Neurology*, *36*(4), 557–565. https://doi.org/10.1002/ana.410360404

Hossmann, K A. (1996). Periinfarct depolarizations. *Cerebrovascular and Brain Metabolism Reviews*, *8*(3), 195–208. Retrieved from http://www.ncbi.nlm.nih.gov/pubmed/8870974

Hossmann, Konstantin Alexander. (2012). The two pathophysiologies of focal brain ischemia: Implications for translational stroke research. *Journal of Cerebral Blood Flow and Metabolism*, *32*(7), 1310–1316. https://doi.org/10.1038/jcbfm.2011.186

Hou, Y., Wang, Y., He, Q., Li, L., Xie, H., Zhao, Y., & Zhao, J. (2018). Nrf2 inhibits NLRP3 inflammasome activation through regulating Trx1/TXNIP complex in cerebral ischemia reperfusion injury. *Behavioural Brain Research*, *336*(April), 32–39. https://doi.org/10.1016/j.bbr.2017.06.027

Howells, D. W., Porritt, M. J., Rewell, S. S., O'Collins, V., Sena, E. S., van der Worp, H. B., … Macleod, M. R. (2010). Different Strokes for Different Folks: The Rich Diversity of Animal Models of Focal Cerebral Ischemia. *Journal of Cerebral Blood Flow & Metabolism*, *30*(8), 1412–1431. https://doi.org/10.1038/jcbfm.2010.66

Hu, D., Serrano, F., Oury, T. D., & Klann, E. (2006). Aging-Dependent Alterations in Synaptic Plasticity and Memory in Mice That Overexpress Extracellular Superoxide Dismutase. *Journal of Neuroscience*, *26*(15), 3933–3941. https://doi.org/10.1523/JNEUROSCI.5566-05.2006

Hu, Q., Ren, J., Li, G., Wu, J., Wu, X., Wang, G., … Li, J. (2018). The mitochondrially targeted antioxidant MitoQ protects the intestinal barrier by ameliorating mitochondrial DNA damage via the Nrf2/ARE signaling pathway. *Cell Death & Disease*, *9*(3), 403. https://doi.org/10.1038/s41419-018-0436-x

Hu, X., Li, P., Guo, Y., Wang, H., Leak, R. K., Chen, S., … Chen, J. (2012). Microglia/Macrophage Polarization Dynamics Reveal Novel Mechanism of Injury Expansion After Focal Cerebral Ischemia. *Stroke*, *43*(11), 3063–3070. https://doi.org/10.1161/STROKEAHA.112.659656

Hu, X., Liou, A. K. F., Leak, R. K., Xu, M., An, C., Suenaga, J., … Chen, J. (2014). Neurobiology of microglial action in CNS injuries: Receptor-mediated signaling mechanisms and functional roles. *Progress in Neurobiology*, *119–120*, 60–84. https://doi.org/10.1016/j.pneurobio.2014.06.002

Huang, L., Wu, Z., Zhuge, Q., Zheng, W., Shao, B., Wang, B., & Sun, F. (2014). Glial Scar Formation Occurs in the Human Brain after Ischemic Stroke. *International Journal of Medical Sciences*, *11*, 344–348. https://doi.org/10.7150/ijms.8140

Huang, X., Gao, Y., Qin, J., & Lu, S. (2018). The mechanism of long non-coding RNA MEG3 for hepatic ischemia-reperfusion: Mediated by miR-34a/Nrf2 signaling pathway. *Journal of Cellular Biochemistry*, *119*(1), 1163–1172. https://doi.org/10.1002/jcb.26286

Hulse, R. E., Winterfield, J., Kunkler, P. E., & Kraig, R. P. (2001). Astrocytic clasmatodendrosis in hippocampal organ culture. *Glia*, *33*(2), 169–179. Retrieved from http://www.ncbi.nlm.nih.gov/pubmed/11180514

Hume, R., Vallance, B. D., & Muir, M. M. (1982). Ascorbate status and fibrinogen concentrations after cerebrovascular accident. *Journal of Clinical Pathology*, *35*(2), 195–199. https://doi.org/10.1136/JCP.35.2.195

Humpel, C. (2015). Organotypic brain slice cultures: A review. *Neuroscience*, *305*, 86–98. https://doi.org/10.1016/J.NEUROSCIENCE.2015.07.086

Iadecola, C. (2013). The Pathobiology of Vascular Dementia. *Neuron*, *80*(4), 844–866. https://doi.org/10.1016/j.neuron.2013.10.008

Iadecola, C., & Alexander, M. (2001). Cerebral ischemia and inflammation. *Current Opinion in Neurology*, *14*(1), 89–94. Retrieved from http://www.ncbi.nlm.nih.gov/pubmed/11176223

Iadecola, C., Zhang, F., Xu, S., Casey, R., & Ross, M. E. (1995). Inducible Nitric Oxide Synthase Gene Expression in Brain following Cerebral Ischemia. *Journal of Cerebral Blood Flow & Metabolism*, *15*(3), 378–384. https://doi.org/10.1038/jcbfm.1995.47

Imai, H., Graham, D. I., Masayasu, H., & Macrae, I. M. (2003). Antioxidant ebselen reduces oxidative damage in focal cerebral ischemia. *Free Radic Biol Med*, *34*(1), 56–63. https://doi.org/S0891584902011802 [pii]

Imai, Y., & Kohsaka, S. (2002). Intracellular Signaling in M-CSF-Induced Microglia Activation: Role of Iba1. *GLIA*, *40*, 164–174. https://doi.org/10.1002/glia.10149

Islam, A., Choudhury, M. E., Kigami, Y., Utsunomiya, R., Matsumoto, S., Watanabe, H., … Tanaka, J. (2018). Sustained anti-inflammatory effects of TGF-β1 on microglia/macrophages. *Biochimica et Biophysica Acta (BBA) - Molecular Basis of Disease*, *1864*(3), 721–734. https://doi.org/10.1016/J.BBADIS.2017.12.022

Ito, D., Tanaka, K., Suzuki, S., Dembo, T., Fukuuchi, Y., Kortaro, T., … Fukuuchi, Y. (2001). Enhanced Expression of Iba1, Ionized Calcium-Binding Adapter Molecule 1, After Transient Focal Cerebral Ischemia In Rat Brain. *Stroke*, *32*, 1208–1215. https://doi.org/10.1161/01.STR.32.5.1208

Itoh, K, Chiba, T., Takahashi, S., Ishii, T., Igarashi, K., Katoh, Y., … Nabeshima, Y. (1997). An Nrf2/small Maf heterodimer mediates the induction of phase II detoxifying enzyme genes through antioxidant response elements. *Biochemical and Biophysical Research Communications*, *236*(2), 313–322. https://doi.org/10.1006/bbrc.1997.6943

Itoh, K, Igarashi, K., Hayashi, N., Nishizawa, M., Yamamoto, M., Itoh, K. E. N., … Nishizawa, M. (1995). Cloning and characterization of a novel erythroid cell-derived CNC family transcription factor heterodimerizing with the small Maf family proteins . Cloning and Characterization of a Novel Erythroid Cell-Derived CNC Family Transcription Factor Heterodimer, *15*(8), 4184–4193.

Itoh, Ken, Tong, K. I., & Yamamoto, M. (2004). Molecular mechanism activating Nrf2-Keap1 pathway in regulation of adaptive response to electrophiles. *Free Radical Biology and Medicine*, *36*(10), 1208–1213. https://doi.org/10.1016/j.freeradbiomed.2004.02.075

Jakel, R. J., Townsend, J. A., Kraft, A. D., & Johnson, J. A. (2007). Nrf2-mediated protection against 6-hydroxydopamine, *4*, 1–10. https://doi.org/10.1016/j.brainres.2007.01.131

Jeong, W., Han, S., Toledano, M. B., & Goo, S. (2012). Free Radical Biology and Medicine Role of sulfiredoxin as a regulator of peroxiredoxin function and regulation of its expression. *Free Radical Biology and Medicine*, *53*(3), 447–456. https://doi.org/10.1016/j.freeradbiomed.2012.05.020

Jha, M. K., Jo, M., Kim, J.-H. H., Suk, K., Mithilesh Kumar Jha, Myungjin Jo, … Kyoungho Suk. (2018). Microglia-Astrocyte Crosstalk: An Intimate Molecular Conversation. *The Neuroscientist*, 107385841878395. https://doi.org/10.1177/1073858418783959

Jiang, T., Chen, N., Zhao, F., Wang, X.-J., Kong, B., Zheng, W., & Zhang, D. D. (2010). High levels of Nrf2 determine chemoresistance in type II endometrial cancer. *Cancer Research*, *70*(13), 5486–5496. https://doi.org/10.1158/0008-5472.CAN-10-0713

Jiao, Y., Wilkinson, J., Di, X., Wang, W., Hatcher, H., Kock, N. D., … Torti, S. V. (2009). Curcumin, a cancer chemopreventive and chemotherapeutic agent, is a biologically active iron chelator. *Blood*, *113*(2), 462–469. https://doi.org/10.1182/blood-2008-05-155952

Jimenez-Blasco, D., Santofimia-Castaño, P., Gonzalez, a, Almeida, a, & Bolaños, J. P. (2015). Astrocyte NMDA receptors' activity sustains neuronal survival through a Cdk5–Nrf2 pathway. *Cell Death and Differentiation*, *22*(11), 1–13. https://doi.org/10.1038/cdd.2015.49

Jing, X., Ren, D., Wei, X., Shi, H., Zhang, X., Perez, R. G., … Lou, H. (2013). Eriodictyol-7-O-glucoside activates Nrf2 and protects against cerebral ischemic injury. *Toxicology and Applied Pharmacology*, *273*(3), 672–679. https://doi.org/10.1016/J.TAAP.2013.10.018

John Lin, C.-C., Yu, K., Hatcher, A., Huang, T.-W., Lee, H. K., Carlson, J., … Deneen, B. (2017). Identification of diverse astrocyte populations and their malignant analogs. *Nature Neuroscience*, *20*(3), 396–405. https://doi.org/10.1038/nn.4493

John Lin, C. C., Yu, K., Hatcher, A., Huang, T. W., Lee, H. K., Carlson, J., … Deneen, B. (2017). Identification of diverse astrocyte populations and their malignant analogs. *Nature Neuroscience*, *20*(3), 396–405. https://doi.org/10.1038/nn.4493

Johnson, C. O., Nguyen, M., Roth, G. A., Nichols, E., Alam, T., Abate, D., … Murray, C. J. L. (2019). Global, regional, and national burden of stroke, 1990–2016: a systematic

analysis for the Global Burden of Disease Study 2016. *The Lancet Neurology*, 439–458. https://doi.org/10.1016/S1474-4422(19)30034-1

Johnson, D. A., Andrews, G. K., Xu, W., & Johnson, J. A. (2002). Activation of the antioxidant response element in primary cortical neuronal cultures derived from transgenic reporter mice. *Journal of Neurochemistry*, *81*(6), 1233–1241. https://doi.org/10.1046/j.1471-4159.2002.00913.x

Johnson, J. A., Johnson, D. A., Kraft, A. D., Calkins, M. J., Jakel, R. J., Vargas, M. R., & Chen, P. C. (2008). The Nrf2-ARE pathway: An indicator and modulator of oxidative stress in neurodegeneration. *Annals of the New York Academy of Sciences*, *1147*, 61–69. https://doi.org/10.1196/annals.1427.036

Jovin, T. G., Chamorro, A., Cobo, E., de Miquel, M. A., Molina, C. A., Rovira, A., … REVASCAT Trial Investigators. (2015). Thrombectomy within 8 Hours after Symptom Onset in Ischemic Stroke. *New England Journal of Medicine*, *372*(24), 2296–2306. https://doi.org/10.1056/NEJMoa1503780

Jyrkkänen, H.-K., Kansanen, E., Inkala, M., Kivelä, A. M., Hurttila, H., Heinonen, S. E., … Levonen, A.-L. (2008). Nrf2 regulates antioxidant gene expression evoked by oxidized phospholipids in endothelial cells and murine arteries in vivo. *Circulation Research*, *103*(1), e1-9. https://doi.org/10.1161/CIRCRESAHA.108.176883

Kadl, A., Meher, A. K., Sharma, P. R., Lee, M. Y., Doran, A. C., Johnstone, S. R., … Leitinger, N. (2010). Identification of a Novel Macrophage Phenotype That Develops in Response to Atherogenic Phospholipids via Nrf2. *Circulation Research*, *107*, 737–746. https://doi.org/10.1161/CIRCRESAHA.109.215715

Kadoya, C., Domino, E. F., Yang, G.-Y. Y., Stern, J. D., & Betz, A. L. Preischemic but not postischemic zinc protoporphyrin treatment reduces infarct size and edema accumulation after temporary focal cerebral ischemia in rats., 26 Stroke § (1995). https://doi.org/https://doi.org/10.1161/str.26.6.1035

Kalaria, R. N. (2000). The role of cerebral ischemia in Alzheimer's disease. *Neurobiology of Aging*, *21*(2), 321–330. https://doi.org/10.1016/S0197-4580(00)00125-1

Kamphuis, W., Kooijman, L., Orre, M., Stassen, O., Pekny, M., & Hol, E. M. (2015). GFAP and vimentin deficiency alters gene expression in astrocytes and microglia in wild-type mice and changes the transcriptional response of reactive glia in mouse model for Alzheimer's disease. *Glia*, *63*(6), 1036–1056. https://doi.org/10.1002/glia.22800

Kanemitsu, H., Nakagomi, T., Tamura, A., Tsuchiya, T., Kono, G., & Sano, K. (2002). Differences in the Extent of Primary Ischemic Damage between Middle Cerebral Artery Coagulation and Intraluminal Occlusion Models. *Journal of Cerebral Blood Flow & Metabolism*, *22*(10), 1196–1204. https://doi.org/10.1097/01.wcb.0000037992.07114.95

Kang, J.-W., & Lee, S.-M. (2012). Melatonin inhibits type 1 interferon signaling of toll-like receptor 4 via heme oxygenase-1 induction in hepatic ischemia/reperfusion. *Journal of Pineal Research*, *53*(1), 67–76. https://doi.org/10.1111/j.1600-079X.2012.00972.x

Kannan, S., Muthusamy, V. R., Whitehead, K. J., Wang, L., Gomes, A. V, Litwin, S. E., … Rajasekaran, N. S. (2013). Nrf2 deficiency prevents reductive stress-induced hypertrophic cardiomyopathy. *Cardiovascular Research*, *100*(1), 63–73. https://doi.org/10.1093/cvr/cvt150

Kanninen, K., Heikkinen, R., Malm, T., Rolova, T., Kuhmonen, S., Leinonen, H., … Koistinaho, J. (2009). Intrahippocampal injection of a lentiviral vector expressing Nrf2 improves spatial learning in a mouse model of Alzheimer's disease. *Proceedings of the National Academy of Sciences of the United States of America*, *106*(38), 16505–16510. https://doi.org/10.1073/pnas.0908397106

Kanninen, K., Malm, T. M., Jyrkkänen, H. K., Goldsteins, G., Keksa-Goldsteine, V., Tanila, H., … Koistinaho, J. (2008). Nuclear factor erythroid 2-related factor 2 protects against beta

amyloid. *Molecular and Cellular Neuroscience*, *39*(3), 302–313. https://doi.org/10.1016/j.mcn.2008.07.010

Kemmerer, Z. A., Ader, N. R., Mulroy, S. S., & Eggler, A. L. (2015). Comparison of human Nrf2 antibodies : A tale of two proteins. *Toxicology Letters*, *238*(2), 83–89. https://doi.org/10.1016/j.toxlet.2015.07.004

Kennedy, K. A. M., Sandiford, S. D. E., Skerjanc, I. S., & Li, S. S.-C. (2012). Reactive oxygen species and the neuronal fate. *Cellular and Molecular Life Sciences*, *69*(2), 215–221. https://doi.org/10.1007/s00018-011-0807-2

Kensler, T. W., & Wakabayashi, N. (2010). Nrf2: friend or foe for chemoprevention? *Carcinogenesis*, *31*(1), 90–99. https://doi.org/10.1093/carcin/bgp231

Kensler, Thomas W, & Wakabayashi, N. (2010). Nrf2: friend or foe for chemoprevention? *Carcinogenesis*, *31*(1), 90–99. https://doi.org/10.1093/carcin/bgp231

Kernan, W. N., Ovbiagele, B., Black, H. R., Bravata, D. M., Chimowitz, M. I., Ezekowitz, M. D., … Wilson, J. A. (2014). Guidelines for the prevention of stroke in patients with stroke and transient ischemic attack: A guideline for healthcare professionals from the American Heart Association/American Stroke Association. *Stroke*, *45*(7), 2160–2236. https://doi.org/10.1161/STR.0000000000000024

Kerr, J. F., Wyllie, A. H., & Currie, A. R. (1972). Apoptosis: a basic biological phenomenon with wide-ranging implications in tissue kinetics. *British Journal of Cancer*, *26*(4), 239–257. https://doi.org/10.1038/bjc.1972.33

Khalilov, I., Esclapez, M., Medina, I., Aggoun, D., Lamsa, K., Leinekugel, X., … Ben-Ari, Y. (1997). A Novel In Vitro Preparation: the Intact Hippocampal Formation. *Neuron*, *19*(4), 743–749. https://doi.org/10.1016/S0896-6273(00)80956-3

Khandelwal, P., Yavagal, D. R., & Sacco, R. L. (2016). Acute Ischemic Stroke Intervention. *Journal of the American College of Cardiology*, *67*(22), 2631–2644. https://doi.org/10.1016/J.JACC.2016.03.555

Kiernan, M. C., Vucic, S., Cheah, B. C., Turner, M. R., Eisen, A., Hardiman, O., … Zoing, M. C. (2011). Amyotrophic lateral sclerosis. *Lancet (London, England)*, *377*(9769), 942–955. https://doi.org/10.1016/S0140-6736(10)61156-7

Kilkenny, C., Browne, W. J., Cuthill, I. C., Emerson, M., & Altman, D. G. (2010). Improving Bioscience Research Reporting : The ARRIVE Guidelines for Reporting Animal Research, *8*(6), 6–10. https://doi.org/10.1371/journal.pbio.1000412

Kissela, B. M., Khoury, J., Kleindorfer, D., Woo, D., Schneider, A., Alwell, K., … Broderick, J. P. (2005). Epidemiology of ischemic stroke in patients with diabetes: the greater Cincinnati/Northern Kentucky Stroke Study. *Diabetes Care*, *28*(2), 355–359. https://doi.org/10.2337/DIACARE.28.2.355

Klein, R. S., Lin, E., Zhang, B., Luster, A. D., Tollett, J., Samuel, M. A., … Diamond, M. S. (2005). Neuronal CXCL10 Directs CD8 T-Cell Recruitment and Control of West Nile Virus Encephalitis. *JOURNAL OF VIROLOGY*, *79*(17), 11457–11466. https://doi.org/10.1128/JVI.79.17.11457-11466.2005

Kliper, E., Bashat, D. Ben, Bornstein, N. M., Shenhar-Tsarfaty, S., Hallevi, H., Auriel, E., … Assayag, E. Ben. (2013). Cognitive decline after stroke: Relation to inflammatory biomarkers and hippocampal volume. *Stroke*, *44*(5), 1433–1435. https://doi.org/10.1161/STROKEAHA.111.000536

Klocke, F. J., Rosing, D. R., & Pittman, D. E. (1969). Inert gas measurements of coronary blood flow. *The American Journal of Cardiology*. https://doi.org/10.1016/0002-9149(69)90008-3

Knoflach, M., Matosevic, B., Rücker, M., Furtner, M., Mair, A., Wille, G., … Austrian Stroke Unit Registry Collaborators, F. the A. S. U. R. (2012). Functional recovery after ischemic stroke--a matter of age: data from the Austrian Stroke Unit Registry. *Neurology*, *78*(4),

279–285. https://doi.org/10.1212/WNL.0b013e31824367ab
Kobayashi, A., Kang, M.-I., Watai, Y., Tong, K. I., Shibata, T., Uchida, K., & Yamamoto, M. (2006). Oxidative and electrophilic stresses activate Nrf2 through inhibition of ubiquitination activity of Keap1. *Molecular and Cellular Biology*, *26*(1), 221–229. https://doi.org/10.1128/MCB.26.1.221-229.2006
Kobayashi, E. H., Suzuki, T., Funayama, R., Nagashima, T., Hayashi, M., Sekine, H., … Yamamoto, M. (2016). Nrf2 suppresses macrophage inflammatory response by blocking proinflammatory cytokine transcription. *Nature Communications*, *7*(May), 1–14. https://doi.org/10.1038/ncomms11624
Koenitzer, J. R., & Freeman, B. A. (2010). Redox signaling in inflammation: interactions of endogenous electrophiles and mitochondria in cardiovascular disease. *Annals of the New York Academy of Sciences*, *1203*, 45–52. https://doi.org/10.1111/j.1749-6632.2010.05559.x
Kohen, R. O. N., Yamamoto, Y., Cundy, K. C., & Ames, B. N. (1988). Antioxidant activity of carnosine , homocarnosine , and anserine present in muscle and brain, *85*(May), 3175–3179.
Koizumi, S., Hirayama, Y., & Morizawa, Y. M. (2018). New roles of reactive astrocytes in the brain; an organizer of cerebral ischemia. *Neurochemistry International*, 1–8. https://doi.org/10.1016/j.neuint.2018.01.007
Kokovay, E., Li, L., & Cunningham, L. A. (2006). Angiogenic recruitment of pericytes from bone marrow after stroke. *Journal of Cerebral Blood Flow & Metabolism*, *26*(4), 545–555. https://doi.org/10.1038/sj.jcbfm.9600214
Kondylis, V., Kumari, S., Vlantis, K., & Pasparakis, M. (2017). The interplay of IKK, NF-κB and RIPK1 signaling in the regulation of cell death, tissue homeostasis and inflammation. *Immunological Reviews*, *277*(1), 113–127. https://doi.org/10.1111/imr.12550
Konnova, E. A., & Swanberg, M. (2018). *Animal Models of Parkinson's Disease*. *Parkinson's Disease: Pathogenesis and Clinical Aspects*. Retrieved from http://www.ncbi.nlm.nih.gov/pubmed/30702844
Korn, S. H., Wouters, E. F., Vos, N., & Janssen-Heininger, Y. M. (2001). Cytokine-induced activation of nuclear factor-kappa B is inhibited by hydrogen peroxide through oxidative inactivation of IkappaB kinase. *The Journal of Biological Chemistry*, *276*(38), 35693–35700. https://doi.org/10.1074/jbc.M104321200
Kornienko, J. S., Smirnova, I. S., Pugovkina, N. A., Ivanova, J. S., Shilina, M. A., Grinchuk, T. M., … Lyublinskaya, O. G. (2019). High doses of synthetic antioxidants induce premature senescence in cultivated mesenchymal stem cells. *Scientific Reports*, *9*(1), 1296. https://doi.org/10.1038/s41598-018-37972-y
Kraft, A. D., Johnson, D. A., & Johnson, J. A. (2004). Nuclear Factor E2-Related Factor 2-Dependent Antioxidant Response Element Activation by tert -Butylhydroquinone and Sulforaphane Occurring Preferentially in Astrocytes Conditions Neurons against Oxidative Insult. *The Journal of Neuroscience*, *24*(5), 1101–1112. https://doi.org/10.1523/JNEUROSCI.3817-03.2004
Kunz, A., & Iadecola, C. (2009). Cerebral vascular dysregulation in the ischemic brain. *Handbook of Clinical Neurology*, *92*, 283. https://doi.org/10.1016/S0072-9752(08)01914-3
Kunze, R. (2017). Dimethyl fumarate for ischemic stroke. *Oncotarget*, 6–7.
Kunze, R., Urrutia, A. A., Hoffmann, A., Liu, H., Helluy, X., Pham, M., … Marti, H. H. (2015). Dimethyl fumarate attenuates cerebral edema formation by protecting the blood–brain barrier integrity. *Experimental Neurology*, *266*, 99–111. https://doi.org/10.1016/j.expneurol.2015.02.022
Kuraoka, M., Furuta, T., Matsuwaki, T., Omatsu, T., Ishii, Y., Kyuwa, S., & Yoshikawa, Y. (2009).

Direct Experimental Occlusion of the Distal Middle Cerebral Artery Induces High Reproducibility of Brain Ischemia in Mice. *Experimental Animals*, *58*(1), 19–29. https://doi.org/10.1538/expanim.58.19

Kwak, M.-K., Itoh, K., Yamamoto, M., & Kensler, T. W. (2002). Enhanced expression of the transcription factor Nrf2 by cancer chemopreventive agents: role of antioxidant response element-like sequences in the nrf2 promoter. *Molecular and Cellular Biology*, *22*(9), 2883–2892. https://doi.org/10.1128/MCB.22.9.2883-2892.2002

Lalancette-Hébert, M., Gowing, G., Simard, A., Weng, Y. C., & Kriz, J. (2007). Selective Ablation of Proliferating Microglial Cells Exacerbates Ischemic Injury in the Brain. *J Neuroscience*, *27*(10), 2596–2605. https://doi.org/10.1523/JNEUROSCI.5360-06.2007

Lanjakornsiripan, D., Pior, B. J., Kawaguchi, D., Furutachi, S., Tahara, T., Katsuyama, Y., … Gotoh, Y. (2018). Layer-specific morphological and molecular differences in neocortical astrocytes and their dependence on neuronal layers. *Nature Communications*, *9*(1). https://doi.org/10.1038/s41467-018-03940-3

LaPash Daniels, C. M., Austin, E. V. E. V., Rockney, D. E., Jacka, E. M., Hagemann, T. L., Johnson, D. A., … Messing, A. (2012). Beneficial Effects of Nrf2 Overexpression in a Mouse Model of Alexander Disease. *J Neuroscience*, *32*(31), 10507–10515. https://doi.org/10.1523/JNEUROSCI.1494-12.2012.Beneficial

LaPash Daniels, C. M., Austin, E. V. E. V. E. V. E. V. E. V. E. V. E. V., Rockney, D. E., Jacka, E. M., Hagemann, T. L., Johnson, D. A., … Messing, A. (2012). Beneficial Effects of Nrf2 Overexpression in a Mouse Model of Alexander Disease. *J Neuroscience*, *32*(31), 10507–10515. https://doi.org/10.1523/JNEUROSCI.1494-12.2012.Beneficial

Laurence, G. (2005). *Brodmann's Localisation in the Cerebral Cortex*. Boston, MA: Springer US. https://doi.org/10.1007/b138298

Lebel, C. P., & Bondy, S. C. (1991). Oxygen radicals: Common mediators of neurotoxicity. *Neurotoxicology and Teratology*, *13*(3), 341–346. https://doi.org/10.1016/0892-0362(91)90081-7

Lebkuechner, I., Wilhelmsson, U., Möllerström, E., Pekna, M., & Pekny, M. (2015). Heterogeneity of Notch signaling in astrocytes and the effects of GFAP and vimentin deficiency. *Journal of Neurochemistry*, *135*(2), 234–248. https://doi.org/10.1111/jnc.13213

Lee, H. K., Koh, S., Lo, D. C., & Marchuk, D. A. (2018). Neuronal IL-4Rα modulates neuronal apoptosis and cell viability during the acute phases of cerebral ischemia. *The FEBS Journal*, *285*(15), 2785–2798. https://doi.org/10.1111/febs.14498

Lee, J.-M. M., Calkins, M. J., Chan, K., Kan, Y. W., & Johnson, J. A. (2003). Identification of the NF-E2-related factor-2-dependent genes conferring protection against oxidative stress in primary cortical astrocytes using oligonucleotide microarray analysis. *Journal of Biological Chemistry*, *278*(14), 12029–12038. https://doi.org/10.1074/jbc.M211558200

Lee, J.-M. M., Shih, A. Y., Murphy, T. H., & Johnson, J. A. (2003). NF-E2-related factor-2 mediates neuroprotection against mitochondrial complex I inhibitors and increased concentrations of intracellular calcium in primary cortical neurons. *Journal of Biological Chemistry*, *278*(39), 37948–37956. https://doi.org/10.1074/jbc.M305204200

Lee, W.-H., Kumar, A., Rani, A., & Foster, T. C. (2014). Role of antioxidant enzymes in redox regulation of N-methyl-D-aspartate receptor function and memory in middle-aged rats. *Neurobiology of Aging*, *35*(6), 1459–1468. https://doi.org/10.1016/J.NEUROBIOLAGING.2013.12.002

Leger, M., Quiedeville, A., Bouet, V., Haelewyn, B., Boulouard, M., Schumann-Bard, P., & Freret, T. (2013). Object recognition test in mice. *Nature Protocols*, *8*(12), 2531–2537. https://doi.org/10.1038/nprot.2013.155

Lei, X., Lei, L., Zhang, Z., & Cheng, Y. (2016). Neuroprotective effects of lycopene

pretreatment on transient global cerebral ischemia-reperfusion in rats: The role of the Nrf2/HO-1 signaling pathway. *Molecular Medicine Reports*, *13*(1), 412–418. https://doi.org/10.3892/mmr.2015.4534

Leonardi, A., Chariot, A., Claudio, E., Cunningham, K., & Siebenlist, U. (2000). CIKS, a connection to Ikappa B kinase and stress-activated protein kinase. *Proceedings of the National Academy of Sciences*, *97*(19), 10494–10499. https://doi.org/10.1073/pnas.97.10.5243

Levine, D. A., Galecki, A. T., Langa, K. M., Unverzagt, F. W., Kabeto, M. U., Giordani, B., & Wadley, V. G. (2015). Trajectory of Cognitive Decline after Incident Stroke. *JAMA*, *314*(1), 41–51. https://doi.org/10.1001/jama.2015.6968

Lewington, S., Clarke, R., Qizilbash, N., Peto, R., & Collins., R. (2002). Age-specific relevance of usual blood pressure to vascular mortality: a meta-analysis of individual data for one million adults in 61 prospective studies. *The Lancet*, *360*(9349), 1903–1913. https://doi.org/10.1016/S0140-6736(02)11911-8

Li, H., Wang, P., Huang, F., Jin, J., Wu, H., Zhang, B., … Wu, X. (2018). Astragaloside IV protects blood-brain barrier integrity from LPS-induced disruption via activating Nrf2 antioxidant signaling pathway in mice. *Toxicology and Applied Pharmacology*, *340*, 58–66. https://doi.org/10.1016/J.TAAP.2017.12.019

Li, J., Johnson, D., Calkins, M., Wright, L., Svendsen, C., & Johnson, J. (2005). Stabilization of Nrf2 by tBHQ Confers Protection against Oxidative Stress-Induced Cell Death in Human Neural Stem Cells. *Toxicological Sciences*, *83*(2), 313–328. https://doi.org/10.1093/toxsci/kfi027

Li, L., Willets, R. S., Polidori, M. C., Stahl, W., Nelles, G., Sies, H., & Griffiths, H. R. (2010). Oxidative LDL modification is increased in vascular dementia and is inversely associated with cognitive performance. *Free Radical Research*, *44*(3), 241–248. https://doi.org/10.3109/10715760903440153

Li, Lisha, Peng, Y., Hui, Y., Zhang, S., Zhou, Y., Li, D., … Gao, X. (2015). Overexpression of Heme Oxygenase 1 Impairs Cognitive Ability and Changes the Plasticity of the Synapse. *Journal of Alzheimer's Disease*, *47*(3), 595–608. https://doi.org/10.3233/JAD-150027

Li, Lizhen, Lundkvist, A., Andersson, D., Wilhelmsson, U., Nagai, N., Pardo, A. C., … Pekny, M. (2008). Protective role of reactive astrocytes in brain ischemia. *Journal of Cerebral Blood Flow & Metabolism*, *28*, 468–481. https://doi.org/10.1038/sj.jcbfm.9600546

Li, S., Zheng, J., & Carmichael, S. T. (2005). Increased oxidative protein and DNA damage but decreased stress response in the aged brain following experimental stroke. *Neurobiology of Disease*, *18*(3), 432–440. https://doi.org/10.1016/j.nbd.2004.12.014

Li, W., Suwanwela, N. C., & Patumraj, S. (2016). Curcumin by down-regulating NF-kB and elevating Nrf2, reduces brain edema and neurological dysfunction after cerebral I/R. *Microvascular Research*, *106*, 117–127. https://doi.org/10.1016/j.mvr.2015.12.008

Liby, K., Hock, T., Yore, M. M., Suh, N., Place, A. E., Risingsong, R., … Sporn, M. B. (2005). The Synthetic Triterpenoids, CDDO and CDDO-Imidazolide, Are Potent Inducers of Heme Oxygenase-1 and Nrf2/ARE Signaling. *Cancer Research*, *65*(11), 4789–4798. https://doi.org/10.1158/0008-5472.CAN-04-4539

Liby, K. T., Yore, M. M., & Sporn, M. B. (2007). Triterpenoids and rexinoids as multifunctional agents for the prevention and treatment of cancer. *Nature Reviews Cancer*, *7*(5), 357–369. https://doi.org/10.1038/nrc2129

Liddell, J. (2017). Are Astrocytes the Predominant Cell Type for Activation of Nrf2 in Aging and Neurodegeneration? *Antioxidants*, *6*(3), 65. https://doi.org/10.3390/antiox6030065

Liddelow, S. A., & Barres, B. A. (2017). Reactive Astrocytes: Production, Function, and Therapeutic Potential. *Immunity*, *46*(6), 957–967.

https://doi.org/10.1016/j.immuni.2017.06.006
Liddelow, S. A., Guttenplan, K. A., Clarke, L. E., Bennett, F. C., Bohlen, C. J., Schirmer, L., … Wilton, D. K. (2017). Neurotoxic reactive astrocytes are induced by activated microglia. *Nature Publishing Group*. https://doi.org/10.1038/nature21029
Liedtke, W., Edelmann, W., Chiu, F.-C., Kucherlapati, R., & Raine, C. S. (1998). *Experimental Autoimmune Encephalomyelitis in Mice Lacking Glial Fibrillary Acidic Protein Is Characterized by a More Severe Clinical Course and an Infiltrative Central Nervous System Lesion*. *American Journal of Pathology* (Vol. 152). Retrieved from https://www.ncbi.nlm.nih.gov/pmc/articles/PMC1858102/pdf/amjpathol00013-0243.pdf
Lin, R., Cai, J., Kostuk, E. W., Rosenwasser, R., & Iacovitti, L. (2016). Fumarate modulates the immune / inflammatory response and rescues nerve cells and neurological function after stroke in rats. *Journal of Neuroinflammation*, 1–15. https://doi.org/10.1186/s12974-016-0733-1
Linder, C. C. (2006). Genetic Variables That Influence Phenotype. *ILAR Journal*, *47*(2), 132–140. https://doi.org/10.1093/ilar.47.2.132
Ling, J., Ji, H., Wang, X., Zhang, Y., Zhang, C., Song, H., … Qian, J. (2015). 5d, a novel analogue of 3-n-butylphthalide, protects brains against nervous injury induced by ischemia/reperfusion through Akt/Nrf2/NOX4 signaling pathway. *RSC Adv.*, *5*(85), 69583–69592. https://doi.org/10.1039/C5RA09941B
Lipton, P. (1999). Ischemic cell death in brain neurons. *Physiological Reviews*, *79*(4), 1431–1568. https://doi.org/10.1016/j.shpsa.2008.02.001
Liu, B., Teschemacher, A. G., & Kasparov, S. (2017). Astroglia as a cellular target for neuroprotection and treatment of neuro-psychiatric disorders. *Glia*, *65*(8), 1205–1226. https://doi.org/10.1002/glia.23136
Liu, D., Smith, C. L., Barone, F. C., Ellison, J. a, Lysko, P. G., Li, K., & Simpson, I. a. (1999). Astrocytic demise precedes delayed neuronal death in focal ischemic rat brain. *Molecular Brain Research*, *68*(1–2), 29–41. Retrieved from http://www.ncbi.nlm.nih.gov/pubmed/10320781
Liu, F., & Mccullough, L. D. (2011). Middle Cerebral Artery Occlusion Model in Rodents: Methods and Potential Pitfalls. *Journal of Biomedicine and Biotechnology*, *2011*. https://doi.org/10.1155/2011/464701
Liu, L., Vollmer, M. K., Ahmad, A. S., Fernandez, V. M., Kim, H., & Doré, S. (2019). Pretreatment with Korean red ginseng or dimethyl fumarate attenuates reactive gliosis and confers sustained neuroprotection against cerebral hypoxic-ischemic damage by an Nrf2-dependent mechanism. *Free Radical Biology and Medicine*, *131*, 98–114. https://doi.org/10.1016/J.FREERADBIOMED.2018.11.017
Liu, R., Pan, M.-X., Tang, J.-C., Zhang, Y., Liao, H.-B., Zhuang, Y., … Wan, Q. (2017). Role of neuroinflammation in ischemic stroke. *Neuroimmunol Neuroinflammation*, *4*, 158–166. https://doi.org/10.20517/2347-8659.2017.09
Liu, X., Liu, J., Zhao, S., Zhang, H., Cai, W., Cai, M., … Hu, X. (2016). Interleukin-4 Is Essential for Microglia/Macrophage M2 Polarization and Long-Term Recovery after Cerebral Ischemia. *Stroke*, *47*(2), 498–504. https://doi.org/10.1161/STROKEAHA.115.012079
Liu, Zhongwu, & Chopp, M. (2016). Astrocytes, therapeutic targets for neuroprotection and neurorestoration in ischemic stroke. *Progress in Neurobiology*, *144*, 103–120. https://doi.org/10.1016/j.pneurobio.2015.09.008
Liu, Zhongwu, Li, Y., Cui, Y., Roberts, C., Lu, M., Wilhelmsson, U., … Chopp, M. (2014). Beneficial Effects of GFAP/Vimentin Reactive Astrocytes for Axonal Remodeling and Motor Behavioral Recovery in Mice after Stroke. *Glia*, *62*(12), 2022–2033. https://doi.org/10.1111/j.1743-6109.2008.01122.x.Endothelial

Liu, Zongjian, Ran, Y., Huang, S., Wen, S., Zhang, W., Liu, X., … Huang, T.-T. (2017). Curcumin Protects against Ischemic Stroke by Titrating Microglia/Macrophage Polarization. *Frontiers in Aging Neuroscience*, *9*, 233. https://doi.org/10.3389/fnagi.2017.00233

Loboda, A., Damulewicz, M., Pyza, E., Jozkowicz, A., & Dulak, J. (2016). Role of Nrf2 / HO-1 system in development , oxidative stress response and diseases : an evolutionarily conserved mechanism. *Cellular and Molecular Life Sciences*, *73*(17), 3221–3247. https://doi.org/10.1007/s00018-016-2223-0

Luca, M., Luca, A., & Calandra, C. (2015). The Role of Oxidative Damage in the Pathogenesis and Progression of Alzheimer's Disease and Vascular Dementia. *Oxidative Medicine and Cellular Longevity*, *2015*(1), 504678. https://doi.org/10.1155/2015/504678

Lucas, D. R., & Newhouse, J. P. (1957). The toxic effect of sodium L-glutamate on the inner layers of the retina. *A.M.A. Archives of Ophthalmology*, *58*(2), 193–201. Retrieved from http://www.ncbi.nlm.nih.gov/pubmed/13443577

Lucas, S.-M., Rothwell, N. J., & Gibson, R. M. (2006). The role of inflammation in CNS injury and disease. *British Journal of Pharmacology*, *147*(S1), S232–S240. https://doi.org/10.1038/sj.bjp.0706400

Luitse, M. J. A., Biessels, G. J., Rutten, G. E. H. M., & Kappelle, L. J. (2012). Diabetes, hyperglycaemia, and acute ischaemic stroke. *The Lancet Neurology*, *11*(3), 261–271. https://doi.org/10.1016/S1474-4422(12)70005-4

Lukaszevicz, A.-C., Sampaïo, N., Guégan, C., Benchoua, A., Couriaud, C., Chevalier, E., … Onténiente, B. (2002). High Sensitivity of Protoplasmic Cortical Astroglia to Focal Ischemia. *Journal of Cerebral Blood Flow & Metabolism*, *22*(3), 289–298. https://doi.org/10.1097/00004647-200203000-00006

Ma, Q. (2013). Role of Nrf2 in Oxidative Stress and Toxicity. *Annu. Rev. Pharmacol. Toxicol*, *53*, 401–426. https://doi.org/10.1146/annurev-pharmtox-011112-140320

Ma, Q., & He, X. (2012). Molecular basis of electrophilic and oxidative defense: promises and perils of Nrf2. *Pharmacological Reviews*, *64*(4), 1055–1081. https://doi.org/10.1124/pr.110.004333

Macciocchi, S. N., Diamond, P. T., Alves, W. M., & Mertz, T. (1998). Ischemic stroke: Relation of age, lesion location, and initial neurologic deficit to functional outcome. *Archives of Physical Medicine and Rehabilitation*, *79*(10), 1255–1257. https://doi.org/10.1016/S0003-9993(98)90271-4

Mackensen, G. B., Patel, M., Sheng, H., Calvi, C. L., Batinić-Haberle, I., Day, B. J., … Warner, D. S. (2001). Neuroprotection from Delayed Postischemic Administration of a Metalloporphyrin Catalytic Antioxidant. *Journal of Neuroscience*, *21*(13), 4582–4592. https://doi.org/10.1523/JNEUROSCI.21-13-04582.2001

Macrae, I. M., & Allan, S. M. (2018). Stroke: The past, present and future. *Brain and Neuroscience Advances*, *2*, 239821281881068. https://doi.org/10.1177/2398212818810689

Macrez, R., Obiang, P., Gauberti, M., Roussel, B., Baron, A., Parcq, J., … Ali, C. (2011). Antibodies Preventing the Interaction of Tissue-Type Plasminogen Activator With N-Methyl-d-Aspartate Receptors Reduce Stroke Damages and Extend the Therapeutic Window of Thrombolysis. *Stroke*, *42*(8). Retrieved from http://stroke.ahajournals.org/content/42/8/2315.long

Maeda, K., Hata, R., & Hossmann, K.-A. A. (1998). Differences in the cerebrovascular anatomy of C57Black/6 and SV129 mice. *NeuroReport*, *9*(7), 1317–1319. https://doi.org/10.1097/00001756-199805110-00012

Magaki, S. D., Williams, C. K., & Vinters, H. V. (2018). Glial function (and dysfunction) in the normal & ischemic brain. *Neuropharmacology*, *134*, 218–225. https://doi.org/10.1016/J.NEUROPHARM.2017.11.009

Magesh, S., Chen, Y., & Hu, L. (2012). Small Molecule Modulators of Keap1-Nrf2-ARE Pathway as Potential Preventive and Therapeutic Agents. *Medicinal Research Reviews*, *32*(4), 687–726. https://doi.org/10.1002/med

Magistretti, P. J., & Allaman, I. (2015). A Cellular Perspective on Brain Energy Metabolism and Functional Imaging. *Neuron*, *86*(4), 883–901. https://doi.org/10.1016/J.NEURON.2015.03.035

Mandal, P. K., Seiler, A., Perisic, T., Kölle, P., Banjac Canak, A., Förster, H., … Conrad, M. (2010). System x(c)- and thioredoxin reductase 1 cooperatively rescue glutathione deficiency. *The Journal of Biological Chemistry*, *285*(29), 22244–22253. https://doi.org/10.1074/jbc.M110.121327

Mangialasche, F., Polidori, M. C., Monastero, R., Ercolani, S., Camarda, C., Cecchetti, R., & Mecocci, P. (2009). Biomarkers of oxidative and nitrosative damage in Alzheimer's disease and mild cognitive impairment. *Ageing Research Reviews*, *8*(4), 285–305. https://doi.org/10.1016/j.arr.2009.04.002

Manwani, B., Liu, F., & .. (2011). Functional recovery in aging mice after experimental stroke. *Brain Behav Immun.*, *25*(8), 1689–1700. https://doi.org/10.1016/j.bbi.2011.06.015.Functional

Mao, L., Yang, T., Li, X., Lei, X., Sun, Y., Zhao, Y., … Zhang, F. (2018). Protective effects of sulforaphane in experimental vascular cognitive impairment: Contribution of the Nrf2 pathway. *Journal of Cerebral Blood Flow & Metabolism*, 0271678X1876408. https://doi.org/10.1177/0271678X18764083

Martin, L. J., Al-Abdulla, N. A., Brambrink, A. M., Kirsch, J. R., Sieber, F. E., & Portera-Cailliau, C. (1998). Neurodegeneration in Excitotoxicity, Global Cerebral Ischemia, and Target Deprivation: A Perspective on the Contributions of Apoptosis and Necrosis. *Brain Research Bulletin*, *46*(4), 281–309. https://doi.org/10.1016/S0361-9230(98)00024-0

Masuda, T., Sankowski, R., Staszewski, O., Böttcher, C., Amann, L., Scheiwe, C., … Prinz, M. (2019). Spatial and temporal heterogeneity of mouse and human microglia at single-cell resolution. *Nature*, *566*(7744), 388. https://doi.org/10.1038/s41586-019-0924-x

Matias, I., Morgado, J., & Gomes, F. C. A. (2019). Astrocyte Heterogeneity: Impact to Brain Aging and Disease. *Frontiers in Aging Neuroscience*, *11*, 59. https://doi.org/10.3389/fnagi.2019.00059

Matsuo, Y., Kihara, T., Ikeda, M., Ninomiya, M., Onodera, H., & Kogure, K. (1995). Role of Neutrophils in Radical Production during Ischemia and Reperfusion of the Rat Brain: Effect of Neutrophil Depletion on Extracellular Ascorbyl Radical Formation. *Journal of Cerebral Blood Flow & Metabolism*, *15*(6), 941–947. https://doi.org/10.1038/jcbfm.1995.119

Matsushima, K., Schmidt-Kastner, R., Hogan, M. J., & Hakim, A. M. (1998). Cortical spreading depression activates trophic factor expression in neurons and astrocytes and protects against subsequent focal brain ischemia. *Brain Research*, *807*(1–2), 47–60. https://doi.org/10.1016/S0006-8993(98)00716-1

McCabe, C., Arroja, M. M., Reid, E., & Macrae, I. M. (2018). Animal models of ischaemic stroke and characterisation of the ischaemic penumbra. *Neuropharmacology*, *134*, 169–177. https://doi.org/10.1016/J.NEUROPHARM.2017.09.022

McColl, B. W., Carswell, H. V., McCulloch, J., & Horsburgh, K. (2004). Extension of cerebral hypoperfusion and ischaemic pathology beyond MCA territory after intraluminal filament occlusion in C57Bl/6J mice. *Brain Research*, *997*(1), 15–23. https://doi.org/10.1016/J.BRAINRES.2003.10.028

Mcdonough, A., Richard, X., Lee, V., Noor, S., Lee, X. C., Le, T., … Weinstein, J. R. (2017). Neurobiology of Disease Ischemia/Reperfusion Induces Interferon-Stimulated Gene Expression in Microglia. *J Neuroscience*, *37*(34), 8292–8308.

https://doi.org/10.1523/JNEUROSCI.0725-17.2017
McMahon, M., Itoh, K., Yamamoto, M., Chanas, S. A., Henderson, C. J., McLellan, L. I., … Hayes, J. D. (2001). The Cap'n'Collar basic leucine zipper transcription factor Nrf2 (NF-E2 p45-related factor 2) controls both constitutive and inducible expression of intestinal detoxification and glutathione biosynthetic enzymes. *Cancer Research*, *61*(8), 3299–3307. Retrieved from http://www.ncbi.nlm.nih.gov/pubmed/11309284
McManus, M., & Liebeskind, D. S. (2016). Blood Pressure in Acute Ischemic Stroke. *Journal of Clinical Neurology (Seoul, Korea)*, *12*(2), 137. https://doi.org/10.3988/JCN.2016.12.2.137
McNaught, K. S. P., & Jenner, P. (1999). Altered Glial Function Causes Neuronal Death and Increases Neuronal Susceptibility to 1-Methyl-4-Phenylpyridinium- and 6-Hydroxydopamine-Induced Toxicity in Astrocytic/Ventral Mesencephalic Co-Cultures. *Journal of Neurochemistry*, *73*(6), 2469–2476. https://doi.org/10.1046/j.1471-4159.1999.0732469.x
Meister, A. (1995). [1] Glutathione metabolism. *Methods in Enzymology*, *251*, 3–7. https://doi.org/10.1016/0076-6879(95)51106-7
Memezawa, H., Smith, M. L., & Siesjö, B. K. (1992). Penumbral tissues salvaged by reperfusion following middle cerebral artery occlusion in rats. *Stroke*, *23*(4), 552–559. https://doi.org/10.1161/01.STR.23.4.552
Mercatelli, R., Lana, D., Bucciantini, M., Giovannini, M. G., Cerbai, F., Quercioli, F., … Nosi, D. (2016). Clasmatodendrosis and b-amyloidosis in aging hippocampus. *FASEB Journal*, *30*(4), 1480–1491. https://doi.org/10.1096/fj.15-275503
Michell-Robinson, M. A., Moore, C. S., Healy, L. M., Osso, L. A., Zorko, N., Grouza, V., … Antel, J. P. (2016). Effects of fumarates on circulating and CNS myeloid cells in multiple sclerosis. *Annals of Clinical and Translational Neurology*, *3*(1), 27–41. https://doi.org/10.1002/acn3.270
Miller, R. H., & Raff, M. C. (1984). Fibrous and protoplasmic astrocytes are biochemically and developmentally distinct. *The Journal of Neuroscience : The Official Journal of the Society for Neuroscience*, *4*(2), 585–592. https://doi.org/10.1523/JNEUROSCI.04-02-00585.1984
Miller, V. V. M. M., Lawrence, D. A. A., Mondal, T. K. K. T., & Seegal, R. R. F. F. (2009). Reduced glutathione is highly expressed in white matter and neurons in the unperturbed mouse brain - implications for oxidative stress associated with neurodegeneration. *Brain Research*, *1276*, 22–30. https://doi.org/10.1016/j.brainres.2009.04.029
Mills Ko, E., Ma, J. H., Guo, F., Miers, L., Lee, E., Bannerman, P., … Pleasure, D. (2014). Deletion of astroglial CXCL10 delays clinical onset but does not affect progressive axon loss in a murine autoimmune multiple sclerosis model. *Journal of Neuroinflammation*, *11*(105). https://doi.org/10.1186/1742-2094-11-105
Min, K.-J., Yang, M., Kim, S.-U., Jou, I., & Joe, E. (2006). Astrocytes Induce Hemeoxygenase-1 Expression in Microglia: A Feasible Mechanism for Preventing Excessive Brain Inflammation. *Journal of Neuroscience*, *26*(6), 1880–1887. https://doi.org/10.1523/JNEUROSCI.3696-05.2006
Minett, T., Classey, J., Matthews, F. E., Fahrenhold, M., Taga, M., Brayne, C., … Boche, D. (2016). Microglial immunophenotype in dementia with Alzheimer's pathology. *Journal of Neuroinflammation*, *13*(1), 1–10. https://doi.org/10.1186/s12974-016-0601-z
Mink, J. W., Blumenschine, R. J., & Adams, D. B. Ratio of central nervous system to body metabolism in vertebrates: Its constancy and functional basis, 10 American Journal of Physiology - Regulatory Integrative and Comparative Physiology § (1981). https://doi.org/10.1152/ajpregu.1981.241.3.r203
Moehlenkamp, J. D., & Johnson, J. A. (1999). Activation of Antioxidant/Electrophile-

Responsive Elements in IMR-32 Human Neuroblastoma Cells. *Archives of Biochemistry and Biophysics*, *363*(1), 98–106. https://doi.org/10.1006/ABBI.1998.1046

Moi, P., Chan, K., Asunis, I., Cao, A., & Kan, Y. W. (1994). Isolation of NF-E2-related factor 2 (Nrf2), a NF-E2-like basic leucine zipper transcriptional activator that binds to the tandem NF-E2/AP1 repeat of the beta-globin locus control region. *Proceedings of the National Academy of Sciences of the United States of America*, *91*(21), 9926–9930. https://doi.org/10.1073/pnas.91.21.9926

Mokin, M., Abou-Chebl, A., Castonguay, A. C., Nogueira, R. G., English, J. D., Farid, H., … Zaidat, O. O. (2018). Real-world stent retriever thrombectomy for acute ischemic stroke beyond 6 hours of onset: analysis of the NASA and TRACK registries. *Journal of NeuroInterventional Surgery*, neurintsurg-2018-014272. https://doi.org/10.1136/NEURINTSURG-2018-014272

Molcho, L., Ben-Zur, T., Barhum, Y., Angel, A., Glat, M., & Offen, D. (2018). Combined Gene Therapy to Reduce the Neuronal Damage in the Mouse Model of Focal Ischemic Injury. *Journal of Molecular Neuroscience*, 1–8. https://doi.org/10.1007/s12031-018-1143-x

Montarolo, P. G., Boelet, P., Castellucci, V. F., Morgan, J., Kandel, E. R., & Schachert, S. (1986). A Critical Period for Macromolecular Synthesis. *Science*, *234*(October), 1249–1254.

Morel, L., Men, Y., Chiang, M. S. R., Tian, Y., Jin, S., Yelick, J., … Yang, Y. (2018). Intracortical astrocyte subpopulations defined by astrocyte reporter Mice in the adult brain. *Glia*. https://doi.org/10.1002/glia.23545

Morioka, T., Kalehua, A. N., & Streit, W. J. (1993). Characterization of microglial reaction after middle cerebral artery occlusion in rat brain. *The Journal of Comparative Neurology*, *327*(1), 123–132. https://doi.org/10.1002/cne.903270110

Morizawa, Y. M., Hirayama, Y., Ohno, N. N. N. N., Shibata, S., Shigetomi, E., Sui, Y., … Koizumi, S. (2017). Reactive astrocytes function as phagocytes after brain ischemia via ABCA1-mediated pathway. *Nature Communications*, *8*(1), 1–15. https://doi.org/10.1038/s41467-017-00037-1

Morrice, J., Gregory-Evans, C., & Shaw, C. (2018). Animal models of amyotrophic lateral sclerosis: A comparison of model validity. *Neural Regeneration Research*, *13*(12), 2050. https://doi.org/10.4103/1673-5374.241445

Morris, G. P., Wright, A. L., Tan, R. P., Gladbach, A., Ittner, L. M., Vissel, B., & Annunziato, L. (2016). A Comparative Study of Variables Influencing Ischemic Injury in the Longa and Koizumi Methods of Intraluminal Filament Middle Cerebral Artery Occlusion in Mice. *PLOS ONE*, *11*(2), e0148503. https://doi.org/10.1371/journal.pone.0148503

Morris, R. (1984). Developments of a water-maze procedure for studying spatial learning in the rat. *Journal of Neuroscience Methods*, *11*(1), 47–60. https://doi.org/10.1016/0165-0270(84)90007-4

Morris, R. S., Jones, P. S., Alawneh, J. A., Hong, Y. T., Fryer, T. D., Aigbirhio, F. I., … Baron, J. (2018). Relationships between selective neuronal loss and microglial activation after ischaemic stroke in man. *Brain*, *141*(May), 2089–2111. https://doi.org/10.1093/brain/awy121

Morrison, H. W., & Filosa, J. A. (2013). A quantitative spatiotemporal analysis of microglia morphology during ischemic stroke and reperfusion. *Journal of Neuroinflammation*, *10*(1), 1. https://doi.org/10.1186/1742-2094-10-4

Moskowitz, M. A., Lo, E. H., & Iadecola, C. (2010). The science of stroke: Mechanisms in search of treatments. *Neuron*, *67*(2), 181–198. https://doi.org/10.1016/j.neuron.2010.07.002

Mozaffarian, D., Benjamin, E. J., Go, A. S., Arnett, D. K., Blaha, M. J., Cushman, M., … Stroke Statistics Subcommittee. (2016). Heart Disease and Stroke Statistics—2016 Update. *Circulation*, *133*(4), e38–e360. https://doi.org/10.1161/CIR.0000000000000350

Mulcahy, N. J., Ross, J., Rothwell, N. J., & Loddick, S. A. (2003). Delayed administration of

interleukin-1 receptor antagonist protects against transient cerebral ischaemia in the rat. *British Journal of Pharmacology*, *140*, 471–476. https://doi.org/10.1038/sj.bjp.0705462

Murphy, T. H., Yu, J., Ng, R., Johnson, D. A., Shen, H., Honey, C. R., & Johnson, J. A. (2001). Preferential expression of antioxidant response element mediated gene expression in astrocytes. *Journal of Neurochemistry*, *76*(6), 1670–1678. https://doi.org/10.1046/j.1471-4159.2001.00157.x

Muruet, W., Rudd, A., Wolfe, C. D. A., & Douiri, A. (2018). Long-Term Survival After Intravenous Thrombolysis for Ischemic Stroke: A Propensity Score-Matched Cohort With up to 10-Year Follow-Up. *Stroke*, *49*(3), 607–613. https://doi.org/10.1161/STROKEAHA.117.019889

Naito, Y., Takagi, T., & Higashimura, Y. (2014). Heme oxygenase-1 and anti-inflammatory M2 macrophages. *ARCHIVES OF BIOCHEMISTRY AND BIOPHYSICS*, *564*, 83–88. https://doi.org/10.1016/j.abb.2014.09.005

Nakamichi, K., Inoue, S., Takasaki, T., Morimoto, K., & Kurane, I. (2004). Rabies virus stimulates nitric oxide production and CXC chemokine ligand 10 expression in macrophages through activation of extracellular signal-regulated kinases 1 and 2. *Journal of Virology*, *78*(17), 9376–9388. https://doi.org/10.1128/JVI.78.17.9376-9388.2004

Narasimhalu, K., Lee, J., Leong, Y. L., Ma, L., De Silva, D. A., Wong, M. C., … Chen, C. (2015). Inflammatory markers and their association with post stroke cognitive decline. *International Journal of Stroke*, *10*(4), 513–518. https://doi.org/10.1111/ijs.12001

Narayanan, S. V., Dave, K. R., Saul, I., & Perez-pinzon, M. A. (2015). Resveratrol Preconditioning Protects Against Cerebral Ischemic Injury via Nuclear Erythroid 2-Related Factor 2. *Stroke*, *46*(6), 1626–1632. https://doi.org/10.1161/STROKEAHA.115.008921

National Institute of Neurological Disorders and Stroke rt-PA Stroke Study Group. (1995). Tissue Plasminogen Activator for Acute Ischemic Stroke. *New England Journal of Medicine*, *333*(24), 1581–1588. https://doi.org/10.1056/NEJM199512143332401

Neuhaus, A. A., Couch, Y., Hadley, G., & Buchan, A. M. (2017). Neuroprotection in stroke: T he importance of collaboration and reproducibility. *Brain*, *140*(8), 2079–2092. https://doi.org/10.1093/brain/awx126

Nguyen, T.-V. V, Hayes, M., Zbesko, J. C., Frye, J. B., Congrove, N. R., Belichenko, N. P., … Doyle, K. P. (2018). Alzheimer's associated amyloid and tau deposition co-localizes with a homeostatic myelin repair pathway in two mouse models of post-stroke mixed dementia. *Acta Neuropathologica Communications*, *6*(1), 100. https://doi.org/10.1186/s40478-018-0603-4

Nihashi, T., Inao, S., Kajita, Y., Kawai, T., Sugimoto, T., Niwa, M., … Yoshida, J. (2001). Expression and distribution of beta amyloid precursor protein and beta amyloid peptide in reactive astrocytes after transient middle cerebral artery occlusion. *Acta Neurochir (Wien)*, *143*(3), 287–295. Retrieved from http://www.ncbi.nlm.nih.gov/entrez/query.fcgi?cmd=Retrieve&db=PubMed&dopt=Citation&list_uids=11460917

Noben-Trauth, N., Shultz, L. D., Brombacher, F., Urban, J. F., Gu, H., & Paul, W. E. (1997). An interleukin 4 (IL-4)-independent pathway for CD4+ T cell IL-4 production is revealed in IL-4 receptor-deficient mice. *Proceedings of the National Academy of Sciences of the United States of America*, *94*(20), 10838–10843. https://doi.org/10.1073/PNAS.94.20.10838

Nogueira, R. G., Jadhav, A. P., Haussen, D. C., Bonafe, A., Budzik, R. F., Bhuva, P., … Jovin, T. G. (2017). Thrombectomy 6 to 24 Hours after Stroke with a Mismatch between Deficit

and Infarct. *New England Journal of Medicine*, *378*(1), 11–21. https://doi.org/10.1056/nejmoa1706442

Norden, D. M., Fenn, A. M., Dugan, A., & Godbout, J. P. (2014). TGFβ produced by IL-10 redirected astrocytes attenuates microglial activation. *Glia*, *62*(6), 881–895. https://doi.org/10.1002/glia.22647

Nunomura, A., Perry, G., Pappolla, M. A., Wade, R., Hirai, K., Chiba, S., & Smith, M. A. (1999). RNA Oxidation Is a Prominent Feature of Vulnerable Neurons in Alzheimer ' s Disease, *19*(6), 1959–1964.

O'Brien, J. T., Erkinjuntti, T., Reisberg, B., Roman, G., Sawada, T., Pantoni, L., … DeKosky, S. T. (2003). Vascular cognitive impairment. *The Lancet Neurology*, *2*(2), 89–98. https://doi.org/10.1016/S1474-4422(03)00305-3

O'Mealey, G. B., Berry, W. L., & Plafker, S. M. (2017). Sulforaphane is a Nrf2-independent inhibitor of mitochondrial fission. *Redox Biology*, *11*, 103–110. https://doi.org/10.1016/j.redox.2016.11.007

O'Sullivan, S. B., & Schmitz, T. J. (2007). *Physical rehabilitation*. F.A. Davis. Retrieved from https://books.google.fr/books/about/Physical_Rehabilitation.html?id=_LNmQgAACAAJ&redir_esc=y

Obrenovich, M. E., Smith, M. A., Siedlak, S. L., Chen, S. G., De La Torre, J. C., Perry, G., & Aliev, G. (2006). Overexpression of GRK2 in alzheimer disease and in a chronic hypoperfusion rat model is an early marker of brain mitochondrial lesions. *Neurotoxicity Research*, *10*(1), 43–56. https://doi.org/10.1007/BF03033333

Ohira, T., Shahar, E., Chambless, L. E., Rosamond, W. D., Mosley, T. H., & Folsom, A. R. (2006). Risk Factors for Ischemic Stroke Subtypes The Atherosclerosis Risk in Communities Study. *Stroke*, *37*(10), 2493–2498. https://doi.org/10.1161/01.STR.0000239694.19359.88

Okada, S., Nakamura, M., Katoh, H., Miyao, T., Shimazaki, T., Ishii, K., … Okano, H. (2006). Conditional ablation of Stat3 or Socs3 discloses a dual role for reactive astrocytes after spinal cord injury. *Nature Medicine*, *12*(7), 829–834. https://doi.org/10.1038/nm1425

Oki, K., Kaneko, N., Kanki, H., Imai, T., Suzuki, N., Sawamoto, K., & Okano, H. (2010). Musashi1 as a marker of reactive astrocytes after transient focal brain ischemia. *Neuroscience Research*, *66*(4), 390–395. https://doi.org/10.1016/J.NEURES.2009.12.013

Oladiran, O., & Nwosu, I. (2019). Stroke risk stratification in atrial fibrillation: a review of common risk factors. *Journal of Community Hospital Internal Medicine Perspectives*, *9*(2), 113–120. https://doi.org/10.1080/20009666.2019.1593781

Olguín-Albuerne, M., & Morán, J. (2018). Redox Signaling Mechanisms in Nervous System Development. *Antioxidants & Redox Signaling*, *28*(18), 1603–1625. https://doi.org/10.1089/ars.2017.7284

Olmez, I., & Ozyurt, H. (2012). Reactive oxygen species and ischemic cerebrovascular disease. *Neurochemistry International*, *60*(2), 208–212. https://doi.org/10.1016/j.neuint.2011.11.009

Olney, J. W. (1969). Brain lesions, obesity, and other disturbances in mice treated with monosodium glutamate. *Science (New York, N.Y.)*, *164*(3880), 719–721. https://doi.org/10.1126/science.164.3880.719

Omura, T., Tanaka, Y., Miyata, N., Koizumi, C., Sakurai, T., Fukasawa, M., … Roman, R. J. (2006). Effect of a New Inhibitor of the Synthesis of 20-HETE on Cerebral Ischemia Reperfusion Injury. *Stroke*, *37*(5), 1307–1313. https://doi.org/10.1161/01.STR.0000217398.37075.07

Orset, C., Macrez, R., Young, A. R., Panthou, D., Angles-Cano, E., Maubert, E., … Vivien, D. (2007). Mouse Model of In Situ Thromboembolic Stroke and Reperfusion. *Stroke*, *38*(10), 2771–2778. https://doi.org/10.1161/STROKEAHA.107.487520

Orsini, F., Villa, P., Parrella, S., Zangari, R., Zanier, E. R., Gesuete, R., … De Simoni, M.-G. (2012). Targeting mannose-binding lectin confers long-lasting protection with a surprisingly wide therapeutic window in cerebral ischemia. *Circulation*, *126*(12), 1484–1494. https://doi.org/10.1161/CIRCULATIONAHA.112.103051

Ovanesov, M. V, Ayhan, Y., Wolbert, C., Moldovan, K., Sauder, C., & Pletnikov, M. V. (2008). Astrocytes play a key role in activation of microglia by persistent Borna disease virus infection. *Journal of Neuroinflammation*, *5*(1), 50. https://doi.org/10.1186/1742-2094-5-50

Ozkul, A., Akyol, A., Yenisey, C., Arpaci, E., Kiylioglu, N., & Tataroglu, C. (2007). Oxidative stress in acute ischemic stroke. *Journal of Clinical Neuroscience*, *14*(11), 1062–1066. https://doi.org/10.1016/J.JOCN.2006.11.008

Paciaroni, M., Caso, V., & Agnelli, G. (2009). The Concept of Ischemic Penumbra in Acute Stroke and Therapeutic Opportunities. *European Neurology*, *61*(6), 321–330. https://doi.org/10.1159/000210544

Panizzon, K. L., Dwyer, B. E., Nishimura, R. N., & Wallis, R. A. (1996). Neuroprotection against CA1 injury with metalloporphyrins. *Neuroreport*, *7*(2), 662–666. Retrieved from http://www.ncbi.nlm.nih.gov/pubmed/8730852

Park, J. H., Cho, J. H., Ahn, J. H., Choi, S. Y., Lee, T.-K., Lee, J.-C., … Kang, I. J. (2018). Neuronal loss and gliosis in the rat striatum subjected to 15 and 30 minutes of middle cerebral artery occlusion. *Metabolic Brain Disease*, *33*(3), 775–784. https://doi.org/10.1007/s11011-018-0192-8

Parodi, B., Rossi, S., Morando, S., Cordano, C., Bragoni, A., Motta, C., … Uccelli, A. (2015). Fumarates modulate microglia activation through a novel HCAR2 signaling pathway and rescue synaptic dysregulation in inflamed CNS. *Acta Neuropathologica*, *130*(2), 279–295. https://doi.org/10.1007/s00401-015-1422-3

Patel, A., Berdunov, V., King, D., Quayyum, Z., Wittenberg, R., & Knapp, M. (2017). Current, future and avoidable costs of stroke in the UK Part 2: Societal costs of stroke in the next 20 years and potential returns from increased spending on research. *Stroke Association*, 12. Retrieved from https://www.stroke.org.uk/sites/default/files/costs_of_stroke_in_the_uk_report_-executive_summary_part_2.pdf

Patel, A. R., Ritzel, R., Mccullough, L. D., & Liu, F. (2013). Microglia and ischemic stroke : a double-edged sword. *International Journal of Physiology, Pathophysiology and Pharmacology*, *5*(2), 73–90.

Pedrono, E., Durukan, A., Strbian, D., Marinkovic, I., Shekhar, S., Pitkonen, M., … Tatlisumak, T. An Optimized Mouse Model for Transient Ischemic Attack, 69 Journal of Neuropathology & Experimental Neurology § (2010). https://doi.org/10.1097/NEN.0b013e3181cd331c

Pekna, M., Pekny, M., Porritt, M. J., Andersson, H. C., Hou, L., & Nilsson, M. (2012). Photothrombosis-Induced Infarction of the Mouse Cerebral Cortex Is Not Affected by the Nrf2-Activator Sulforaphane. *PloS One*, *7*(7), 17–19. https://doi.org/10.1371/journal.pone.0041090

Pekny, M., & Nilsson, M. (2005). Astrocyte activation and reactive gliosis. *Glia*, *50*(4), 427–434. https://doi.org/10.1002/glia.20207

Pekny, M., & Pekna, M. (2004). Astrocyte intermediate filaments in CNS pathologies and regeneration. *The Journal of Pathology*, *204*(4), 428–437. https://doi.org/10.1002/path.1645

Pekny, M., Pekna, M., Messing, A., Steinhäuser, C., Lee, J. M., Parpura, V., … Verkhratsky, A. (2016). Astrocytes: a central element in neurological diseases. *Acta Neuropathologica*, *131*(3), 323–345. https://doi.org/10.1007/s00401-015-1513-1

Pekny, M., Wilhelmsson, U., Tatlisumak, T., & Pekna, M. (2019). Astrocyte activation and reactive gliosis—A new target in stroke? *Neuroscience Letters*, *689*(July 2018), 45–55. https://doi.org/10.1016/j.neulet.2018.07.021

Pellegrini, G. G., Cregor, M., McAndrews, K., Morales, C. C., McCabe, L. D., McCabe, G. P., … Bellido, T. (2017). Nrf2 regulates mass accrual and the antioxidant endogenous response in bone differently depending on the sex and age. *PLOS ONE*, *12*(2), e0171161. https://doi.org/10.1371/journal.pone.0171161

Pendlebury, S. T., & Rothwell, P. M. (2009). Prevalence, incidence, and factors associated with pre-stroke and post-stroke dementia: a systematic review and meta-analysis. *The Lancet Neurology*, *8*(11), 1006–1018. https://doi.org/10.1016/S1474-4422(09)70236-4

Pendlebury, S. T., & Rothwell, P. M. (2019). Incidence and prevalence of dementia associated with transient ischaemic attack and stroke: analysis of the population-based Oxford Vascular Study. *The Lancet Neurology*, *18*(3), 248–258. https://doi.org/10.1016/S1474-4422(18)30442-3

Peng, H., Li, H., Sheehy, A., Cullen, P., Allaire, N., & Scannevin, R. H. (2016). Dimethyl fumarate alters microglia phenotype and protects neurons against proin fl ammatory toxic microenvironments. *Journal of Neuroimmunology*, *299*, 35–44. https://doi.org/10.1016/j.jneuroim.2016.08.006

Perego, C., Fumagalli, S., & De Simoni, M.-G. (2011). Temporal pattern of expression and colocalization of microglia/macrophage phenotype markers following brain ischemic injury in mice. *Journal of Neuroinflammation*, *8*(1), 174. https://doi.org/10.1186/1742-2094-8-174

Pérez-Torres, I., Guarner-Lans, V., & Rubio-Ruiz, M. E. (2017). Reductive Stress in Inflammation-Associated Diseases and the Pro-Oxidant Effect of Antioxidant Agents. *International Journal of Molecular Sciences*, *18*(10), 2098. https://doi.org/10.3390/ijms18102098

Petrovic-Djergovic, D., Hyman, M. C., Ray, J. J., Bouis, D., Visovatti, S. H., Hayasaki, T., & Pinsky, D. J. (2012). Tissue-Resident Ecto-5′ Nucleotidase (CD73) Regulates Leukocyte Trafficking in the Ischemic Brain. *The Journal of Immunology*, *188*(5), 2387–2398. https://doi.org/10.4049/JIMMUNOL.1003671

Phillips, A. A., Chan, F. H., Mu, M., Zheng, Z., Krassioukov, A. V, Ainslie, P. N., … Ainslie, P. N. (2016). Neurovascular coupling in humans: Physiology, methodological advances and clinical implications. *Journal of Cerebral Blood Flow & Metabolism*, *36*(4), 647–664. https://doi.org/10.1177/0271678X15617954

Pluta, R., Ułamek, M., & Jabłon, M. (2009). Alzheimer ' s Mechanisms in Ischemic Brain Degeneration. *The Anatomical Record*, *292*, 1863–1881. https://doi.org/10.1002/ar.21018

Popa-Wagner, A., Carmichael, S. T., Kokaia, Z., Kessler, C., & Walker, L. C. (2007). The response of the aged brain to stroke: too much, too soon? *Current Neurovascular Research*, *4*(3), 216–227. https://doi.org/10.2174/156720207781387213

Popa-Wagner, A., Schroder, E., Schmoll, H., Walker, L. C., & Kessler, C. (1999). *Upregulation of MAPIB and MAP2 in the Rat Brain After Middle Cerebral Artery Occlusion: Effect of Age*. *Journal of Cerebral Blood Flow and Metabolism* (Vol. 19). Retrieved from https://journals.sagepub.com/doi/pdf/10.1097/00004647-199904000-00008

Popp, A., Jaenisch, N., Witte, O. W., & Frahm, C. (2009). Identification of Ischemic Regions in a Rat Model of Stroke, *4*(3). https://doi.org/10.1371/journal.pone.0004764

Pradillo, J. M., Denes, A., Greenhalgh, A. D., Boutin, H., Drake, C., McColl, B. W., … Allan, S. M. (2012). Delayed administration of interleukin-1 receptor antagonist reduces ischemic brain damage and inflammation in comorbid rats. *Journal of Cerebral Blood Flow & Metabolism*, *32*(9), 1810–1819. https://doi.org/10.1038/jcbfm.2012.101

Pratico, D., Uryu, K., Leight, S., Trojanoswki, J. Q., & Lee, V. M. (2001). Increased Lipid Peroxidation Precedes Amyloid Plaque Formation in an Animal Model of Alzheimer Amyloidosis, *21*(12), 4183–4187.

Prust, M., Wang, J., Morizono, H., Messing, A., Brenner, M., Gordon, E., … Vanderver, A. (2011). GFAP mutations, age at onset, and clinical subtypes in Alexander disease. *Neurology*, *77*(13), 1287–1294. https://doi.org/10.1212/WNL.0b013e3182309f72

Puig, B., Brenna, S., Magnus, T., Puig, B., Brenna, S., & Magnus, T. (2018). Molecular Communication of a Dying Neuron in Stroke. *International Journal of Molecular Sciences*, *19*(9), 2834. https://doi.org/10.3390/ijms19092834

Qin, C., Fan, W. H., Liu, Q., Shang, K., Murugan, M., Wu, L. J., … Tian, D. S. (2017). Fingolimod protects against ischemic white matter damage by modulating microglia toward M2 polarization via STAT3 pathway. *Stroke*, *48*(12), 3336–3346. https://doi.org/10.1161/STROKEAHA.117.018505

Radak, D., Katsiki, N., Resanovic, I., Jovanovic, A., Sudar-Milovanovic, E., Zafirovic, S., … R. Isenovic, E. (2017). Apoptosis and Acute Brain Ischemia in Ischemic Stroke. *Current Vascular Pharmacology*, *15*(2), 115–122. https://doi.org/10.2174/1570161115666161104095522

Radi, R., Beckman, J. S., Bush, K. M., & Freeman, B. a. (1991). Peroxynitrite-induced membrane lipid peroxidation: the cytotoxic potential of superoxide and nitric oxide. *Archives of Biochemistry and Biophysics*, *288*(2), 481–487. Retrieved from http://www.ncbi.nlm.nih.gov/pubmed/1654835

Raghunath, A., Sundarraj, K., Nagarajan, R., Arfuso, F., Bian, J., Kumar, A. P., … Perumal, E. (2018). Antioxidant response elements: Discovery, classes, regulation and potential applications. *Redox Biology*, *17*, 297–314. https://doi.org/10.1016/J.REDOX.2018.05.002

Raina, A. K., Perry, G., Nunomura, A., Sayre, L. M., & Smith, M. A. (2000). Histochemical and immunocytochemical approaches to the study of oxidative stress. *Clin Chem Lab Med*, *38*(2), 93–97. https://doi.org/10.1515/CCLM.2000.015

Rajan, W. D., Wojtas, B., Gielniewski, B., Gieryng, A., Zawadzka, M., & Kaminska, B. (2018). Dissecting functional phenotypes of microglia and macrophages in the rat brain after transient cerebral ischemia. *Glia*. https://doi.org/10.1002/glia.23536

Rakers, C., Schleif, M., Blank, N., Matušková, H., Ulas, T., Händler, K., … Petzold, G. C. (2018). Stroke target identification guided by astrocyte transcriptome analysis. *Glia*, *67*(4), 619–633. https://doi.org/10.1002/glia.23544

Rakers, C., Schmid, M., Petzold, G. C., & Gabor Petzold, C. C. (2017). TRPV4 channels contribute to calcium transients in astrocytes and neurons during peri-infarct depolarizations in a stroke model. *Glia*, *65*(9), 1550–1561. https://doi.org/10.1002/glia.23183

Ransohoff, R. M. (2016). A polarizing question: do M1 and M2 microglia exist? *Nature Neuroscience*, *19*(8), 987–991. https://doi.org/10.1038/nn.4338

Rappert, A., Bechmann, I., Pivneva, T., Mahlo, J., Biber, K., Nolte, C., … Helmut. (2004). CXCR3-Dependent Microglial Recruitment Is Essential for Dendrite Loss after Brain Lesion. *The Journal of Neuroscience : The Official Journal of the Society for Neuroscience*, *24*(39), 8500–8509. https://doi.org/https://doi.org/10.1523/JNEUROSCI.2451-04.2004

Rappert, A., Biber, K., Nolte, C., Lipp, M., Schubel, A., Lu, B., … Kettenmann, H. W. G. M. B. H. (2002). Secondary Lymphoid Tissue Chemokine (CCL21) Activates CXCR3 to Trigger a Cl − Current and Chemotaxis in Murine Microglia. *Journal of Immunology (Baltimore, Md. : 1950)*, *168*, 3221–3226. https://doi.org/https://doi.org/10.4049/jimmunol.168.7.3221

Reddy, P. H. (2006). Amyloid precursor protein-mediated free radicals and oxidative damage : Implications for the development and progression of Alzheimer ' s disease, 1–

13. https://doi.org/10.1111/j.1471-4159.2005.03530.x

Redondo-Castro, E., Cunningham, C., Miller, J., Martuscelli, L., Aoulad-Ali, S., Rothwell, N. J., … Pinteaux, E. (2017). Interleukin-1 primes human mesenchymal stem cells towards an anti-inflammatory and pro-trophic phenotype in vitro. *Stem Cell Research & Therapy*, *8*(1), 79. https://doi.org/10.1186/s13287-017-0531-4

Remington, L. T., Babcock, A. A., Zehntner, S. P., & Owens, T. (2007). Microglial recruitment, activation, and proliferation in response to primary demyelination. *The American Journal of Pathology*, *170*(5), 1713–1724. https://doi.org/10.2353/ajpath.2007.060783

Ren, H. L., Lv, C. N., Xing, Y., Geng, Y., Zhang, F., Bu, W., & Wang, M. W. (2018). Downregulated Nuclear Factor E2-Related Factor 2 (Nrf2) Aggravates Cognitive Impairments via Neuroinflammation and Synaptic Plasticity in the Senescence-Accelerated Mouse Prone 8 (SAMP8) Mouse: A Model of Accelerated Senescence. *Medical Science Monitor : International Medical Journal of Experimental and Clinical Research*, *24*, 1132–1144. Retrieved from http://www.ncbi.nlm.nih.gov/pubmed/29474348

Resende, R., Isabel, P., Proença, T., Deshpande, A., Busciglio, J., Pereira, C., & Resende, C. (2008). Free Radical Biology & Medicine Brain oxidative stress in a triple-transgenic mouse model of Alzheimer disease, *44*, 2051–2057. https://doi.org/10.1016/j.freeradbiomed.2008.03.012

Rider, P., Carmi, Y., Guttman, O., Braiman, A., Cohen, I., Voronov, E., … Apte, R. N. (2011). IL-1α and IL-1β recruit different myeloid cells and promote different stages of sterile inflammation. *Journal of Immunology (Baltimore, Md. : 1950)*, *187*(9), 4835–4843. https://doi.org/10.4049/jimmunol.1102048

Roberts, E. L., Chih, C. P., & Rosenthal, M. (1997). Age-related changes in brain metabolism and vulnerability to anoxia. *Advances in Experimental Medicine and Biology*, *411*, 83–89. Retrieved from http://www.ncbi.nlm.nih.gov/pubmed/9269414

Robertson, C. A., Mccabe, C., Lopez-Gonzalez, M. R., Deuchar, G. A., Dani, K., Holmes, W. M., … Macrae, I. M. (2015). Detection of ischemic penumbra using combined perfusion and T2* oxygen challenge imaging. *International Journal of Stroke*, *10*(1), 42–50. https://doi.org/10.1111/ijs.12327

Robinson, M. J., Macrae, I. M., Todd, M., Reid, J. L., & McCulloch, J. (1990). Reduction of local cerebral blood flow to pathological levels by endothelin-1 applied to the middle cerebral artery in the rat. *Neuroscience Letters*, *118*(2), 269–272. Retrieved from http://www.ncbi.nlm.nih.gov/pubmed/2274283

Rodríguez García, P. L., & Rodríguez García, D. (2015). Diagnosis of vascular cognitive impairment and its main categories. *Neurología (English Edition)*, *30*(4), 223–239. https://doi.org/10.1016/j.nrleng.2011.12.013

Rojas-Gutierrez, E., Muñoz-Arenas, G., Treviño, S., Espinosa, B., Chavez, R., Rojas, K., … Guevara, J. (2017). Alzheimer's disease and metabolic syndrome: A link from oxidative stress and inflammation to neurodegeneration. *Synapse*, *71*(10), 1–21. https://doi.org/10.1002/syn.21990

Rojas, J. I., Zurrú, M. C., Romano, M., Patrucco, L., & Cristiano, E. (2007). Acute ischemic stroke and transient ischemic attack in the very old - risk factor profile and stroke subtype between patients older than 80 years and patients aged less than 80 years. *European Journal of Neurology*, *14*(8), 895–899. https://doi.org/10.1111/j.1468-1331.2007.01841.x

Rojo, A. I., Innamorato, N. G., Martín-Moreno, A. M., De Ceballos, M. L., Yamamoto, M., & Cuadrado, A. (2010). Nrf2 regulates microglial dynamics and neuroinflammation in experimental Parkinson's disease. *Glia*, *58*(5), 588–598. https://doi.org/10.1002/glia.20947

Rojo, R., Raper, A., Ozdemir, D. D., Lefevre, L., Grabert, K., Wollscheid-Lengeling, E., … Hume,

D. A. (2019). Deletion of a Csf1r enhancer selectively impacts CSF1R expression and development of tissue macrophage populations. *Nature Communications*, *6*, 14. https://doi.org/10.1038/s41467-019-11053-8

Rosell, A., Agin, V., Rahman, M., Morancho, A., Ali, C., Koistinaho, J., … Montaner, J. (2013). Distal Occlusion of the Middle Cerebral Artery in Mice: Are We Ready to Assess Long-Term Functional Outcome? *Translational Stroke Research*, *4*(3), 297–307. https://doi.org/10.1007/s12975-012-0234-1

Rothhammer, V., Borucki, D. M., Tjon, E. C., Takenaka, M. C., Chao, C.-C., Ardura-Fabregat, A., … Quintana, F. J. (2018). Microglial control of astrocytes in response to microbial metabolites. *Nature*, 1. https://doi.org/10.1038/s41586-018-0119-x

Rushmore, T. H., Morton$, M. R., & Pickett, C. B. (1991). The Antioxidant Responsive Element. Activation By Oxidative Stress And Identification Of The DNA Consensus Sequence Required For Functional Activity. *The Journal Of Biological Chemistry*, *266*(18), 11632–11639. Retrieved from http://www.jbc.org/content/266/18/11632.full.pdf

Ryan, C. L., Doucette, T. A., Gill, D. A., Langdon, K. D., Liu, Y., Perry, M. A., & Tasker, R. A. (2006). An improved post-operative care protocol allows detection of long-term functional deficits following MCAo surgery in rats. *Journal of Neuroscience Methods*, *154*(1–2), 30–37. https://doi.org/10.1016/J.JNEUMETH.2005.11.009

Ryou, M., & Mallet, R. T. (2018). An In Vitro Oxygen–Glucose Deprivation Model for Studying Ischemia–Reperfusion Injury of Neuronal Cells (pp. 229–235). Humana Press, New York, NY. https://doi.org/10.1007/978-1-4939-7526-6_18

Ryter, S. W., & Tyrrell, R. M. (2000). The heme synthesis and degradation pathways: role in oxidant sensitivity: Heme oxygenase has both pro- and antioxidant properties. *Free Radical Biology and Medicine*, *28*(2), 289–309. https://doi.org/10.1016/S0891-5849(99)00223-3

Saab, K. R., Kendrick, J., Yracheta, J. M., Lanaspa, M. A., Pollard, M., & Johnson, R. J. (2015). New insights on the risk for cardiovascular disease in African Americans: the role of added sugars. *Journal of the American Society of Nephrology : JASN*, *26*(2), 247–257. https://doi.org/10.1681/ASN.2014040393

Sahlas, D. J., Bilbao, J. M., Swartz, R. H., & Black, S. E. (2002). Clasmatodendrosis correlating with periventricular hyperintensity in mixed dementia. *Annals of Neurology*, *52*(3), 378–381. https://doi.org/10.1002/ana.10310

Saido, T. comings, & ... (1994). Spatial Resolution of the Primary p-Amyloidogenic Process Induced in Postischemic Hippocampus*, *269*(21), 15253–15257.

Salinet, A. S. M., Robinson, T. G., & Panerai, R. B. (2015). Effects of cerebral ischemia on human neurovascular coupling, CO_2 reactivity, and dynamic cerebral autoregulation. *Journal of Applied Physiology*, *118*(2), 170–177. https://doi.org/10.1152/japplphysiol.00620.2014

Salter, M. W., & Stevens, B. (2017). Microglia emerge as central players in brain disease. *Nature Medicine*, *23*(9), 1018–1027. https://doi.org/10.1038/nm.4397

Sandberg, M., Patil, J., D'Angelo, B., Weber, S. G., Mallard, C., D'Angelo, B., … Mallard, C. (2014). NRF2-regulation in brain health and disease: Implication of cerebral inflammation. *Neuropharmacology*, *79*, 298–306. https://doi.org/10.1016/j.neuropharm.2013.11.004

Sasaki, H., Sato, H., Kuriyama-Matsumura, K., Sato, K., Maebara, K., Wang, H., … Bannai, S. (2002). Electrophile response element-mediated induction of the cystine/glutamate exchange transporter gene expression. *The Journal of Biological Chemistry*, *277*(47), 44765–44771. https://doi.org/10.1074/jbc.M208704200

Satoh, J., Kino, Y., Asahina, N., Takitani, M., Miyoshi, J., Ishida, T., & Saito, Y. (2016). TMEM119 marks a subset of microglia in the human brain, (July 2015), 39–49.

https://doi.org/10.1111/neup.12235
Satoh, S., Kobayashi, T., Hitomi, A., Ikegaki, I., Suzuki, Y., Shibuya, M., … Asano, T. (1999). Inhibition of neutrophil migration by a protein kinase inhibitor for the treatment of ischemic brain infarction. *Japanese Journal of Pharmacology*, *80*(1), 41–48. Retrieved from http://www.ncbi.nlm.nih.gov/pubmed/10446755
Savard, A., Lavoie, K., Brochu, M.-E., Grbic, D., Lepage, M., Gris, D., & Sebire, G. (2013). Involvement of neuronal IL-1β in acquired brain lesions in a rat model of neonatal encephalopathy. *Journal of Neuroinflammation*, *10*(1), 880. https://doi.org/10.1186/1742-2094-10-110
Scannevin, R. H., Chollate, S., Jung, M. -y., Shackett, M., Patel, H., Bista, P., … Rhodes, K. J. (2012). Fumarates Promote Cytoprotection of Central Nervous System Cells against Oxidative Stress via the Nuclear Factor (Erythroid-Derived 2)-Like 2 Pathway. *Journal of Pharmacology and Experimental Therapeutics*, *341*(1), 274–284. https://doi.org/10.1124/jpet.111.190132
Schilling, M., Besselmann, M., Leonhard, C., Mueller, M., Ringelstein, E. B., Kiefer, R., … David, S. (2003). Microglial activation precedes and predominates over macrophage infiltration in transient focal cerebral ischemia: a study in green fluorescent protein transgenic bone marrow chimeric mice. *Experimental Neurology*, *183*(1), 25–33. https://doi.org/10.1016/S0014-4886(03)00082-7
Schilling, M., Besselmann, M., Müller, M., Strecker, J. K., Ringelstein, E. B., & Kiefer, R. (2005). Predominant phagocytic activity of resident microglia over hematogenous macrophages following transient focal cerebral ischemia: An investigation using green fluorescent protein transgenic bone marrow chimeric mice. *Experimental Neurology*, *196*(2), 290–297. https://doi.org/10.1016/J.EXPNEUROL.2005.08.004
Schipper, H. M., Song, W., Tavitian, A., & Cressatti, M. (2019). The sinister face of heme oxygenase-1 in brain aging and disease. *Progress in Neurobiology*, *172*, 40–70. https://doi.org/10.1016/j.pneurobio.2018.06.008
Schippers, J. H. M., Nguyen, H. M., Lu, D., Schmidt, R., & Mueller-Roeber, B. (2012). ROS homeostasis during development: an evolutionary conserved strategy. *Cellular and Molecular Life Sciences*, *69*(19), 3245–3257. https://doi.org/10.1007/s00018-012-1092-4
Schulz, J. B., Weller, M., Matthews, R. T., Heneka, M. T., Groscurth, P., Martinou, J.-C., … Klockgether, T. (1998). Extended therapeutic window for caspase inhibition and synergy with MK-801 in the treatment of cerebral histotoxic hypoxia. *Cell Death & Differentiation*, *5*(10), 847–857. https://doi.org/10.1038/sj.cdd.4400420
Schulze-Topphoff, U., Varrin-Doyer, M., Pekarek, K., Spencer, C. M., Shetty, A., Sagan, S. A., … Zamvil, S. S. (2016). Dimethyl fumarate treatment induces adaptive and innate immune modulation independent of Nrf2. *Proceedings of the National Academy of Sciences of the United States of America*, *113*(17), 4777–4782. https://doi.org/10.1073/pnas.1603907113
Scremin, O. U. (1995). Cerebral vascular system. In *G. Paxinos (Ed.), The Rat Nervous System, Academic Press, London,* (pp. 3–35).
Seifert, H. A., Benedek, G., Liang, J., Nguyen, H., Kent, G., Vandenbark, A. A., … Offner, H. (2017). Sex differences in regulatory cells in experimental stroke. *Cellular Immunology*, *318*(May), 49–54. https://doi.org/10.1016/j.cellimm.2017.06.003
Seo, H.-A., & Lee, I.-K. (2013). The role of Nrf2: adipocyte differentiation, obesity, and insulin resistance. *Oxidative Medicine and Cellular Longevity*, *2013*(184598), 1–7. https://doi.org/10.1155/2013/184598
Shah, Z. A. A., Li, R.-C. C., Thimmulappa, R. K. K., Kensler, T. W. W., Yamamoto, M., Biswal, S., & Doré, S. (2007). Role of reactive oxygen species in modulation of Nrf2 following

ischemic reperfusion injury. *Neuroscience*, *147*(1), 53–59. https://doi.org/10.1016/j.neuroscience.2007.02.066

Shannon, C., Salter, M., & Fern, R. (2007). GFP imaging of live astrocytes: Regional differences in the effects of ischaemia upon astrocytes. *Journal of Anatomy*, *210*(6), 684–692. https://doi.org/10.1111/j.1469-7580.2007.00731.x

Shen, X. N., Lu, Y., Tan, C. T. Y., Liu, L. Y., Yu, J. T., Feng, L., & Larbi, A. (2019). Identification of inflammatory and vascular markers associated with mild cognitive impairment. *Aging*, *11*(8), 2403–2419. https://doi.org/10.18632/aging.101924

Shi, K., Tian, D.-C., Li, Z.-G., Ducruet, A. F., Lawton, M. T., & Shi, F.-D. (2019). Global brain inflammation in stroke. *The Lancet Neurology*. https://doi.org/10.1016/S1474-4422(19)30078-X

Shi, Q., Chowdhury, S., Ma, R., Le, K. X., Hong, S., Caldarone, B. J., … Lemere, C. A. (2017). Complement C3 deficiency protects against neurodegeneration in aged plaque-rich APP/PS1 mice. *Science Translational Medicine*, *9*(392). Retrieved from http://stm.sciencemag.org/content/scitransmed/9/392/eaaf6295.full.pdf

Shibasaki, T., Iuchi, Y., Okada, F., Kuwata, K., Yamanobe, T., Bannai, S., … Fujii, J. (2009). Aggravation of ischemia–reperfusion-triggered acute renal failure in xCT-deficient mice. *Archives of Biochemistry and Biophysics*, *490*(1), 63–69. https://doi.org/10.1016/J.ABB.2009.08.008

Shigemoto-Mogami, Y., Hoshikawa, K., & Sato, K. (2018). Activated Microglia Disrupt the Blood-Brain Barrier and Induce Chemokines and Cytokines in a Rat in vitro Model. *Frontiers in Cellular Neuroscience*, *12*, 494. https://doi.org/10.3389/fncel.2018.00494

Shih, A. Y., Johnson, D. A., Wong, G., Kraft, A. D., Jiang, L., Erb, H., … Murphy, T. H. (2003). Coordinate Regulation of Glutathione Biosynthesis and Release by Nrf2-Expressing Glia Potently Protects Neurons from Oxidative Stress. *The Journal of Neuroscience*, *23*(8), 3394–3406.

Shih, Andy Y, Imbeault, S., Barakauskas, V., Erb, H., Jiang, L., Li, P., & Murphy, T. H. (2005). Induction of the Nrf2-driven antioxidant response confers neuroprotection during mitochondrial stress in vivo. *The Journal of Biological Chemistry*, *280*(24), 22925–22936. https://doi.org/10.1074/jbc.M414635200

Shih, Andy Y, Li, P., & Murphy, T. H. (2005a). A Small-Molecule-Inducible Nrf2-Mediated Antioxidant Ischemia In Vivo. *Journal of Neuroscience*, *25*(44), 10321–10335. https://doi.org/10.1523/JNEUROSCI.4014-05.2005

Shih, Andy Y, Li, P., & Murphy, T. H. (2005b). A Small-Molecule-Inducible Nrf2-Mediated Antioxidant Response Provides Effective Prophylaxis against Cerebral Ischemia In Vivo. *Journal of Neuroscience*, *25*(44), 10321–10335. https://doi.org/10.1523/JNEUROSCI.4014-05.2005

Shin, J. A., Park, E.-M., Choi, J.-S., Seo, S.-M., Kang, J. L., Lee, K.-E., & Cho, S. (2009). Ischemic preconditioning-induced neuroprotection is associated with differential expression of IL-1β and IL-1 receptor antagonist in the ischemic cortex. *Journal of Neuroimmunology*, *217*(1–2), 14–19. https://doi.org/10.1016/J.JNEUROIM.2009.06.001

Shinozaki, Y., Shibata, K., Yoshida, K., Shigetomi, E., Gachet, C., Ikenaka, K., … Koizumi, S. (2017). Transformation of Astrocytes to a Neuroprotective Phenotype by Microglia via P2Y1 Receptor Downregulation. *Cell Reports*, *19*(6), 1151–1164. https://doi.org/10.1016/J.CELREP.2017.04.047

Shiva Shankar Reddy, C. S., Subramanyam, M. V. V., Vani, R., & Asha Devi, S. (2007). In vitro models of oxidative stress in rat erythrocytes: Effect of antioxidant supplements. *Toxicology in Vitro*, *21*(8), 1355–1364. https://doi.org/10.1016/j.tiv.2007.06.010

Si, Z., Wang, X., Zhang, Z., Wang, J., Li, J., Li, J., … Gao, X. (2018). Heme Oxygenase 1 Induces Tau Oligomer Formation and Synapse Aberrations in Hippocampal Neurons. *Journal of*

Alzheimer's Disease : JAD, *65*(2), 409–419. https://doi.org/10.3233/JAD-180451

Sieber, M. W., Claus, R. A., Witte, O. W., & Frahm, C. (2011). Attenuated inflammatory response in aged mice brains following stroke. *PloS One*, *6*(10), e26288. https://doi.org/10.1371/journal.pone.0026288

Sieber, M. W., Guenther, M., Jaenisch, N., Albrecht-Eckardt, D., Kohl, M., Witte, O. W., & Frahm, C. (2014). Age-specific transcriptional response to stroke. *Neurobiology of Aging*, *35*(7), 1744–1754. https://doi.org/10.1016/J.NEUROBIOLAGING.2014.01.012

Siegler, J. E., Boehme, A. K., Kumar, A. D., Gillette, M. A., Albright, K. C., & Martin-Schild, S. (2013). What Change in the National Institutes of Health Stroke Scale Should Define Neurologic Deterioration in Acute Ischemic Stroke? *Journal of Stroke and Cerebrovascular Diseases*, *22*(5), 675–682. https://doi.org/10.1016/J.JSTROKECEREBROVASDIS.2012.04.012

Sigfridsson, E., Marangoni, M., Johnson, J. A., Hardingham, G. E., Fowler, J. H., & Horsburgh, K. (2018). Astrocyte-specific overexpression of Nrf2 protects against optic tract damage and behavioural alterations in a mouse model of cerebral hypoperfusion. *Scientific Reports*, *8*(1), 12552. https://doi.org/10.1038/s41598-018-30675-4

Silva, B., Sousa, L., Miranda, A., Vasconcelos, A., Reis, H., Barcelos, L., … Rachid, M. A. (2015). Memory deficit associated with increased brain proinflammatory cytokine levels and neurodegeneration in acute ischemic stroke. *Arquivos de Neuro-Psiquiatria*, *73*(8), 655–659. https://doi.org/10.1590/0004-282X20150083

Sims, N. R., & Yew, W. P. (2017). Reactive astrogliosis in stroke: Contributions of astrocytes to recovery of neurological function. *Neurochemistry International*, *107*, 88–103. https://doi.org/10.1016/J.NEUINT.2016.12.016

Singh, U. P., Singh, R., Singh, S., Karls, R. K., Quinn, F. D., Taub, D. D., & Lillard, J. W. (2008). CXCL10+ T cells and NK cells assist in the recruitment and activation of CXCR3+ and CXCL11+ leukocytes during Mycobacteria-enhanced colitis. *BMC Immunology*, *9*(1), 25. https://doi.org/10.1186/1471-2172-9-25

Skrobot, O. A., Black, S. E., Chen, C., DeCarli, C., Erkinjuntti, T., Ford, G. A., … Kehoe, P. G. (2018). Progress toward standardized diagnosis of vascular cognitive impairment: Guidelines from the Vascular Impairment of Cognition Classification Consensus Study. *Alzheimer's and Dementia*, *14*(3), 280–292. https://doi.org/10.1016/j.jalz.2017.09.007

Smith, A. M., Gibbons, H. M., Oldfield, R. L., Bergin, P. M., Mee, E. W., Faull, R. L. M., & Dragunow, M. (2013). The transcription factor PU.1 is critical for viability and function of human brain microglia. *Glia*, *61*(6), 929–942. https://doi.org/10.1002/glia.22486

Smith, H. K., Russell, J. M., Granger, D. N., & Gavins, F. N. E. (2015). Critical differences between two classical surgical approaches for middle cerebral artery occlusion-induced stroke in mice. *Journal of Neuroscience Methods*, *249*, 99–105. https://doi.org/10.1016/j.jneumeth.2015.04.008

Smith, M. A., Richey Harris, P. L., Sayre, L. M., Beckman, J. S., & Perry, G. (1997). Widespread peroxynitrite-mediated damage in Alzheimer's disease. *The Journal of Neuroscience : The Official Journal of the Society for Neuroscience*, *17*(8), 2653–2657. https://doi.org/10.1523/JNEUROSCI.17-08-02653.1997

Snider, B. J., Gottron, F. J., & Choi, D. W. (1999). Apoptosis and Necrosis in Cerebrovascular Disease. *Annals of the New York Academy of Sciences*, *893*(1 OXIDATIVE/ENE), 243–253. https://doi.org/10.1111/j.1749-6632.1999.tb07829.x

Sofroniew, M. V. (2009). Molecular dissection of reactive astrogliosis and glial scar formation. *Trends in Neurosciences*, *32*(12), 638–647. https://doi.org/10.1016/J.TINS.2009.08.002

Sofroniew, M. V., & Vinters, H. V. (2010). Astrocytes: Biology and pathology. *Acta Neuropathologica*, *119*(1), 7–35. https://doi.org/10.1007/s00401-009-0619-8

Soriano, F. X., Baxter, P., Murray, L. M., Sporn, M. B., Gillingwater, T. H., & Hardingham, G. E.

(2009). Transcriptional Regulation of the AP-1 and Nrf2 Target Gene Sulfiredoxin. *Molecules and Cells*, *27*(3), 279–282. https://doi.org/10.1007/s10059-009-0050-y

Soriano, F. X., Léveillé, F., Papadia, S., Higgins, L. G., Varley, J., Baxter, P., … Hardingham, G. E. (2008). Induction of sulfiredoxin expression and reduction of peroxiredoxin hyperoxidation by the neuroprotective Nrf2 activator 3H-1,2-dithiole-3-thione. *Journal of Neurochemistry*, *107*(2), 533–543. https://doi.org/10.1111/j.1471-4159.2008.05648.x

Spanakis, E. K., & Golden, S. H. (2013). Race/ethnic difference in diabetes and diabetic complications. *Current Diabetes Reports*, *13*(6), 814–823. https://doi.org/10.1007/s11892-013-0421-9

Srivastava, S., Alfieri, A., Siow, R., Mann, G., & Fraser, P. A. (2013). Temporal and spatial distribution of Nrf2 in rat brain following stroke: quantitation of nuclear to cytoplasmic Nrf2 content using a novel immunohistochemical technique. *The Journal of Physiology*, *14*, 3525–3538. https://doi.org/10.1113/jphysiol.2013.257964

Stocker, R., Yamamoto, Y., McDonagh, A. F., Glazer, A. N., & Ames, B. N. (1987). Bilirubin is an antioxidant of possible physiological importance. *Science (New York, N.Y.)*, *235*(4792), 1043–1046. https://doi.org/10.1126/science.3029864

Strecker, J.-K., Minnerup, J., Gess, B., Ringelstein, E. B., Schäbitz, W.-R., & Schilling, M. (2011). Monocyte Chemoattractant Protein-1-Deficiency Impairs the Expression of IL-6, IL-1β and G-CSF after Transient Focal Ischemia in Mice. *PLoS ONE*, *6*(10), e25863. https://doi.org/10.1371/journal.pone.0025863

Suh, J. H., Shenvi, S. V, Dixon, B. M., Liu, H., Jaiswal, A. K., Liu, R., & Hagen, T. M. (2004). Decline in transcriptional activity of Nrf2 causes age-related loss of glutathione synthesis , which is reversible with lipoic acid, (24).

Sun, M., Jin, H., Sun, X., Huang, S., Zhang, F.-L., Guo, Z., & Yang, Y. (2018). Free Radical Damage in Ischemia-Reperfusion Injury: An Obstacle in Acute Ischemic Stroke after Revascularization Therapy. *Oxidative Medicine and Cellular Longevity*, *2018*, 1–17. https://doi.org/10.1155/2018/3804979

Swanson, R. A., Ying, W., & Kauppinen, T. M. (2004). Astrocyte Influences on Ischemic Neuronal Death, 193–205.

Tajima, Y., Takuwa, H., Kokuryo, D., Kawaguchi, H., Seki, C., Masamoto, K., … Ito, H. (2014). Changes in cortical microvasculature during misery perfusion measured by two-photon laser scanning microscopy. *Journal of Cerebral Blood Flow & Metabolism*, *34*(10), 1363–1372. https://doi.org/10.1038/jcbfm.2014.91

Takano, T., Oberheim, N. A., Cotrina, M. L., & Nedergaard, M. (2009). Astrocytes and ischemic injury. *Stroke*, *40*(3 SUPPL. 1), 8–13. https://doi.org/10.1161/STROKEAHA.108.533166

Takaya, K., Suzuki, T., Motohashi, H., Onodera, K., Satomi, S., Kensler, T. W., & Yamamoto, M. (2012). Validation of the multiple sensor mechanism of the Keap1-Nrf2 system. *Free Radical Biology and Medicine*, *53*(4), 817–827. https://doi.org/10.1016/j.freeradbiomed.2012.06.023

Tamura, A., Graham, D. I., McCulloch, J., & Teasdale, G. M. (1981). Focal Cerebral Ischaemia in the Rat: 1. Description of Technique and Early Neuropathological Consequences following Middle Cerebral Artery Occlusion. *Journal of Cerebral Blood Flow & Metabolism*, *1*(1), 53–60. https://doi.org/10.1038/jcbfm.1981.6

Tanaka, J., Toku, K., Zhang, B., Ishihara, K., Sakanaka, M., & Maeda, N. (1999). Astrocytes prevent neuronal death induced by reactive oxygen and nitrogen species. *Glia*, *28*(2), 85–96. https://doi.org/10.1002/(SICI)1098-1136(199911)28:2<85::AID-GLIA1>3.0.CO;2-Y

Tanaka, N., Ikeda, Y., Ohta, Y., Deguchi, K., Tian, F., Shang, J., … Abe, K. (2010). Expression of Keap1 – Nrf2 system and antioxidative proteins in mouse brain after transient middle

cerebral artery occlusion. *Brain Research*, *1370*, 246–253. https://doi.org/10.1016/j.brainres.2010.11.010

Tanaka, R., Komine-Kobayashi, M., Mochizuki, H., Yamada, M., Furuya, T., Migita, M., … Urabe, T. (2003). Migration of enhanced green fluorescent protein expressing bone marrow-derived microglia/macrophage into the mouse brain following permanent focal ischemia. *Neuroscience*, *117*(3), 531–539. https://doi.org/10.1016/S0306-4522(02)00954-5

Tang, Y., & Le, W. (2016). Differential Roles of M1 and M2 Microglia in Neurodegenerative Diseases. *Molecular Neurobiology*, *53*(2), 1181–1194. https://doi.org/10.1007/s12035-014-9070-5

Teh, D. B. L., Prasad, A., Jiang, W., Ariffin, M. Z., Khanna, S., Belorkar, A., … ALL, A. H. (2017). Transcriptome Analysis Reveals Neuroprotective aspects of Human Reactive Astrocytes induced by Interleukin 1β. *Scientific Reports*, *7*(1), 13988. https://doi.org/10.1038/s41598-017-13174-w

Thiels, E., Urban, N. N., Gonzalez-Burgos, G. R., Kanterewicz, B. I., Barrionuevo, G., Chu, C. T., … Klann, E. (2000). Impairment of long-term potentiation and associative memory in mice that overexpress extracellular superoxide dismutase. *The Journal of Neuroscience : The Official Journal of the Society for Neuroscience*, *20*(20), 7631–7639. Retrieved from http://www.ncbi.nlm.nih.gov/pubmed/11027223

Thomalla, G., Simonsen, C. Z., Boutitie, F., Andersen, G., Berthezene, Y., Cheng, B., … Gerloff, C. (2018). MRI-Guided Thrombolysis for Stroke with Unknown Time of Onset. *New England Journal of Medicine*, *379*(7), 611–622. https://doi.org/10.1056/NEJMoa1804355

Thrane, A. S., Rangroo Thrane, V., & Nedergaard, M. (2014). Drowning stars: Reassessing the role of astrocytes in brain edema. *Trends in Neurosciences*, *37*(11), 620–628. https://doi.org/10.1016/j.tins.2014.08.010

Thun, M. J., Apicella, L. F., & Henley, S. J. (2000). Smoking vs Other Risk Factors as the Cause of Smoking-Attributable Deaths. *JAMA*, *284*(6), 706. https://doi.org/10.1001/jama.284.6.706

Tian, X., Peng, J., Zhong, J., Yang, M., Pang, J., Lou, J., … Dong, Z. (2016). β-Caryophyllene protects *in vitro* neurovascular unit against oxygen-glucose deprivation and re-oxygenation-induced injury. *Journal of Neurochemistry*, *139*(5), 757–768. https://doi.org/10.1111/jnc.13833

Titova, E., Ostrowski, R. P., Adami, A., Badaut, J., Lalas, S., Ghosh, N., … Obenaus, A. (2011). Brain irradiation improves focal cerebral ischemia recovery in aged rats. *Journal of the Neurological Sciences*, *306*, 143–153. https://doi.org/10.1016/j.jns.2011.02.034

Tomimoto, H., Akiguchi, I., Wakita, H., Suenaga, T., Nakamura, S., & Kimura, J. (1997). Regressive changes of astroglia in white matter lesions in cerebrovascular disease and Alzheimer's disease patients. *Acta Neuropathologica*, *94*(2), 146–152. https://doi.org/10.1007/s004010050686

Tönnies, E., & Trushina, E. (2017). Oxidative Stress, Synaptic Dysfunction, and Alzheimer's Disease. *Journal of Alzheimer's Disease*, *57*(4), 1105–1121. https://doi.org/10.3233/JAD-161088

Tramutola, A., Lanzillotta, C., Perluigi, M., & Butterfield, D. A. (2017). Oxidative stress, protein modification and Alzheimer disease. *Brain Research Bulletin*, *133*, 88–96. https://doi.org/10.1016/j.brainresbull.2016.06.005

Trendelenburg, G., & Dirnagl, U. (2005). Neuroprotective role of astrocytes in cerebral ischemia: Focus on ischemic preconditioning. *Glia*, *50*(4), 307–320. https://doi.org/10.1002/glia.20204

Trotman-Lucas, M., Kelly, M. E., Janus, J., Fern, R., & Gibson, C. L. (2017). An alternative

surgical approach reduces variability following filament induction of experimental stroke in mice. *Disease Models & Mechanisms*, *10*(7), 931–938. https://doi.org/10.1242/dmm.029108

Trueman, R. C., Diaz, C., Farr, T. D., Harrison, D. J., Fuller, A., Tokarczuk, P. F., … Dunnett, S. B. (2017). Systematic and detailed analysis of behavioural tests in the rat middle cerebral artery occlusion model of stroke : Tests for long-term assessment. *Journal of Cerebral Blood Flow & Metabolism*, *37*(4), 1349–1361. https://doi.org/10.1177/0271678X16654921

Tsuchiya, D., Hong, S., Kayama, T., Panter, S. S., & Weinstein, P. R. (2003). Effect of suture size and carotid clip application upon blood flow and infarct volume after permanent and temporary middle cerebral artery occlusion in mice. *Brain Research*, *970*(1–2), 131–139. Retrieved from http://www.ncbi.nlm.nih.gov/pubmed/12706254

Turner, R. J., & Sharp, F. R. (2016). Implications of MMP9 for Blood Brain Barrier Disruption and Hemorrhagic Transformation Following Ischemic Stroke. *Frontiers in Cellular Neuroscience*, *10*(March), 1–13. https://doi.org/10.3389/fncel.2016.00056

Tymianski, M., Christopher Wallace, M., Spigelman, I., Uno, M., Carlen, P. L., Tator, C. H., & Charlton, M. P. (1993). Cell-permeant Ca2+ chelators reduce early excitotoxic and ischemic neuronal injury in vitro and in vivo. *Neuron*, *11*(2), 221–235. https://doi.org/10.1016/0896-6273(93)90180-Y

Uesugi, M., Kasuya, Y., Hayashi, K., & Goto, K. (1998). SB209670, a potent endothelin receptor antagonist, prevents or delays axonal degeneration after spinal cord injury. *Brain Research*, *786*(1–2), 235–239. Retrieved from http://www.ncbi.nlm.nih.gov/pubmed/9555032

Umegaki, M., Sanada, Y., Waerzeggers, Y., Rosner, G., Yoshimine, T., Heiss, W.-D., & Graf, R. (2005). Peri-Infarct Depolarizations Reveal Penumbra-Like Conditions in Striatum Peri-Infarct Depolarizations Reveal Penumbra-Like Conditions in Striatum. *J. Neurosci.*, *23*(37), 11602–11610. https://doi.org/10.1523/jneurosci.4182-04.2005

Urushihata, T., Takuwa, H., Seki, C., Tachibana, Y., Takahashi, M., Kershaw, J., … Obata, T. (2018). Water diffusion in the brain of chronic hypoperfusion model mice: A study considering the effect of blood flow. *Magnetic Resonance in Medical Sciences*, *17*(4), 318–324. https://doi.org/10.2463/mrms.mp.2017-0149

Vaas, M., Enzmann, G., Perinat, T., Siler, U., Reichenbach, J., Licha, K., … Klohs, J. (2017). Non-invasive near-infrared fluorescence imaging of the neutrophil response in a mouse model of transient cerebral ischaemia. *Journal of Cerebral Blood Flow & Metabolism*, *37*(8), 2833–2847. https://doi.org/10.1177/0271678X16676825

Vara, D., & Pula, G. (2014). Reactive Oxygen Species: Physiological Roles in the Regulation of Vascular Cells. *Current Molecular Medicine*, *14*(9), 1103–1125. https://doi.org/10.2174/1566524014666140603114010

Vargas, M. R., Johnson, D. A., Sirkis, D. W., Messing, A., Johnson, A., Johnson, J. A., & Johnson, A. (2008). Nrf2 activation in astrocytes protects against neurodegeneration in mouse models of familial amyotrophic lateral sclerosis. *Annual Review of Neuroscience*, *28*(50), 13574–13581. https://doi.org/10.1523/JNEUROSCI.4099-08.2008

Veerhuis, R., Nielsen, H. M., & Tenner, A. J. (2011). Complement in the brain. *Molecular Immunology*, *48*(14), 1592–1603. https://doi.org/10.1016/j.molimm.2011.04.003

Venugopal, R., & Jaiswal, A. K. (1996). Nrf1 and Nrf2 positively and c-Fos and Fra1 negatively regulate the human antioxidant response element-mediated expression of NAD(P)H:quinone oxidoreductase1 gene. *Proceedings of the National Academy of Sciences*, *93*(25), 14960–14965. https://doi.org/10.1073/PNAS.93.25.14960

Verkhratsky, A., & Nedergaard, M. (2017). Physiology Of Astroglia. *Physiological Reviws*, *98*, 239–389. Retrieved from

http://www.physiology.org/doi/pdf/10.1152/physrev.00042.2016
Vermeer, S. E., Prins, N. D., den Heijer, T., Hofman, A., Koudstaal, P. J., & Breteler, M. M. (2003). Silent brain infarcts and the risk of dementia and cognitive decline. *N Engl J Med*, *348*(13), 1215–1222. https://doi.org/10.1056/NEJMoa022066
Vijayan, M., & Reddy, P. H. (2016). Stroke, Vascular Dementia, and Alzheimer's Disease: Molecular Links. *Journal of Alzheimer's Disease*, *54*(2), 427–443. https://doi.org/10.3233/JAD-160527
Villarreal, A., Rosciszewski, G., Murta, V., Cadena, V., Usach, V., Dodes-traian, M. M., … Ramos, A. J. (2016). Isolation and Characterization of Ischemia-Derived Astrocytes (IDAs) with Ability to Transactivate Quiescent Astrocytes, *10*(June), 1–16. https://doi.org/10.3389/fncel.2016.00139
Vogel, C., & Marcotte, E. M. (2012). Insights into the regulation of protein abundance from proteomic and transcriptomic analyses. *Nature Reviews Genetics*, *13*(4), 227–232. https://doi.org/10.1038/nrg3185
Wagner, D. C., Scheibe, J., Glocke, I., Weise, G., Deten, A., Boltze, J., & Kranz, A. (2013). Object-based analysis of astroglial reaction and astrocyte subtype morphology after ischemic brain injury. *Acta Neurobiologiae Experimentalis*, *73*(1), 79–87.
Wallin, A., Kapaki, E., Boban, M., Engelborghs, S., Hermann, D. M., Huisa, B., … Rosenberg, G. (2017). Biochemical markers in vascular cognitive impairment associated with subcortical small vessel disease-A consensus report. *BMC Neurology*, *17*(102), 1–12. https://doi.org/10.1186/s12883-017-0877-3
Walsh, J., Jenkins, R. E., Wong, M., Olayanju, A., Powell, H., Copple, I., … Park, B. K. (2014). Identification and quantification of the basal and inducible Nrf2-dependent proteomes in mouse liver: Biochemical, pharmacological and toxicological implications. *Journal of Proteomics*, *108*, 171–187. https://doi.org/10.1016/J.JPROT.2014.05.007
Wang, A., Liu, J., Meng, X., Li, J., Wang, H., Wang, Y., … Wang, Y. (2018). Association between oxidized low-density lipoprotein and cognitive impairment in patients with ischemic stroke. *European Journal of Neurology*, *25*(1), 185–191. https://doi.org/10.1111/ene.13497
Wang, B., Zhu, X., Kim, Y., Li, J., Huang, S., Saleem, S., … Cao, W. (2012). Histone deacetylase inhibition activates transcription factor Nrf2 and protects against cerebral ischemic damage. *Free Radical Biology and Medicine*, *52*(5), 928–936. https://doi.org/10.1016/j.freeradbiomed.2011.12.006
Wang, C.-Y., Wang, Z.-Y., Xie, J.-W., Cai, J.-H., Wang, T., Xu, Y., … An, L. (2014). CD36 Upregulation Mediated by intranasal LV-Nrf2 treatment Mitigates Hypoxia-induced Progression of Alzheimer's-like Pathogenesis. *Antioxidants & Redox Signaling*, *21*(16), 2208–2231. https://doi.org/10.1089/ars.2014.5845
Wang, J., Xing, H., Wan, L., Jiang, X., Wang, C., & Wu, Y. (2018). Treatment targets for M2 microglia polarization in ischemic stroke. *Biomedicine & Pharmacotherapy*, *105*, 518–525. https://doi.org/10.1016/J.BIOPHA.2018.05.143
Wang, M., Iliff, J. J., Liao, Y., Chen, M. J., Shinseki, M. S., Venkataraman, A., … Nedergaard, M. (2012). Cognitive Deficits and Delayed Neuronal Loss in a Mouse Model of Multiple Microinfarcts. *Journal of Neuroscience*, *32*(50), 17948–17960. https://doi.org/10.1523/JNEUROSCI.1860-12.2012
Wang, P., Liang, X., Lu, Y., Zhao, X., & Liang, J. (2016). MicroRNA-93 Downregulation Ameliorates Cerebral Ischemic Injury Through the Nrf2 / HO-1 Defense Pathway. *Neurochemical Research*, (40), 1–9. https://doi.org/10.1007/s11064-016-1975-0
Wang, Y., Huang, Y., Xu, Y., Ruan, W., Wang, H., Zhang, Y., … Pang, T. (2018). A Dual AMPK/Nrf2 Activator Reduces Brain Inflammation After Stroke by Enhancing Microglia M2 Polarization. *Antioxidants*, *28*(2), 141–163. https://doi.org/10.1089/ars.2017.7003

Wanner, I. B., Anderson, M. A., Song, B., Levine, J., Fernandez, A., Gray-Thompson, Z., … Sofroniew, M. V. (2013). Glial scar borders are formed by newly proliferated, elongated astrocytes that interact to corral inflammatory and fibrotic cells via STAT3-dependent mechanisms after spinal cord injury. *The Journal of Neuroscience : The Official Journal of the Society for Neuroscience*, *33*(31), 12870–12886. https://doi.org/10.1523/JNEUROSCI.2121-13.2013

Wardlaw, J. M., & Bath, P. M. (2019). Stroke research in 2018: extended time windows, refined benefit, and lifestyle prevention targets. *The Lancet Neurology*, *18*(1), 2–3. https://doi.org/10.1016/S1474-4422(18)30457-5

Watakabe, A., Komatsu, Y., Nawa, H., & Yamamori, T. (2006). Gene expression profiling of primate neocortex: molecular neuroanatomy of cortical areas. *Genes, Brain, and Behavior*, *5 Suppl 1*, 38–43. https://doi.org/10.1111/j.1601-183X.2006.00193.x

Watson, B. D., Dietrich, W. D., Busto, R., Wachtel, M. S., & Ginsberg, M. D. (1985). Induction of reproducible brain infarction by photochemically initiated thrombosis. *Annals of Neurology*, *17*(5), 497–504. https://doi.org/10.1002/ana.410170513

Weber, B., & Barros, L. F. (2018). The Astrocyte: Powerhouse and Recycling Center, 1–16. https://doi.org/10.1101/cshperspect.a020396

Wehr, H., Ryglewicz, D., Rodo, M., Poźniak, M., Swiderska, M., Panczenko, B., & Stajniak, A. (2000). [In vitro oxidation of low density lipoproteins in patients after ischemic stroke]. *Neurologia i Neurochirurgia Polska*, *34*(3), 447–456. Retrieved from http://www.ncbi.nlm.nih.gov/pubmed/10979539

White, B. J., Tarabishy, S., Venna, V. R., Manwani, B., Benashski, S., McCullough, L. D., & Li, J. (2012). Protection from cerebral ischemia by inhibition of TGFβ-activated kinase. *Experimental Neurology*, *237*(1), 238–245. https://doi.org/10.1016/j.expneurol.2012.05.019

White, C. S., Lawrence, C. B., Brough, D., & Rivers-Auty, J. (2017). Inflammasomes as therapeutic targets for Alzheimer's disease. *Brain Pathology*, *27*(2), 223–234. https://doi.org/10.1111/bpa.12478

White, H., Boden-Albala, B., Wang, C., Elkind, M. S., Rundek, T., Wright, C. B., & Sacco, R. L. (2005). Ischemic Stroke Subtype Incidence Among Whites, Blacks, and Hispanics The Northern Manhattan Study. *Circulation*, *111*(10), 1327–1331. https://doi.org/10.1161/01.CIR.0000157736.19739.D0

Wojtovich, A. P., & Brookes, P. S. (2008). The endogenous mitochondrial complex II inhibitor malonate regulates mitochondrial ATP-sensitive potassium channels: Implications for ischemic preconditioning. *Biochimica et Biophysica Acta (BBA) - Bioenergetics*, *1777*(7–8), 882–889. https://doi.org/10.1016/J.BBABIO.2008.03.025

Wolf, P. A., D'Agostino, R. B., Kannel, W. B., Bonita, R., & Belanger, A. J. (1988). Cigarette Smoking as a Risk Factor for Stroke. *JAMA*, *259*(7), 1025. https://doi.org/10.1001/jama.1988.03720070025028

Wolf, P. A., Mitchell, J. B., Baker, C. S., Kannel, W. B., & D'Agostino, R. B. (1998). Impact of Atrial Fibrillation on Mortality, Stroke, and Medical Costs. *Archives of Internal Medicine*, *158*(3), 229. https://doi.org/10.1001/archinte.158.3.229

Won, S. J., Kim, J.-E., Cittolin-Santos, G. F., & Swanson, R. a. (2015). Assessment at the Single-Cell Level Identifies Neuronal Glutathione Depletion As Both a Cause and Effect of Ischemia-Reperfusion Oxidative Stress. *Journal of Neuroscience*, *35*(18), 7143–7152. https://doi.org/10.1523/JNEUROSCI.4826-14.2015

Woo, H. A., Jeong, W., Chang, T.-S., Park, K. J., Park, S. J., Yang, J. S., & Rhee, S. G. (2005). Reduction of cysteine sulfinic acid by sulfiredoxin is specific to 2-cys peroxiredoxins. *The Journal of Biological Chemistry*, *280*(5), 3125–3128. https://doi.org/10.1074/jbc.C400496200

Wu, G., Zhu, L., Yuan, X., Chen, H., Xiong, R., Zhang, S., … Zhang, W. (2017). Britanin Ameliorates Cerebral Ischemia – Reperfusion Injury. *Antioxidants & Redox Signaling*, *00*(00), 1–15. https://doi.org/10.1089/ars.2016.6885

Wu, J., Chen, Y., Yu, S., Li, L., Zhao, X., Li, Q., … Zhao, Y. (2017). Neuroprotective effects of sulfiredoxin-1 during cerebral ischemia/reperfusion oxidative stress injury in rats. *Brain Research Bulletin*, *132*(May), 99–108. https://doi.org/10.1016/j.brainresbull.2017.05.012

Wu, Le, Liu, Z. J., Miao, S., Zou, L. B., Cai, L., Wu, P., … Li, H. H. (2013). Lipoxin A4 ameliorates cerebral ischaemia/reperfusion injury through upregulation of nuclear factor erythroid 2-related factor 2. *Neurological Research*, *35*(9), 968–975. https://doi.org/10.1179/1743132813Y.0000000242

Wu, Lingfeng, Zhang, K., Hu, G., Yang, H., Xie, C., & Wu, X. (2014). Inflammatory response and neuronal necrosis in rats with cerebral ischemia, *9*(19). https://doi.org/10.4103/1673-5374.143419

Wu, Q. J., & Tymianski, M. (2018). Targeting nmda receptors in stroke: New hope in neuroprotection. *Molecular Brain*, *11*(1), 1–14. https://doi.org/10.1186/s13041-018-0357-8

Wu, Z., Rademakers, T., Kiessling, F., Vogt, M., Westein, E., Weber, C., … van Zandvoort, M. (2017). Multi-photon microscopy in cardiovascular research. *Methods*, *130*, 79–89. https://doi.org/10.1016/J.YMETH.2017.04.013

Xia, C.-Y., Zhang, S., Gao, Y., Wang, Z.-Z., & Chen, N.-H. (2015). Selective modulation of microglia polarization to M2 phenotype for stroke treatment. *International Immunopharmacology*, *25*(2), 377–382. https://doi.org/10.1016/J.INTIMP.2015.02.019

Xia, M. Q., Bacskai, B. J., Knowles, R. B., Qin, S. X., & Hyman, B. T. (2000). Expression of the chemokine receptor CXCR3 on neurons and the elevated expression of its ligand IP-10 in reactive astrocytes: in vitro ERK1/2 activation and role in Alzheimer's disease. *Journal of Neuroimmunology*, *108*(1–2), 227–235. https://doi.org/10.1016/S0165-5728(00)00285-X

Xiong, X., Barreto, G. E., Xu, L., Ouyang, Y. B., Xie, X., Giffard, R. G., … Giffard, R. G. (2011). Increased Brain Injury and Worsened Neurological Outcome in Interleukin-4 Knockout Mice After Transient Focal Cerebral Ischemia. *Stroke*, *42*(7), 2026–2032. https://doi.org/10.1161/STROKEAHA.110.593772

Xue, F., Huang, J., Ding, P., Zang, H., Kou, Z., Li, T., … Yan, W. (2016). Nrf2 / antioxidant defense pathway is involved in the neuroprotective effects of Sirt1 against focal cerebral ischemia in rats after hyperbaric oxygen preconditioning. *Behavioural Brain Research*, *309*, 1–8. https://doi.org/10.1016/j.bbr.2016.04.045

Xue, Q., Liu, Y., Qi, H., Ma, Q., Xu, L., Chen, W., … Xu, X. (2013). A Novel Brain Neurovascular Unit Model with Neurons, Astrocytes and Microvascular Endothelial Cells of Rat. *Int. J. Biol. Sci*, *9*(2), 174–189. https://doi.org/10.7150/ijbs.5115

Yabuki, Y., & Fukunaga, K. (2013). Oral administration of glutathione improves memory deficits following transient brain ischemia by reducing brain oxidative stress. *Neuroscience*, *250*, 394–407. https://doi.org/10.1016/j.neuroscience.2013.07.017

Yager, J. Y., Kala, G., Hertz, L., & Juurlink, B. H. (1994). Correlation between content of high-energy phosphates and hypoxic-ischemic damage in immature and mature astrocytes. *Brain Research. Developmental Brain Research*, *82*(1–2), 62–68. Retrieved from http://www.ncbi.nlm.nih.gov/pubmed/7842520

Yamagami, S., Tamura, M., Hayashi, M., Endo, N., Tanabe, H., Katsuura, Y., & Komoriya, K. (1999). Differential production of MCP-1 and cytokine-induced neutrophil chemoattractant in the ischemic brain after transient focal ischemia in rats. *Journal of Leukocyte Biology*, *65*(6), 744–749. https://doi.org/10.1002/jlb.65.6.744

Yamamoto, T., Suzuki, T., Kobayashi, A., Wakabayashi, J., Maher, J., Motohashi, H., & Yamamoto, M. (2008). Physiological significance of reactive cysteine residues of Keap1 in determining Nrf2 activity. *Molecular and Cellular Biology*, *28*(8), 2758–2770. https://doi.org/10.1128/MCB.01704-07

Yamashita, K., Vogel, P., Fritze, K., Back, T., Hossmann, K.-A., & Wiessner, C. (1996). Monitoring the temporal and spatial activation pattern of astrocytes in focal cerebral ischemia using in situ hybridization to GFAP mRNA: comparison withsgp-2 andhsp70 mRNA and the effect of glutamate receptor antagonists. *Brain Research*, *735*(2), 285–297. https://doi.org/10.1016/0006-8993(96)00578-1

Yamauchi, K., Nakano, Y., Imai, T., Takagi, T., Tsuruma, K., Shimazawa, M., … Hara, H. (2016). A Novel Nuclear Factor Erythroid 2-Related Factor 2 (Nrf2) Activator Rs9 Attenuates Brain Injury After Ischemia Reperfusion In Mice. *Neuroscience*, *2*(July). https://doi.org/10.1016/j.neuroscience.2016.07.035

Yang, B., Strong, R., Sharma, S., Brenneman, M., Mallikarjunarao, K., Xi, X., … Savitz, S. I. (2011). Therapeutic Time Window and Dose Response of Autologous Bone Marrow Mononuclear Cells for Ischemic Stroke. *Journal of Neuroscience Research*, *89*, 833–839. https://doi.org/10.1002/jnr.22614

Yang, C., Zhang, X., Fan, H., & Liu, Y. (2009). Curcumin upregulates transcription factor Nrf2 , HO-1 expression and protects rat brains against focal ischemia. *Brain Research*, *1282*, 133–141. https://doi.org/10.1016/j.brainres.2009.05.009

Yang, Y., Xi, Z., Xue, Y., Ren, J., Sun, Y., Wang, B., … Bian, L. (2017). Hemoglobin pretreatment endows rat cortical astrocytes resistance to hemin-induced toxicity via Nrf2/HO-1 pathway. *Experimental Cell Research*, *361*(2), 217–224. https://doi.org/10.1016/j.yexcr.2017.10.020

Yang, Z., & Wang, K. K. W. (2015). Glial fibrillary acidic protein: From intermediate filament assembly and gliosis to neurobiomarker. *Trends in Neurosciences*, *38*(6), 364–374. https://doi.org/10.1016/j.tins.2015.04.003

Yao, Y., Miao, W., Liu, Z., Han, W., Shi, K., Shen, Y., … Shi, F. D. (2016). Dimethyl Fumarate and Monomethyl Fumarate Promote Post-Ischemic Recovery in Mice. *Translational Stroke Research*, *7*(6), 535–547. https://doi.org/10.1007/s12975-016-0496-0

Ye, Z.-W., Zhang, J., Townsend, D. M., & Tew, K. D. (2015). Oxidative stress, redox regulation and diseases of cellular differentiation. *Biochimica et Biophysica Acta (BBA) - General Subjects*, *1850*(8), 1607–1621. https://doi.org/10.1016/J.BBAGEN.2014.11.010

Yeager, R. L., Reisman, S. A., Aleksunes, L. M., & Klaassen, C. D. (2009). Introducing the ‘“ TCDD-Inducible AhR-Nrf2 Gene Battery ,”’ *111*(2), 238–246. https://doi.org/10.1093/toxsci/kfp115

Yoon, J. S., Jo, D., Lee, H.-S., Yoo, S.-W., Lee, T.-Y., Hwang, W. S., … Suh-Kim, H. (2018). Spatiotemporal Protein Atlas of Cell Death-Related Molecules in the Rat MCAO Stroke Model. *Experimental Neurobiology*, *27*(4), 287–298. https://doi.org/10.5607/en.2018.27.4.287

Yoshizaki, K., Adachi, K., Kataoka, S., Watanabe, A., Tabira, T., Takahashi, K., & Wakita, H. (2008). Chronic cerebral hypoperfusion induced by right unilateral common carotid artery occlusion causes delayed white matter lesions and cognitive impairment in adult mice. *Experimental Neurology*, *210*(2), 585–591. https://doi.org/10.1016/j.expneurol.2007.12.005

Yu, Q., Tian, D.-L., Tian, Y., Zhao, X.-T., & Yang, X.-Y. (2018). Elevation of the Chemokine Pair CXCL10/CXCR3 Initiates Sequential Glial Activation and Crosstalk During the Development of Bimodal Inflammatory Pain after Spinal Cord Ischemia Reperfusion. *Cellular Physiology and Biochemistry : International Journal of Experimental Cellular Physiology, Biochemistry, and Pharmacology*, *49*(6), 2214–2228.

https://doi.org/10.1159/000493825
Zagorski, J. W., Maser, T. P., Liby, K. T., & Rockwell, C. E. (2017). The Nrf2 activators tBHQ and CDDO-Im have both Nrf2-dependent and – independent effects on human Jurkat T cell activation, as determined by CRISPR-Cas9 gene editing. *The Journal of Immunology*, *198*(1 Supplement).
Zakkar, M., Van der Heiden, K., Luong, L. A., Chaudhury, H., Cuhlmann, S., Hamdulay, S. S., … Evans, P. C. (2009). Activation of Nrf2 in endothelial cells protects arteries from exhibiting a proinflammatory state. *Arteriosclerosis, Thrombosis, and Vascular Biology*, *29*(11), 1851–1857. https://doi.org/10.1161/ATVBAHA.109.193375
Zamanian, J. L., Xu, L., Foo, L. C., Nouri, N., Zhou, L., Giffard, R. G., & Barres, B. A. (2012). Genomic Analysis of Reactive Astrogliosis, *32*(18), 6391–6410. https://doi.org/10.1523/JNEUROSCI.6221-11.2012
Zamboni, G., Griffanti, L., Jenkinson, M., Mazzucco, S., Li, L., Küker, W., … Rothwell, P. M. (2017). White Matter Imaging Correlates of Early Cognitive Impairment Detected by the Montreal Cognitive Assessment after Transient Ischemic Attack and Minor Stroke. *Stroke*, *48*(6), 1539–1547. https://doi.org/10.1161/STROKEAHA.116.016044
Zarruk, J. G., Greenhalgh, A. D., & David, S. (2017). Microglia and macrophages differ in their inflammatory profile after permanent brain ischemia. *Experimental Neurology*, (August). https://doi.org/10.1016/j.expneurol.2017.08.011
Zbesko, J. C., Nguyen, T. V, Yang, T., Frye, J. B., Hayes, M., Chung, A., … Facility, C. (2018). Glial scars are permeable to the neurotoxic environment of chronic stroke infarcts. *Neurobiology of Disease*, *112*, 63–78. https://doi.org/10.1016/j.nbd.2018.01.007.Glial
Zeng, Z., Miao, N., & Sun, T. (2018). Revealing cellular and molecular complexity of the central nervous system using single cell sequencing. *Stem Cell Research and Therapy*, *9*(1), 1–11. https://doi.org/10.1186/s13287-018-0985-z
Zerna, C., Thomalla, G., Campbell, B. C. V, Rha, J.-H., & Hill, M. D. (2018). Current practice and future directions in the diagnosis and acute treatment of ischaemic stroke. *The Lancet*, *392*(10154), 1247–1256. https://doi.org/10.1016/S0140-6736(18)31874-9
Zeynalov, E., Shah, Z. A., Li, R. chi, & Dor??, S. (2009). Heme oxygenase 1 is associated with ischemic preconditioning-induced protection against brain ischemia. *Neurobiology of Disease*, *35*(2), 264–269. https://doi.org/10.1016/j.nbd.2009.05.010
Zhai, Q.-H., Futrell, N., & Chen, F.-J. (1997). Gene expression of IL-10 in relationship to TNF-α, IL-1β and IL-2 in the rat brain following middle cerebral artery occlusion. *Journal of the Neurological Sciences*, *152*(2), 119–124. https://doi.org/10.1016/S0022-510X(97)00154-8
Zhai, X., Chen, X., Shi, J., Shi, D., Ye, Z., Liu, W., … Sun, X. (2013). Lactulose ameliorates cerebral ischemia – reperfusion injury in rats by inducing hydrogen by activating Nrf2 expression. *Free Radical Biology and Medicine*, *65*, 731–741. https://doi.org/10.1016/j.freeradbiomed.2013.08.004
Zhang, C., Zhu, Y., Wang, S., Zachory Wei, Z., Jiang, M. Q., Zhang, Y., … Wei, L. (2018). Temporal Gene Expression Profiles after Focal Cerebral Ischemia in Mice. *Aging and Disease*, *9*(2), 249–261. https://doi.org/10.14336/AD.2017.0424
Zhang, D. D., & Hannink, M. (2003). Distinct cysteine residues in Keap1 are required for Keap1-dependent ubiquitination of Nrf2 and for stabilization of Nrf2 by chemopreventive agents and oxidative stress. *Molecular and Cellular Biology*, *23*(22), 8137–8151. https://doi.org/10.1128/MCB.23.22.8137-8151.2003
Zhang, Hongqiao, Davies, K. J. A., & Formana, H. J. (2015). Oxidative stress response and Nrf2 signaling in aging. *Free Radical Biology and Medicine*, *65*, 314–336. https://doi.org/10.1016/j.freeradbiomed.2013.07.003
Zhang, Hongqiao, Liu, H., Davies, K. J. A., Sioutas, C., Finch, C. E., Morgan, T. E., & Forman, H.

J. (2012). Nrf2-regulated phase II enzymes are induced by chronic ambient nanoparticle exposure in young mice with age-related impairments. *Free Radical Biology & Medicine*, *52*(9), 2038–2046. https://doi.org/10.1016/j.freeradbiomed.2012.02.042

Zhang, Hongxia, Lin, S., Chen, X., Gu, L., Zhu, X., Zhang, Y., … Jin, K. (2018). The effect of age, sex and strains on the performance and outcome in animal models of stroke. *Neurochemistry International*. https://doi.org/10.1016/J.NEUINT.2018.10.005

Zhang, L., Zhang, R. L., Jiang, Q., Ding, G., Chopp, M., & Zhang, Z. G. (2015). Focal embolic cerebral ischemia in the rat. *Nature Protocols*, *10*(4), 539–547. https://doi.org/10.1038/nprot.2015.036

Zhang, M., An, C., Gao, Y., Leak, R. K., Chen, J., & Zhang, F. (2013). Emerging Roles of Nrf2 and Phase II Antioxidant Enzymes in Neuroprotection. *Progress in Neurobiology*, *100*, 30–47. https://doi.org/10.1016/j.pneurobio.2012.09.003.

Zhang, P., Singh, A., Yegnasubramanian, S., Esopi, D., Kombairaju, P., Bodas, M., … Biswal, S. (2010). Loss of Kelch-like ECH-associated protein 1 function in prostate cancer cells causes chemoresistance and radioresistance and promotes tumor growth. *Molecular Cancer Therapeutics*, *9*(2), 336–346. https://doi.org/10.1158/1535-7163.MCT-09-0589

Zhang, R., Xu, M., Wang, Y., Xie, F., Zhang, G., & Qin, X. (2017). Nrf2—a Promising Therapeutic Target for Defensing Against Oxidative Stress in Stroke. *Molecular Neurobiology*, *54*(8), 6006–6017. https://doi.org/10.1007/s12035-016-0111-0

Zhang, X., Yeung, P. K. K., McAlonan, G. M., Chung, S. S. M., & Chung, S. K. (2013). Transgenic mice over-expressing endothelial endothelin-1 show cognitive deficit with blood–brain barrier breakdown after transient ischemia with long-term reperfusion. *Neurobiology of Learning and Memory*, *101*, 46–54. https://doi.org/10.1016/j.nlm.2013.01.002

Zhang, Y.-J., Song, J.-R., & Zhao, M.-J. (2019). NR4A1 regulates cerebral ischemia-induced brain injury by regulating neuroinflammation through interaction with NF-κB/p65. *Biochemical and Biophysical Research Communications*, *518*(1), 59–65. https://doi.org/10.1016/J.BBRC.2019.08.008

Zhang, Yan, Sano, M., Shinmura, K., Tamaki, K., Katsumata, Y., Matsuhashi, T., … Fukuda, K. (2010). 4-Hydroxy-2-nonenal protects against cardiac ischemia–reperfusion injury via the Nrf2-dependent pathway. *Journal of Molecular and Cellular Cardiology*, *49*(4), 576–586. https://doi.org/10.1016/J.YJMCC.2010.05.011

Zhang, Ye, Chen, K., Sloan, S. A., Bennett, M. L., Scholze, A. R., O'Keeffe, S., … Wu, J. Q. (2014). An RNA-sequencing transcriptome and splicing database of glia, neurons, and vascular cells of the cerebral cortex. *The Journal of Neuroscience : The Official Journal of the Society for Neuroscience*, *34*(36), 11929–11947. https://doi.org/10.1523/JNEUROSCI.1860-14.2014

Zhao, H., Zheng, T., Yang, X., Fan, M., Zhu, L., Liu, S., … Sun, C. (2019). Cryptotanshinone Attenuates Oxygen-Glucose Deprivation/ Recovery-Induced Injury in an in vitro Model of Neurovascular Unit. *Frontiers in Neurology*, *10*, 381. https://doi.org/10.3389/fneur.2019.00381

Zhao, L., Mulligan, M. K., & Nowak, T. S. (2017). Substrain- and sex-dependent differences in stroke vulnerability in C57BL/6 mice. *Journal of Cerebral Blood Flow and Metabolism*, *39*(3), 426–438. https://doi.org/10.1177/0271678X17746174

Zhao, S. C., Ma, L. S., Chu, Z. H., Xu, H., Wu, W. Q., & Liu, F. (2017). Regulation of microglial activation in stroke. *Acta Pharmacologica Sinica*, *38*(4), 445–458. https://doi.org/10.1038/aps.2016.162

Zhao, X., Sun, G., Zhang, J., Strong, R., Dash, P. K., Kan, Y. W., … Aronowski, J. (2007). Transcription factor Nrf2 protects the brain from damage produced by intracerebral hemorrhage. *Stroke*, *38*(12), 3280–3286. https://doi.org/10.1161/STROKEAHA.107.486506

Zhu, H., Santo, A., & Li, Y. (2012). The antioxidant enzyme peroxiredoxin and its protective role in neurological disorders. *Experimental Biology and Medicine (Maywood, N.J.)*, *237*(2), 143–149. https://doi.org/10.1258/ebm.2011.011152

Zhu, W., Casper, A., Libal, N. L., Murphy, S. J., Bodhankar, S., Offner, H., & Alkayed, N. J. (2015). Preclinical Evaluation of Recombinant T-cell Receptor Ligand RTL1000 as a Therapeutic Agent in Ischemic Stroke. *Transl Stroke Res*, *6*(1), 60–68. https://doi.org/10.1007/s12975-014-0373-7

Zlokovic, B. V. (2008). The blood-brain barrier in health and chronic neurodegenerative disorders. *Neuron*, *57*(2), 178–201. https://doi.org/10.1016/j.neuron.2008.01.003

Zonta, M., Angulo, M. C., Gobbo, S., Rosengarten, B., Hossmann, K.-A., Pozzan, T., & Carmignoto, G. (2003). Neuron-to-astrocyte signaling is central to the dynamic control of brain microcirculation. *Nature Neuroscience*, *6*(1), 43–50. https://doi.org/10.1038/nn980

Zrzavy, T., Machado-Santos, J., Christine, S., Baumgartner, C., Weiner, H. L., Butovsky, O., & Lassmann, H. (n.d.). Dominant role of microglial and macrophage innate immune responses in human ischemic infarcts. *Brain Pathology*, *28*(6), 791–805. https://doi.org/10.1111/bpa.12583

Zuloaga, K. L., Johnson, L. A., Roese, N. E., Marzulla, T., Zhang, W., Nie, X., … Alkayed, N. J. (2016). High fat diet-induced diabetes in mice exacerbates cognitive deficit due to chronic hypoperfusion. *Journal of Cerebral Blood Flow and Metabolism*, *36*(7), 1257–1270. https://doi.org/10.1177/0271678X15616400

Zuloaga, K. L., Zhang, W., Yeiser, L. A., Stewart, B., Kukino, A., Nie, X., … Alkayed, N. J. (2015). Neurobehavioral and Imaging Correlates of Hippocampal Atrophy in a Mouse Model of Vascular Cognitive Impairment. *Transl Stroke Res*, *6*(5), 390–398. https://doi.org/10.1007/s12975-015-0412-z

8. Appendixes

8.1. Reagent recipes

Phosphate buffer

Phosphate buffer (PB) was made 10-times concentrated by dissolving 2.57 g of mono-sodium phosphate (NaH_2PO_4; Sigma) and 11.95 g di-sodium phosphate (Na_2HPO_4; Sigma) in distilled water to make up for 1 litre. This solution was then filtered and was diluted a tenth in order to be used.

Phosphate buffer saline

Phosphate buffer saline (PBS) was made 10-times concentrated by dissolving 2.57 g of mono-sodium phosphate (NaH_2PO_4; Sigma) and 11.95 g di-sodium phosphate (Na_2HPO_4; Sigma) in distilled water. After adjusting the pH to 7.4, 90 g of sodium chloride was added, and the final solution was filled with distilled water to make up for 1 litre. This solution was then filtered and was diluted a tenth in order to be used.

Tris buffer

Tris buffer (TB) was made 10-times concentrated by dissolving 60.6 g of Trizma HCl (Sigma) and 13.9 g of Trizma base (Sigma) in distilled water to make up for 1 litre. This solution was then adjusted for a 7.6 pH and filtered. In order to be used, this solution was diluted a tenth.

Paraformaldehyde 4%

After heating 800 ml of PB at 60°C, 40 g of P6148 paraformaldehyde (Sigma) was added to the hot PB and let to stir for 15 minutes. After cooling down, the final solution was filled with distilled water to make up for 1 litre. This solution was then adjusted to a pH of 7.4 and filtered.

8.2. Glial response in the peri-infarct compared to the core of chronic ischaemia and compared with lesion

8.2.1. Peri-infarct results in the chronic phase of ischaemia were a mean value of core and healthy for Glial marker GFAP and Iba1

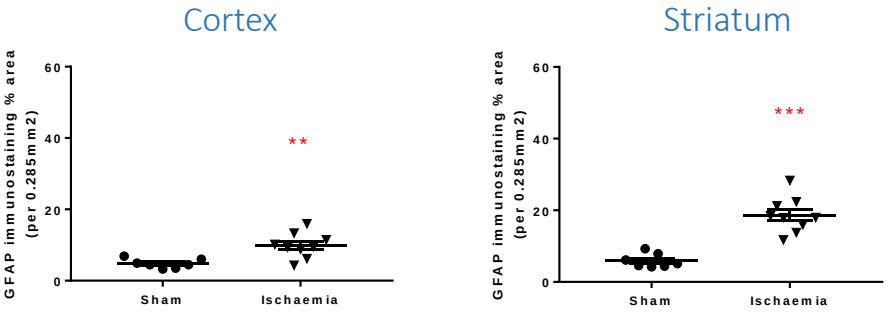

Figure 8-1 GFAP immunostaining quantified with %area was increased in the peri-infarct 4 weeks following ischaemia.

Quantification of GFAP immunostaining by assessing %area revealed significant differences between shams and 15 minutes ischaemia in the cortex peri-infarct ($t_{(14)}$=3.635, p=0.0027) and the striatum ($t_{(14)}$=6.414, p<0.0001).

*Data presented as mean ± SEM. Student's t-test (N= 7 to 9 per group). **p<0.01, ***p<0.001.*

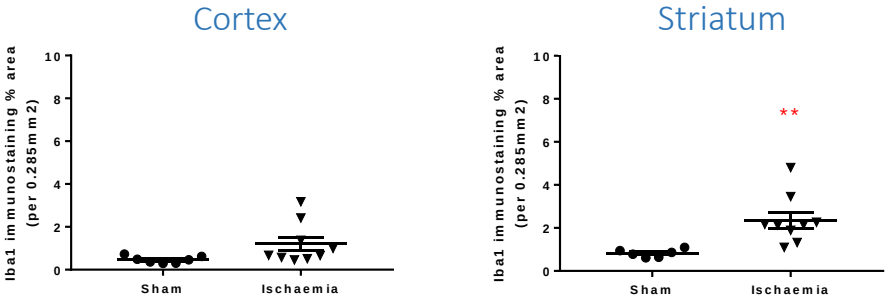

Figure 8-2 Iba1 immunostaining quantified with %area was increased in the peri-infarct 4 weeks following ischaemia.

Quantification of Iba1 immunostaining by assessing %area revealed significant differences between shams and 15 minutes ischaemia in the striatum ($t_{(14)}$=3.278, p=0.0060), but not in the cortex peri-infarct ($t_{(14)}$=1.989, p=0.0666) and

*Data presented as mean ± SEM. Student's t-test (N= 7 to 9 per group). **p<0.01.*

8.2.2. Correlations of the lesion volume with GFAP and Iba1 marker in the chronic response to ischaemia

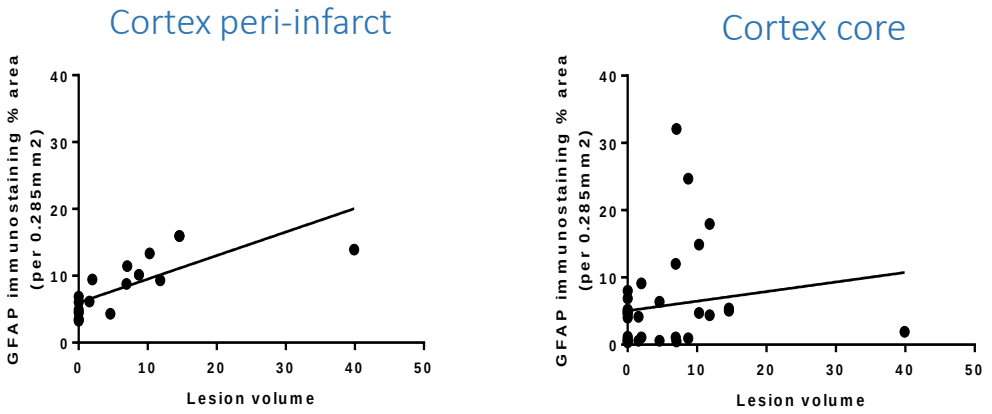

Figure 8-3 GFAP %area in the cortex peri-infarct is correlated with the lesion volume at 4 weeks but not the core.

Study of GFAP immunostaining %area compared with lesion volume revealed significant a positive correlation in the peri-infarct (R=0.7338, p<0.0001) but not in the cortex core (R=0.1544, p=0.3908).

Regression curve after Rho of Pearson correlation study (N= 7 to 9 per group).

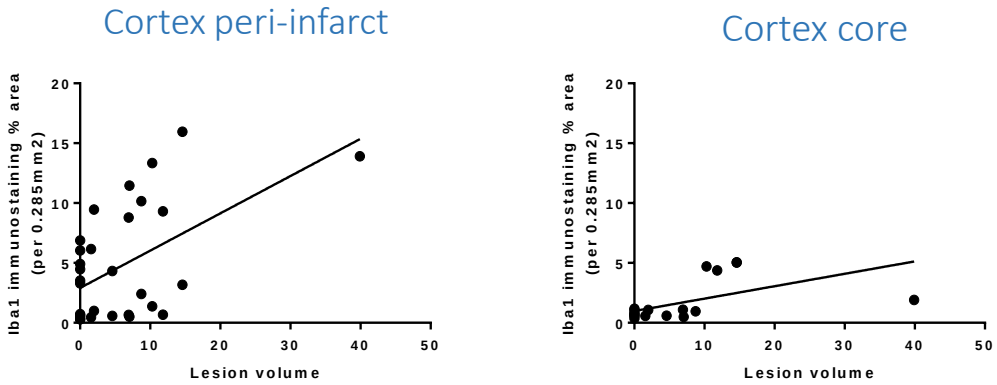

Figure 8-4 Iba1 %area in the cortex is correlated with the lesion volume at 4 weeks

Study of Iba1 immunostaining %area compared with lesion volume revealed significant a positive correlation in the peri-infarct (R=0.5333, p=0.0014) and core (R=0.5252, p=0.0017).

Regression curve after Rho of Pearson correlation study (N= 7 to 9 per group).

8.3. Astrocytic overexpression of Nrf2 did not modify cerebral blood flow 4 weeks after ischaemia

In order to verify cerebral blood flow (CBF) reduction in our model, laser speckle technique was used. The laser speckle software created a map of the blood flow with pseudo colours, ranging from blue (low) to red (high; Fig 8.4 A). This technique presented difficulties as the wound on the skull had to be reopened 4 weeks after the first reading and the scar compromised the reading of a few animals (13 animals excluded: 4 sham wild-type, 3 sham GFAP-Nrf2, 4 ischaemic wild-type and 2 ischaemic GFAP-Nrf2). The quantification is presented with ipsilateral CBF normalised to the contralateral CBF levels, with contralateral being 100%. Sham animals presented similar CBF readings before and 4 weeks after surgery. There was a significant effect of the surgery with decreased CBF in the ipsilateral side of ischaemic animals compared to shams ($F_{(1, 35)}$=8.19, p=0.0071) and there was no effect of the genotype or interaction ($F_{(1, 35)}$=0.102, p=0.75 and $F_{(1, 35)}$=0.029, p=0.86 respectively; Fig. 8.4 B).

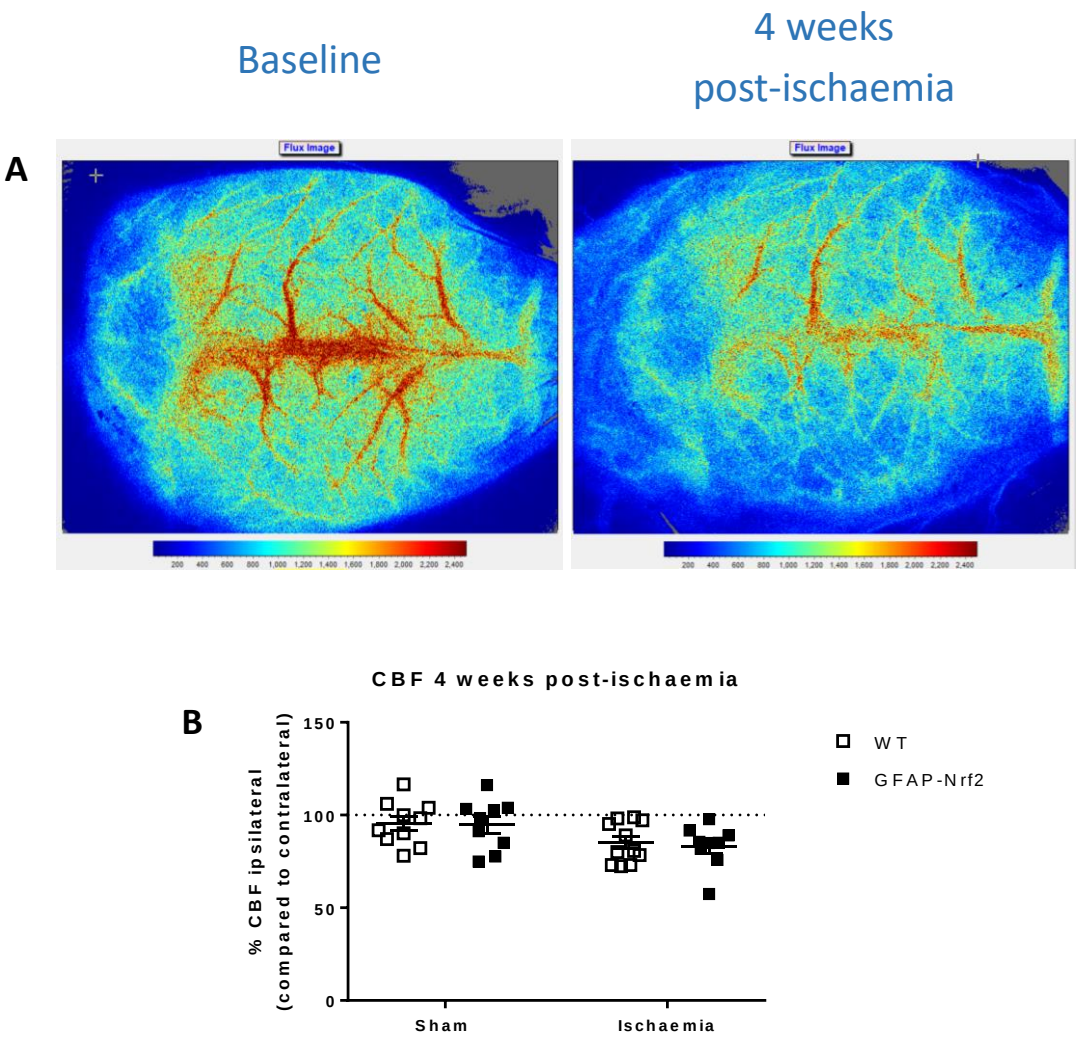

Figure 8-5. Nrf2 overexpression in astrocytes does not modify cerebral blood flow (CBF) reduction observed after mild ischaemia 4 weeks post-injury.

(A) Representative images of the cerebral blood flow (CBF) with intensity colours (from blue low CBF to red high CBF). Ischaemia reduces the CBF in the ipsilateral side (right hand side), four weeks after the injury.

(B) Quantification of CBF in the ipsilateral side to the lesion, normalised on the contralateral CBF, showed a reduction four weeks after 15 minutes of ischaemia ($F_{(1, 35)}$=8.19, p=0.0071). There was no effect of genotype ($F_{(1, 35)}$=0.102 p=0.75).

*Dotted line indicates contralateral CBF level. Data presented as mean ± SEM. Two-way ANOVA followed by post hoc comparisons with Bonferroni (N= 11 to 15 per group). *p<0.05, **p<0.01, ***p<0.001.*

Using the same model, Sigfridsson and colleagues found unchanged CBF was reduced 6 weeks after bilateral common carotid artery stenosis but not altered between Gfap-Nrf2 and wild-type mice (Sigfridsson et al., 2018). Other authors modulating Nrf2 in models of ischaemia did not find an effect on CBF (Shah et al., 2007; Yang et al., 2018; Wu et al., 2017). Interestingly, cognitive functions were impaired in GFAP-Nrf2 animals at 4 weeks after

ischaemia. This result is unlikely related to the cerebral blood flow modulation as GFAP-Nrf2 mice had comparable CBF levels to wild-type ischaemic animals. It suggests that this effect is independent of CBF modulation.

However, this result is limited by the comparison technique used to assess the perfusion is a comparison to contralateral side and not baseline. This method was preferred as many technical problems were encountered and some animal reading had to be excluded.